# Integrating Signals in Placode Progenitor Development

Hintze, Mark

*Awarding institution:*
King's College London

# Integrating Signals in Placode Progenitor Development

**BY**

**Mark Hintze**

**A thesis submitted to the King's College London higher degrees office in partial fulfilment for the degree of**

**Doctor of Philosophy**

**Craniofacial Development & Stem Cell Biology**
**Floor 27, Tower Wing**
**Guy's Hospital**
**London SE1 9RT**

**February 2016**

**Mark Hintze, London, UK**

# Abstract

Crucial parts of the sense organs arise from common precursors in the pre-placodal region (PPR). The PPR is marked by the factors *Six1*/4 and *Eya2*, which are both sufficient and required for PPR properties. Their induction requires signals from the head and prechordal mesoderm and the adjacent neural plate has also been implicated. However, their relative contribution has not been established.

Using a differential screen new PPR regulators as well as genes, which define the PPR spatially, were identified. Using these I dissected the transcriptional hierarchy downstream of PPR-inducing tissues. Both lateral head and prechordal mesoderm initially induce the same set of genes, but these responses diverge later, providing some rostro-caudal bias. However, grafts of neural plate alone do not induce a PPR, but provides further regional identity. Combining mesodermal tissue with neural plate tissue in an axial homotypic manner induces placodes with distinct identities, relative to the axial origin of the inducing tissue, while heterotypic grafts resulted in undefined domains. These results suggest a model for placode induction: initial induction generates a generic state, from which cells diverge under the influence of local signals.

The PPR is positioned by FGF and Wnt and Bmp antagonists emanating from the underlying mesoderm. To determine the genes regulated by each signal I combined tissue grafts, inhibitors and agonists of each pathway and determined the changes of gene expression in the responding tissue over time. This analysis reveals that all three pathways are required for PPR formation. FGF signalling appears to act early to specify a common domain, with some input from BMP antagonists, with later PPR regulation requiring combined input from all three signal factors.

# Contents

# Table of figures

# Tables

# Acknowledgements

Well this is an incredibly long way from where I was 10 years ago, when I decided that putting sausage rolls on a tray might not live up to my expectations in life. Even then I couldn't imagine 10 years later I would be submitting a PhD at King's College London.

First I would like to thank Andrea for being a great supervisor and putting in a lot of effort and support to help me get to this point and also giving me an opportunity to even do a PhD. Thanks also go to Stephen Price and Sarah Guthrie who helped me along the way towards a Masters and then a PhD. I would also like to thank Karen Liu who was really supportive of me as a second supervisor. Thanks also goes Claudio Stern and his lab as well as the Green group.

Next I want to thank everyone in the Streit lab for their support. A special mention goes to Monica Tambalo (the best dissector!) and Anneliese Norris 'the small gang', they helped set me up in the lab and we had a lot of fun. I wouldn't have been able to do the bioinformatics in this thesis without the help of Maryam, who started at the same time as me on this journey. Thanks as well to Jing Chen, Ramya, Ravindra, Mohi, Alice, who put up with my crazy ideas. I also want to thank Ewa for great technical assistance and the past lab techs Gael and Annabelle. Thanks to Basil and Jenny for helping me out when I needed it.

A huge thank you to my parents, without their support I would never have even picked myself up and dusted myself off after leaving school, I would also like to thank Kat Connor and her family for their support in the past.

Lastly a special thank you goes to Rebecca Williams, who without I may have descended into chaos and never finished this. Without your help I would never have got this far.

I find this very strange to be finishing, so know this even before you have begun to read my thesis you have read the last words that I wrote here……

For in the end although it is hard to see from the beginning as time moves inexhaustibly forward, we always get there.

# Abbreviations

| | |
|---|---|
| aNP | Anterior neural plate |
| ANOVA | Analysis of variance |
| aPPR | anterior pre placodal region |
| Ap2/Tfap2a | Transcription Factor AP-2 Alpha |
| BMP | Bone morphogentic protein |
| Bp | Base pair |
| cDNA | complementary Deoxyribonucleic acid |
| Dac | dachshund |
| Dlx | Distal-less homeobox |
| DMSO | Dimethyl sulfoxide |
| DNA | Deoxyribonucleic acid |
| ERNI | early response to neural induction |
| EST | expressed sequence tag |
| Etv | ets variant |
| Eya | Eyes absent |
| F/C | Fold change |
| FGF | Fibroblast growth factor |
| FGFR | Fibroblast growth factor receptor |
| Fox | Forkhead box |
| Gata | globin transcription factor |
| Gbx | gastrulation brain homeobox |
| GFP | Green fluorescent protein |
| GRN | Gene regulatory network |
| HH | Hamburger and Hamilton |
| Irx/Xiro | Iroquois homeobox /Xenopus Iroquois homeobox protein |
| lHM | Lateral head mesoderm |
| LOP | Lens olfactory progenitors |
| mmV | maxillomandibular |
| mRNA | messenger Deoxyribonucleic acid |
| Msx | Msh homeobox |
| NNE | Non neural ectoderm |
| Node | Hensen’s node |
| NP | neural plate |

| | |
|---|---|
| NPB | neural plate border |
| OEP | otic epibranchial progenitors |
| oPV | ophthalmic |
| Otx | Orthodenticle Homeobox |
| Pax | Paired box homeodomain |
| pME | Pre-chordal mesendoderm |
| pNP | Posterior neural plate |
| RA | Retinoic acid |
| SEM | Standard error of the mean |
| Shh | Sonic hedgehog |
| Six | Sine Oculis Homeobox |
| So | Sine Oculis |
| Sox | SRY-related HMG-box |
| WNT | wingless-type MMTV |
| Zic | Zinc finger of the cerebellum |

# 1. Introduction

## 1.1 Early processes in chick embryo development

The chick, a domesticated fowl (*Gallus Gallus Domesticus*), has been used as a model system in science since Aristotle studied the development of chicken embryos in ancient Greece. It is an excellent model organism as eggs are easily obtained and can be incubated to a variety of stages, making it simple to analyse a wide range of developmental processes. The large size of the embryo makes it easy to manipulate, it can also be cultured ex vivo. Chickens are of the amniote clade of tetrapod vertebrates and are similar in development and molecular biology to many mammals including humans. Therefore, the present study uses chick embryos to investigate the patterning, formation and regulation of the pre-placodal region and subsequent formation of cranial placode progenitors in early embryonic development.

### 1.1.2 Blastula and gastrula stages

The oocyte is fertilised in the oviduct of the hen with the albumen and shell secreted around the ovum as it resides in the shell gland. The egg is telolecithal (the yolk is concentrated at one pole) and therefore undergoes discoidal meroblastic cleavage (Bellairs, 1993; Bellairs et al., 1978). As cleavage begins, all cells are "open" to the yolk until the 64 cell stage when the blastodisc is formed on top of the yolk (Bellairs, 1993; Bellairs et al., 1978; *Eya*l-Giladi and Kochav, 1976; Stern and Downs, 2012). When the egg is laid, the blastodisc is already divided into two regions: the area pellucida, which gives rise to the embryo proper, and the outer area opaca, which forms extraembryonic tissues. Once this thin disc of cells is complete, the next major morphogenetic movement begins with cells shedding from the epiblast into the sub-germinal space between the epiblast and the yolk. This shedding of cells creates small islands of cells that later join in a posterior to anterior progression, forming a cell layer known as the hypoblast (*Eya*l-Giladi and Kochav, 1976; Fabian and *Eya*l-Giladi, 1981; Stern and Downs, 2012; Stern and Ireland, 1981). The rotation of the egg within the oviduct in conjunction with gravity causes the yolk to shift, tipping the blastodisc up at one end. This shift in the blastodisc is thought to create an accumulation of cells at one edge and thus position the anterior and posterior axis (*Eya*l-Giladi and Fabian, 1980; Kochav and *Eya*l-Giladi, 1971). The marginal zone forms at the edge of the area opaca and the area pellucida, with the most caudal region being the posterior marginal zone (PMZ). The PMZ has the same properties as the Nieuwkoop Centre in frogs in that it is able to induce organiser properties (Bachvarova et al., 1998; Nieuwkoop, 1977). Closely associated with the PMZ is a local thickening of cells known as Koller's sickle, which

contributes to the hypoblast and may also participate in primitive streak initiation in the epiblast (Bachvarova et al., 1998; Stern, 1990). The primitive streak is first seen at Hamburger and Hamilton stage 2 (Hamburger and Hamilton, 1951) and is the site of gastrulation, where cells that form the endoderm and mesoderm ingress to form the three germ layers. Over the next few hours the streak extends from posterior to anterior between HH3 and HH4$^{+}$ and the primitive groove becomes apparent. At the very tip of the streak is Hensen's node, the amniote organiser, which has neural inducing and patterning properties. Mesodermal cells that form axial and lateral tissues are organised along the anterior-posterior axis of the streak, with cells from the node generating notochord, prechordal mesoderm and medial somites and cells from the posterior streak generating lateral and extraembryonic mesoderm (Psychoyos and Stern, 1996; Schoenwolf et al., 1992; Selleck and Stern, 1992).

### 1.1.3 Neural plate stages

Once the embryo reaches HH4$^{+}$, notochord and prechordal progenitors emerge from the tip of the node and the node begins to regress, it lays down the axial mesoderm (Meier, 1981; Psychoyos and Stern, 1996; Seifert et al., 1993). At HH5, there is a clear separation of the prechordal mesendoderm and the notochord. The anterior ectoderm can now be divided into three regions: the neural plate, which eventually gives rise to the central nervous system, the future epidermis surrounding it and the neural plate border, in which both territories overlap. Next to the primitive streak the epiblast still contains a mixture of ectoderm and mesoderm precursors, with the latter ingressing as the streak continues to regress (Psychoyos and Stern, 1996; Schoenwolf et al., 1992; Selleck and Stern, 1992) . At HH4$^{+}$ the neural plate begins to express the definitive neural marker *Sox2* (Kamachi et al., 1995; Streit and Stern, 1999), while genes such as *ERNI* and *Sox3,* which begin to be expressed earlier, straddle both the neural plate and its border (Rex et al., 1997; Streit et al., 2000). The non-neural ectoderm (NNE) is marked by genes including *Gata2* and *-3* (Sheng and Stern, 1999).

The neural plate border is characterised by the overlapping expression of early pre-neural and non-neural transcripts and contains precursors for the neural plate, the epidermis, the neural crest and the sensory placodes (Bhattacharyya et al., 2004; Groves and Labonne, 2014; Keller, 1976; Kozlowski et al., 1997; Pieper et al., 2011; Streit, 2002; Xu et al., 2008). By HH6, the head fold forms anterior to the neural plate. At this point, sensory placode progenitors surround the anterior neural plate and can be identified by expression of *Six* and *Eya* family members as the pre-placodal region (PPR) (Bhattacharyya et al., 2004; Brugmann and Moody, 2005; Dutta et al., 2005; Pieper et al., 2011; Streit, 2002). As

development proceeds, cells of different fates segregate, with neural crest cells being concentrated at the neural dorsal folds and placode cells remaining in the more lateral, non-neural ectoderm. The neural folds later elevate towards the midline (from HH8 onwards) and ultimately merge and separate from the epidermis to form the neural tube. (Kalcheim and Le Douarin, 1986). At HH7, the formation of the somites begins from the pre-somitic mesoderm and a pair of somites is generated every 90 minutes (Palmeirim et al., 1997). Shortly thereafter, localised thickenings of ectoderm adjacent to the neural tube begin to develop, forming the cranial placodes (For review: Baker and Bronner-Fraser, 2001).

In chick, the first cranial placode to form at HH10 is the otic placode next to rhombomeres 5 and 6 of the hindbrain, while the olfactory placode forms last around HH15 at the very anterior tip of the embryo next to the telencephalon (Baker and Bronner-Fraser, 2001; Streit, 2004 Summarised in Figure 1.1). Although cranial placodes are visually distinct only by neural tube stages, the cells that comprise them begin to be induced at a much earlier stage. Some tissues and signals which play a role in the induction of early progenitors have been identified and characterised (Baker and Bronner-Fraser, 2001; Jacobson, 1966; Schlosser, 2010). Experimental evidence shows that cells must go through a "PPR-state" before they can respond to placode inducing signals (Martin and Groves, 2006). Therefore, the main focus of this study is to investigate and understand PPR development by focusing on the tissues and signals involved in its induction and regionalisation. The following paragraphs briefly describe the formation of the mesodermal tissues implicated in PPR and placode formation.

## 1.2 The origin and role of the avian mesoderm in early development

In the avian embryo, the mesoderm is formed when cells ingress through the primitive streak and migrate to form the intermediate germ layer (Hatada and Stern, 1994; Redkar et al., 2001; Schoenwolf et al., 1992). This layer of tissue can be divided into head and trunk mesoderm. The cranial mesoderm gives rise to key elements of the cranial skull base as well as the craniofacial musculature (Bothe and Dietrich, 2006; Noden and Francis-West, 2006). It can be divided into the lateral head mesoderm (lHM) (which includes the heart mesoderm), the paraxial mesoderm and the axial notochord and prechordal mesendoderm (pME) at its tip (Adelmann, 1922; Couly et al., 1992; DeHaan, 1963; Noden, 1988; Seifert et al., 1993). Both the lHM and pME have been implicated in providing signals that pattern the overlying ectoderm (Foley et al., 1997; Litsiou et al., 2005; Lleras-Forero et al., 2013; Pera and Kessel, 1997).

### 1.2.1 The lateral head mesoderm

The lateral head mesoderm gives rise to numerous muscles in the development, which contribute to the movement of the head and jaw (Couly et al., 1992). Many fate maps show the early origin of this mesoderm is spread across the developing epiblast at pre-streak stages and that the lHM migrates through the anterior two thirds of the primitive streak (Hatada and Stern, 1994; Psychoyos and Stern, 1996; Redkar et al., 2001; Schoenwolf et al., 1992). The lHM gives rise to the cardiac progenitors that provide the cells for the structures of the heart and the electrical activity that provides the heart beat (DeHaan, 1963; Redkar et al., 2001; Sater and Jacobson, 1989). lHM ablation leads to disruption of heart formation as well as disrupting the PPR genes in the overlying ectoderm, seen as a loss of *Six1* and *Eya2* (Litsiou et al., 2005; Redkar et al., 2001). Interestingly, many genes involved in heart development e.g. *Nkx2.5* (Redkar et al., 2001) are expressed in the mesoderm with a pattern reminiscent of *Six* and *Eya* family members in the overlying ectoderm (Ehrman and Yutzey, 1999; Esteve and Bovolenta, 1999; Ishihara et al., 2008a; Lopez-Sanchez et al., 2009; Yuan and Schoenwolf, 2000). Indeed, *Six1*, *Six4*, *Eya1* and *Eya2* themselves are also present in the head mesoderm, as well as the first 5 somites (Ishihara et al., 2008a; Sato et al., 2012).

### 1.2.2 Prechordal mesendoderm

The prechordal mesendoderm (pME) is a fan shaped tissue arising from the anterior tip of the primitive streak. It comprises of both mesoderm and, at its more anterior region, a mixture of mesoderm and endoderm cells, while no chordamesoderm (notochord) is present (Adelmann, 1922; Noden, 1988; Seifert et al., 1993). The pME originates from Hensen's node and its precursors ingress through the node as the first axial mesoderm (Noden, 1988; Schoenwolf et al., 1992). Although a prominent structure in early development, once the head fold has formed the pME will integrate with the paraxial mesoderm and become indistinguishable as a single population of cells (Noden, 1988). The origin of the cells that form the pME has been much debated. The most anterior structure, the prechordal plate, is continuous with the prechordal mesendoderm and is endodermal in origin, while the more posterior prechordal mesendoderm has a mesodermal origin (Adelmann, 1922; Seifert et al., 1993). As both of these populations are very difficult to distinguish and separate reliably, the prechordal mesendoderm (pME) will refer to the fan shaped structure that arises from the node, which is distinct by HH5 at the tip of the notochord.

Quail and chick chimeras show that the pME contributes to various structures including the muscles of the eye: *m.rectus ventralis*, *m.rectus medialis* and the *m.obliqous ventralis* (Couly et al., 1992). Importantly, it is also involved in patterning of various structures of the developing vertebrate head. pME cells, when cultured with prospective neuroectoderm, will induce a nervous system (Hara, 1961). While more recent experiments have shown that the pME can induce different fates, although the results are not definitive. One study showed that the pME, when grafted ectopically close to the neural plate/tube will impart anterior character to posterior structures, but cannot induce neural tissue on its own (Foley et al., 1997). However, a second study showed that the pME can induce a forebrain like vesicle in the future epidermis (Pera and Kessel, 1997). In the second study, pME grafts were close to the endogenous forebrain and recruitment of prospective forebrain cells from the host can therefore not be ruled out. In addition, the lack of donor markers makes it difficult to assess the contribution of host and donor tissue (Pera and Kessel, 1997). A third, more recent study, has shown that the pME is the source of neuropeptides, which control the expression of *Pax6* a key anterior placode marker and the PPR marker *Eya2* (Li et al., 1994; Lleras-Forero et al., 2013).

Although it is clear that the pME has inducing capabilities and provides possible cues for the induction of PPR related markers, it is unclear if the pME can induce Six and *Eya*. Therefore, the role of the pME in PPR development will be investigated further.

## 1.3 The neural plate border and the positioning of the PPR

### 1.3.1 Overlapping gene expression defines the neural plate border

At gastrula stages, the cells that form the PPR are widespread and intermingled with precursors for many other tissues, shown by fate map analysis in different species (Garcia-Martinez et al., 1993; Hatada and Stern, 1994; Keller, 1976; Kozlowski et al., 1997; Rudnick, 1935; Streit, 2002). As the neural plate is established centring around the node (HH4/4$^{+}$) its edges continue to overlap with precursors for other ectodermal derivatives (neural crest, placodes, epidermis) in a territory referred to as the “border” (Dickinson et al., 1995; LaBonne and Bronner-Fraser, 1998; Liem et al., 1995; Moury and Jacobson, 1990; Selleck and Bronner-Fraser, 1995; Streit and Stern, 1999). Lateral to the neural plate border the epiblast contains only future epidermal cells. Molecularly, the neural plate border can be defined by the overlapping expression of genes from both the early neural plate and the NNE (For review: Grocott et al., 2012; Streit, 2007). At gastrula stages, among the pre-

neural/neural genes that extend from the neural plate into the border region are *ERNI, Dlx3*, *Sox3*, *Zic1*, *N-myc* and *Sall4* (Spalt4) (Barembaum and Bronner-Fraser, 2007; Hong and Saint-Jeannet, 2007; Khudyakov and Bronner-Fraser, 2009; Rex et al., 1997). In contrast, genes from the lateral epidermal region extend to overlap with genes from the neural plate and include *Gata2*, *Dlx5*, *Msx1*, *Pax7* and *Tfap2a* (Ap2) and *Dlx3* in *Xenopus* (Basch et al., 2006; Kwon et al., 2010; Pera et al., 1999; Sheng and Stern, 1999; Streit and Stern, 1999; Woda et al., 2003).

At late gastrula/head process stages, the border territory becomes more defined with genes such as *ERNI* becoming confined to it and the onset of *Irx1* expression (Glavic et al., 2004; Khudyakov and Bronner-Fraser, 2009; Streit et al., 2000). Gradually more transcripts become expressed in, restricted to or increased in the border region. These include *Foxi3*, *Msx1*, *Pax3*, *Pax7*, *Gata3* and the *Dlx* genes (Brown et al., 2005; Khudyakov and Bronner-Fraser, 2009; McLarren et al., 2003). The *Dlx* genes do not correspond across species with changes in nomenclature and expression. *Dlx3* is expressed in the non-neural ectoderm in *Xenopus*, resembling *Dlx5* in amniotes (Pieper et al., 2012), while in amniotes *Dlx*3 is enriched in the neural plate at gastrulation stages and will go on to be expressed in the otic placode (Bhattacharyya and Bronner-Fraser, 2008; Khudyakov and Bronner-Fraser, 2009). Gene duplication in zebrafish leads to further differences to *Xenopus* and amniotes, therefore *Xenopus Dlx3/5*, amniotes *Dlx*5/6 and zebrafish *Dlx3b/4b* will be considered as equivalent in terms of expression domains, while amniote *Dlx3* will remain as a separate entity.

Finally at head fold stages, the embryo begins to express the definitive neural plate marker *Sox2.* The neural plate border then begins to be refined into the PPR and neural crest domains with the onset of expression of PPR markers *Six1/4* and *Eya2* and neural crest genes *C-myc*, *Slug* (*Snail2*) and *Foxd3* (Brugmann et al., 2004; Esteve and Bovolenta, 1999; Ishihara et al., 2008a; Khudyakov and Bronner-Fraser, 2009; LaBonne and Bronner-Fraser, 2000; Mancilla and Mayor, 1996).

Many of the TFs described above are not only good markers for the border and its derivatives, but also play a critical role in positioning it. *Dlx* genes play a crucial role in border specification. In chick, misexpression of *Dlx5* in the neural plate leads to the loss of the neural markers *Sox2/3*, while the border markers *Msx1* and *BMP4* are expanded. Ectopic expression of *Dlx5* also leads to the induction of *Six4* (McLarren et al., 2003). Therefore, *Dlx5* is important in positioning the neural plate border and is involved in PPR formation. However, ectopic *Dlx5* cannot induce neural crest or placodal cell fates, which are

derivatives of the border (McLarren et al., 2003). Morphants for *Dlx3b/4b* in zebrafish showed a loss of Six4 and Eya1, indicating their necessity at the border in promoting PPR fate (Esterberg and Fritz, 2009) In Xenopus, gain-of-function of *Dlx3* leads to a loss of neural plate markers, but does not expand the epidermal markers such as *Keratin19* (Woda et al., 2003). Repressing or activating *Dlx3* at different times in the neural plate border showed that it is required until the end of gastrulation to position it. Further experiments revealed a role for *Dlx3* in neural crest and PPR formation: grafts of neural plate into the non-neural ectoderm normally will induce both tissues; however when *Dlx3* expression is attenuated no induction of *Slug* (neural crest) or *Six1* (PPR) is observed (Woda et al., 2003). This indicates that *Dlx* genes are important for the neural plate border to form and for its derivatives but are not sufficient for further induction (Woda et al., 2003). In *Xenopus*, *Dlx3* creates a competence region in the non-neural ectoderm for PPR markers (Pieper et al., 2012) and knock down of *Dlx3* leads to an expansion of *Sox3* a neural marker and a loss of neural crest (*Foxd3)*, PPR (*Six1*, *Eya1*) and non-neural ectoderm markers (*Keratin19*), while misexpression leads to an induction of non-neural markers (Pieper et al., 2012). In fish, neural plate grafts into the non-neural ectoderm normally induce the PPR marker *Six1*, however when *Dlx3* expression is abolished no induction is seen. This indicates that *Dlx* is not only a competence factor, but it is also required cell autonomously for *Six1* expression (Pieper et al., 2012). Recently, *Dlx5* has also been shown to regulate *Six1* directly in a positive fashion through a *Six1* enhancer which is active in the anterior PPR (Sato et al., 2010). Taken together these results show that across different species *Dlx factors* are vital for the positioning of the border region and the formation of neural crest and PPR cells. Using similar loss- and gain-of-functions experiments, *Gata2* was also shown to be similar to *Dlx3* in *Xenopus*, acting as a competence factor for PPR genes, but crucially it could not induce ectopic non-neural markers (Pieper et al., 2012). Another member of the Gata family *Gata3* also acts as a competence factor in zebrafish in conjunction with *Tfap2a/c* and *Foxi1*, promoting a PPR competence domain (Kwon et al., 2010).

In contrast to *Dlx* genes which promote placodal fate, *Msx1* is also expressed at the border, but in a narrower domain where it is involved in the promotion of neural crest over PPR fate. Misexpression of *Msx1* induces neural cells and attenuation of *Msx*1 in *Dlx3b/4b* zebrafish mutants will rescue placodal fate (Monsoro-Burq et al., 2005; Phillips et al., 2006). *Msx1* also directly represses *Six1* through interaction with the aPPR *Six1* enhancer (Sato et al., 2010). Therefore, a complex interaction takes place within the border region between *Dlx* and *Msx* to refine and promote placodal or neural crest fate, respectively.

*Foxi* genes are important in the specification of the neural plate border, loss- and gain-of-function experiments of *Foxi1* in *Xenopus* show a loss of non-neural genes or an expansion of neural markers, respectively (Matsuo-Takasaki et al., 2005). *Foxi1* also acts in a partnership with *Tfap2a/c* and *Gata3* to create an early domain of competence, under the control of BMP, which forms the PPR (Kwon et al., 2010). in Zebrafish the identification of two mutants *Hearsay* and *Foo/Foo,* which display otic placode progenitor disruption, both had mutations in the *Foxi1* gene and morphants for *Foxi1* phenocopied the *Hearsay* mutant (Nissen, 2003; Solomon, 2003). While, knockdown of *Foxi1* leads to a loss of *Dlx3*, important in PPR and placode formation as well as being involved in the neural plate border (Nissen, 2003). *Foxi3*, is suggested to be equivalent in chick to *Foxi1* in zebrafish and can induce *Dlx5* and the PPR markers *Six1* and *Eya* when ectopically expressed (Khatri et al., 2014), while knockdown of *Foxi3* leads to the loss of the otic placode at later stages (Khatri et al., 2014).

*Irx1*, a known transcriptional repressor, is expressed in the border region and subsequent PPR (Glavic et al., 2004; Khudyakov and Bronner-Fraser, 2009), plays an important role in the specification of placodal cells from. Overexpression of the *Irx1* homeodomain fused to an engrailed repressive construct lead to an expansion of *Six1* and placode markers (Glavic et al., 2004). Therefore, *Irx1* may play a role in PPR formation by repressing genes that prevent formation of the PPR

In *Xenopus*, *Zic1* and *Pax3* play a role in determining the fate of cells in the border region, the overexpression of *Zic1* promotes PPR genes, while knockdown leads to loss of both neural crest and PPR markers. The overexpression of *Pax3* at high concentrations leads to the increase in hatching gland fate and at low concentrations leads to an expansion of neural crest fate. The combined overexpression of *Pax3* and *Zic1* leads to promotion of neural crest markers and not PPR genes (Hong and Saint-Jeannet, 2007). This suggests that varying levels of *Zic1* and *Pax3* at the border will determine cell fate outcomes and that *Zic1* is important for *Six1* induction.

The early ectoderm can be divided into 3 domains along the medio-lateral axis (neural plate, border and non-neural ectoderm), but it can also be divided anterior to posterior by various transcription factors. *Otx2* and *Gbx2* mark the distinction between these two domains (Bally-Cuif et al., 1995; Shamim and Mason, 1999; Steventon et al., 2012). *Otx*2 and *Gbx*2 are mutually repressive, with the misexpression of one leading to the repression of the other and a shift of the anterior and posterior boundary (Katahira et al., 2000; Millet et al., 1999). Experiments using constitutively active constructs showed that the activation of *Otx2* targets is required for the formation of anterior placode structures

(olfactory, lens and trigeminal), while *Gbx2* activation is required for the otic placode (Steventon et al., 2014). Misexpression experiments in the neural plate have shown that other factors such as *Six3* and *Irx3* further subdivide the neural plate through mutual repression. Gain- or loss-of-function of *Six3* or *Irx3* did not affect *Otx2* or *Gbx2* expression, suggesting that this later division does not affect the previous boundary formation. There is a possibility that this may also apply to the subdivision of the PPR, however this remains to be tested.

While the overlapping expression and mutual repression of transcription factors plays a role in the positioning of the neural plate border (Summarised in Figure 1.2), signalling molecules secreted from surrounding tissues are also important in setting up the early domains that transcription factors subsequently through interaction refine into defined cell fates.

### 1.3.2 Signals that promote the neural plate border

During the development of the border region and subsequently, the PPR, signalling factors from surrounding tissues play a role in promoting the border/PPR. FGF signalling has been implicated in different aspects of ectodermal patterning. *FGF receptors 1* and *4* are already expressed in the pre-streak epiblast, with *FGFr1* remaining upregulated in the neural plate and its border and subsequently in the neural tube at HH10 (Lunn et al., 2007). *FGFr4* is expressed in the anterior neural plate and tube at HH stages 4/5 and 6 (Lunn et al., 2007). *FGFr2* and *-3* are first expressed in the neural plate at HH3 and 4, respectively. FGFr2 remains upregulated in the neural plate, while *FGFr3* becomes restricted to the anterior neural plate and then is expressed in the somites by HH8 – 10 (Lunn et al., 2007). There is also expression of *Pea3* and *Erm*, both of which are involved in the FGF pathway (Roehl and Nüsslein-Volhard, 2001), along with phosphorylated Erk (pERK) in ectoderm that will go one to form the neural plate border and subsequently the PPR and neural crest domain (Lunn et al., 2007). Thus, FGF receptors and signalling read outs are present as the neural plate border is established and PPR cells are set aside.

Grafts of FGF4 and FGF8 coated beads placed in the extraembryonic region of the chick induce the border marker *Msx1* (Streit and Stern, 1999) and overexpression of FGF8 in *Xenopus* also showed an upregulation of *Msx1* (Monsoro-Burq et al., 2005) In addition, FGF8 induces pre-neural markers *ERNI* and *Sox3,* but not the definitive neural marker *Sox2*, while FGF inhibition prevents their induction by an organiser graft (Streit et al., 2000). Misexpression of dominant negative FGF receptors caused the lateral expression of the

neural crest marker *Msx1* and the NNE marker *BMP4* (Stuhlmiller and García-Castro, 2012), suggesting FGF helps set the boundaries of the neural plate border. In addition, beads coated with FGF4 also initiate the neural crest cascade in the chick extraembryonic ectoderm with the upregulation of *Pax*7 (Yardley and García-Castro, 2012). However, the induction of *Pax*7 was only robust when beads were grafted in the presence of a neural promoting media (N2), so it is difficult to assess if this is an FGF only effect. In *Xenopus*, FGF has been shown to regulate factors at the neural plate border; overexpression leads to an expansion of *Zic1* and *Pax3*, two factors involved in the specification of the border and its derivatives (Hong and Saint-Jeannet, 2007). In contrast, a loss of FGF signalling results in a loss of *Zic1* in the posterior neural plate border but *Zic1* is expanded anteriorly, while *Pax3* is reduced throughout (Hong and Saint-Jeannet, 2007). Together these findings suggest that FGF is important for gene expression in the neural plate border, but may have different effects depending on the axial position.

These findings suggest that FGF initiates the expression of genes involved in the setting up the early neural plate border. Interestingly, with respect to PPR induction, FGF is only required for an initial period in line with the findings summarised above that it is sufficient and required for early expression of genes in the border. While FGF is important for the induction of early neural factors, other signalling factors to promote the formation of NNE such as WNTs and BMPs.

WNT signalling has been shown to be important for the positioning of the neural plate border, promoting important transcription factors involved in its specification. WNTS are expressed in the non-neural ectoderm and in the lateral region of the early chick epiblast (Skromne and Stern, 2001; Wilson et al., 2001). WNT signalling negatively regulates early neural and border markers in explant cultures. Medial explants from pre-streak chick embryos loose expression of *Sox2/3* and *Otx2* in the presence of WNT, but upregulate the border marker *Msx1*. In contrast, lateral epiblast explants lost the expression of *Msx1* in the presence of a WNT inhibitor and upregulate neural markers (Wilson et al., 2001). Likewise, in *Xenopus* overactivation of WNT1 induces the border factors *Pax3* and *Zic1* (Hong and Saint-Jeannet, 2007). These findings suggest that the level of WNT signalling determines the boundaries between neural and border genes. In addition, at slightly later stages WNT signalling is involved in anterior-posterior and medial-lateral patterning of the ectoderm. The WNT pathway caudalises anterior border cells as demonstrated by the induction of *Snail2* in chick and *Xslug* in *Xenopus* (Patthey et al., 2008; Villanueva et al., 2002). Likewise, activation of the WNT pathway represses anterior character (*Otx2* expression), while

promoting posterior identity (Nordström et al., 2002). At mid- and hindbrain levels the border generates both neural crest and placodes, and here WNT promotes the activation of neural crest factors at the expense of placodal character. Overexpression of β-catenin leads to the expansion of the crest marker *Pax*7 into the PPR territory, while its inhibition has the opposite effect (Litsiou et al., 2005; García-Castro et al., 2002; Basch et al., 2006). In chick explant culture WNT will induce neural crest from naive neural plates (García-Castro et al., 2002). In *Xenopus,* expression of a *XWNT7b* leads to the expansion of the neural crest gene *Xtwist* and when expressed with noggin in ectodermal explant cultures will promote neural crest markers *Xslug* and *Xtwist* (Chang and Hemmati-Brivanlou, 1998). Conversely, when WNT signalling is blocked in the *Xenopus* ectoderm the neural plate is expanded (Heeg-Truesdell and LaBonne, 2006). Recently mouse mutants have shown that *Grainy Head like 3* regulates the specification of the neural plate border in surface ectoderm under the control of WNT (Kimura-Yoshida et al., 2015). Therefore, WNT signalling is clearly key to the induction of early border markers and the subsequent promotion of neural crest.

A number of BMPs and BMP antagonists are involved in the promotion of factors important for the positioning of the neural plate border and its subsequent derivatives. In frog, fish and chick BMPs (*BMP4, BMP7*) and its targets (e.g. *Msx1*) are generally broadly expressed in the non-neural ectoderm (Streit and Stern, 1999), although timing and patterns differ slightly, It has been thought that a graded response to levels of BMPs determine the fate of tissues across the early embryonic ectoderm, with high levels being responsible for non-neural fate and low or abolished signalling important for neural fate (De Robertis and Kuroda, 2004; Harland, 2000; Weinstein and Hemmati-Brivanlou, 1999). Indeed experiments in *Xenopus* where BMP was added to animal caps or inhibited with a dominant negative BMP receptor, showed that high levels of BMP promoted epidermal fates, while inhibition led to neural fates (Wilson et al., 1997). BMP signalling also represses neural fates in early chick embryos: exposure of early embryonic ectoderm to BMP led to a loss of neural factors (Wilson et al., 2001). At this stage, inhibition of FGF shows an up regulation of BMP, suggesting that FGF signalling normally represses BMPs subsequently promoting neural and border fate (Wilson et al., 2001). However, at gastrulation stage misexpression of BMP inhibitors is not sufficient to induce ectopic neural markers (Linker and Stern, 2004; Streit et al., 1998; Wawersik et al., 2005), but does expand the neural, border and neural crest factors *Sox*2, *Msx1* and *Pax*7 respectively (Linker et al., 2009; Streit and Stern, 1999). Targeted misexpression of BMP inhibitors in *Xenopus* (*Smad6*) shows similar results (Linker and Stern, 2004). Together these findings indicate that at gastrulation stages only cells at the border are sensitive to levels of BMP signalling. Indeed, at this stage

phosphorylation of Smad1/5/8, key intracellular proteins which mediate BMP, is first present in the non-neural and border ectoderm of the neurula stage chick embryo (Faure et al., 2002; Stuhlmiller and García-Castro, 2012), in a pattern similar to the neural crest marker *Pax*7 and other neural crest genes (Stuhlmiller and García-Castro, 2012). This suggests that BMP signalling may be important for the positioning of the border and determining the size of the neural plate.

In support of this idea, a number of border genes are positively regulated by BMP and inhibition of BMP. Graded levels of Noggin showed that intermediate levels of BMP are required for WNTs to activate *Zic1* (Hong and Saint-Jeannet, 2007). A reduction in BMP signalling in *Xenopus*, using a dominant negative BMP receptor, leads to an expansion of the border and PPR marker *Irx1* (Glavic et al., 2004). *Dlx* genes important in the formation of the border and the refinement of the boundary between the neural plate and non-neural ectoderm are negatively regulated by the BMP antagonist Chordin (Luo et al., 2001), while the border and neural crest gene *Msx1* is induced by BMP in chick and frog (Suzuki et al., 1997; Wilson et al., 2001). These results implicate BMP signalling as upstream regulators of border and crest transcripts. Recent studies in zebrafish (Kwon et al., 2010) have extended these experiments to assess when BMP signalling is required for PPR induction demonstrating a dual role. At early stages, abolishing BMP signalling leads to the loss of *Tfap2a/c*, *Foxi1* and Gata2, four factors shown to be competence factors for the later expression of PPR markers (Kwon et al., 2010). However, at later stages BMP signalling must be inhibited for PPR markers to be expressed. These findings provide evidence for a twostep process where BMP is required initially to create a competence domain and subsequently BMP needs to be attenuated to allow PPR formation. Likewise, in *Xenopus* BMP antagonism promotes the induction of the PPR marker *Six1* (Brugmann et al., 2004)

In summary, it is clear that early on levels of WNT, FGF and BMP are required to split the early embryo into neural and non-neural domains. While at later stages further refinement of these signals into discrete domains of expression will refine these two domains into the neural plate, border and NNE from which different cell fates are derived.

### 1.3.3 The binary competence model

The above paragraphs describe some of the evidence for the existence of a territory called 'neural plate border', from which PPR and neural crest cells are specified by early neural fold stages. The border model proposes that cell fate is acquired gradually and that this corresponds to the gradual expression and refinement of transcription factors controlled by different signalling factors. These factors regulate each other and thus define restricted cell fates successively. Initially, there is an overlap of pre-neural and non-neural gene expression in the ectoderm where cells of different fates reside (Dickinson et al., 1995; Grocott et al., 2012; Liem et al., 1995; Schlosser, 2010; Selleck and Bronner-Fraser, 1995). Segregation of different cell lineages is mimicked by the onset of new transcription factors or changing expression of others. The above sections describe the evidence for the overlap of transcription factors and the functions that these play in promoting neural crest and PPR cell fates. However, there is further evidence that transcription factors at the border region cross repress each other to create more discrete domains. In *Xenopus*, misexpression of *Six1* leads to the expansion of *Zic2* and repression of neural (*Sox2,Dlx6*) and neural crest markers (*Foxd3*), *Six1* knockdown leads to a reduction of *Dlx5* and *Eya1* (border, PPR) (Brugmann et al., 2004). In contrast, misexpression of *Sox2* led to a reduction in *Six1*, while misexpression of *Foxd3* also led to a loss of *Six1* (Brugmann et al., 2004). Showing mutual interactions between transcription factors define the neural, neural crest and PPR domains. Similar results are observed in chick; while misexpression of *Six1* and *Eya2* leads to the repression of *Pax*7 (neural crest) and *Sox*2 (neural), it promotes *Six4* (PPR), *Dlx*5 and *Gata3* (border) (Christophorou et al., 2009). These results show that factors induced in early overlapping domains eventually refine through cross repressive interactions. Fate maps also show that cell fates are refined within the border region around the same time (Fernández-Garre et al., 2002; Streit, 2002). Together, these observations suggest that cell fates become refined through the cross-repressive action of transcription factors over time.

However, another model for the specification of placodal and neural crest identity has been proposed recently. The binary competence model suggests that the early ectoderm is separated into two regions the neural ectoderm and the non-neural ectoderm and cells in one region cannot acquire the fate of the other region (Schlosser, 2006; Schlosser, 2010). Much of the evidence for this model comes from *Xenopus*. Grafts of neural plate into belly ectoderm show induction of the PPR marker *Six1* only in the host ectoderm, which is non-neural and not in the grafted neural plate (Ahrens and Schlosser, 2005; Glavic et al., 2004). Assessing the competence of non-neural ectoderm to generate PPR this

ectoderm was grafted into the neural plate border; while PPR markers are induced in the graft, neural crest markers are induced in the host neural plate (Pieper et al., 2011).These findings have been interpreted to support the binary competence model. However, they are in contrast to earlier findings in *Xenopus*, where neural crest markers are induced from both the neural and non-neural ectoderm (Dickinson et al., 1995; Mancilla and Mayor, 1996; Moury and Jacobson, 1990), as well as numerous studies in the chick (Litsiou et al., 2005; Selleck and Bronner-Fraser, 1995; Streit and Stern, 1999) and lineage tracing experiments (Selleck and Bronner-Fraser, 1995). In addition, experiments by Pieper and colleagues themselves demonstrate that at early stages both tissues, neural plate and non-neural ectoderm, are competent to give rise to both PPR and neural crest but that this changes over time. This is remarkably similar to the successive refinement of fates proposed by the border model. Thus, the apparent discrepancy can be resolved when developmental timing is considered.

## 1.4 The pre placodal region

In the early ectoderm neural crest and placode progenitors are mixed, however these cells will eventually separate; the neural crest will move towards the neural folds and PPR cells will remain adjacent to the neural plate. Following this separation PPR cells will eventually give rise to all the cranial placodes (Baker and Bronner-Fraser, 2001; Grocott et al., 2012; Schlosser, 2010; Streit, 2007).

The idea that all cranial placodes, thickened regions of ectoderm in the developing vertebrate head, originate from a single band of ectoderm next to the developing CNS has been around for decades. Knouff described a morphologically distinct region and early experimental embryology suggested that a relatively large territory is competent to give rise to any placode (Knouff, 1935; Stone, 1924; Stone, 1928; Stone, 1931). The following section will summarise the properties on this territory, which is here referred to as the pre-placodal region (PPR).

### 1.4.1 A common region of origin for all sensory placodes

In some amphibians and fish a morphological ectodermal thickening, the PPR, can be seen surrounding the neural plate (Miyake et al., 1997; Verwoerd and van Oostrom, 1979). However, these thickenings are absent in chick and frog (Couly and Le Douarin, 1985; Northcutt and Brandle, 1995; Schlosser and Northcutt, 2000). Some of the first evidence for

a common placode territory came from experiments in *Taricha torosa* (Jacobson, 1963a; Jacobson, 1963b; Jacobson, 1963c). Jacobson dissected a strip of ectoderm next to the anterior neural plate, reversed its anterior-posterior orientation before transplanting it back into a host embryo. When performed at early neurula stages, placodes formed in their normal position indicating that cells developed according to their new position and that for example future otic cells had acquired anterior identity, while olfactory cells were re-specified as posterior placode. However, if the same transplantation was performed at late neurula stages, the ectoderm was no longer able to respond to signals from its new environment and developed according to its original fate. Thus, a posterior placode (otic) formed anteriorly, while an anterior placode (olfactory) formed posteriorly (Jacobson, 1963c). These experiments suggested that initially cells along the neural plate edge are competent to form any placode, but as development proceeds this ability is lost. These observations raised the possibility that there is indeed a common territory from which all placodes arise and are the first real demonstration that there is a short window of competence for all cranial placodes.

Following this fate maps in teleost, amphibians and chick have shown that the ectoderm surrounding the neural plate corresponds to a similar region in Jacobson's experiments. Lineage labelling shows that ectodermal cells next to the anterior neural plate give rise to all sensory placodes (Bhattacharyya and Bronner-Fraser, 2008; Couly and Le Douarin, 1985; Dutta et al., 2005; Garcia-Martinez et al., 1993; Groves and Labonne, 2014; Kozlowski et al., 1997; McCabe et al., 2009; Pieper et al., 2011; Streit, 2002; Xu et al., 2008: For review; Keller, 1976;). Although experimental evidence and fates maps showed that the origin and properties of the ectoderm surrounding the neural plate is fated for placode, it was not until recently that this region was found to be molecularly distinct. There are a set of genes that all PPR cells express, separating them from the neural plate, neural crest and NNE cells. These are factors from the *Six* and *Eya* families: they are expressed in the entire PPR surrounding the neural plate and include *Six1* and *-4*, *Eya1* (*Xenopus*) and *Eya2* (chick) (Ahrens and Schlosser, 2005; Brugmann et al., 2004; Esteve and Bovolenta, 1999; Ishihara et al., 2008a; Kobayashi et al., 2001; Litsiou et al., 2005; Pandur and Moody, 2000). It has also been shown that these factors persist in all placode derivatives with the exception of the lens (Bessarab et al., 2004; Esteve and Bovolenta, 1999; Ghanbari et al., 2001; Ishihara et al., 2008a; Ishihara et al., 2008b; Oliver et al., 1995a; Schlosser and Ahrens, 2004; Xu et al., 1997). Their function will be described below.

The importance of a "PPR cell state" for the development of cranial placodes has been shown through a number of experiments. Misexpression of various transcription

factors including *Sall4*, *Sox3*, *Six3* and *Pax6* in chick, mouse, medaka and Xenopus generates ectopic placodes (Barembaum and Bronner-Fraser, 2007; Chow et al., 1999; Kobayashi et al., 1998; Köster et al., 2000) However, these ectopic structures appear to arise only very close to the neural tube, presumably from PPR cells suggesting that the PPR may have special properties. An elegant experiment further demonstrated that the acquisition of PPR makers is critical for cells to become placodes. When PPR ectoderm fated to become otic or trigeminal placodes is cultured in the presence of FGF2, the otic marker *Pax2* is induced. This is not true for early embryonic ectoderm taken from stages $HH3^{+}$ (Martin and Groves, 2006). However, if this ectoderm is first grafted into the PPR of a host embryo, it will upregulate PPR markers and then, when exposed to FGFs, go on to express *Pax2* an otic marker (Martin and Groves, 2006). Together, these results suggest that placode cells must pass through a PPR cell state before they are able to respond to placode inducing signals and that there is a two stage process to placode formation.

The evidence above shows that placode cells are derived from a common territory and must have passed through a PPR state to become placodes. In addition, they also appear to share common properties. Experiments in chick have shown that the PPR is intrinsically biased towards a lens placode fate (Bailey et al., 2006). PPR ectoderm surrounding the neural plate was dissected from different anterior and posterior positions and then cultured in the absence of any inductive signals for up to 72 hours. PPR ectoderm from all anterior-posterior levels quickly upregulated *Six1* and *Eya2*, as well as the anterior PPR marker *Pax6*, which is normally never expressed in posterior placode progenitors. Following this PPR tissue from all levels initiated the lens programme by upregulating *L-maf*, *Foxc1* and finally d- and a-crystallin (Bailey et al., 2006). In contrast, non-PPR ectoderm did not upregulate any PPR or lens markers. These results show that PPR cells are intrinsically biased towards a placode fate, while cells in the early embryo are not. Importantly, these findings also demonstrate that irrespective of their later fate all placode progenitors are initially specified as lens tissue and hence share a common developmental potential.

Taken to together these results show that cranial placodes are derived from a distinct region in the embryo, the PPR, distinguished by molecular markers (*Six* and *Eya*), initially share common properties being intrinsically biased towards a single placode fate and can be differentiated into other placodes depending on external signals.

## 1.4.2 The Six and Eya gene families

Members of the *Six* and *Eya* gene families are important factors in the specification of sensory placode progenitors and are necessary for normal cranial placode development in vertebrates. In addition, a number of human syndromes associated with sensory defects, for example Branchio-oto-renal syndrome, arise through mutations in *Six* and *Eya* factors (Abdelhak et al., 1997; Ruf et al., 2004). Working as a transcriptional activator complex, S*ix* and *Eya* factors together with *Dach1/2* promote sensory progenitor fate (Brugmann et al., 2004; Ohto et al., 1999; Silver et al., 2003; Tootle et al., 2003) and are expressed in the PPR and remain upregulated throughout placode development (Baker and Bronner-Fraser, 2001; Esteve and Bovolenta, 1999; Grocott et al., 2012; Ishihara et al., 2008a; Litsiou et al., 2005; Pieper et al., 2011; Schlosser, 2010; Streit, 2002, Christophorou, 2008; Christophorou et al., 2009; Pandur and Moody, 2000; Schlosser et al., 2008).

### 1.4.2.1 The Six gene family

*Sine Oculis* (*So*) was originally discovered in *Drosophila melanogaster* as a key regulator of eye formation: *So* is expressed in the imaginal disc of the eye and is essential for optic lobe development, mutations in *So* result in an absence of eyes (Cheyette et al., 1994). *So* forms a complex with *Eyes Absent* and *Dachshund* and together they determine eye and retinal development. While, early experiments of ectopic expression using the UAS/Gal4 system of *So* alone does not induce ectopic eyes, when co-expressed with *Eyes Absent* (*Eya*) ectopic eyes were induced (Pignoni et al., 1997). This suggests that *So* and *Eya* synergise in eye development in the fly. Indeed, the N-terminal domain of *Eya* interacts with the Six domain of *So*, reporter constructs containing the n-terminal domain of Eya was shown to fuse to the Six domain in yeast and *in vitro* screens (Bonini et al., 1993; Bonini et al., 1997; Chen et al., 1997; Cheyette et al., 1994; Pignoni et al., 1997). However, recent experiments using the UAS/GAL4 system showed that *So* alone could induce ectopic eyes in domains separate from *Eya* but only in specific tissues, the antenna and head cuticle (Weasner et al., 2007). Because of *So's* crucial role in eye development, vertebrate homologs were quickly identified, with conserved family members found in mouse, *Xenopus*, zebrafish, chick and human (Boucher et al., 1996; Bovolenta et al., 1998; Esteve and Bovolenta, 1999; Kawakami et al., 1996a; Oliver et al., 1995b; Seo et al., 1998a; Seo et al., 1998b; Zuber et al., 1999). There are six genes in the *Six* family, grouped by structural sequence similarities in their Six and homeobox domain. *Six1/4*, *Six2/6* and *Six4/5* (Seo et al., 1999) have a six domain and a six-type homeodomain, which mediates co-factor interaction and DNA binding (Kawakami et al., 2000). The sequence structure of *Six4* and *5* suggested that each contained its own

transactivation domain. Only *Six4* has been experimentally verified to have a transactivation domain, a portion of the C-terminal domain was found to activate reporter construct *in vitro* (Kawakami et al., 1996b; Kawakami et al., 2000). The *Six* gene family is thought to have developed through gene duplication; an initial Six cluster was created in bilaterians, which was then duplicated when urochordate and vertebrates split during evolution (Gallardo et al., 1999; Kawakami et al., 2000). *Six2* and *-3* loci are located close together on mouse chromosome 17 and human chromosome 2 (Toy et al., 1998), while *Six1*, *Six4* and *Six6* are all localised close to each other on chromosome 14 (Human) and *Six5* is locaed on chromosome 19 (Human) (Gallardo et al., 1999).

In *Drosophila, So* lies downstream of the *Pax6* homolog *Eyeless* (*Ey*): *Ey* mutants have no compound eye and show a loss of both *So* and *Eya* (Halder et al., 1998). However, *Ey* function depends on the presence of both So and Eya: ectopic expression of *Ey* in *So* or *Eya* mutants will not induce ectopic eyes. Together these experiments suggest that *So* and *Eya* act downstream of *Ey* and activate targets necessary for eye determination (Halder et al., 1998). So changes its function depending on the presence of different co-factors. Yeast two hybrid screens show So in a complex with the repressor *Groucho* (Giot et al., 2003) and in the imaginal disc together they repress the antennal gene *Cut,* which in turn promotes the eye forming region and allows the retinal determination program to take place (Anderson et al., 2012). Further support for this comes from experiments here misexpression of engrailed repressor constructs containing So into regions that normally form the antenna caused a down regulation of *Cut* and a loss of antennal fate (Anderson et al., 2012). Thus, in fly *So* is a critical component of the eye determination network; it acts downstream of Eyeless (Ey) and depending on the availability of co-factors can act as a transcriptional repressor or activator.

Other family members in *Drosophila* also contribute to eye formation. The *Six3* ortholog *Optix* can induce ectopic eyes: when an active form of *Optix* is targeted to the antenna forming region formation of ectopic eyes occurs (Seimiya and Gehring, 2000). However, *Optix* functions independent of *Eyes absent* suggesting that there are different eye determination pathways and functions for these related genes (Seimiya and Gehring, 2000). Misexpression of a repressive form of Optix in the antenna forming region of the fly show that similar to *So* it also represses the antennal gene *Cut* (Anderson et al., 2012). Finally, the *Six5* homolog *D-six4* does not play a role in sense organ formation, but is involved in gonad and muscle development (Kirby et al., 2001).

In vertebrate development, *Six* genes are expressed in various locations in the developing embryo and play a role in different tissues and organs. *Six1* and *Six4* are expressed in the cranial placodes, sensory progenitors, branchial arches, dorsal root ganglia, somites, limb and mesenchyme (Esteve and Bovolenta, 1999; Sato et al., 2012). *Six2* is expressed in sensory progenitors, head mesoderm, branchial arches, fore and midgut and limb mesenchyme (Toy et al., 1998). *Six3* and Six6 have a large amount of overlap in their domains of expression including the forebrain, optic chiasm, olfactory placode and lens placode while very little is known about *Six5* expression in vertebrates (Bovolenta et al., 1998; Esteve and Bovolenta, 1999; Kawakami et al., 1996a; Kawakami et al., 2000; Oliver et al., 1995b; Sato et al., 2010; Seimiya and Gehring, 2000; Seo et al., 1998a; Toy et al., 1998). Careful analysis of Six gene mutant phenotypes has elucidated some of the functions of members of this family.

In humans, mutations in *Six1* cause Branchio-Oto-Renal syndrome (BOR), characterised by hearing, kidney and branchial defects (Ruf et al., 2004). The causative mutations in *Six1* occur in the homeodomain crucial for the *Eya-Dach-Six* transcriptional activator complex preventing DNA binding of *Six1* (Ruf et al., 2004; Winchester et al., 1999). Mouse mutants for *Six1* show various development deficiencies including craniofacial, ear and nose defects and an absence of kidneys, suggesting a similarity to the human BOR syndrome (Xu et al., 2003; Zheng et al., 2003). With respect to sensory systems, homozygous mouse mutants have defects in the inner ear with a failure to progress beyond the otic vesicle stage, the vestibuloacoustic (gVIII) and petrosal (gIX) were also absent (Zheng et al., 2003). Therefore, *Six1* mutant mice have defects in the derivatives of the cranial placode at a late stage, but there does not seem to be a failure in the formation of sensory progenitor cells, given the co-expression of other Six family members there may be compensation. Unlike *Six1*, loss of *Six4* function does not result in an obvious phenotype. However, double knockouts for *Six1* and *Six4* show severe placodal defects, for example there is complete loss the olfactory placode and the neurons that are derived from it (Chen et al., 2009; Ikeda et al., 2007) indicating the proposed redundancy has been removed. Surprisingly, placode progenitors appear to be normal and there are no PPR defects. It is possible that another Six gene, *Six2*, which is expressed at PPR stages (Toy et al., 1998) may at least partially compensate for loss of *Six1* and *-4*.

While mouse mutants so far have not implicated Six family members in PPR specification, experiments in chick and *Xenopus* do shed some light on their role at this early stage. Gain- and loss-of-function experiments in *Xenopus* show that *Six1* is important in the

formation of the PPR and involved in the cross repression of factors important for the neural crest and epidermal region, while promoting PPR specific genes (Brugmann et al., 2004). Likewise in chick, activation of *Six1* target genes is also required for PPR formation: misexpression of *Six1* and *Eya2* induces ectopic *Six4* in non-placodal cells, while repressing *Sox2/3* and *Pax7*, neural an neural crest markers respectively (Christophorou et al., 2009) In contrast, constitutive repressor forms of *Six1* lead to a loss of *Six4* and *Eya2* (Christophorou et al., 2009). Together these data implicate the Six/*Eya* network in the specification of placode progenitors at PPR stages in both chick and frog.

Interestingly, while in invertebrates, *So* is downstream of the *Pax6* homologs *Eyeless* and *Toy* during eye formation, in vertebrates this relationship in PPR development seems to be reversed. In chick, expression of *Six1*-EnR leads to the loss of *Pax6* in lens progenitors, *Pax2* in the future otic placode and *Pax3* in the trigeminal region (Christophorou et al., 2009). However, in zebrafish morphants for *Six1* there were less sensory progenitor defects with only a loss of hair cells in the inner ear. This suggests that *Six1* has a role in sensory organ development across species but its importance in sensory progenitor development may differ across species. Further evidence for a cross species role in PPR specification comes from a conserved Six1 enhancer that was found in mouse, *Xenopus*, chick and Zebrafish; this enhancer was identified as Six1-14 and shown to be active in the aPPR in *Xenopus*, mouse and chick (Sato et al., 2010). The Six gene family plays a crucial role in the development of many structures within the developing embryo. In combination with co-factors Six genes promote the formation of placode progenitors and the formation of the derivatives that are crucial for sensory structures within the vertebrate head. Therefore, they are a crucial marker for sensory progenitor fate.

#### 1.4.2.2 The *Eya* gene family

*Eyes absent* (Eya) was first identified in *Drosophila*, where mutants lacked compound eyes due to a failure of differentiation in the eye imaginal disc (Bonini et al., 1993; Bonini et al., 1997; Chen et al., 1997). Expression of *Eya* in the antenna forming region of the fly leads to formation of ectopic eyes (Bonini et al., 1997). *Eya* mutant flies lose eye disc progenitors and this can be rescued by expressing *Eya* cDNA (Bonini et al., 1993). Co-expression of *Eya* with So also showed an induction of ectopic eyes with increased frequency (Pignoni et al., 1997). Therefore, *Eya* was identified as important in eye formation.

Molecularly, *Eya* is a protein tyrosine phosphatase and a transcriptional co-activator, but as it lacks a DNA binding domain it cannot bind directly to DNA (Jemc and Rebay, 2007; Silver et al., 2003; Tootle et al., 2003). The *Eya* proteins are homologous through the conserved *Eya* domain in the C-terminal region and a 271 amino acid domain is responsible for the binding of the *Dach* and *Six* proteins (Ikeda et al., 2002; Jemc and Rebay, 2007; Li et al., 2003; Ohto et al., 1999; Tadjuidje and Hegde, 2013) The enzymatic activity of *Eya* may not play a role in synergising with *Six* as the protein crystal structure shows the catalytic domain and *Six* binding domain on opposite sides of the protein (Jung et al., 2010). *Eya* is thought to have differing roles depending on its location in the cell; within the cytoplasm it is involved in cell immunity, polarity and cell motility and when bound to a co-factor such as *Six1,* it can translocate to the nucleus and act as a regulator of transcription, DNA damage repair and cell proliferation (Tadjuidje and Hegde, 2013)

There are 4 members of the *Eya* gene family in vertebrates. All family members, except *Eya3,* are expressed in the PPR and sensory placodes in addition to the somites, heart and kidney (Bessarab et al., 2004; Esteve and Bovolenta, 1999; Ishihara et al., 2008b; Modrell and Baker, 2012; Sato et al., 2010). There are some species-specific differences, with *Eya1* being present in the PPR in frog and fish, while *Eya2* is PPR-specific in chick (Ishihara et al., 2008b; Sahly et al., 1999; Schlosser and Ahrens, 2004; Xu et al., 1997).

In different species, mutations in *Eya* genes produce various phenotypes consistent with a role of these proteins in sensory organ formation. Humans with BOR were found to have mutations within the *Eya1* gene that consisted of either exon insertions or deletions resulting in a defective protein (Abdelhak et al., 1997). Loss of *Eya1* function in mice shows some similarity to the phenotype of BOR syndrome in humans; these mice lack ears and kidneys and have an abnormally high amount of apoptosis in their organ primordia (Xu et al., 1999). *Eya1* also regulates epithelium growth and functionally synergises with *Pax2* in inner ear development (Zou et al., 2006), and may be in regionalisation of the otic placode (Zou et al., 2006). Compound *Six1* and *Eya1* mouse mutants show a loss of limb muscle, severe pituitary defects and kidney hypoplasia (Li et al., 2003). In zebrafish, *Eya1* mutants have smaller and malformed otic vesicles (Kozlowski et al., 2005) and differentiation defects in cell lineages derived from the adenohypophysis (Nica et al., 2006). Gain- and loss-of-function experiments in *Xenopus* show that *Eya1* in combination with *Six1* promotes neuronal differentiation in neurogenic placodes through *Soxb1* in a dose dependent manner (Schlosser et al., 2008). High levels of *Eya1* and *Six1* prevent cells from differentiation into neurons and maintain them in a proliferative state, whereas low levels promote neuronal differentiation (Schlosser et al., 2008). In chick misexpression of *Eya2* combined with *Six1*

induces PPR and border markers *Six4, Dlx*5 and *Gata3* (Christophorou et al., 2009). However, this does not lead to the induction of mature placodes, marked by *Pax* genes, suggesting that although they can confer a sensory progenitor identity, additional factors are needed for placode development (Christophorou et al., 2009).

Mutations in the human *Eya4* gene cause sensorineural hearing loss (Schonberger et al., 2005) and have also been implicated in late onset deafness (Wayne et al., 2001). In zebrafish *Eya4* morphants display a decrease of sensory hair cells in the otic vesicle and it has been suggested that the regulation of Na+/K+-ATPase by Eya4 is crucial for development of these sensory hair cells.

In summary, Eya factors are involved in fly eye formation and in sense organ development and cell specification in vertebrates. In humans, mutations in Eya factors are associated with complex syndromes that include sensory defects. Together these findings make Eya proteins together with Six family members important factors in the development of the cranial sensory placodes.

### 1.4.3 The regulation of *Six1/4* and *Eya1/2* in the PPR by tissues and signals

The tissues that induce the PPR have been characterised in classical experimental embryology experiments. With the availability of molecular markers for the PPR, including *Six1/4* and *Eya1/2* many of these have been repeated in different species and the molecular mechanisms and signals that control their PPR specific expression have been explored.

In the 1960's, Jacobsen described the role of the surrounding tissues in placode development (Jacobson, 1963a; Jacobson, 1963b; Jacobson, 1963c; Jacobson, 1966 review). The first set of experiments all conducted in *Taricha torosa,* explanted the prospective placode epidermis either alone, with surrounding tissues such as the neural plate, endoderm, mesoderm or combinations of all 3 (Jacobson, 1963a; Jacobson, 1963b). A second set of experiments rotated the anterior and posterior axis of the placode epidermis or the adjacent tissues to investigate the effects of placode positon (Jacobson, 1963c). Explanting the placode territory alone showed no formation of the olfactory, lens or otic placodes. This strongly suggested that the surrounding tissues were necessary to provide signals for placode induction (Jacobson, 1963a). When the placode territory was explanted with only the anterior endoderm there was no formation of placode structures. However, when explanted with the heart mesoderm and neural plate there was an induction of all three placode territories. When either the neural plate or mesoderm were explanted alone

or together with the placode territory (minus the endoderm) there was induction in a small number of explants of lens or otic placodes but never all three placodes (Jacobson, 1963a). Although the neural plate and mesoderm can induce the lens and otic placodes, there is no induction of the olfactory placode, suggesting that the endoderm plays a positive role but is not solely responsible for its induction. Indeed, ablation of the endoderm did not lead to a complete loss of placodes but did affect the formation of the olfactory placode (Jacobson, 1963b). Recent experiments in chick show that the prechordal mesendoderm is necessary for the expression of the PPR marker *Eya2* and the anterior PPR markers *Pax6* and *pNoc* and somatostatin signalling at least in part mediates this function (Lleras-Forero et al., 2013). The effect of prechordal mesendoderm ablation is rescued by somatostatin. In both chick and fish, somatostatin loss of function prevents PPR formation: somatostatin antagonists or somatostatin receptor knockdown leads to the loss of *Pax6* in chick, and of *Pax6* and *Pitx3* in fish (Lleras-Forero et al., 2013). Therefore, similar to the previous experiments by Jacobson the anterior mesendoderm affects anterior placode development.

Jacobson investigated the role of the heart mesoderm that is adjacent to the placode territory in explant experiments (Jacobson, 1963a). Explants of the placode territory and the heart mesoderm alone did not generate any placodes; occasionally explants of the heart mesoderm together with the ventral endoderm led to the induction of olfactory and otic placodes in the ectoderm(Jacobson, 1963a). Further combinations of explants showed that otic placodes generally only formed in the presence of the heart mesoderm, suggesting that it is important for the formation of posterior placodes (Jacobson, 1963a). Indeed, signals from the mesoderm play a role in PPR induction. In chick, ablation of the lHM leads to the loss of PPR markers, while lHM grafts induce *Six1/4* and *Eya2* ectopically after a relatively short amount of time (*Six4*; 8hrs, *Eya2*; 12hrs; Christophorou, 2008; Litsiou et al., 2005), the lHM comparatively to the heart mesoderm in Jacobson's experiments cannot induced placode domains. In *Xenopus*, the endomesoderm is also required for *Six1* expression in the PPR, but does not ectopically induce them (Ahrens and Schlosser, 2005). Together, these experiments implicate signals from both the neural plate and mesoderm in the formation of placode progenitors, however, the relative contribution of each tissue may differ in different species.

As Jacobson's experiments reveal the addition of the neural plate to presumptive placode explants cultured with mesoderm or endoderm is important for the induction of the placode territories (Jacobson, 1963a). However, the neural plate can also induce otic placodes when explanted alone with the prospective placode ectoderm suggesting that it may play a significant role in its induction (Jacobson, 1963a). This idea is supported by the

following experiments: rotation of the neural plate along the anterior-posterior axis leads to a loss of the lens and otic placode (Jacobson, 1963c). More recently, similar experiments have been performed using the PPR markers *Six1/4* and *Eya1/2* as readouts and the neural plate has been implicated in PPR induction. In chick, the neural plate rarely induces *Six1* in competent non-placodal ectoderm, and 16hrs of contact are required. In contrast, the graft itself starts to express *Six1* much more frequently (Litsiou et al., 2005). In *Xenopus*, removal of the neural plate leads to loss of *Six1* in a small number of embryos, while neural plate grafts induce ectopic *Six1* in a ring around the graft in the host ectoderm and not in the donor ectoderm (Ahrens and Schlosser, 2005). However, *Eya1* is only induced in 50% of these grafts indicating that the induced territory is not a complete PPR (Ahrens and Schlosser, 2005). Thus, there are slight differences in chick and frog, which may reflect the timing of when experiments were performed (neurula stages in *Xenopus* vs. gastrula stages in chick) or different properties of the responding tissue (belly ectoderm in *Xenopus* vs. extraembryonic epiblast in chick). While these experiments implicate signals from the neural plate in PPR induction, they also suggest that other tissues may be involved.

In addition to these classical and more recent experiments on the tissues involved in the induction of the placode territories, a number of experiments have asked which signals are responsible for PPR induction and from which tissues they emanate. Signals implicated include FGFs, WNT antagonists and BMP antagonists, while recently other signals such as neuropeptides have also been connected to PPR and placode formation.

FGF as discussed above (Section 1.3.2) is important for the induction of the neural plate and neural plate border, but it also involved in the induction of the PPR. Both the mesoderm underlying the PPR express *FGF4* and *FGF8* in the chick, while the neural plate in *Xenopus* expresses *FGF8* (Ahrens and Schlosser, 2005; Litsiou et al., 2005). In addition, in chick the prechordal mesendoderm may also be a source of FGFs (Sanchez-Arrones et al., 2012). In chick, grafts of the lHM induce PPR markers in non-placodal cells. However, when the graft is surrounded by SU5402 beads *Six4* induction is reduced (Litsiou et al., 2005). Furthermore, grafts of FGF8 beads leads to the induction of *Eya2* but not *Six1*, suggesting that FGF can induce some border markers but not a full PPR (Litsiou et al., 2005). Similarly, reduction of FGF signalling from the neural plate in *Xenopus* leads to loss of *Six1* (Ahrens and Schlosser, 2005), while ectopic FGF in the presence of a BMP inhibitor induces it. (Ahrens and Schlosser, 2005). Experiments using a constitutively active FGF receptor in *Xenopus* showed expansion of *Foxd3*, a neural crest marker, at the expense of *Six1* (Brugmann et al., 2004). Recent experiments have shown FGF to induce an ectopic neural crest domain, however the presence of a neural prompting media, N2, suggests that other

factors are involved in this induction (Yardley and García-Castro, 2012). Therefore, FGF may have both repressive and activating roles at different time points in PPR development. FGF may in fact induce an early domain that is similar to the border and subsequently depending on other surrounding factors different fates will be induced.

As discussed above (section 1.3.2) BMP signalling is important for the induction of different regions in the early embryo. At early stages BMP is required for the expression of a competence domain for PPR induction. The application of a small molecule BMP inhibitor (Dorsomorphin) at early blastula stages in zebrafish abolishes *Tfap2a/c*, *Foxi1* and *Gata3* (Kwon et al., 2010). Gain- and loss-of-function experiments show that these factors cross-activate and -repress each other to set up the domain in which *Six1* will be expressed. Likewise, in chick and frog *BMP4* and *-7* are expressed at high levels in the lateral ectoderm and neural plate border (Fainsod et al., 1994; Streit and Stern, 1999) and BMP signalling is necessary for the induction of certain border markers (*Msx*1/*Dlx* see above; section 1.3.2) (Luo et al., 2001; McLarren et al., 2003; Wilson et al., 2001). However, at later stage the attenuation of BMP is needed for the induction of the PPR (Ahrens and Schlosser, 2005; Kwon et al., 2010; Litsiou et al., 2005). In chick, electroporation of the BMP inhibitor *Smad6* into the lateral ectoderm expands the PPR markers *Six4* and *Eya2* (Litsiou et al., 2005). However, the misexpression of *Smad6* into the extraembryonic region never induces PPR markers suggesting that BMP inhibition is necessary but not sufficient for PPR induction. This is similar to the result from *Xenopus* where ectopic beads of Noggin could not induce *Six1,* but BMP inhibition in combination with FGF could (Ahrens and Schlosser, 2005).

As described above (Section 1.3.2) WNT plays a role in early ectodermal patterning and its negative regulation is important for PPR marker expression. In chick, misexpression of WNT antagonists such as *Crescent* and N-*Frizzled8* expand the PPR , while activation of WNT causes the loss of the PPR markers *Six1*/4 and *Eya2* (Litsiou et al., 2005). However, WNT antagonists electroporated into the extraembryonic region alone cannot induce ectopic PPR markers (Litsiou et al., 2005). In *Xenopus* a combination of dominant negative WNT and Noggin leads to the induction of *Six1* throughout the ectoderm (Brugmann et al., 2004). Together these results suggest that WNT attenuation is necessary for positioning of the PPR but that it is not sufficient to induce it.

The above results suggest that a combination of signalling is necessary for PPR induction. In chick, the lateral head mesoderm is a source of FGFs and the WNT and BMP antagonists Dan and Cerberus, respectively and the lHM can induce an ectopic PPR

(Chapman et al., 2002; Litsiou et al., 2005; Lunn et al., 2007; Ogita et al., 2001; Rodríguez Esteban et al., 1999). All three signals from the lHM are required to induce the PPR, but they seem to act at different times. FGF beads alongside co-electroporation of *Smad6* (BMP inhibitor) and Crescent (WNT inhibitor) induce *Six4* expression (Litsiou et al., 2005). Interestingly, FGF is only required for the first 5 hours of this induction: replacement of FGF beads with beads soaked in SU5402 (FGF inhibitor) still lead to induction of *Six4* (Litsiou et al., 2005). This fits with the idea that FGF may induce an early border state, which subsequently adopts different fates depending on other factors present.

Recently other signals have been identified that mediate some aspect of PPR and placode development. Loss-of-function experiments have shown that Somatostatin from the pME is at least in part responsible for the induction of anterior PPR markers *Pax6, pNoc* and *SSTR5*, as well as for the general PPR marker *Eya2* (Lleras-Forero et al., 2013). In addition, the neural plate border is a source of retinoic acid which is involved in positioning the PPR and *Six1* expression (Jaurena et al., 2015). In *Xenopus*, *RALDH2* and *Lipocalin-type prostaglandin D2 synthase* (*LPGDS*), which synthesise and transport retinoic acid (RA), respectively, are expressed in anterior neural plate under the control of *Zic1*. LPDGS loss leads the loss of *Six1* expression in the PPR (Jaurena et al., 2015) suggesting that RA signalling cooperates with other signalling pathways to promote placode progenitor formation. These recent findings show that while the 'big three' (FGF, WNT and BMP) play a vital role in PPR induction, other signals are also important and their roles uncovered. This is summarised in Figure 1.3

### 1.4.4 Transcriptional regulation upstream of *Six1/4* and *Eya1/2* in the PPR

Transcription factors upstream of *Six* and *Eya* have only recently been characterised in detail. There are numerous factors that promote the expression of *Six1/4* and *Eya1/2* and hence placode progenitor identity. The *Dlx* family is involved in their regulation: misexpression of *Dlx5* in chick or *Dlx3* in *Xenopus* represses neural fate, but promotes *Six1/4* and *Eya1/2* and thus expands the PPR (Esterberg and Fritz, 2009; McLarren et al., 2003; Pieper et al., 2012; Woda et al., 2003). *Dlx3* loss-of-function in *Xenopus* leads to a reduction in *Eya1* and *Six1* (Pieper et al., 2012) and *Dlx* genes in zebrafish play a similar role. In *Dlx3b/4b* mutants, PPR markers are reduced and misexpression leads to their expansion (Kaji and Artinger, 2004). The *Dlx* genes work by creating a favourable environment for PPR induction by modulating the levels of BMP: loss of *Dlx* leads to a transient increase in BMP and thus preventing PPR formation, while low levels in the presence of *Dlx* genes allow FGF

to induce PPR markers (Esterberg and Fritz, 2009). Supporting a crucial role of *Dlx* protein function, in chick *Dlx*5 directly controls *Six1* expression and positively regulates its anterior PPR enhancer (*Six1*-14) (Sato et al., 2010). Misexpression of *Dlx*5 alongside electroporation of a reporter construct containing the aPPR enhancer showed an increased domain in which the enhancer was active (Sato et al., 2010). In contrast, siRNA knock down of *Dlx5* leads to a reduction of the region in which Six1-14 is active (Sato et al., 2010). Finally, *Dlx5* directly binds the enhancer and thus is directly involved in the positive regulation of *Six1*. However, *Dlx* factors may have dual role in PPR and neural crest formation. While most evidence points towards a positive regulation of PPR markers, there is evidence from frog that *Dlx3* can promote neural crest formation. Loss of function leads to a reduction in the crest marker *Foxd3* and a broader domain of expression for the PPR markers (Pieper et al., 2012). Overall, *Dlx* genes are clearly important for the induction of Six and *Eya*, while also defining the boundaries that separate the neural crest and PPR.

*Zic1* also seems to act upstream of *Six1* with a high levels promoting *Six1* expression and its misexpression induces PPR transcripts (Hong and Saint-Jeannet, 2007). However, in conjunction with *Pax3*, *Zic1* enhances neural crest cell formation (Hong and Saint-Jeannet, 2007). Therefore, *Zic1* alone controls PPR targets but its function changes depending on the presence of other genes. As discussed earlier (Section 1.3.2), in zebrafish *Tfap2a/c*, *Foxi1* and *Gata3,* under the control of BMP, create a competence domain for *Six1* expression (Bhat et al., 2013; Kwon et al., 2010). These two results clearly indicate that the combination of genes plays a role in the outcome of cell fate.

*Irx1* has also been implicated upstream of *Six1*; it is expressed prior to the onset of *Six1*/4 and *Eya1*/2 in the chick and the frog (Glavic et al., 2004; Khudyakov and Bronner-Fraser, 2009). Knock down of *Irx1* leads to a loss of *Six1* in *Xenopus*, while its overactivation leads to an expansion of *Six1* and the placodal markers *Sox2* and *Pax2* (Glavic et al., 2004). Although it is unknown how *Irx* interacts with *Six1*, it is a homeobox transcription factor and the *Six1* aPPR enhancer has a number of homeobox binding sites (Bellefroid et al., 1998; Glavic et al., 2004) through which this interaction may occur.

*Sox* genes also seem to interact with *Six* and *Eya* genes. In medaka ectopic *Sox3* expression induces ectopic placodes that express *Eya1* and *Pax6*, but not *Six3* (Köster et al., 2000). However, other Six transcripts have not been investigated and it is unclear whether *Sox3* plays are role in PPR specification.

In contrast, other transcription factors play a negative role in regulating *Six1/4* and *Eya1/2* such as the neural crest markers *Msx1*, *Pax3* and *Pax7*. In *Xenopus* misexpression

of *Pax3* represses *Six1* and PPR fate (Hong and Saint-Jeannet, 2007). *Msx* and *Dlx* factor levels are thought to cross regulate PPR and neural crest induction. The depletion of *Msx* genes in zebrafish leads a loss of neural crest cells, while placodes are normal, and *Dlx3* expression is shifted dorsally (Phillips et al., 2006). In *Dlx3b/4b* mutants there is a loss of PPR markers, and this phenotype can be rescued by attenuating *Msx* signalling (Phillips et al., 2006). These results suggest that *Dlx* and *Msx* genes mutually oppose each other to create the domains that define the neural crest and PPR. In support of this experiments in chick show that *Msx1* has a direct role in *Six1* regulation. The anterior PPR enhancer Six1-14 contains homeobox and paired box binding sites (Sato et al., 2010). *Msx*1 binds directly to the aPPR enhancer and overexpression of *Msx*1 together with the aPPR reporter construct showed a reduced enhancer activity (Sato et al., 2010). Likewise, *Pax*7 misexpression negatively regulates the aPPR enhancer, however it was not shown to directly bind to the enhancer, so this interaction may be indirect. These results show that factors which promote the neural crest negatively regulate PPR genes

Overall genes such as *Irx1* and *Zic1* positively regulate *Six1*, while competence factors *Tfap2a/c*, *Foxi1* and *Gata* genes provide a domain of competence for PPR induction. Conversely, *Six1*/4 and *Eya1*/2 are negatively regulated by factors that promote neural crest formation e.g. *Msx*1 and *Pax3*/7. Although a number of factors have been implicated in the regulation of Six and *Eya*, the hierarchy of transcriptional regulation and the temporal structure behind this input remains poorly understood.

### 1.4.5 The anterior and posterior subdivision of the PPR into placode domains

The anterior and posterior patterning of the PPR initially comprises many factors discussed above in the formation of the neural plate border (Section 1.3). These include the mutual repression between *Otx*2 and *Gbx*2, which define anterior and posterior identity, respectively (Katahira et al., 2000; Millet et al., 1999; Steventon et al., 2012). Knockdown and misexpression of *Otx*2 and *Gbx*2 in *Xenopus* also shows that they are required for the activation of anterior and posterior placode genes, respectively (Steventon et al., 2012). While other transcription factors such as *Six3* and *Irx3* then subdivide the PPR into smaller molecular domains their role in placode progenitors has not been assessed (Kobayashi et al., 2002). As the PPR is regionalised the expression of markers for placode subgroups is initiated with lens/olfactory progenitor (LOP) marker *Pax6*, second the otic/epibranchial progenitor (OEP) marker *Pax2* (*Pax*8 in *Xenopus*) and finally the trigeminal progenitor (TP) marker *Pax3*. The placodal domains are further refined due to the mutually repressive

properties of the *Pax* genes. In chick misexpression experiments show that *Pax3* and *Pax6* repress each other (Wakamatsu, 2011), that *Pax6* and *Pax3* represses *Pax2* (Wakamatsu, 2011) (Dude et al., 2009). These results suggest that a repressive interaction between the *Pax* genes sets up the placodal territories and may segregate cell fates.

## 1.5 Cranial placodes

Once the PPR is subdivided into anterior, middle and posterior territories, placodes with distinct character are established. In this section I will summarise the derivatives and function of each placode and how they are induced from progenitors. However, only placodes related to the PPR will discussed, placodes in the cranial region also give rise to the taste buds, teeth and other non-sensory structures.

### 1.5.1 Adenohypophysis

The adenohypophyseal placode is located in the anterior midline ventral to the diencephalon. After its initial formation at early somite stages (chick, somite stage 3; mouse, somite stage 13-20; frog, somite stage 14 (Baker and Bronner-Fraser, 2001)) it forms an out-pocketing in the midline oral ectoderm, Rathke's pouch. Together with the neurohypophysis, which arises from the ventral hypothalamus, the anterior pituitary forms the future pituitary gland (Baker and Bronner-Fraser, 2001). Fate maps using quail and chick chimeras and lineage tracing in rat, showed that the anterior neural ridge including the adjacent non-neural ectoderm form the adenohypophyseal placode (Couly and Le Douarin, 1985; Kouki et al., 2001). Ablation of the anterior neural plate at somite stage 2-4 in chick caused a loss of the adenohypophysis (elAmraoui and Dubois, 1993). This suggest that the anterior neural plate/ridge forms the adenohypophysis. While explant experiments show ectoderm from the head region was competent to form the adenohypophyseal placode up to the 12 somite stage (Gleiberman et al., 1999).

Various tissues are involved in the induction of the of the adenohypophyseal placode; chick explants of the ventral diencephalon together with head ectoderm from 6-12 somites showed the induction of the adenohypophyseal placode and adrenocorticotropic cells (Gleiberman et al., 1999). This induction was enhanced by the addition of mesenchyme from the 1-4 somite stage, while transplantation of notochord to the presumptive otic ectoderm showed induction of a structure similar to Rathke's pouch (Gleiberman et al., 1999; Kawamura et al., 2002 review).

FGF has been recently implicated in adenohypophysis induction with mouse mutants for FGFr2 showing severe defects in the development of the adenohypophysis (De Moerlooze et al., 2000) . Shh misexpression in zebrafish represses lens fate, while loss of Shh leads to ectopic lens formation in the presumptive adenohypophysis ectoderm (Dutta et al., 2005) suggesting that Shh sets up the adenohypophysis by repressing lens fate. However, as of yet, no signal has been found to be sufficient for induction (Baker and Bronner-Fraser, 2001).

There are a number of transcription factors that label the hypophyseal placode and play an important role for its formation. The transcription factors *Pax6* and *Six3* mark the anterior forebrain as well as anterior placodes (Bovolenta et al., 1998; Oliver et al., 1995b). While *Pax6* mutant mice initially develop a normal placode, they have dorsal-ventral patterning defects in the pituitary gland as well as depleted somatotropes and lactotropes (Kioussi et al., 1999). In zebrafish *Six3* is expressed in the anterior neural plate and the adenohypophysis, misexpression of *Six3* expands the region from which the adenohypophysis is derived (Kobayashi et al., 1998). Mouse mutants for *Hesx1* fail to form Rathke's pouch; this disruption is enhanced when *Six3* is also knocked out (Gaston-Massuet et al., 2008). Another anterior specific gene is involved in the development of the adenohypophysis; mutations in *Otx2* cause defects in the formation of the pituitary gland through lowering FGF signalling (Mortensen et al., 2014). Conditional knockouts of *Otx*2 in the neural ectoderm lead to a smaller adenohypophysis and is in part caused by the loss of FGF10 due to *Otx*2 deletion (Mortensen et al., 2014).

The *Pitx* family of genes is also involved in the formation of the adenohypophyseal placode with both *Pitx1* and *2* being expressed in adenohypophysis in mice (Szeto et al., 1999). The *Pitx1* mutant has normal adenohypophysis development, however the mice exhibit minor defects in hormone cell lineage specification (Szeto et al., 1999) suggesting a later role in adenohypophysis development. Single mutant mice for *Pitx2* show an increased amount of cell death in the adenohypophysis leading to hypoplasia of the structure (Charles et al., 2005). Double *Pitx1* and *-2* mutants display a more severe phenotype, with severe adenohypophysis hypoplasia and failure to express *Lhx3 a key* adenohypophysis gene (Charles et al., 2005). Mouse mutants show that *Lhx3* is important for the growth and development of Rathke's pouch. While its formation is unaffected later the anterior and intermediate lobes of the pituitary are missing. The role of *Pitx* genes is also seen in zebrafish. *Pitx3* is expressed in the adenohypophysis (Dutta et al., 2005). *Pitx*3 mutants exhibit pre-placodal defects with morpholino knockdowns leading to the loss of adenohypophysis placode structures (Dutta et al., 2005). Finally, *Eya1* zebrafish mutants

show a lineage specification defect in the pituitary which can be enhanced when combined with the loss of *Six1* (Nica et al., 2006).

In summary, the adenohypophysis arises from anterior midline ectoderm and is induced by the surrounding ventral diencephalon and mesenchyme and signalling molecules that include FGFs and Shh. Furthermore, the development of the adenohypophysis depends on the transcriptions factors including *Pitx1/2*, *Lhx3, Pax6* and *Six3.*

### 1.5.2 Olfactory placode

The olfactory placode generates the olfactory epithelium that lines the caudal region of the nasal cavity. In addition to olfactory sensory neurons, which are responsible for smell perception, it contains a population of stem cells that continuously renew these neurons throughout life. The olfactory placode also generates several migratory neurons such as GnRH neurons, somatostatin positive, calbindin positive neurons, which leave the placode to enter the forebrain. initially, it is the origin of pheromone receptor neurons that are formed in the vomeronasal organ (unique to tetrapods), severing the connection between the vomeronasal interferes with pheromone but not general odour sensing (Baker and Bronner-Fraser, 2001; Buck, 2000). Thus, the olfactory placode produces a large number of different cell types, and has been subject to many investigations due to its capacity of neuronal regeneration.

The olfactory placode is only morphologically visible in chick at somite stage 19 ($HH13^{+}$ (Bhattacharyya and Bronner-Fraser, 2008) with the earliest molecular markers of olfactory fate, *Dlx*3/5 and *Pax6*, being present just prior to this stage (Bhattacharyya and Bronner-Fraser, 2008). Quail and chick transplantation experiments showed that a broad area encompassing the anterior ectoderm and anterior lateral neural folds contained olfactory precursors (Couly and Le Douarin, 1985). More recent fate map studies in chick and zebrafish showed that olfactory precursors overlap with lens precursors in the anterior ectoderm before becoming restricted to the very anterior tip of the ectoderm and then forming the olfactory pit (Bhattacharyya et al., 2004; Xu et al., 2008).

Thus, olfactory precursors come from a broad area and competence studies have shown that a large region of the early ectoderm is competent to give rise to the olfactory placode but becomes refined over time. Quail to chick grafting studies showed early pre-streak ectoderm is component to form an olfactory placode when grafted in the anterior neural folds at HH8 (Bhattacharyya and Bronner-Fraser, 2008). However, later grafts of

head, mid or trunk ectoderm from stage HH8 shows only head ectoderm is competent to form the olfactory placode (Bhattacharyya and Bronner-Fraser, 2008). A restriction in competence is also seen in experiments in *Taricha Torosa.* Explants and grafting studies show that neuroectoderm is competent up until mid neurula stage to form the placode (Jacobson, 1963a; Jacobson, 1966). This shows that early on a broad set of cells in the ectoderm can give rise to the olfactory placode, but later olfactory competence is restricted to the head ectoderm.

Tissues involved in the induction of the olfactory placode include the underlying endoderm: in *Taricha Torosa* removal of the endoderm disrupted the formation of the olfactory placode more than any other placode (Jacobson, 1963b). Explants of olfactory ectoderm alone do not develop into olfactory placodes, however when combined with the anterior neural plate they do suggesting that the anterior neural plate plays a role in nasal placode induction (Jacobson, 1963a). Ablation experiments conducted in chick support a role for anterior neural tissue in olfactory induction. Forebrain tissue was removed and embryos were allowed to develop further: the forebrain 'repaired' and induced an olfactory placode on the ablated side (Waddington, 1936). Recent results suggest that the anterior mesendoderm is also involved in the development of anterior placodal structures, as ablation leads to the loss of early olfactory placode marker *Pax6* (Lleras-Forero et al., 2013).

Various signals promote formation of the olfactory placode and its derivatives. A recent study showed that neuropeptide signalling, namely somatostatin, is necessary for the induction of lens and olfactory progenitors at PPR stages: somatostatin knockdown in fish and chick led to the loss of *Pax6* (Lleras-Forero et al., 2013). In addition, FGF8 promotes the development of olfactory precursors in the chick (Bailey et al., 2006). *FGF8* is expressed in the anterior neural ridge, next to the future placode and at HH10 is present in the placode itself (Bailey et al., 2006), along with pERK, a readout of active FGF signalling. Grafts of beads coated in FGF8 expand the olfactory territory at the expense of the lens placode and explants of the lens and olfactory precursors upregulate *GnRH,* a marker for the early placode, when exposed to FGF (Bailey et al., 2006). FGF8 mutant mice show increased apoptosis and a failure to form the nasal cavity, leading to olfactory defects (Kawauchi et al., 2005). Although the olfactory pit initially forms as development progresses the placode is either lost or reduced in size (Kawauchi et al., 2005). Later, BMP has a role in the anterior and posterior patterning of the olfactory placode and the differentiation of neurons (LaMantia et al., 2000; Shou et al., 2000). When BMP signalling is inhibited in explants of the mouse olfactory epithelium BMP neuronal markers fail to be expressed, while BMP4

exposure promotes neuronal cell survival (Shou et al., 2000). Experiments using dominant negative BMP constructs showed disruption of the olfactory nerve and that BMP effected Notch signalling which is also crucial in later patterning of the olfactory placode (Maier et al., 2011). Loss-of-function of Notch leads to a disruption of the olfactory placode (Maier et al., 2011)

The neural crest has been implicated as a source of retinoic acid (RA); RA is involved in olfactory placode patterning and its action is opposed by FGF signalling (Bhasin et al., 2003; Sabado et al., 2012) *Raldh3* is expressed in the lateral edge of the olfactory placode, while *FGF8* is present in the medial ectoderm. While RA promotes lateral character, FGF signalling has the opposite effect (LaMantia et al., 2000) . It seems that both signals oppose each other by negative cross talk (Sabado et al., 2012). Placement of beads soaked in RA, negatively regulated *FGF8* and *Sprouty2*, while attenuating FGF signalling lead to the expansion of *Raldh3* (Sabado et al., 2012). However, this only worked in a short period of time, when specification of Gnrh-1 neurons, a specific population of cells derived from the olfactory placode occurs.

As discussed above, the olfactory placode precursors first originate from a broad area and become refined to the anterior tip of the ectoderm. This refinement can also be seen at the molecular level: a number of transcription factors mimics this process and appear to play a role in olfactory cell fate determination. These include *Pax6* and *Dlx5*, which appear to control the sorting of cells into the correct placodal domains (Bhattacharyya et al., 2004). At early stages the lens and olfactory precursor cells occupy a common domain *Pax6* and *Dlx5* are co-expressed in these progenitors (Bhattacharyya et al., 2004). As cell fates segregate *Pax6* and *Dlx5* expression domains separate to label lens and olfactory cells, respectively (Bhattacharyya et al., 2004). Overexpression of *Dlx5* led to the formation of smaller lens and an accumulation of cells in the olfactory region, suggesting that *Dlx5* promotes olfactory fate and that its downregulation is necessary for lens cell fate (Bhattacharyya et al., 2004). Another factor crucial for the early olfactory placode, *Otx2,* controls *Dmrt4/5* in *Xenopus*, which is responsible for olfactory neurogenesis later (Parlier et al., 2013; Steventon et al., 2012). The overexpression of a constitutive repressor form of *Otx*2 leads to the loss of early olfactory placode makers including *Dmrt4* (Steventon et al., 2012). Knockdown of *Dmrt4* or *5*, while leaving the placode intact, leads to the loss of neurogenesis (Huang et al., 2005; Parlier et al., 2013) suggesting that *Otx*2 is important for early specification of the placode but also promotes later neurogenesis through positive regulation of *Dmrt4/5*. A number of mouse mutants reveal the importance of different

transcription factors during olfactory development. Absence of *Foxg1* causes a complete loss of olfactory structures, the epithelium, bulb, and vomeronasal organs. This was due to a failure in proliferation of an initial precursor population which formed normally (Duggan et al., 2008), while *Emx2* null mice have disorganised placodes at later stages (Simeone et al., 1992)

Overall olfactory precursors arise from a broad region in the early head ectoderm becoming refined to the very anterior tip of the ectoderm. This induction and refinement may be controlled by the underlying mesendoderm and the adjacent anterior neural plate. A number of signals have been implicated at various steps including neuropeptides, FGF, BMP and RA signalling. At the same time, certain transcription factors including *Pax6*, *Dlx*3/*5*, *Otx*2 and *Foxg1* play a role at different steps of cell fate specification. However the temporal hierarchy of these tissues, signals and transcription factors that determines this placode remains to be investigated.

### 1.5.3 Trigeminal placode

The trigeminal placode arises from intermediate PPR ectoderm, lying between the anterior lens and the epibranchial placodes. The trigeminal placode comprises the ophthalmic (Opv) and maxillomandibular (Mmv) placodes in amniotes; in anamniotes the ophthalmic is referred to as the profundal and the maxillomandibular (Baker and Bronner-Fraser, 2001).In most organisms the Opv and the Mmv fuse to create a single structure (Baker and Bronner-Fraser, 2001), however in frogs they are mostly separate only fusing at their proximal ends (Schlosser and Northcutt, 2000). These placodes give rise to sensory neurons of the trigeminal ganglion forming the trigeminal nerve (cranial nerve V); the ganglion also receives contribution from neural crest cells (D'Amico-Martel and Noden, 1983). Its ophthalmic branch innervates the muscles of the forehead, upper eyelid and front of nose, while the maxillary branch innervates the muscles of the cheeks, lower eyelid, upper jaw and sides of the nose; the mandibular branch innervates the lower jaw (Baker and Bronner-Fraser, 2001; Gray and Leonard, 1983; Schlosser, 2006; Schlosser, 2010).

Quail to chick transplantations have shown that at the 3 somite stage the head ectoderm rostral to the first somite is competent to form the trigeminal placode when grafted to the Opv region (Baker et al., 1999). By the 8 somite stage prospective trigeminal ectoderm is committed and this coincides with the onset of *Pax3* expression (Baker et al., 1999).

Experiments by Stark, where the neural tube was separated physically from the placode region, showed that the neural tube is necessary for the expression of *Pax3* (Stark et al., 1997). However, when a physical barrier with perforations was used, *Pax3* induction was normal suggesting that a diffusible signal from the neural tube promotes trigeminal fate (Stark et al., 1997). Recent experiments have tried to understand which signalling molecules might determine trigeminal fate. Inhibition of WNT signalling from the neural tube prevents *Pax3* expression (Lassiter et al., 2007), however WNT alone is not sufficient to induce it ectopically (Lassiter et al., 2007). Although these results implicate WNT as a candidate for trigeminal induction, WNT is not necessary for the maintenance of *Pax3* expression: WNT electroporation of dominant negative WNT1 showed no loss of *Pax3* (Canning et al., 2008b). In fact, FGF signalling is thought to cooperate with WNT to induce *Pax3*: activation of FGF receptors is crucial for WNT activation and subsequent *Pax3* expression (Canning et al., 2008b). In addition, at later stages trigeminal neurogenesis also requires FGF signalling, as a dominant negative FGFr caused a loss of neurogenesis markers (Lassiter et al., 2009). Recently experiments have identified a number of other signalling molecules that may play a role in the induction of *Pax3*. A signalling molecule screen has shown a possible role for Platelet derived growth factors, insulin growth factors and SHH in trigeminal placode development, validated by in situ hybridisation, as well as identifying numerous factors from the WNT and FGF family (McCabe et al., 2007)

In addition, the cell surface glycoprotein CD151, part of the cell signalling scaffold web tetrasapanin, has been implicated in controlling the onset of *Pax3* expression in the trigeminal placode (McCabe and Bronner, 2011). A knock down of CD151 lead to a loss of *Pax3*, as *Pax3* is expressed before CD151, this suggests a role as a maintenance factor for *Pax3*, rather than an inducer.

The earliest marker for the Opv in chick or profundal placode in frog is *Pax3*, expressed at HH9 in chick and slightly later in *Xenopus* (Baker et al., 1999; Dude et al., 2009; Pieper et al., 2011; Schlosser, 2006; Stark et al., 1997; Xu et al., 2008). Explant cultures of trigeminal ectoderm shows the onset of *Pax3* is connected with the commitment to form trigeminal neurons, suggesting that it is a marker of trigeminal cell determination (Baker et al., 1999). Thus, currently little is known about the transcriptional network that controls trigeminal fate.

### 1.5.4 Lateral line placode

Multiple lateral line placodes are only present in aquatic vertebrates where they give rise to the lateral line system. The lateral line system detects movement through electric fields and vibrations within the water through the use of specialised cell types: neuromasts, which will detect the vibrations in the water and the electric field sensing ampulary organ (Baker and Bronner-Fraser, 2001; Schlosser, 2010). The lateral line placodes undergo an extraordinary migration, where they leave lateral line organs across the head and body of the embryo. There is little known about these placodes except their early origin, anterior to and next to the epibranchial and otic placodes.

There are few distinct markers for the lateral line; *Tbx3* is the only distinguishing transcription factor (Schlosser, 2006). No signalling molecules have been discovered which induce or specify the lateral line (Baker and Bronner-Fraser, 2001; Schlosser, 2010). However, *Eya4* and *Parvalbumen3* have recently been shown to mark mechanosensory hair cells in the lateral line *Eya4* has been suggested to be a conserved marker for lateral line placodes in jawed vertebrates (Modrell and Baker, 2012). Overall, even though the morphology, migration and origins of the lateral line have been studied for more than a century; very little is known about how the lateral line develops after the early placode stage (Piotrowski and Baker, 2014).

### 1.5.5 Hypobranchial placodes

There is very little information available on the hypobranchial placode, for it was only recently located and has not been shown to be present in all vertebrates (Baker and Bronner-Fraser, 2001). The hypobranchial placodes are two extra placodes found in *Xenopus*, which can be seen at the 32 somite stage and 36 somite stage when they are marked by *Ngnr1* and *NeuroD*. They form ventral to the second and third pharyngeal pouch (Schlosser and Northcutt, 2000). The hypobranchial placodes are not well understood and have only been shown to give rise to neurons which contribute to a previously unknown structure called the hypobranchial ganglia; its function remains unknown (Schlosser, 2003).

### 1.5.6 Lens placode

The lens placode is a non-neurogenic placode and is responsible for the formation of the transparent lens structure of the eye, by providing the correct refraction of light on to the

retina for subsequent visualisation. The transparency of the lens depends on the presence of crystallin proteins which have been co-opted from other cellular functions throughout evolution such as stress protection and enzymatic function (Cvekl and Piatigorsky, 1996; Piatigorsky, 1998; Simpson et al., 1995; Tomarev and Piatigorsky, 1996). At early neural tube stages the presumptive lens ectoderm overlies the optic vesicle, which evaginates from the ventral diencephalon. As contact between the lens ectoderm and the optic vesicle is established the placode thickens and invaginates to form the lens vesicle, which subsequently differentiates into the lens. The formation of the functional eye depends on the continued interaction between the optic cup and lens (Coulombre and Coulombre, 1963; Lang, 2004).

Experiments by Spemann in 1901 on *Rana Pipens* showed that the ablation of the optic cup leads to the loss of the lens (Spemann, 1901) suggesting that the optic vesicle plays an important role in lens induction. However, soon thereafter conflicting evidence was obtained in other amphibian species (King, 1904; Lewis W H, 1901) and whether or not the optic vesicle indeed is the lens inducer has been debated. Mouse mutants that lack the optic vesicle including *Lhx2*, *Rx* and *BMP4* mutants (Furuta and Hogan, 1998; Mathers et al., 1997; Porter et al., 1997), also show a loss of lens tissue apparently lending support to the idea that the optic vesicle induces a lens. In chick, the sufficiency of the optic cup to induce lens was shown by quail-chick chimera experiments, where the optic cup was transplanted into the trunk ectoderm and induced ectopic lenses (Karkinen-Jääskeläinen, 1978). However, within their experiments they added a protein supplement to the nutrient medium which proved vital to lens formation, suggesting that other unknown factors may be involved in lens formation. While, reinvestigation of the grafting experiments, using vital dyes to mark host and donor tissue, in *Xenopus* and *Rana palustris* showed that the optic vesicle was a weak inducer of lens fate if at all and that it was often very difficult to not transplant lens cells from the donor (Grainger et al., 1988). The model of lens formation has since been revised and there is evidence that lens specification occurs long before the optic vesicle forms. With experiments from chick showing that the lens was specified (marked by *Pax6* expression) at PPR stages (Bailey et al., 2006)

Classical grafting experiments in amphibians and chick showed that a large region of the ectoderm is initially competent to give rise to the lens, when exposed to the appropriate signals. This include the non-neural ectoderm as well as the neural plate (Jacobson, 1963a; Servetnick and Grainger, 1991) in amphibians and the trunk ectoderm in chick (Jorquera et al., 1989). In addition, it was suggested that the extra-embryonic region in chick is also competent to give rise to lenses: optic cups grafts into this territory generated

lenses (Clark and Fowler, 1960; Waddington, 1936). However, since no host-donor markers were used it is difficult to assess whether these lenses arise from the graft itself or are induced. Extensive analysis of competence was carried out in Xenopus (Gallagher et al., 1996; Grainger et al., 1988; Servetnick and Grainger, 1991; Zygar et al., 1998) These studies revealed that at early stages a large region of ectoderm is competent, however this is successively restricted as the embryo develops until at the 10 somite stage competence matches the lens placode.

While it is clear that the competence for lens extends to a large region of the ectoderm over a long period of early development, many different tissues are presumed to be involved in lens induction. These tissues have been thought to incrementally shift the fate of the presumptive ectoderm towards lens and include the endoderm, heart mesoderm, retina and neural plate (Jacobson, 1966). These studies often used the morphological formation of lens to analyse the end result and only recently a number of molecular markers have been used. More recently experiments in chick have asked the question of when lens fate is specified (Bailey et al., 2006). These studies revealed that already at head process stages before somite formation cells in the pre-placodal ectoderm are specified as lens. Surprisingly however not only lens precursors, but also precursors for all other placodes undergo lens formation when cultured in isolation in the absence of other inducing signals. PPR explants switch on *Pax6* followed by *L-Maf* , *Foxe3* and the lens differentiation genes ð- and α-crystalline. These findings have led to the suggestion that the PPR, but not other ectoderm, has the tendency to develop into lenses and that induction of other placodes requires lens repression as well as inducing signals. In addition, these findings suggest that since lens specification occurs long before the optic vesicle is formed, this tissue cannot be the primary inducer of lens fate.

How is lens fate restricted to its normal position? Initially, FGF signalling seems to play a crucial role. FGF8 from the anterior neural ridge represses *Pax6* and imparts olfactory character (Bailey et al., 2006) (See above section 1.5.2), while FGF signalling from the mesoderm underlying otic progenitors has a similar function in the posterior PPR (Lleras-Forero et al., 2013). Interestingly, FGF signalling has been implicated in the induction of many placodes including the otic, trigeminal and epibranchial territories (Bhattacharyya and Bronner-Fraser, 2008; Canning et al., 2008b; Freter et al., 2008; Ladher et al., 2000; Lassiter et al., 2009; Wright and Mansour, 2003) suggesting that lens repression by FGF may be a general mechanism for all placodes. In addition, in fish Shh promotes the development of the adenohypophysis over lens, while a knockdown of Shh leads to an expansion of lens cell markers (Dutta et al., 2005). This suggests that shh signalling restricts lens cell fate

anteriorly. Finally, neural crest cells have been implicated in lens repression at later stages. Ablation of neural crest cells leads to ectopic lens formation (Bailey et al., 2006). The neural crest are a source of TGF-β, which suppresses lens formation in explant cultures and in vivo (Grocott et al., 2011). TGF-β induces WNT2b expression in the overlying non-lens ectoderm, which in turn represses lens. Indeed in mouse, inactivation of β-catenin in the ectoderm surrounding the lens results in ectopic lenses. While gain-of-function of β-catenin will supress normal lens development (Smith et al., 2005). Together, these findings suggest migrating neural crest cells are important in preventing the expansion of the lens placode and that a number of signalling pathways are involved in this process. Overall, it seems that a combination of Shh, FGF and WNT signalling is needed to suppress the lens fate and allow the formation of other placodal territories.

While the above factors are important in restricting the lens domain other signals have been shown to be positive regulators of lens fate. Recent experiments in the chick have shown a role for the prechordal mesendoderm, which underlies the future lens and olfactory region. Ablation of the pME displayed a loss of *Pax6* and further investigation showed that a neuropeptide, somatostatin was involved in the induction of *Pax6* in the lens region (Lleras-Forero et al., 2013). Knockdown of somatostatin signalling by small molecule inhibitors or morpholino targeting its receptor leads to a loss of *Pax6* in chick and fish and as a consequence lens malformations (Lleras-Forero et al., 2013). BMP signalling has been implicated at early stages of lens precursor formation and suggested to be sufficient and required for *Pax6* expression and promoting lens over olfactory fate (Sjödal et al., 2007). Exposing explants of early chick anterior neural ectoderm (HH5) to BMP lead to the induction of crystallin proteins. Interestingly, culturing the olfactory and lens precursory ectoderm for 12 hours and then adding BMP induced crystallin and blocked olfactory induction (Sjödal et al., 2007) . This suggests that while BMP promotes lens formation from the neural plate, presumably by transforming it into PPR, the timing of the BMP signal is also important to differentiate between lens and olfactory precursors. In mouse, BMP signalling from the optic vesicle and in the lens ectoderm itself are crucial for lens formation. Loss of BMP4 function results in the absence of a lens placode and the failure of upregulation of Sox2 (Furuta and Hogan, 1998). On the other hand *BMP7* is expressed in the surface ectoderm where it is required for lens formation (Wawersik et al., 1999). While FGF signalling at early stages is involved in lens repression, at placode stages it is required for its formation. Mouse mutants for FRS2α a docking protein crucial for downstream FGF signalling and overexpression of a dominant negative FGFR showed loss of *Pax6* and disruption of lens formation (Faber et al., 2001; Gotoh et al., 2004; Smith et al., 2010)

In summary, a number of signals are repeatedly used during lens placode formation and have different functions at different time points of placode formation.

While tissues and signalling inputs are vital to the formation of the lens, it is impossible to ignore the transcriptional hierarchy that promotes lens fate. The master eye regulators in *Drosophila, eyeless* and *twin of eyeless*, are responsible for the onset of the retinal determination network. In vertebrates, there is only one homolog *Pax6* and this factor is key lens formation (Chen et al., 1997; Collinson et al., 2000; Quinn et al., 1996). Fly mutants for eyeless do not develop compound eyes, while misexpression of eyeless induces ectopic eyes. Likewise, misexpression of vertebrate *Pax6* in *Xenopus* leads to ectopic lens formation, largely associated with neural tissue (Chow et al., 1999). *Pax6* mutant mice showed small eye phenotypes and mutations in *Pax6* have also been found in human patients with eye defects (Fujiwara et al., 1994; M.Hanson et al., 1993; Tang et al., 1997). Haploinsufficiency of *Pax6* is a causative factor in aniridia (absence of the iris), mutant mice where *Pax6* has been reduced in the lens showed a failure in the formation of eye structures disrupting the correct angle of refraction by the lens required for clear vision (Kroeber et al., 2010). Mutations in *Pax6* have been found in humans with aniridia (Kang et al., 2012). Therefore, even a reduction in the level of *Pax6* is sufficient to cause lens defects.

*Pax6* is clearly one of the key factors for lens fate but numerous other factors have been proposed as upstream regulators in vertebrates. In the PPR, activation of *Six1* target genes is required for *Pax6* expression. Overexpression of a constitutive repressor form of *Six1* in the PPR lead to a loss of *Pax6* (Christophorou et al., 2009). Another *Six* gene, *Six3* is also involved in lens formation: its overexpression in medaka leads to ectopic lenses which express *Pax6* (Loosli et al., 1999). In mouse, lens specific *Sox3* deletion prevents placode formation and *Pax6* expression, and *Six3* may directly regulate its expression by binding to the *Pax6* lens ectoderm enhancer (Liu et al., 2006). Misexpression of *Six3* in chick expands the presumptive lens ectoderm (Liu et al., 2006). Thus, *Six3* appears to be an important upstream regulator of *Pax6*. However, it also has another role: *Six3* regulates anterior ectoderm fate repressing the posterior marker *Irx3*, thereby creating an anterior domain within which *Pax6* can be expressed (Kobayashi et al., 2002). *Otx2* is expressed in much of the anterior ectoderm including the neural plate and placode territory. *Otx2* target activation is required for normal lens development and seems to lie upstream of *Pax6* (Steventon et al., 2012).

Other transcription factors such as the Hmg-box transcription factors *Sox2* and *Sox3* are expressed in the forming lens and together with *Pax6* activate δ-crystalline by binding to the DC2 enhancer (Kamachi et al., 1995; Kamachi et al., 1998).

In summary, lens fate is specified early during development and PPR cells have the autonomous tendency to develop into lenses. A complex signalling network represses lens specification to confine lens development to its appropriate place next to the optic vesicle. Subsequently, continued interaction between the vesicle and the lens are required for normal eye development a number of signals are also known to promote lens formation, and some of the key transcription factors include members of the Pax and Six families.

### 1.5.7 The Epibranchial placodes

The epibranchial placodes originate from the posterior PPR and are initially part of the combined otic and epibranchial progenitor domain (OEPD) (Baker and Bronner-Fraser, 2001; Grocott et al., 2012; Schlosser, 2010). The OEPD is marked by *Pax2* at the 4 somite stage in chick and by the 8 somite stage in *Xenopus* (Groves and Bronner-Fraser, 2000; Heller and Brandli, 1997). In Xenopus and fish, *Pax8* labels this territory earlier at neural plate stages (Mackereth et al., 2005).The epibranchial placode can be distinguished from the otic placed by its expression of *Sox3* (Abu-Elmagd et al., 2001). There are few fate maps that investigated the location of epibranchial precursors at early somite stages. In chick, epibranchial and otic progenitors appear to be mixed early on (Streit, 2002), while lineage tracing of *Pax2* positive cells in fish provides evidence that epibranchial cells are derived from *Pax2*+ cells: while high levels of *Pax2* expression biases cells towards otic fate, cells expressing low levels contribute to epibranchial placodes (McCarroll et al., 2012).in comparison, Fate maps in Xenopus, show precursors of the otic and epibranchial placode partially overlap in the posterior PPR (Pieper et al., 2011).

The epibranchial placodes do not undergo the complex morphogenetic changes as the olfactory, lens and otic placodes, but instead generates neuroblasts that contribute to the cranial sensory ganglia. There are three epibranchial placodes forming in the ectoderm close to branchial clefts where the pharyngeal endoderm makes contact with the overlying ectoderm (Webb and Noden, 1993). The most anterior placode is the geniculate, which forms dorsal to the first branchial arch, giving rise to the geniculate ganglion that contributes to cranial nerve VII (facial). The second is the petrosal placode, forming dorsal to the second branchial cleft and contributing to cranial nerve IX (glossopharyngeal). Lastly, the third is the nodose placode, which forms dorsally to the third branchial cleft and

contributes neurons to cranial nerve X (vagus). (Baker and Bronner-Fraser, 2001; Begbie et al., 1999; D'Amico-Martel and Noden, 1983; Ladher et al., 2010; Schlosser, 2010). Axons emanating from these ganglia convey viscerosensory and gustatory information from the orpharynegeal cavity as well as the heart and other organs. The superior (IX) Jugular (X) ganglia are of neural crest origin, as are the glial cells that envelop their axons (D'Amico-Martel and Noden, 1983)

A number of experiments in chick showed that various tissues are competent up until the early somite stages to give rise to epibranchial placodes. Heterotypic grafts of placode territories showed that the presumptive otic ectoderm could be induced to become epibranchial when transplanted to the epibranchial domain, this was also true for trunk ectoderm (Vogel and Davies, 1993). In a similar manner presumptive trigeminal placode can adopt epibranchial fate when transplanted. However, as soon as trigeminal cells start to express *Pax3* they are unable to do so (Baker and Bronner-Fraser, 2000).

Cephalic mesoderm and endoderm are sources of FGF signalling, which is required for early epibranchial development. In zebrafish, FGF3 hypomorph mutants show a loss of the glossopharyngeal placode and smaller vagal placodes (Nechiporuk et al., 2007) . However, this phenotype can be rescued with a graft of cephalic mesoderm, restoring the FGF signalling (Nechiporuk et al., 2007). FGF10 works with FGF3 to specify the epibranchial placode. Combining an FGF10 morpholino with the FGF3 mutant zebrafish, showed a loss of the facial placode and near total loss of the glossopharyngeal and vagal placodes (McCarroll and Nechiporuk, 2013). Showing that a combination of FGF signalling is required for epibranchial formation. In addition, pharyngeal endoderm can induce epibranchial markers and is thought to do this through the provision of BMP7 (Begbie et al., 1999). BMP7 is sufficient to induce *Phox2a* epibranchial neurons from competent head ectoderm (Begbie et al., 1999). Explant cultures of cranial ectoderm in the presence of BMP7 induces *Phox2a* expressing cells. While, co-culture of the pharyngeal mesoderm and cranial ectoderm in the presence of a BMP inhibitor does not induce *Phox2a* cells (Begbie et al., 1999).

The OEPD is first specified in chick around the 4 somite stage, when *Pax2* begins to be expressed. There is ample evidence in chick, mouse and zebrafish that OEPD induction is mediated by FGF signalling. In fish, knockdown FGF8 mutants (ace) develop a smaller OEPD (Kwon and Riley, 2009; Léger and Brand, 2002; Maroon et al., 2002), as do FGF3 morphants. When FGF3 is knocked down in ace mutants the *Pax2* expression is completely lost and the OEPD does not form (Léger and Brand, 2002; Maroon et al., 2002; Sun et al., 2007). Another transcription factor that labels the OEPD is *Foxi1* and ectopic expression of

*FGF3* and *-8* can induce this marker and cells induced to express *Foxi1* go onto generate *Phox2a* positive cells, suggesting epibranchial fate (Nechiporuk et al., 2007). Epibranchial defects have also been seen in mice deficient in *Sprouty1 and 2*, in the mutants the epibranchial placode is enlarged, this could be due to the loss of the negative feedback on FGF signalling, allowing unchecked FGF to induce a larger region to epibranchial fate (Simrick et al., 2011). In contrast, in mouse *FGF10* is expressed in the mesoderm underlying the OPED, while *FGF3* is present in the neuroectoderm, where the PPR will form (Wright and Mansour, 2003) While single knockouts show a disruption of the otic placode and later defects in the patterning of the inner ear (Hatch et al., 2007; Wright and Mansour, 2003), mice mutant for both FGF3 and 8 have virtually no OEPD, although the epibranchial phenotype has not been examined (Wright and Mansour, 2003). Finally, in chick mesoderm-derived *FGF19* promotes OEPD fate. Ectodermal explants exposed to FGF19 begin to express *Pax2* and other otic markers, although future epibranchial fate was not assessed in these experiments (Ladher et al., 2010).

While there is a large amount of evidence for a common progenitor domain for the otic and epibranchial placodes (For reiview Grocott et al., 2012; Streit, 2004) more recently this has been challenged and signals from the otic placode were suggested to induce the epibranchial territory (Padanad and Riley, 2011). This study suggests that the otic placode forms first and upregulates *FGF24* under the control of *Pax2*. Subsequently, FGF24 is then thought to induce the *Sox3* expressing domain of the epibranchial placode because FGF24 knockdown causes epibranchial defects.

Canonical Wnt signalling is crucial for the separation of otic and epibranchial cells from the OEPD. In fish, high levels of *Pax2a* expression bias cells towards otic fate, while low level of *Pax2a* cells contribute to epibranchial placodes. WNT signalling appears to control *Pax2* levels and its misexpression induces higher levels, shifting cell fate towards the otic (McCarroll et al., 2012). Likewise, experiments in mouse provide evidence that otic cells close to the neural tube receive high levels of Wnt signalling, while epibranchial precursors located more lateral receive no or low levels of Wnt (Ohyama et al., 2006). In mouse, inactivation of β-catenin leads to a loss of the otic placode and an expansion of epidermis, while increased levels of Wnt expanded the otic domain. Although epibranchial identity was not assessed in these experiments, findings in chick suggest that Wnt signalling is inhibitory for epibranchial fate. When FGF was over expressed in the OEPD, the region was expanded, however otic fate was lost, suggesting a promotion of early OEPD fate but not later otic or epibranchial fate (Freter et al., 2008). However, when WNT signalling was over activated by the expression of a stabilised β-catenin construct, *Foxi2* was lost and epibranchial fate was

inhibited (Freter et al., 2008). WNT therefore inhibits epibranchial fate, consequently promoting otic fate.

In summary FGF signalling is critical for the induction of the OEPD; while prolonged FGF exposure leads to loss of otic fate, it promotes epibranchial identity. In contrast, Wnt signalling from the neural tube promotes otic, but inhibits epibranchial cells.

Although the epibranchial and otic progenitor cells are initially mixed, there are molecular differences in their transcriptional regulation .Zebrafish mutants for *Dlx3b/Dlx4b* show only otic, but no epibranchial defects (Sun et al., 2007). It has also been established that the transcription factors *Foxi1* and *Pax2* are essential for the formation of the OEPD v(Solomon, 2003; Sun et al., 2007). As mentioned above, levels of *Pax2* expression seem to differentiate between otic and epibranchial progenitors. Misexpression of *Pax2*a in zebrafish lead to an increase in otic placode size as well as cell number, where as a lowering of *Pax2*a and *Pax8* lead to a high number of epibranchial cells (McCarroll et al., 2012). At later stages *Six1* and *Eya1* have a role in the regulation of neuronal differentiation in the epibranchial placode. *Six1* and *Eya1* mutant mice show a loss of the neuronal differentiation and maintenance markers *Neurog1* and *Phox2* (Zou et al., 2004).

Overall the epibranchial placodes are responsible for the formation of three important sensory ganglia. Their induction is initiated by FGF signalling before being separated from the otic placode by graded levels of WNT signalling.

### 1.5.8 Otic placode

The vertebrate inner ear is responsible for hearing and balance. The cristae are sensory patches associated with each semi-circular canal responsible for balance perception. In addition, there are the utricle and saccule. The cochlea or cochlear duct contains the sensory hair cells responsible for the perception of sound called Organ of Corti in mammals or basilar papilla birds (Noramly and Grainger, 2002). There is evidence in fish that the saccule and utricle are responsible for hearing (Kever et al., 2014; Popper et al., 2005).These structures as well as the vestibuloaccoustic ganglion, which innervates these sensory cells, develop from the otic placode originally located next to the hindbrain. The otic placode is derived from the posterior PPR, and initially the otic progenitors are part of a common domain with epibranchial precursors (Baker and Bronner-Fraser, 2001; Grocott et al., 2012; Schlosser, 2010).

The otic placode forms the entire inner ear and undergoes complex morphological changes after forming an initial ectoderm thickening (Baker and Bronner-Fraser, 2001;

Torres and Giráldez, 1998). In amniotes, the otic placode invaginates to form the otic vesicle (Groves and Bronner-Fraser, 2000; Ladher et al., 2010; Torres and Giráldez, 1998). While, in anamniotes cells accumulate to form a condensed 'ball' which subsequently generates a lumen during cavitation (Haddon and Lewis, 1996; Hoijman et al., 2015) Subsequently, the vesicle is regionalised as evidenced by differential gene expression and differential proliferation, apoptosis, growth and cell rearrangements generate the complex structures of the inner ear (For review Torres and Giráldez, 1998)

Initially large parts of the developing embryonic ectoderm are competent to give rise to otic placodes. In amphibians, both head and trunk ectoderm are competent to form the otic placode (Jacobson, 1963a). In *Xenopus* belly ectoderm loses competence around mid neurula stage (Baker and Bronner-Fraser, 2001; Gallagher et al., 1996), although other experiments show that trunk ectoderm at mid neurula stage is still able to from otic vesicles when exposed to FGF (Gallagher et al., 1996; Lombardo and Slack, 1998). Likewise in chick, a relatively large portion of the head ectoderm from 4-6 somite stages is competent to form the otic placode (Groves and Bronner-Fraser, 2000). However, competence is restricted to posterior cranial ectoderm after the 10 somite stage (Groves and Bronner-Fraser, 2000). More recent experiments show that competence is restricted to the PPR. When exposed to otic inducing signals (FGF) $HH3^{+}$ ectoderm does not express otic genes. However, when the same ectoderm is first grafted to the PPR and then explanted and cultured with FGF explants upregulated the otic marker *Pax2* (Martin and Groves, 2006). Therefore, before they can acquire otic identity cells must go through a PPR state.

Numerous tissues provide signals to restrict and promote otic development. In amphibians, experiments using explants of presumptive placodal tissue showed that occasionally heart mesoderm in combination with endoderm will induce otic placodes (Jacobson, 1963a). However, endoderm in combination with posterior neural plate will induce otic fate more often (Jacobson, 1963a), while, the neural plate and fold will always induce otic placodes in explants (Jacobson, 1963a). However, in the absence of molecular markers and techniques to label inducing and responding tissue, it is difficult to interpret some of the experiments. However, they do show that the surrounding tissue provide otic inducing signals and suggest that the neural plate may be most important, together with contribution from the mesoderm and endoderm. In *Ambystoma*, transient cell to cell contacts from the hindbrain were suggested to influence the development of the ear (Model et al., 1981). Fine structural analysis showed cellular processes extending from the hindbrain to the otic region, which disappeared upon otic induction, raising the possibility that a signal passes between the both tissues (Model et al., 1981). There is also historical

evidence that the hindbrain when grafted ectopically in *Amblystoma* can induce a region that resembles an ear like structure (Stone, 1931). More recent evidence in zebrafish suggested that the hindbrain does have a role in otic induction with ectopic hindbrain grafts leading to the formation of ectopic otic vesicles (Woo and Fraser, 1997). Experiments in chick provide a controversial view for the role for neural tissue in otic development. Explants of prospective otic tissue with or without neural plate show that the neural plate plays a role in the maintenance of the otic marker *Lmx-1* (Giraldez, 1998). However, ablation of the neural tube does not impact on the formation of the otic placode (Waddington, 1937). However, more recent experimental evidence show that otic competence and specification had most likely begun before the point at which Waddington had removed the neural tube (see above Groves and Bronner-Fraser, 2000). Therefore, it is difficult to reliably determine from these experiments if the neural tube is not involved in otic placode specification.

Other recent experiments in chick and quail suggest the role of the hindbrain is in the patterning of the otic vesicle rather than induction. Vitamin A deficient quails have neural tube patterning defects, but otic induction occurs normally. However, expression of *Pax2*, *EphA4*, *SoHo1* and *WNT3a* was disrupted leading to the conclusion patterning of the inner ear was defective (Kil et al., 2005). This is supported further by rotation experiments: rotating the hindbrain along the dorso-ventral axis leads to dorso-ventral patterning defects of the otic vesicle (Bok et al., 2005). In mouse, mutants that display hindbrain patterning defects also show abnormal otic patterning (Mendonsa and Riley, 1999; Ruben, 1973; Sadl et al., 2003; For review Trainor, 2003). Together, these experiments implicate signals form the neural plate in otic development, however the exact role and timing of these events remains elusive.

Other experiments have implicated the mesodermal signals in initiating otic development in particular inducing the OEPD. In fish, mutants that lack mesoderm show a delay in placode formation (Mendonsa and Riley, 1999). In chick ablation of the mesoderm underlying the otic region leads to a loss of otic markers and grafting of this mesoderm adjacent to the trigeminal region induces the OEPD marker *Pax2* (Kil et al., 2005). Performing ablation experiments at different times reveals that mesodermal signals are required early, but not after the 4 somite stage. However, mesoderm grafts cannot induce ectopic otic placodes (Christophorou, 2008). These experiments suggest that while mesodermal signals are important for otic development they must cooperate with other signals from different tissues. Indeed, explants experiments in chick show that only when

neural tissue is included future otic placode cells express definitive otic markers (Ladher et al., 2000)

As already discussed above, otic precursors are initially intermingled with epibranchial progenitors in the OEPD and FGFs have been implicated in its induction.

Numerous FGFs are surrounding the otic territory including FGF3, 4 and 19 (Maroon et al., 2002; Paxton et al., 2010; For review Schimmang, 2007; Wright and Mansour, 2003). A number of FGFs are expressed in the mesoderm underlying the OEPD (mouse: FGF10 (Wright and Mansour, 2003), chick: FGF19 (Ladher et al., 2000), zebrafish: FGF3 (Phillips et al., 2001) and mesodermal FGF expression generally precedes FGF ligand expression in the neural tube, FGF3 in mouse, chick and Xenopus (Lombardo and Slack, 1998; Mahmood et al., 1995; Mahmood et al., 1996) FGF8 in zebrafish (Phillips et al., 2001).

In mouse, loss of *FGF3* leads to reduced levels of *Pax2,* although the otic placode is present, but later patterning is abnormal (Mansour et al., 1993; *Pax*ton et al., 2010). Likewise, in the absence of FGF10 the otic vesicle is smaller (Ohuchi et al 2000). However, when both FGFs are deleted, the otic placode is missing completely highlighting the importance of FGF signalling for otic development (Wright and Manour, 2003). In chick blocking FGF signalling using small molecule inhibitors in explants or FGF19 or -3 knockdown in vivo leads to the absence of *Pax2* (Freter et al., 2008, Martin and groves 2006), while in fish loss of both FGF3 and -8 results in the absence of the otic vesicle (Léger and Brand, 2002; Maroon et al., 2002) (Léger and Brand, 2002; Maroon et al., 2002; Phillips et al., 2001). Thus, FGF signalling is required for otic placode formation.

FGF misexpression experiments in different species support a role for FGF signalling in OEPD induction. Misexpression of FGF19, -3 or -10 induces otic vesicles in mouse or chick (Alvarez et al., 2003; Kil et al., 2005; Ladher et al., 2000; Phillips et al., 2004; Vendrell et al., 2000) while in fish expansion of the otic placode is observed (Padanad et al., 2012). However FGF signalling is not enough to convert non-neural/non-PPR tissue to an otic fate. While FGF19 from the mesoderm can induce *Pax2* expressing domains in neural explants, it cannot do so in uncommitted non-neural tissue (Ladher et al., 2000) suggesting that other signals are required. One such signal is the canonical Wnt pathway. In chick ectoderm from HH7, before otic commitment, was cultured with WNT8c and FGF19 and showed an upregulation of *Pax2, Dlx5* and *Soho1* (Ladher et al., 2000). FGF19 derived from the mesoderm induced *WNT8C* in neural tube tissue and together they induce otic cells from the OEPD (Ladher et al., 2000). In mouse, TCF/Lef-lacZ reporter activity shows that canonical Wnt signalling is

active in the medial, but not lateral OEPD and activation of β-catenin in *Pax2* positive cells leads to the expansion of the otic placode at the expense of epidermis (Ohyama et al., 2006). While, inactivation of the pathway has the opposite effect. Similar results are observed in chick, where activation of Wnt signalling promotes otic, but inhibits epibranchial fates (Freter et al., 2008). Activation of the Wnt pathway is clearly under FGF control. As described above, FGF19 induces *Wnt8c* in the neural tube (Ladher et al., 2000); inactivation of the FGF antagonist *Sprouty1* in mouse leads to the expansion of the Wnt expression domain and a larger otic placode (Rogers et al., 2012). Thus, FGF signalling controls Wnt expression and graded Wnt activity establishes the difference between otic and epibranchial cells.

The transcriptional network that controls otic development acts largely downstream of FGF signalling. The *Pax2/5/8* family is important in the development of the inner ear. Mouse mutants for *Pax2* show inner ear defects, including the loss of the cochlea (Torres and Giráldez, 1998). A number of human patients with high frequency hearing loss, have mutations in *Pax2* (Eccles and Schimmenti, 1999; Favor et al., 1996; Torres et al., 1996). *Pax2* mutant mice display similar phenotypes with renal, ear, eye and brain defects (Favor et al., 1996). Furthermore, *Pax8* mutant mice have hearing loss, along with thyroid defects (Christ et al., 2004). In zebrafish double mutants for *Pax2* and *8* show otic placode defects, while *Pax2* mutant ears have only partial defects (Mackereth et al., 2005) suggesting that *Pax8* may substitute for *Pax2* function. Finally, in the chick *Pax2* is essential for otic placode formation, regulating epithelial morphogenesis and cell fate (Christophorou et al., 2010). *Pax2* gain-of-function induces ectopic cell adhesion markers and a loss of function leads to loss of the characteristic cell shape associated with the otic placode, in addition to the loss of otic markers (Christophorou et al., 2010). These results show that *Pax2/5/8 are* important in the early specification of otic placode cells, but may also play a role in cell shape and morphogenesis.

A number of patients with BOR syndrome have mutations in *Eya1*. In agreement with this finding, *Eya1* mutant mice lack ears and kidneys, both structures affected in BOR syndrome (Abdelhak et al., 1997; Xu et al., 1999). Other transcription factor are also important for otic development including *Gbx2*, which represses anterior genes including *Otx2* and is required for otic placode development (Kobayashi et al., 2002; Steventon et al., 2012). Misexpression of *Sox3* occasionally induces ectopic *Pax2* expressing domains in Medaka, suggesting a possible role upstream of *Pax2* in otic induction (Köster et al., 2000).

Another family of genes important in otic specification are the *Foxi* genes, with *Foxi1* and *Foxi3* having important roles in inner ear development. Zebrafish mutants for *Foxi1* indicate its requirement for *Pax8* expression and *Foxi1* can activate ectopic *Pax8* (Solomon, 2003). Misexpression of *Foxi1* showed ectopic induction of *Pax8* in regions away from the otic placodes, morphants for *Foxi1* showed a loss of otic placodes and *Foxi1* mutants lack *Pax8* expression and display disorganised *Pax2* expression causing disruption of the otic placode (Nissen, 2003).There is also a role for *Foxi1* in FGF signalling, which is important for *Pax2/8* induction (Nissen, 2003). FGF3 mutants and morphants abolish *Foxi1* and subsequently *Pax8*, while *Foxi1* mutants and morphants show loss of *Pax*8 but not FGF3 (Nissen, 2003) suggesting a hierarchy where FGF controls *Foxi1*, which in turn controls *Pax*8. Recent experiments indicate that *Foxi3* is involved in creating the conditions for an FGF signalling response (Khatri et al., 2014). Knockdown of *Foxi3* in the chick left PPR induction intact but lead to a failure of otic induction. This was suggested to be due to a failure to respond to FGF signalling (Khatri et al., 2014): in the absence of *Foxi3* presumptive otic cells are unable to respond to FGF signalling (Khatri et al., 2014). However, misexpression of *Foxi3* does not confer competence to respond to FGF signalling to non-otic ectoderm. These findings suggest that *Foxi3* is required for the response to FGF, but alone is not sufficient to confer this ability. Taken together these experiments show a transcriptional hierarchy that allows PPR tissue to respond to signals from surrounding tissues and upregulate key otic genes such as *Pax2/5/8*.

In summary, the otic placode forms next to posterior neural plate by a twostep model involving signals from the mesoderm and neural plate. These signals include FGF and WNT and they combine synergistically to induce the otic placode. However, the transcriptional hierarchy that moves the PPR to the otic placode and the temporal order in which this hierarchy occurs needs further investigation.

## 1.6 Aims

As described in sections 1.4, Six1/4 and Eya1/2 are key markers for the PPR and functionally involved in specification of sensory progenitors or placode formation. However, the upstream regulators of these genes are poorly understood. The PPR inducing tissues and signals have been characterised, but the sequence and timing of signalling is poorly understood and the contribution of different tissues and signals to PPR induction are unclear. A recent microarray screen has identified a large number of transcription factors that appear to be co-regulated with the Six and Eya cassette, and seems to act upstream or

in parallel with these genes. These genes can now be used to assess the response to PPR-inducing tissues and signals, and establish a temporal hierarchy.

Thus, this thesis aims to characterise the response of naive ectoderm to PPR inducing tissues, the lateral head mesoderm and prechordal mesendoderm over time and thus identify putative upstream regulators of *Six1* and *Eya2*. The second aim was to dissect the contribution of different tissues, namely the mesoderm and neural plate, to PPR induction and subdivision of the PPR into more defined domains. Finally, this thesis investigates the role of different signalling pathways in PPR induction and how they relate to different tissues.

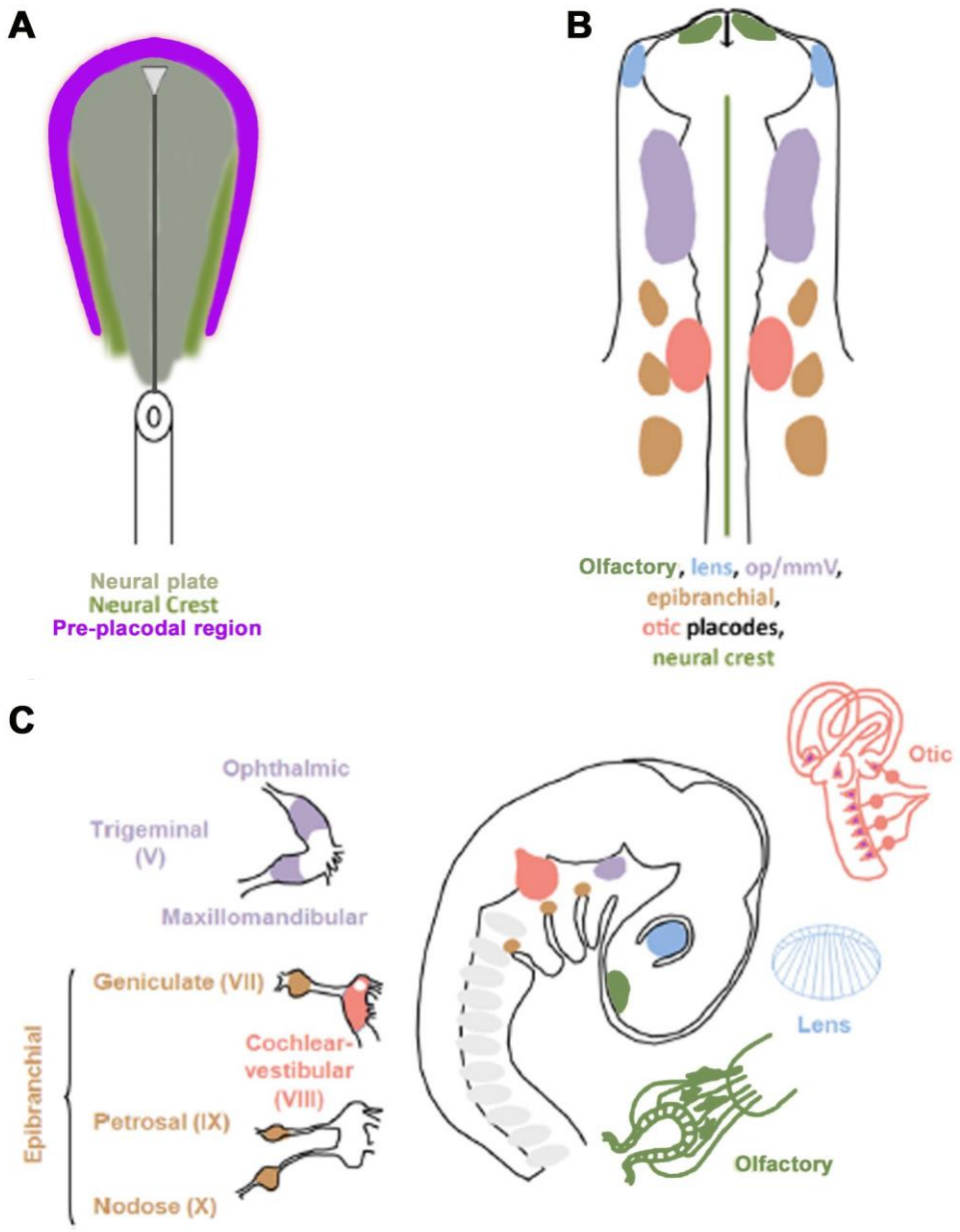


Figure 1.1: PPR, cranial placodes and their derivatives

**A**. At neurula stages of development the pre-placodal region (**purple**) surrounds the neural plate (**grey**), the neural crest (**green**) lies between these two domains. At this stage these domains still overlap and cells are intermingled. **B.** At HH stage 10 the PPR cells have formed distinct regions of thickened ectoderm along the anterior and posterior axis of the embryo, which are the cranial placodes. **C.** The cranial placodes will form structures of the sensory organs (**Right**) and sensory ganglia (**Left**) at development proceeds. (modified from Grocott et al., 2012 and Webb and Noden, 1993).

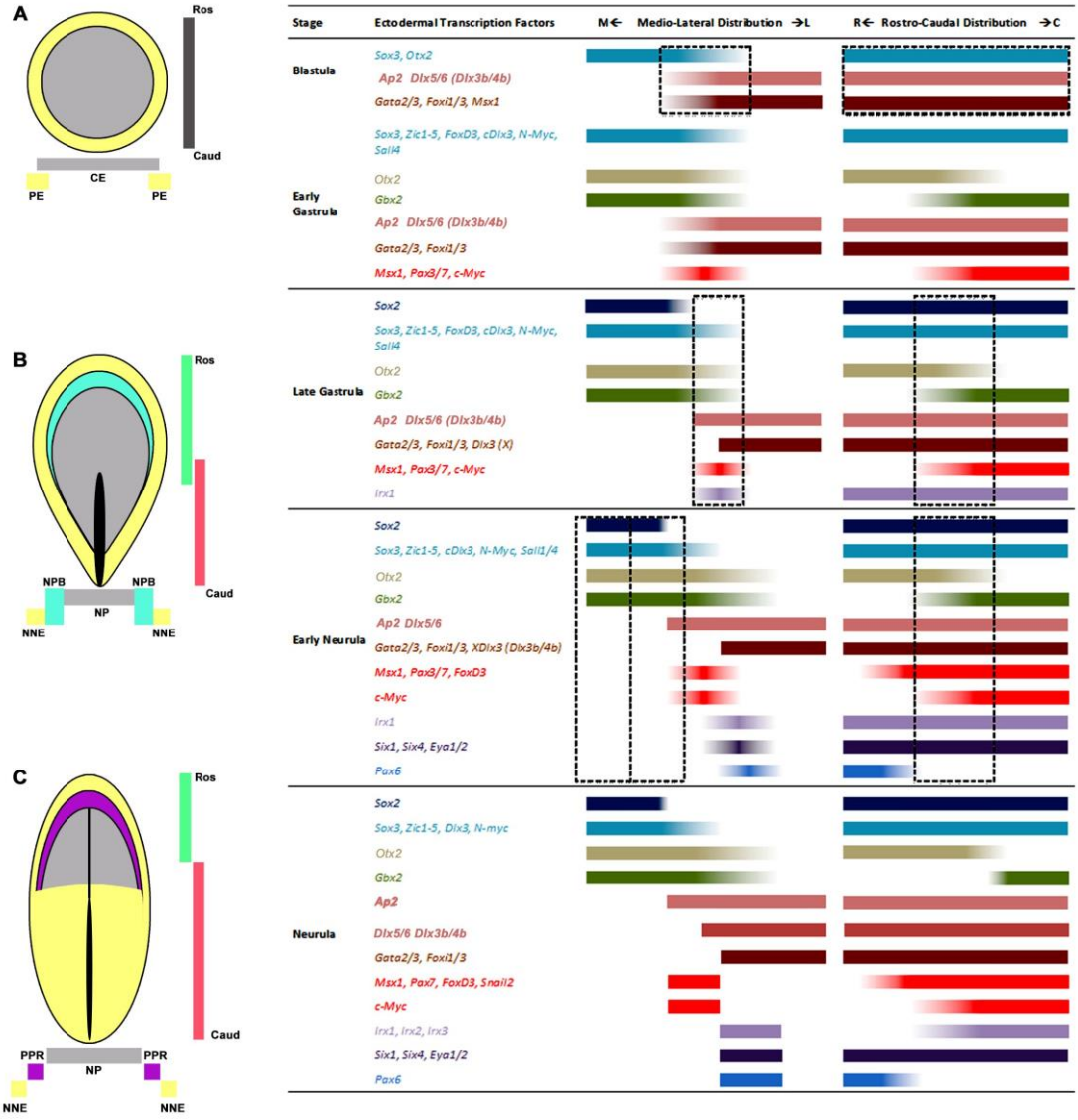


Figure 1.2: Overlapping gene expression defines the neural plate border

**A.** At blastula stages the genes expressed in the epiblast overlap at the border of the central and peripheral epiblast (**CE, PE**). While, the rostral (**Ros**) and caudal (**Caud**) distribution is uniform **B.** At gastrula stages the expression of transcripts from the early neural plate (**NP, grey**) and non-neural ectoderm (**NNE, yellow**) overlap in the neural plate border (**NPB, turquoise**). At this stage rostral and caudal domains come to be defined by distinct domains of gene expression. **C.** By neurula stages he PPR (**purple**) has formed and transcription factors specific for each domain are expressed; *Sox2* neural plate; *Six1* PPR; *Snail2* neural crest. Hatched boxes represent regions of overlap in gene expression (modified from Grocott et al., 2012).

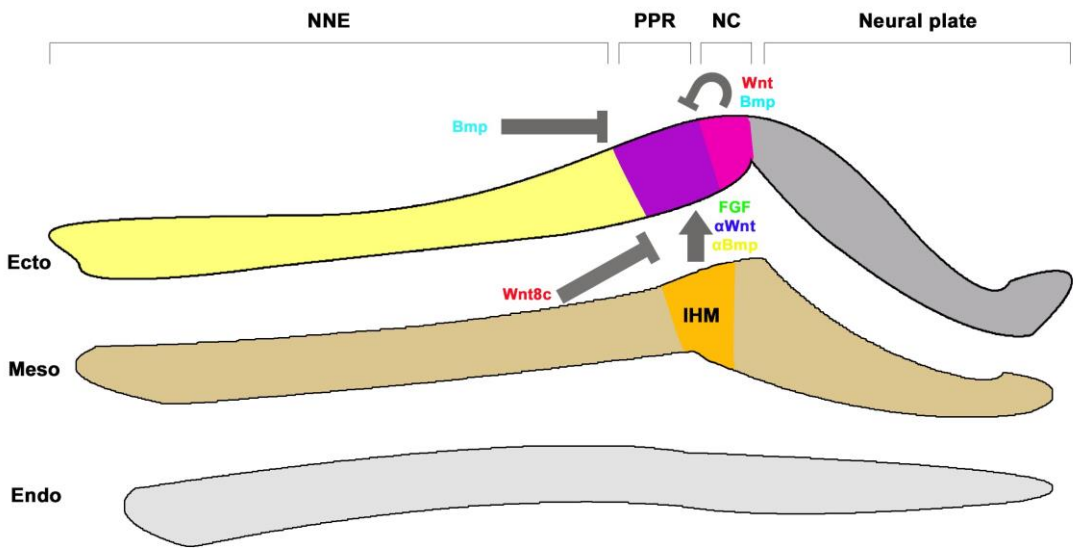


Figure 1.3: Local signalling promotes and restricts PPR position and fate

The PPR (**purple**) forms in the ectoderm adjacent to the neural plate and neural crest. Signals from surrounding tissue promote or restrict the PPR to its location. The lateral head mesoderm (**lHM, orange**) lies underneath the PPR and provides the three signals necessary for PPR induction, FGF (**green**), WNT antagonists (**blue**) and BMP antagonists (**yellow**). The adjacent paraxial mesoderm restricts the boundaries of the PPR through WNT (**Red**) signalling which negatively regulates PPR markers. While, BMP (**light blue)** and WNT signals from the adjacent neural plate/neural crest (**pink**) prevent the PPR expanding medially and lateral expansion is prevented by BMP signalling from the NNE (**yellow**).

# 2. Materials and Methods

The materials and methods has been divided into two sections, in the first I will describe the embryonic dissections and manipulations. The second section will describe the molecular biology and other analysis used on the manipulations performed.

## 2.1 Embryonic manipulations

### 2.1.1 Embryos

Fertilised chicken eggs were obtained from Winter and Steward farms (UK), Fertilised GFP chicken eggs were obtained from the Roslin Transgenic Chicken Facility (The Roslin Institute) and fertilised Japanese quail eggs were obtained from BC Potter Farm (Cambridge). All eggs were incubated to the required Hamburger and Hamilton stages from 2-30hrs in a humidified incubator at 38°C (Hamburger and Hamilton, 1951). All experiments were carried out using an Olympus SZ60 dissecting microscope with either transmitted light or illumination from the top using a cold light source.

### 2.1.2 Harvesting embryos

Embryos were harvested from the egg by the following procedure. First the shell was removed from one end of the egg with blunt forceps. The albumin was removed and the yolk was rotated to leave the embryo visible. A small square was cut around the embryo, which was then removed from the yolk together with the attached vitelline membrane using a small spoon. The embryo was then placed into phosphate buffered saline (PBS, 37mM NaCl, 2.7mM KCL, 10mM $Na_2HPO_4$, 1.8mM $KH_2PO_4$ ) before fixation or into Tyrode's saline (137mM NaCl, 2.7mM KCl, 320µM $NaH_2PO_4x2H_2O$, 5.6mM glucose) for dissection (Section 2.1.4). Embryos were cleaned by gently blowing saline with a Pasteur pipette and the vitelline membrane was removed, leaving the embryo ready for further manipulation. Embryos for fixation were placed in 4% paraformaldehyde in PBS for 4 hours at room temperature or overnight at 4°C. Afterwards, they were stored at -20°C in methanol, before being further processing.

## 2.1.3 Culturing techniques

Embryos were cultured for tissue grafting or bead placement by using either New culture (New, 1955; Stern and Ireland, 1981) or Whatman filter paper culture (Chapman et al., 2001).

### 2.1.3.1 New culture

The egg shell was broken using a coarse forceps; the thick albumin was discarded and the thin albumin collected. The intact yolk was placed into a Pyrex dish containing Pannet-Compton (PC) saline (82.8mM NaCl, 8.3mM KCl, 2.8mM $CaCl_2.2H_2O$, 2.5mM $MgCl_2.6H_2O$, 8mM $Na_2HPO_4.2H_2O$, 7.2□M $NaH_2PO_4.2H_2O$) and any remaining thick albumin on the yolk was removed using blunt forceps or a fire-polished glass Pasteur pipette. Using sharp scissors, the yolk is cut around the equator and the vitelline membrane with the embryo attached was removed. It was then placed onto a watch glass with the embryo ventral side up and a glass ring was placed onto the membrane so that the embryo is in the centre. The membrane was then folded over the edges of the ring. The ring and watch glass were removed from the dish to a microscope, where the membrane is stretched until tight and any remaining liquid inside the ring is removed using a glass pipette. The ring is then filled with PC solution and placed in a covered humid chamber until further use. Once further manipulations (tissue/bead grafting Section 2.1.5, 2.1.6) are complete, all liquid is removed from inside and outside the ring, which is then transferred to a 35mm Petri dish containing thin albumin and placed in the incubator at 38˚C, for 3, 6, 12 or 24 hours. This procedure was used for all tissue grafting experiments.

### 2.1.3.2 Whatman filter paper culture

This filter paper culture technique is a modified version of New culture technique where Whatman (No.1-5) laboratory filter paper is used instead of a glass ring. The filter paper is cut into squares (approx. 1.5cm x 1.5cm) and a 7.5mm hole was made in the centre with a single hole punch, it was then autoclaved. The shell of the egg is broken with blunt forceps and the thin albumin collected. The yolk is orientated so that the embryo is on the top and any remaining thick albumin is removed using blunt forceps and folded tissue paper. Using fine forceps, the filter paper is then placed with the centre of the hole over the embryo and a small amount of force is applied to the filter paper and yolk to create a strong adherence

between the filter paper and the membrane. The vitelline membrane is then cut around all 4 edges of the paper and both were removed with the embryo attached at an oblique angle following the flow of the yolk. The filter paper was then placed in a dish containing Tyrode's saline with the embryo facing upwards. Using a fire polished glass Pasteur pipette any remaining yolk can be cleaned from the embryo and membrane. After further manipulations (Sections 2.1.4, 2.1.6) the embryo was placed in a 35mm Petri dish containing thin albumin and incubated in a humid environment at 38°c for 3 or 6 hours. This procedure was used mainly for experiments involving beads coated with proteins or drugs (Section 2.1.6) or for when drugs were directly added to the albumin.

## 2.1.4 Tissue dissections

Embryos were collected in Tyrode's saline (Section 2.1.2). For all dissections embryos were immersed in a 35mm petri dish lined with Sylgard, containing Tyrode's saline and pinned out ventral side up with insect pins. To aid with tissue dissection dispase at 1µg/ml was added to the Tyrode's saline.

### 2.1.4.1 Lateral head mesoderm dissection

For dissection of the lateral head mesoderm (lHM) embryos were incubated to HH 5/6 (26-28hrs). With the embryo facing ventral side up the endoderm and mesoderm in the required region (Figure 2.1 (B), Orange rectangle) was scored in a rectangular manner at only three edges using a fine syringe needle (3mm, 30 half gauge; BD MicrolanceTM3). The needle was then used to peel off the mesoderm and endoderm away from the underling ectoderm. Since the top layer of endoderm remains attached to one edge, it is easily visible and is cut away to leave only the mesoderm attached to the ectoderm. The lHM is then cut away from the ectoderm and removed using a 20µl pipette, placed in a 35mm Petri dish containing Tyrode's saline and stored on ice to await the grafting procedure (Section 2.1.5).

### 2.1.4.2 Pre-chordal mesendoderm dissection

To obtain pre-chordal mesendoderm (pME) embryos were incubated to HH 5 (22-24hrs). The pME is a triangular structure at the tip of the developing notochord (Figure 2.1 (A), Light blue triangle). This triangle was scored using a fine syringe needle and peeled from underlying ectoderm in a posterior to anterior movement, leaving it attached at the most anterior edge. The final cut at the anterior edge of the pME was then made, the tissue

collected using a 20µl pipette and placed into a 35mm Petri dish containing Tyrode's saline and stored on ice to await the grafting procedure (Section 2.1.5).

#### 2.1.4.3 Anterior and posterior neural plate dissection

Both the anterior and posterior neural plate (aNP, pNP) were excised in the same way, with only the axial position differing between the dissections. The aNP was defined as the anterior third of the neural plate at HH6, while the pNP was defined as its posterior third with the most caudal point starting at the level of the first forming somite (Figure 2.1,B). Embryos were incubated to HH 6 (28 hrs) and the endoderm and mesoderm overlying the aNP and pNP were scored on four sides with fine syringe needles (Figure 2.1, B). This tissue was removed and discarded, and the underlying neural plate was cut to exclude the midline and transferred using a 20µl pipette to a 35mm Petri dish containing Tyrode's saline until further use (Section 2.1.5).

### 2.1.5 Tissue grafting and induced ectoderm dissection.

All tissues were grafted into the inner third of the area opaca of host embryos at stage $3^{+}/4^{-}$ (16 hrs) and cultured using New culture (section 2.1.3.1). Dissected induced ectoderm was collected for mRNA analysis by NanoString (Section 2.2.2).

Host embryos were set up in a 35mm Petri dish containing thin albumin. Using a fine syringe needle, a pocket was made in the yolky cells in the area opaca close to its inner margin leaving a small flap to cover grafted tissues. Using a 20µl pipette the tissue (lHM, pME, aNP or pNP) to be grafted was placed onto the host embryo and then pushed into the pocket. The area around the graft was dried using a pulled fine glass needle and the flap of yolk cells was replaced over the graft to secure it in place. The host was then transferred to the incubator for the required time (3, 6, 12, 16 or 24 hours). After incubation the host was removed from the vitelline membrane by filling the ring with PBS and the embryo was removed from the membrane and processed for fixation (Section *2.1.2*) and subsequent analysis (Section 2.2.3).

For the dissection of the host epiblast underlying the graft, the following procedure was used. The host embryo was covered with RNAse free PBS and the grafted tissue was removed using a fine needle (30-33G). To show that donor tissue can be removed completely control experiments using grafts from GFP chick embryos were carried out (Figure 2.2 A-D). The ectoderm underlying the graft was cut and then removed using a 20µl pipette and transferred to a 0.2ml Eppendorf tube on ice. For NanoString nCounter analysis

5-1 explants were collected; the tube was spun at 100rpm for 10 seconds to collect tissues. Using a pulled fine glass needle and air pressure the remaining PBS was aspirated and replaced with 5µl of lysis buffer (RNAqueous-Micro Kit, Ambion). The samples were snap frozen and stored at -80°C until further analysis.

## 2.1.6 Protein and Drug treatments

### 2.1.6.1 FGF and SU5402 treatment

Heparin beads (Sigma) were washed in sterile PBS, removed and incubated in 50µg/ml of recombinant Mouse FGF8 isoform b (R&D Systems) on ice for two hours. Subsequently, they were placed into the area opaca of stage HH4$^{-}$ host embryos, which were then cultured for 3 or 6 hours in New culture (Section 2.1.3.1). The ectoderm underlying each bead was then excised and collected as described above (Section 2.1.5).

SU5402 (Tocris Bioscience), an inhibitor of FGF signalling through tyrosine kinase inhibition, was used to attenuate FGF signalling. SU5402 was dissolved in dimethyl sulfoxide (DMSO; Sigma) to make a stock concentration of 10mM; a 25µM solution was used as working solution. AG1X2 beads were incubated in DMSO (1:1000; controls) or DMSO containing SU5402 (25µM) for 2 hours at room temperature. The beads were then washed in PBS for 15 minutes before use to remove excess DMSO and SU5402. Host embryos of stage HH4$^{-}$ were prepared in New culture, lHM or pME donor tissues were prepared as described above (Section 2.1.4.1, 2.1.4.2) and grafted together with 1-2 beads into the extra embryonic region. The embryos were then incubated at 38°C for the required time (3, 6 or 12 hours). After incubation the graft and beads were removed and the underling tissue was processed and collected as above for mRNA analysis (Section 2.1.5*).*

### 2.1.6.2 Dorsomorphin and Bmp4 treatment

Dorsomorphin dihydrochloride (6-[4-[2-(1-Piperidinyl) ethoxy] phenyl]-3-(4-pyridinyl)-pyrazolo [1, 5-a] pyrimidine dihydrochloride, Tocris Bioscience) is a potent inhibitor of BMP signalling, (via the inhibition of Bmp type1 receptors). Dorsomorphin was diluted in DMSO to a stock solution of 10mM; a working concentration of 10µM was prepared in albumin and Tyrode's saline. Embryos at stage HH4$^{-}$ were prepared using the Whatman filter paper culture method (section2.1.3.2) and then immersed in Tryode's saline containing Dorsomorphin (10µM) or DMSO (1:1000) as control, for 20 minutes, before being placed

into a 35mm Petri dish containing 1ml of thin albumin with drug or DMSO. The embryos were then incubated for 3 or 6 hours and subsequently processed for fixation. For mRNA analysis, the area opaca epiblast was collected. Embryo were immersed in RNAse-free PBS on a Slygard coated dish to aid dissection.

Recombinant mouse BMP4 (R&D Systems) was reconstituted at a concentration of 100 µg/ml in sterile 4 mM HCl containing 0.1% bovine serum albumin. Heparin beads were incubated in 1µg/ml BMP4 for 1 hr on ice. Stage HH4$^{-}$ hosts were prepared for New culture and lHM or pME tissues were prepared for grafting as described above (Section 2.1.4). lHM and pME grafts were placed into the area opaca of host embryos together with 1-2 BMP4 coated beads (Section 2.1.5) before being incubated for the required time 3 or 6 hours. Host embryos were processed for fixation or mRNA collection (Section 2.1.5).

#### 2.1.6.3 BIO treatment

To attenuate WNT antagonism from the mesoderm the drug BIO ((2'Z, 3'E)-6-Bromoindirubin-3'-oxime, Sigma Aldrich) a powerful agonist of WNT through its inhibition of GSK-3α/β, was used. A stock concentration of 10mM was made by diluting BIO in DMSO, and then diluted to a 2.5µM working stock. AG1X2 beads were then immersed in BIO at 2.5µM for 2 hours at room temperature before being grafted along with either lHM or pME hosts at stage HH4$^{-}$. The hosts were then incubated for 3, 6 or 12 hours before being processed for either fixation or mRNA collection (Section 2.1.2, 2.1.5)

## 2.2 Molecular biology and analysis

### 2.2.1 Microarray

A microarray screen was previously performed in our lab (Christophorou, 2008) to identify genes induced in response to the lHM that are also present in the pre-placodal region. This screen used lHM-induced area opaca (MIE), non-induced area opaca (NIE), anterior and posterior pre-placodal region (aPPR and pPPR) to compare the transcriptome in all four tissues (Lleras-Forero et al., 2013). The data were analysed the following way, using GeneSpring software (version 7.3.1; Agilent Technologies, UK). To determine whether the data sets were suitable for further analysis and to determine the relationship between and within the biological replicates, principle components analysis and hierarchical clustering

were used. A step-wise process determined differential expression between the conditions under investigation. Samples were first normalized to the 50th percentile across the whole expression dataset and then each gene was normalized to the median of its own expression across each cell type. Prior to statistical analysis, genes classed as being not expressed (absent in biological replicates) or not varying their expression above a twofold level in all cell types were removed from the analysis. Then, one way analysis of variance (ANOVA; p=0.05) was used on the remaining set of genes to determine which genes showed a significant difference in expression levels between each cell type. Those found to be significant were subsequently subjected to the following hierarchical clustering analysis.

The R-statistical packages Hclust and Heatmap.2 were used (Source code appendix 9.2). First a row z score is generated for each gene across all conditions (NIE, MIE, aPPR and pPPR). The value for each individual condition is then compared to the row Z score and the gene is classified as enriched, present or under represented for each condition. Next each gene is scored for its similarity to another and over a number of iterations clusters are generated, being subsequently visualised through a heatmap.

### 2.2.2 NanoString

Extraembryonic epiblast exposed to the different grafts was collected as described (Section *2.1.5*) and stored at -80°C. Following storage, the samples were hybridised according to the nCounter Gene Expression Assay Manual. A NanoString probe set was designed using the results from the described microarray and known genes involved in PPR development from the literature (List of genes- appendix 9.3). The RNA samples were hybridised with capture and reporter probes at 65°c for 16 hours and then transferred to the nCounter Prep Station, where the excess capture and reporter probes were removed. The now purified RNA complex is immobilized and aligned for reading on the imaging plate. This is then transferred to the nCounter Analyser Station, where 600 fields of view are analysed and counted for each sample analysed (Figure 2.3; (Fortina and Surrey, 2008; Geiss et al., 2008).

The resulting data were analysed according to the nCounter Data Analysis Guidelines. The NanoString code sets contain positive and negative control probes for normalisation. First, the positive controls for each lane are summed and then an average is generated across all replicates. To create a positive normalisation factor for each lane, the sum of the positive spike probes is calculated. The sum of each lane is then averaged across the replicates. The summed value of each positive probe set is then divided by the average to create the positive normalisation factor. Following this, an average and standard

deviation are produced for each lane from the negative probe values, the average is added to 2 times the standard deviation, generating a negative normalisation factor. To generate the normalised counts for each mRNA sample the following method is used. First the raw counts are multiplied by the positive lane normalisation factor and the negative normalisation factor is then subtracted for each individual probe value. To remove infinities from the final fold change analysis, any values below the negative normalisation factor are classed as absent, and replaced with the negative normalisation factor. Next, the lanes are normalised to the total amount of mRNA in each lane: the counts for each lane are summed and each individual value is then divided by the lane total, producing a normalised value that can be further analysed.

For each experiment three biological replicates were carried out, their average normalised counts were calculated and this was then used to compare fold changes and p-values (<0.05, unpaired t-test) between different conditions. The p-value and fold change were used to identify significantly changing genes.

One final threshold was applied to identify genes, which could be classed as biologically present in the extra embryonic region. A statistical analysis of the area opaca analysis revealed genes that changed significantly in the extra embryonic region over 3, 6 and 12 hours. Genes which had a positive fold change and a p-value <0.05 were correlated with the raw expression value. Genes were then classed as present if they had a raw count average above 5. This correlated with known expression patterns such as Kremen1.

## 2.2.3 Whole mount in situ hybridisation

### 2.2.3.1 Generation of Dioxigenin (DIG) labelled antisense probes

All cDNAs for antisense probe production were in pBluescript SK or pGEM-T-easy vectors. These plasmids either contain the T7 and T3 or T7 and SP6 RNA polymerase binding sites, respectively. To linearize plasmids they were digested with appropriate enzymes at the correct temperature (Table 1.2), for 4-5 hours or overnight. Linearization of the plasmids was checked by gel electrophoresis by running 1/25th of the reaction on a 1% agarose gel (Sigma) in TAE buffer (242g Tris base; 57.1 ml glacial acetic acid; 100ml 0.5M EDTA pH 8.0 in 1L H2O). A phenol-chloroform extraction was performed to isolate the DNA, which was then precipitated using 1/10x volume of 4M sodium acetate (Sigma) and 2.5x volume of absolute ethanol at -20˚C for a minimum of 1 hour or overnight. The precipitated DNA was

centrifuged at 1600rpm at 4°C for 15 minutes and then washed with 150µl of 70% ethanol followed by 50µl of absolute ethanol, creating a DNA pellet. The pellet was then air dried and subsequently dissolved in 50µl of dd$H_2O$. Transcription reactions using the polymerase T3 (Promega), T7 (New England Biolabs) or SP6 (New England Biolabs) and dNTPs ( Roche) containing 10 mM dATP, 10mM dCTP, 10 mM dGTP, 6.5 mM dTTP and 3.5 mM digoxigenin-11-UTP were set up (Table 1.3) and incubated at 37˚C for 2 hours. After incubation, the DNA template was degraded by adding 1µl of DNase (Promega) for thirty minutes and the correct band size was checked by agarose gel electrophoresis (Table 1.2). This reaction was then precipitated twice using 1/10x volume 4M LiCl and 2.5x absolute ethanol for a minimum of 1 hour or overnight at -20˚C. The precipitated mRNA is obtained by centrifugation at 4˚C at 16100rcf for 15 minutes. The mRNA pellet is then dissolved in 50µl of ddH2O at 37˚C for 15 minutes before being denatured at 95˚C for 3 minutes. It is then immediately put on ice for 5 minutes. A final antisense probe is then made up to approximately 1µg/ml with hybridization buffer and stored at -20˚C.

### 2.2.3.2 Whole mount in situ hybridisation

Chick embryos were collected as described above (Section 2.1.2). They were rehydrated through stepwise incubations of 75%, 50% and 25% absolute methanol in PBS containing 0.1% Tween-20 (BDH; PTW). The rehydrated embryos were incubated in PTW twice for 10 minutes, following this 1µl of Proteinase K (10µg/ml; Sigma) was added. They were then incubated again for 10-30 minutes depending on the stage of the embryo. After incubation, embryos were rinsed with PTW and then placed in 4% formaldehyde, 0.1% glutaraldehyde in PTW (Sigma) for 30-60 minutes. They were washed twice in PTW and transferred to hybridisation solution [50% formamide (BDH); 1.3x SSC pH 5.3(Sodium Chloride Sodium Citrate; BDH); 5mM EDTA; 50µg/ml yeast RNA (Promega); 0.002% Tween-20 (100%; BDH); 0.005% CHAPS (10%; Sigma); 100µg/ml Heparin (50µg/ml Sigma)], for a pre hybridisation step at 70˚Cfor 2-6 hours. Following pre-hybridisation the embryos were transferred to a hybridisation solution containing the antisense probe and incubated at 70˚C overnight. The probe was removed and retained at -20˚C for further use and the embryos were washed 3 times, 30 minutes each, in fresh hybridisation solution at 70˚C. Embryos were washed in a 1:1 hybridisation solution combined with Tris-buffered saline containing 1% Tween20 (TBST; 0.05M Tris, 0.15M NaCl, 1% Tween-20) at 70˚C and subsequently rinsed 3 times in TBST. TBST was used to wash embryos twice for 10 minutes at room temperature; embryos were then incubated in blocking buffer for 3 hours [5% heat inactivated sheep serum (Sigma), 1mg/ml BSA (Sigma) in TBST] before being incubated in anti Digoxigenin antibody

(0.2-0.4µg/ml Anti-sheep/goat IgG-AP, Roche) at 1:2500 in blocking buffer overnight at 4˚C on a rocking platform. The solution containing the antibody is removed and recycled for further use and the embryos are washed 3 times in TBST for 1 hour each. They are then washed in NTMT (0.1M NaCl; 0.1M Tris HCl (pH 9.5); 50mM MgCl2; 1% Tween-20) for 10 minutes and subsequently placed in a foil covered vial with developing solution containing NBT (Nitro Blue Tetrazolium; Sigma) and BCIP (5-Bromo-4 Chloro-3 Indodyl Phosphate; Sigma) as substrates (4.5µl 50mg/ml NBT in N,N-Dimethylformamide (DMF) and 3.5µl 50mg/ml BCIP in 70% DMF per 1.5 ml NTMT). The vial is then placed on a rocking platform at room temperature. Staining was allowed to develop until a dark blue stain was visualised and the embryo was then washed in TBST and placed in 4% formaldehyde until subsequent processing.

| Insert | length | Vector | restriction enzyme | RNA polymerase |
|---|---|---|---|---|
| Ccnd1 | 1230bp | PCR2.1 | // | T7 |
| Eya2 | 2400bp | pbs sk | Not1 | T7 |
| Gbx2 | 900 | // | Bglc2 | T3 |
| Otx2 | 1600bp | Pbs sk | Xho1 | T3 |
| Sall1 | 842 | Pbs sk | // | T3 |
| Six1 | Pbs sk | pbs sk | BamH1 | T3 |
| Sox2 | 500bp | | Xba1 | T7 |
| Sox3 | 100bp | pbs sk | Xba1 | T7 |
| Znf462 | 500bp | Pbs sk | // | T7 |

Table 2.1: Dig labelled riboprobes

| Component | Sp6/T7 RNA polymerase | T3 RNA polymerase |
|---|---|---|
| DNA 3µg/µl | 3µl | 3µl |
| Water | 27µl | 22µl |
| 10x (T7/Sp6: promega) or 5x (T3; NEB) Transcription buffer | 5µl | 10µl |
| 10x DIG nucleotide mix (Roche) | 5µl | 5µl |
| 0mM Dithiothreitol (DTT; Promega) | - | 5µl |
| 1-2mg/µl RNAsin (Promega) | 1µl | 1µl |
| Enzyme (SP6, T7, T3) | 5µl | 5µl |
| Total | 50µl | 50µl |

Table 2.2: Transcription mix

## 2.2.4 Immunocytochemistry

Donor quail tissue was visualised using immunocytochemistry. Embryos were fixed for about 30 minutes following in situ hybridisation and washed extensively in PBS. Next samples were put into blocking buffer (1% goat serum (Sigma), 1% Triton-X100 (Sigma) in PBS for one hour and subsequently incubated in blocking buffer with 1:5 QCPN antibody (Mouse Monoclonal, Developmental Studies Hybridoma Bank, maintained by the Department of Pharmacology and Molecular Sciences, The Johns Hopkins University School of Medicine, Baltimore, MD 21205 and the Department of Biological Sciences, University of Iowa, Iowa City 52242, under contract N01-HD-2-3144 from NICHD) for 2 days at 4°C. The embryos were then washed in PBS 3x30 minutes before being incubated in blocking buffer with horse radish peroxidase conjugated secondary antibody 1:1500 (Goat anti-mouse IgG-HRP, Jackson Immunoresearch Laboratories) for 2 days at 4°C.

After incubation, 3, 3'-diaminobenzidine (DAB) was used to detect and visualise HRP. Embryos were washed in 100mM Tris, pH 7.4 for 5-15 minutes and then incubated in 0.5mg/ml DAB in 100 mM Tris, pH 7.4 in the dark for 5-10 minutes. A concentration of 0.003% $H_2O_2$ was used to start the reaction, the reaction was stopped after sufficient brown staining was visualised. The reaction was then stopped in $H_2O$, and the embryos were then placed in 4% paraformaldehyde in PBS and subsequently processed for photography and wax sectioning (Section 2.2.5, 2.2.6).

## 2.2.5 Wax sectioning

Embryos processed for wax sectioning were placed in Methanol for 10 minutes followed by 10 minutes in Propan-2-ol. They were then transferred to tetrahydronapthalene for 30 minutes at 60˚C and subsequently placed in a 1:1 tetrahydronapthalene: wax solution for 30 minutes and then in wax alone 3 time for 30 minutes each. Next, they were placed in moulds and covered with wax and left to set overnight. The blocks are sectioned into 10um sections on a Lecia RM2245 microtome and are collected on slides. These slides were then left to dry overnight, dewaxed in Histoclear, and then mounted with coverslips using DPX mounting medium (Solmedia).

## 2.2.6 Microscopy

Photographs of whole mount embryos after in situ hybridisation were viewed with an Olympus SZX12 dissecting microscope. Sections were viewed and imaged using an AxioVert 300 M (Zeiss). Pictures were taken with an AxioCam HR digital camera or a Retiga2000 digital camera, the resulting digital files were uniquely named and stored.

## 2.2.7 Bioinformatics analysis

### 2.2.7.1 Clover analysis

The Six1-14 aPPR enhancer sequence was obtained through sequencing of plasmids containing the enhancer construct (kind gifts from Shigeru Sato). This sequence was then compared to sequence taken from a BLAST search using the primers that were described in the supplementary information from the paper (Sato et al., 2010) and found to match. To analyse the Six1-14 aPPR enhancer the Cis-eLement OVERrepresentation (CLOVER) tool was used to discover over represented transcription factor binding motifs. In short, CLOVER analyses the given sequence against a library of transcription factor binding sites against a control input. A combined Transfac and Jaspar vertebrate library was used, and as control the Six1-14 aPPR enhancer sequence was shuffled 1000 times. This generates a P-value for the likelihood of a transcription factor binding site being enriched or occurring by chance and a cut off of $p<0.05$ was used. Clover also generates the position of the binding site within the analysed sequence.

### 2.2.7.2 GENIE3 analysis

An inferred GRN network was created in the following way from NanoString data. The data sets from all tissue grafting experiments were used to generate this network. The mean expression values for each gene under each condition were analysed by the GENIE3 algorithm. In brief, n genes are decomposed into n different regression problems. For each of the regression problems, the expression profile of one gene (target gene) is predicted from the expression profiles of all of other genes (input genes), using tree based ensemble methods. Within this the importance of a single input gene in explaining the profile of the target gene is assessed and an importance measure is generated. This importance measure is then used to predict the regulatory links and their direction within the network. Following

the analysis the top 1000 interactions were isolated, based on the strength of their importance measure and the network was viewed using Cytoscape. For subsequent analysis genes of interest were highlighted with their first neighbours (putative regulators and targets) and small networks were created.

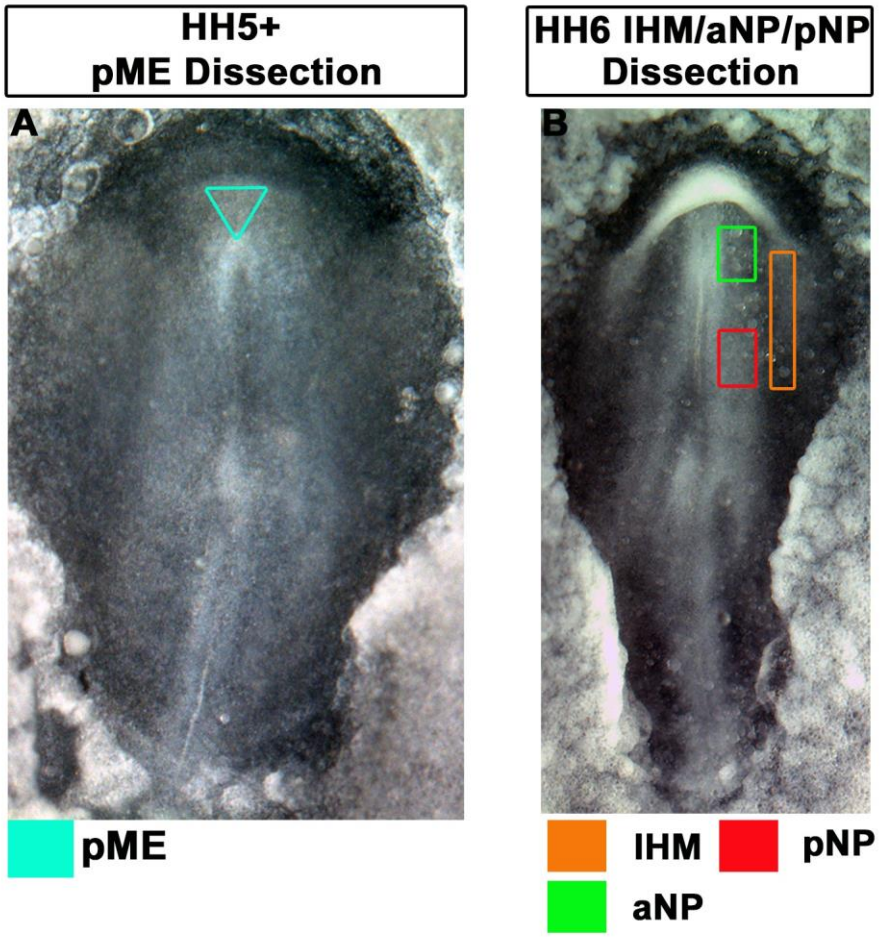


Figure 2.1: Tissues dissected for grafting experiments

**A.** Blue outline shows location of pME dissection at HH stage $5^{+}$. **B**. Outlines of lHM (orange), aNP (green) and pNP (red) dissection at HH stage 6.

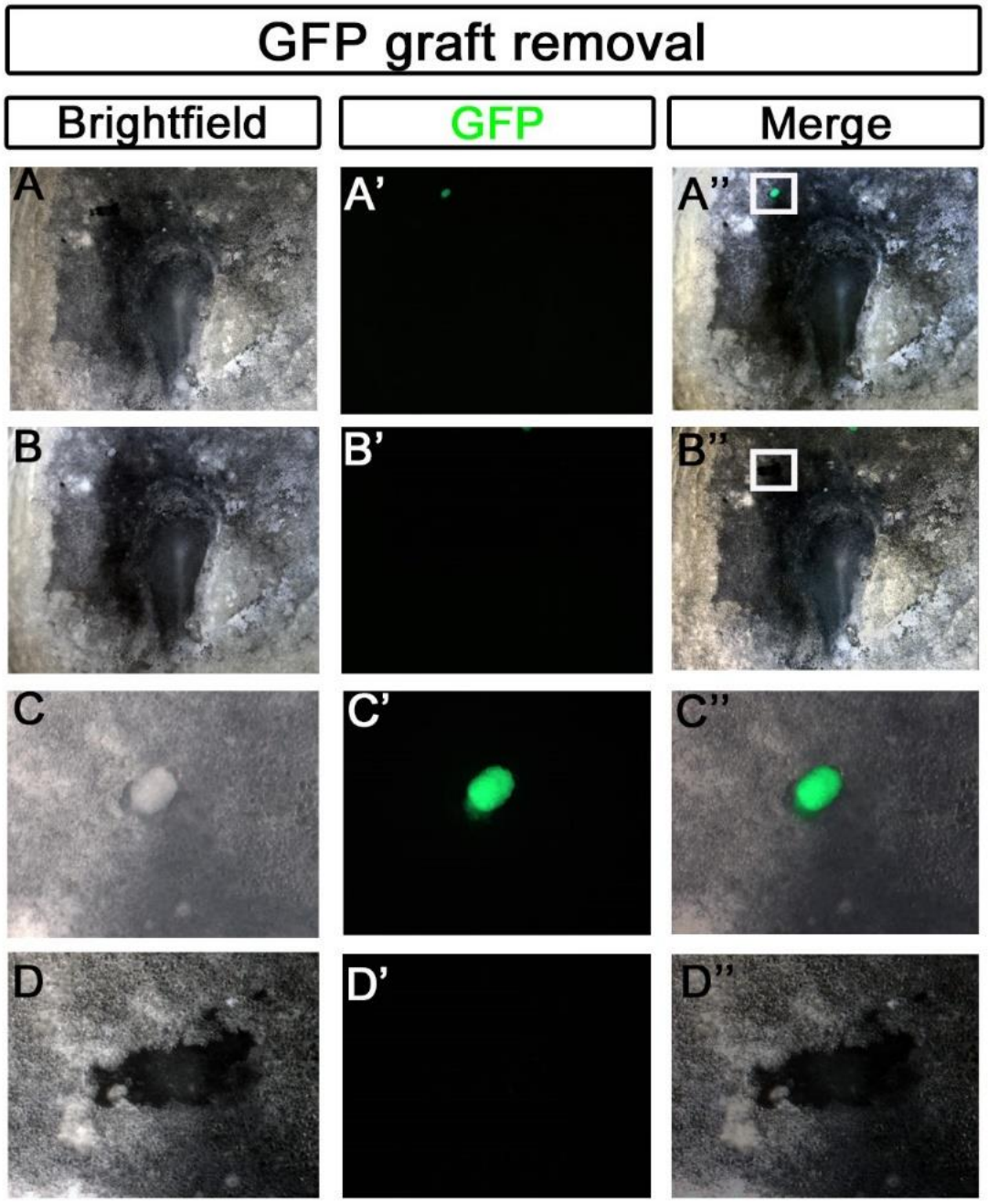


Figure 2.2: Graft removal efficiency

To examine if any cells of the grafted tissue were left behind during removal of the donor tissue, GFP expressing pME was grafted to a HH4- host. After 6 hours the tissue was removed and the host ectoderm underneath was left intact (**A-D**). **A- A''**, Images display location of graft. **B-B''**, images show that the graft has been removed and is not left in the vicinity of the region to be excised. **C** and **D** are higher magnification images of the white boxes in **A''** and **B''.**

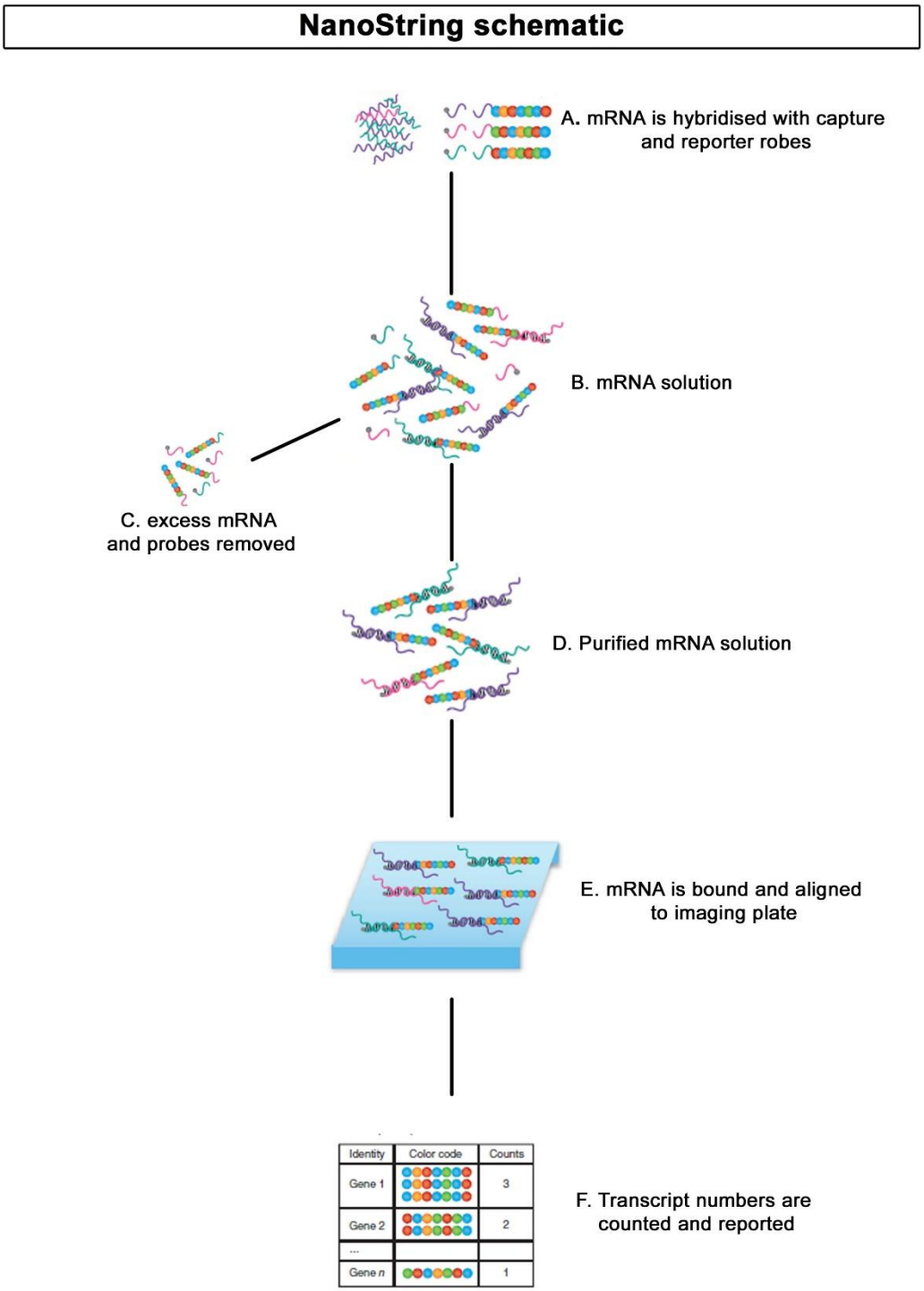


Figure 2.3: NanoString schematic

**A.** NanoString capture and reporter probes are mixed directly with the mRNA. This solution is then purified with excess mRNA and probes removed. **B and C**. This purified mRNA solution is then bound to an imaging plate and the number of reporters, each representing an individual gene copy, are counted. **D and F**. Adapted from Fortina and Surrey 2008).

| Experiment/ time | 3 hours | 6 hours | 12 hours |
|---|---|---|---|
| Lateral head mesoderm | ● | ● | ● |
| Prechordal mesoderm | ● | ● | ● |
| Anterior neural plate | ● | ● | ● |
| Posterior neural plate | ● | ● | ● |
| lHM/aNP | | ● | ● |
| lHM/pNP | | ● | ● |
| pME/aNP | | ● | ● |
| pME/pNP | | ● | ● |
| lHM/Su5402 | ● | ● | ● |
| lHM/BIO | ● | ● | |
| lHM/Bmp4 | ● | ● | |
| pME/Su5402 | ● | ● | |
| pME/BIO | ● | ● | |
| pME/Bmp4 | ● | ● | |
| FGF8b | ● | ● | |
| Dorsomorphin | ● | ● | |

Table 2.3: Experimental conditions

A table displaying the conditions of each experiment and the time points at which these were carried out.

# 3. A screen for new regulators in the pre-placodal region

## 3.1 Introduction

The process of early PPR development and the regulation of *Six* and *Eya* genes, key PPR regulators, is not well known. To understand transcriptional regulation of *Six* and *Eya* and how the anterior-posterior axis of the PPR is set up, a microarray screen was carried out. The lHM, which underlies the PPR and plays a key role in its induction, can induce ectopic *Six1/4* and *Eya2* after 12 hours (Christophorou, 2008; Litsiou et al., 2005). The expression of factors acting upstream should also be initiated within this time frame, and comparison of mesoderm-induced ectoderm (MIE) and non-induced ectoderm (NIE) should reveal such factors. Four cell populations were collected for this screen: MIE and NIE, as well as endogenous anterior and posterior PPR ectoderm (aPPR, pPPR). This comparison will highlight genes involved in PPR regulation and putative regulators of *Six* and *Eya* (Figure 3.1).

Although the PPR can be defined as one continuous piece of ectoderm surrounding the neural plate (Grocott et al., 2012; Schlosser, 2010; Streit, 2007), it can also be separated into anterior and posterior regions. As described above the first markers, which separate the PPR axially are *Otx2* and *Gbx2* (Bally-Cuif et al., 1995; Shamim and Mason, 1999), later followed by genes such as *Six3* and the *Irx* genes, which define new subdomains (Ghanbari et al., 2001; Glavic et al., 2002; Goriely et al., 1999). Subsequently, *Pax* genes are expressed in regions that give rise to different placodal derivatives (Baker and Bronner-Fraser, 2001; Schlosser, 2010). It is not well understood how these spatial differences are regulated and subsequently lead to placodal fate. To understand the spatial difference, aPPR and pPPR tissues was collected, using the visible boundaries of the underlying mesoderm as guideline and analysed separately. Therefore separating the a and pPPR will provide information on spatial differences in the PPR (Figure 3.1, A).

Three replicates for each tissue were collected, lysed and 5ng of total mRNA was hybridised to chick Affymetrix gene chip arrays (Chambers and Lumsden, 2009). The data were analysed by Dr David Chambers using Genespring Gx (Agilent Technologies). First, the data were normalised to separate biological variance from background variance due to technical differences. The raw value of each gene is divided by the mean value of all present genes (Quackenbush, 2001). Subsequently, normalised data were plotted to view equal distribution, 11 samples were equally distributed around 1 and only one sample of the aPPR replicates showed unequal variance (Figure 3.2, A). Next each gene is normalised by the

calculating the average from the biological replicates, these averages are then used to compare values across the different populations and generate statistics.

The validity of the array can be checked by comparing raw values of genes from each cell population with their known spatial expression *in vivo* and their known behaviour in response to a mesoderm graft. The aPPR and pPPR sample can be validated by *Eya2* and *Sox3*, both PPR markers (Litsiou et al., 2005): both samples contain these two genes (Figure 3.2, B). *Eya2*, which is upregulated after 12 hours by the lHM, is present in the MIE sample, but not in the NIE. Raw values for *Six4* are too low across all four cell populations to be considered confirming its low expression level compared to other PPR markers. As expected *Gbx2*, a posterior marker (Steventon et al., 2012), is expressed in the pPPR, but only weakly in the aPPR (Figure 3.2, B), while *Six3* and *Pax6*, markers of anterior fate (Bailey et al., 2006; Ghanbari et al., 2001), are expressed in the aPPR. The neural marker *Sox2* (Streit et al., 1997) is absent from all samples as are two neural crest markers, *Pax7* and *Snail2* (Basch et al., 2006; LaBonne and Bronner-Fraser, 2000) (Figure 3.2, B). Taken together the above correlations suggest the microarray data is valid and reproduces experimental data previously known. It should be noted that not all genes in the chicken genome are represented on the Affymetrix gene chip set. For example, the PPR marker *Six1* is missing from the array.

There are 38,535 probes on the chicken Affymetrix gene chip, of these 12,000 were determined to be of too low a value to be biologically relevant and were classed as absent. To refine the data set, aPPR, pPPR and MIE data were compared to the NIE; all genes with more than a 2-fold change were retained; 10,621 probes met this criterium. A one–way ANOVA determined 3,471 probes to be significant, which were then annotated to gene names using the Affymetrix *chicken.na33.annot.csv* annotation file or by blasting the probe sequence using Basic Local Alignment Search Tool (BLAST, NCBI). This resulted in the removal of 603 duplicate probes, leaving 2,868 unique genes with significant changes of 2-fold and more in at least one cell population (Figure 3.3 A).

The aim of this microarray is firstly to determine genes, which may be involved in PPR formation, and secondly to investigate the role of the lHM in PPR induction. The array was further used to understand spatial differences inherent in PPR development. Finally, the results of this microarray were used to generate a NanoString probe set to investigate PPR development further. To find define genes relevant to these processes hierarchical clustering was subsequently performed on the mean expression value of each of the 2,868

genes. Genes within each cluster were then compared to their endogenous expression at PPR stages (HH6-7), thus identifying genes which are indeed expressed in the PPR or its subdomains and therefore are putative regulators.

## 3.2 Hierarchical clustering distinct gene categories and putative regulators of PPR development

The 2,868 genes were clustered using Spearman correlation in a customised R-statistical script incorporating the H-clust and Heatmap.2 scripts. The original heatmap showed distinct groups for the aPPR, pPPR, MIE and NIE (Figure 3.3, B). To focus on putative regulators of the PPR the 2,868 genes were grouped into functional categories and only putative transcription factors (205 genes) and signalling pathway related molecules (36 genes) were kept for further analysis, leaving a total of 241 genes (8% of total significant genes). Analysis of these showed seven distinct clusters across the 4 populations (Figure 3.3 C). In The heatmap the NIE and MIE appear more similar to each other, while the aPPR and pPPR appear very different from the previous two populations. Although the MIE can induce a number of genes involved in PPR specification, it should be pointed out that the transplanted mesoderm may not fully repress the entirety of genes expressed in the NIE. Another possibility is that the mesoderm transplanted is only partially responsible for PPR fate and cannot induce all of the genes associated with PPR cell fate. It is also possible that the aPPR and pPPR samples contain genes expressed in the adjacent neural plate due to the limitations of the dissection techniques. These three possibilities may explain their similarity to each other than to the PPR samples. However, this does not detract from the changes between the NIE and MIE, which will highlight genes involved in PPR development. The genes which do not change between the NIE and MIE and do not appear in the PPR samples may also provide an indication of genes that repress PPR fate

Cluster 1 (Figure 3.4, A) contains a large number of transcripts (77 genes), showing high expression in both the aPPR and pPPR, low expression in the MIE and little to no expression in the NIE. This is validated when looking at the raw values for a selection of genes in this cluster (Figure 3.4, B). This result suggests that a large number of these genes should be expressed in the aPPR and pPPR with some of them being induced by the lHM. This makes them good candidates for *Six* and *Eya* regulators as well as potential PPR markers. However, a microarray cannot provide distinct spatial information and cannot determine if transcripts are also expressed in other tissues. To look at spatial information the genes in each cluster were compared with their in situ expression at PPR stages (HH

stages $5^{+}$/7) using literature searches, the Gallus Expression In Situ Hybridisation database (GEISHA (Antin et al., 2007) or by carrying out in situ hybridisation. The majority of transcripts in cluster 1 are expressed in the neural plate with weak expression in the PPR, e.g. *Trim24* (Figure 3.4, C), with only *Homer2* (Figure 3.4, D) displaying a similar pattern to *Six1*/*Eya2*. (Many of the insitu hybridisation patterns were done by Monica Tambalo for her PhD thesis, Tambalo 2014) Thus many genes identified as putative PPR regulators are not only present in the PPR, but also in the neural plate and PPR cells.

The largest cluster is cluster 2 (118 genes), which shows high expression in the NIE; many transcripts are induced by the lHM (MIE) while others are down regulated. Generally, there is no expression of these genes in the aPPR and pPPR (Figure 3.5 A, B). In situ hybridisation confirms that these are not expressed in the neural plate or PPR, with many expressed in the non-neural ectoderm, e.g. *Hand1* (Figure 3.5, C). There are also a number of genes in this cluster that are normally considered to be neural crest markers such as *Msx1*, *Msx2* and *Snail2*; indeed some of these are known to be expressed in the non-neural ectoderm and the area opaca (Mancilla and Mayor, 1996; Streit and Stern, 1999) Taken together this suggests that these genes could be good candidates to be repressors of PPR fate and as markers of non-neural ectoderm.

A small set of aPPR enriched genes (16 genes) can be seen in Cluster 3 (Figure 3.6 A) including the known anterior markers *Pax6* and *SSTR5* (Bhattacharyya et al., 2004; Lleras-Forero et al., 2013) as well as a novel aPPR marker *Nfkb1* (Figure 3.6, B, C). Most of these genes are weakly induced by the MIE except for *Nkx2.1, Pax6, SStr5* and *Dido1*. (Figure 3.6, A; MIE). Cluster 4 (Figure 3.7, A) shows a set of genes enriched in the pPPR (13 genes) including *Gbx2* and *Irx2* both known posterior markers (Goriely et al., 1999; Katahira et al., 2000; Shamim and Mason, 1999; Steventon et al., 2012; Tour et al., 2002) and *Ccnd1* (Figure 3.7 B, C). *Gbx2*, *Irx2* and *Ccnd1* are also present in the MIE and therefore may be induced by the lHM. Both clusters contain genes differentially expressed in the aPPR and pPPR, with most genes being induced by the lHM although induction is much stronger for pPPR-enriched transcripts. Members of both clusters can therefore be used to investigate further the regulation of PPR development and its spatial differences.

The final three clusters are much smaller with cluster 5 containing eight genes, cluster 6 and 7 five transcripts each (Figure 3.8, A). In cluster 5, the PPR marker *Eya2* is present (Figure 3.8 D). However, there appears to be contamination from the underlying mesoderm in both aPPR and MIE. This is apparent from the presence of cardiac precursor markers including *Nkx2.5*, *Isl2*, *Fgf8* and *Tbx2* (Lopez-Sanchez et al., 2009; Yamada et al.,

2000; Yuan and Schoenwolf, 2000). This mesoderm underlies the PPR in a crescent similar to the horseshoe shaped pattern of PPR markers, as that of *Eya*2. Cluster 6 contains genes, which are expressed in the posterior neural plate and PPR as well as extending to the non-neural ectoderm, *Zeb2* (GEISHA). Cluster 7 similar to cluster 5, shows another group of transcripts, normally expressed in the pre-cardiac mesoderm and endoderm e.g. *Gata4* , and *Hhex* (Lopez-Sanchez et al., 2009).

In summary, hierarchical clustering reflects known as well as newly defined gene expression patterns and known behaviour of transcripts in the PPR induction assay. Therefore, this strategy can be used to define and predict spatial gene expression patterns and also provide clues as to genes, which may regulate *Six1* and *Eya2* expression and/or PPR development. Using the above genes in conjunction with known genes from the literature a NanoString probe set was designed to analyse the behaviour of all of these genes in experimental manipulations.

## 3.3 Discussion

The PPR is the only region of the ectoderm that is competent to give rise to all placodes (Baker and Bronner-Fraser, 2001; Grocott et al., 2012; Schlosser, 2010; Streit, 2007). While *Six1*, *Six4* and *Eya2* are expressed in a continuous territory surrounding the neural plate, other transcripts already subdivide the PPR along the anterior-posterior axis. Cranial placodes arise from the PPR in a spatially precise manner along the developing central nervous system (Baker and Bronner-Fraser, 2001; Schlosser, 2010). Although some of the signals that mediate these processes have been characterised (Baker and Bronner-Fraser, 2001; Brugmann and Moody, 2005; Brugmann et al., 2004; Glavic et al., 2004; Grocott et al., 2012; Litsiou et al., 2005; Pieper et al., 2012; Stuhlmiller and García-Castro, 2012; Wilson et al., 2001), the transcriptional regulation is less well understood. In particular, we know little about the upstream factors that initiate and restrict Six and Eya gene expression and which factors are responsible for rostro-caudal patterning.

The microarray screen was designed to investigate how the PPR is established and, in particular, which transcripts are involved upstream of the Six/Eya cassette. The lHM is a known inducer of the PPR: when grafted next to competent epiblast it can induce a full set of known PPR markers in the chick embryo (Litsiou et al., 2005) and it is necessary for PPR development in *Xenopus* (Ahrens and Schlosser, 2005). This experimental set up therefore provides a useful assay to identify novel putative PPR regulators. Comparing mesoderm-

induced transcripts with those present in the endogenous a- and pPPR refines candidate genes further to those actually co-expressed with *Six1/4* and *Eya2* at some point.

Sato has identified an aPPR Six enhancer which is conserved in mouse, fish and chicken (Sato et al., 2010), numerous transcription factor binding sites were identified for this enhancer including binding sites for homeodomain transcription factors. The Homeodomain transcription factor *Dlx5* was shown to positively regulate the expression of this enhancer in chick (Sato et al., 2010). *Dlx6* falls into the aPPR cluster in the above screen and therefore its enrichment in the aPPR may indicate its involvement in the positive regulation of Six1 in the aPPR. Conversely, *Msx1* falls into the NNE enriched factors and its expression pattern shows that it is enriched in the posterior ectoderm and future neural crest matching its role as a repressor of the aPPR Six1 enhancer (Betancur et al., 2010; Khudyakov and Bronner-Fraser, 2009; Sato et al., 2010; Streit and Stern, 1999; Yardley and García-Castro, 2012).

Although a number of competence factors for the PPR genes *Six1* and *Eya2* have been discovered including *Gata3*, *Foxi1* and *Tfap2a/c* (Bhat et al., 2013; Kwon et al., 2010) none of these genes were found to be enriched in the array. It is possible that as they are expressed in a large domain spanning the NNE up to the neural plate and that the described dissections do no provide a great enough resolution to allow for their detection. Another possibility is the requirement of these factors at early blastula/gastrula stages means that they are no longer present at high enough levels to be detected.

The array was designed to uncover potential regulators of *Six* and *Eya*, while it has provided a number of genes that are present in the region that the PPR forms it is not possible to look for genes which are directly clustered with the Six genes for the following reasons. The Affymetrix annotation for chicken does not contain a probe that can be attributed to Six1, therefore it is absent from our data set. The probe for *Six4* showed little or no activity across the 4 sets and therefore was not enriched in any of the 4 conditions and genes which may have clustered with either of these two genes could not be identified. *Eya2* was present in the screen and did cluster with a number of genes however a large number of upregulated genes were cardiac progenitor markers: *Nkx2.5*, *Isl2*, *Fgf8, Tbx2, Gata4* and *Hhex* (Lopez-Sanchez et al., 2009; Yamada et al., 2000; Yuan and Schoenwolf, 2000) and are a result of contamination from the underlying mesoderm. Therefore the cluster containing *Eya2* is not ideal to identify genes which may regulate *Eya2*.

The majority of transcripts fall into two clusters the NNE and the NP/PPR clusters, interestingly this fits with the region that PPR cells originate from; the neural plate border.

The neural plate border is the region in which genes from the neural plate and NNE overlap; this overlap in genes that will come to be expressed in either the neural plate or the NNE is present at primitive streak stages and PPR stages (Baker and Bronner-Fraser, 2001; Basch et al., 2006; Betancur et al., 2010; Grocott et al., 2012; Pieper et al., 2012; Schlosser, 2006; Schlosser, 2010; Streit and Stern, 1999). Therefore the array has identified genes of either of these two categories (NP or NNE) but very few genes that are specific to the PPR.

A number of genes were found to have a similar pattern of expression (Cluster 1Figure 3-4). These included *Trim24*, *N-myc*, *Otx2*, *Zic3* and *Homer2*. When analysing the in situ hybridisation patterns of these genes, only *Homer2* stood out as marking the same precise territory of placode precursor cells that *Six1* and *Eya2* mark, suggesting that *Homer2* can be a new PPR cell marker. Although *Homer2* is extremely interesting due to its spatial expression and members of the *Homer* family have been shown to interact with *Pax6* (Cooper and Hanson, 2005), its functional role remains to be investigated.

Expression patterns of induced genes were looked at from multiple sources (Tambalo, 2014; Trevers, 2015). Genes in this cluster had a broader expression pattern at PPR stages, encompassing not only the PPR but also the neural plate at primitive streak stages. A number of these genes are expressed well before *Six1* and *Eya2*; with the genes *Otx2*, *Trim24*, *Zic3, Mier1, Sox11* and *N-myc* all found to be expressed during pre-streak stages (Bally-Cuif et al., 1995, Trevers 2015). This suggest that the neural plate and PPR have a large similarity in gene expression and there is a similarity to the pre streak stage embryo, this similarity will be investigated in later experiments. Overall these genes are expressed in the neural plate and PPR and expression pattern analysis reveals a number are expressed before *Six1* and *Eya2* and therefore may be putative regulators of the PPR.

The microarray screen shows a large set of genes (Cluster2, Figure 3.5) which are highly expressed in the NIE and not in the PPR including *Msx1*, *Msx2* and *Hand1*. These genes are markers of non-neural ectoderm and in the case of *Msx1* have been shown to repress the expression of and anterior PPR enhancer associated with *Six*1 (Sato et al., 2010). The expression of these genes such as *Hand1* and *Msx2* in the NNE may suggest that they are negative regulators of the PPR which confine the expression of PPR genes such as *Msx1* or are positive regulators of the PPR which were present in the neural plate border but have become refined to the NNE. When comparing the pre-streak patterns of these genes to those discussed earlier (e.g. *Trim24*, Cluster1) it was found that they had a complementary expression pattern, where they are expressed around the edge of the embryo in the

peripheral epiblast rather than the central epiblast of the previous group. Therefore, it is possible that these genes are regulators of the PPR in either a negative or positive manner.

A smaller set of genes is found to be enriched in either the aPPR or pPPR. Indeed, analysis of their spatial pattern matches the array results with *Nfkb1*, *Sall1* and *Pax6* being predominantly expressed in the aPPR and *Gbx2*, *Irx2* and *Ccnd1* in the pPPR. The MIE values suggest there is induction of certain targets in both sets, there is stronger induction and similarity in the pPPR. This raises the possibility that the MIE is much closer in composition to the pPPR. The aPPR expresses *Pax6*, the marker of lens fate, the pPPR shows no expression of the otic marker *Pax2* and neither are induced by the lHM. In the case of the pPPR it is not surprising as *Pax2* expression has not begun at the time the tissue was dissected. Subsequently, these targets are possible regulators of spatial differences in the PPR and their function in subdividing PPR needs to be established in the future and how they cooperate with each other and with *Six*/Eya needs to be established. The nested expression of these genes may define small subdomains of PPR cells that later develop into olf, lens, tri, epi, otic, and may help understand the transcription factor code that determines individual placodes.

The potential role of the lHM can be uncovered through the comparisons of the lHM enriched genes and the genes which are enriched in the aPPR and pPPR conditions. A large majority of genes in cluster 1 are induced by the lHM and these may be good candidates for regulating *Six1* and *Eya2* in the PPR. The lHM also negatively regulates a number of the genes in the NNE cluster (Cluster2), suggesting that these genes need to be down regulated for the gene cascade that is responsible for the induction of *Six1* and *Eya2* to be activated (e.g. Msx1 (Sato et al., 2010)). There are a small number of genes that are not enriched in the NIE but are induced by the lHM such as *Irx4*, the role of these genes which are enriched by the lHM but not present in the NIE or a and pPPR needs to be investigated further as their role is unknown. The lHM also induces genes in the aPPR and pPPR clusters, although aPPR induction is to a lesser extent than pPPR induction and is most likely due to the location of the lHM. As the lHM resides under the pPPR and is more likely to be involved in pPPR induction. Consequently, the lHM induces a PPR like character and represses the NNE character and this repression may be the first step in the induction of a PPR domain and then the PPR gene cascade can occur.

Although the lHM is required for PPR formation and sufficient to initiate characteristic gene expression (Ahrens and Schlosser, 2005; Litsiou et al., 2005) unlike the endogenous PPR, ectopic lHM-induced PPR cells are not lens specified, nor do they switch

on otic markers when exposed to an otic inducing signal, FGF2 (Christophorou, 2008; Martin and Groves, 2006). This suggests additional signals or factors are missing that allow the induced cells to develop into cranial placodes. To uncover such factors it will be interesting to determine which PPR expressed transcripts from cluster 1 (neural plate/PPR), cluster 2 (NNE/PPR), cluster 3 (aPPR) and cluster 4 (pPPR) are not mesoderm-induced. These genes might provide some insight into the missing factors that require further investigation.

In conclusion this screen has provided a large number of new genes, which can be used to investigate further how the PPR is set up and subdivided in the embryo. In addition to analysing the function of individual genes in this process, the data presented here allow me to dissect the response to mesoderm-derived signals further and to ask whether this tissue sets up initial patterning of the placode territory.

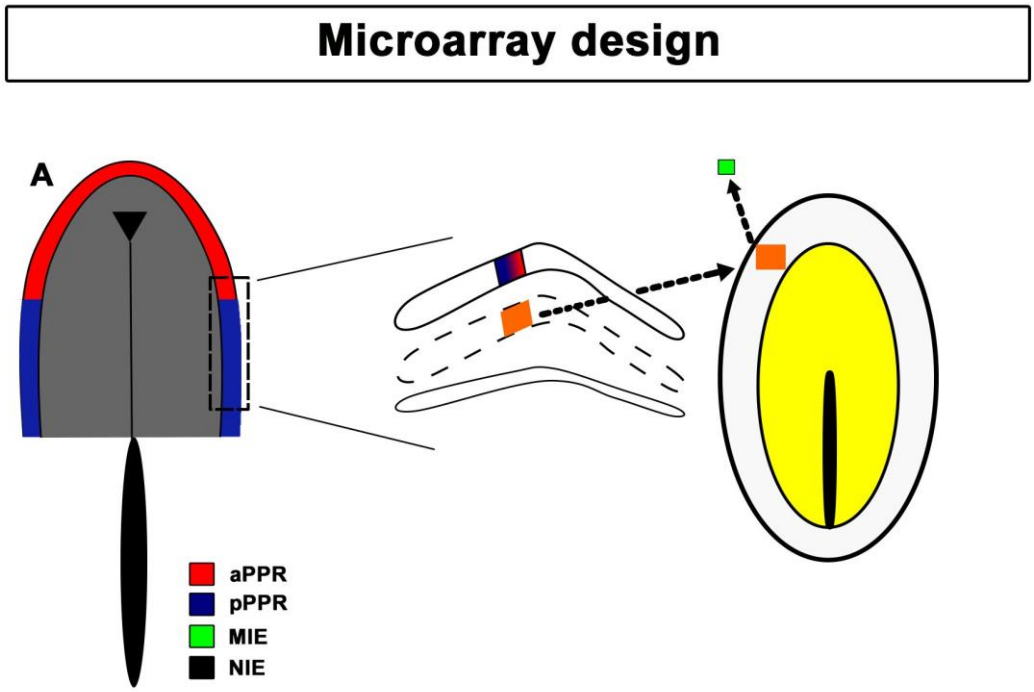


B

| | NIE | MIE | aPPR | pPPR |
|---|---|---|---|---|
| Area opaca enriched | + | - | - | - |
| Mesoderm induced | - | + | + | + |
| PPR enriched | - | -/+ | + | + |
| aPPR enriched | - | -/+ | + | - |
| pPPR enriched | - | -/+ | - | + |
| PPR inhibitory | + | -/+ | - | - |

Figure 3.1: Experimental design of microarray

**A.** diagram showing the location of tissues dissected for the screen: non-induced ectoderm – black square (**NIE**), mesoderm-induced ectoderm - green square (**MIE**), anterior PPR – red territory (**aPPR**) and posterior PPR – dark blue territory (**pPPR**). **B.** Expected patterns of enrichment defining each territory.

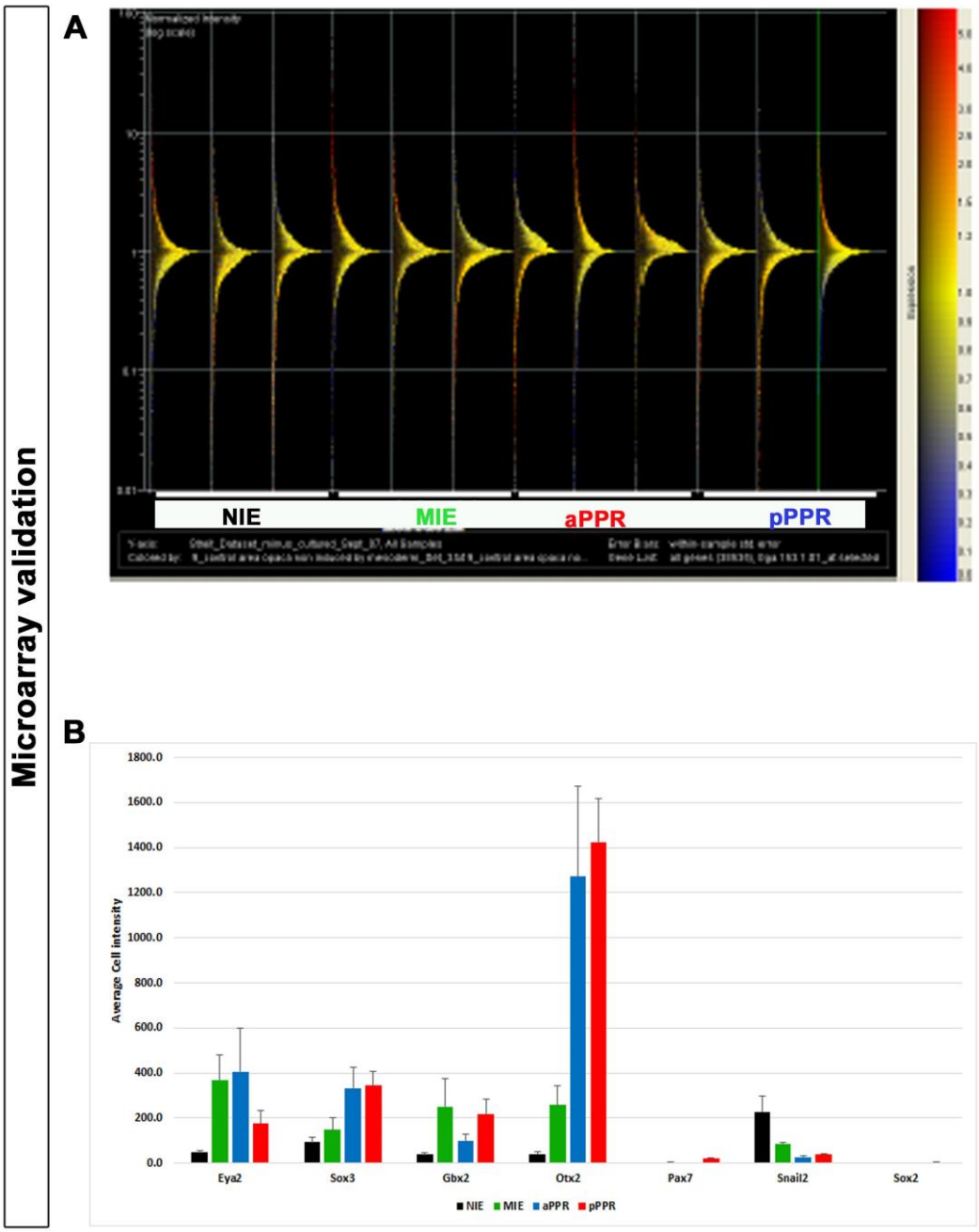


Figure 3.2: Microarray validation

**A.** Normalised microarray data showing equal distribution around 1 for 11 of 12 samples, only sample 9 (**aPPR-3**) showed unequal variance. **B.** Graph of average cell intensity values for all four populations. Genes of known behaviour and expression patterns show the expected values indicating that that the array data are a valid representation of the PPR and mesoderm induced PPR. Error bars represent standard error

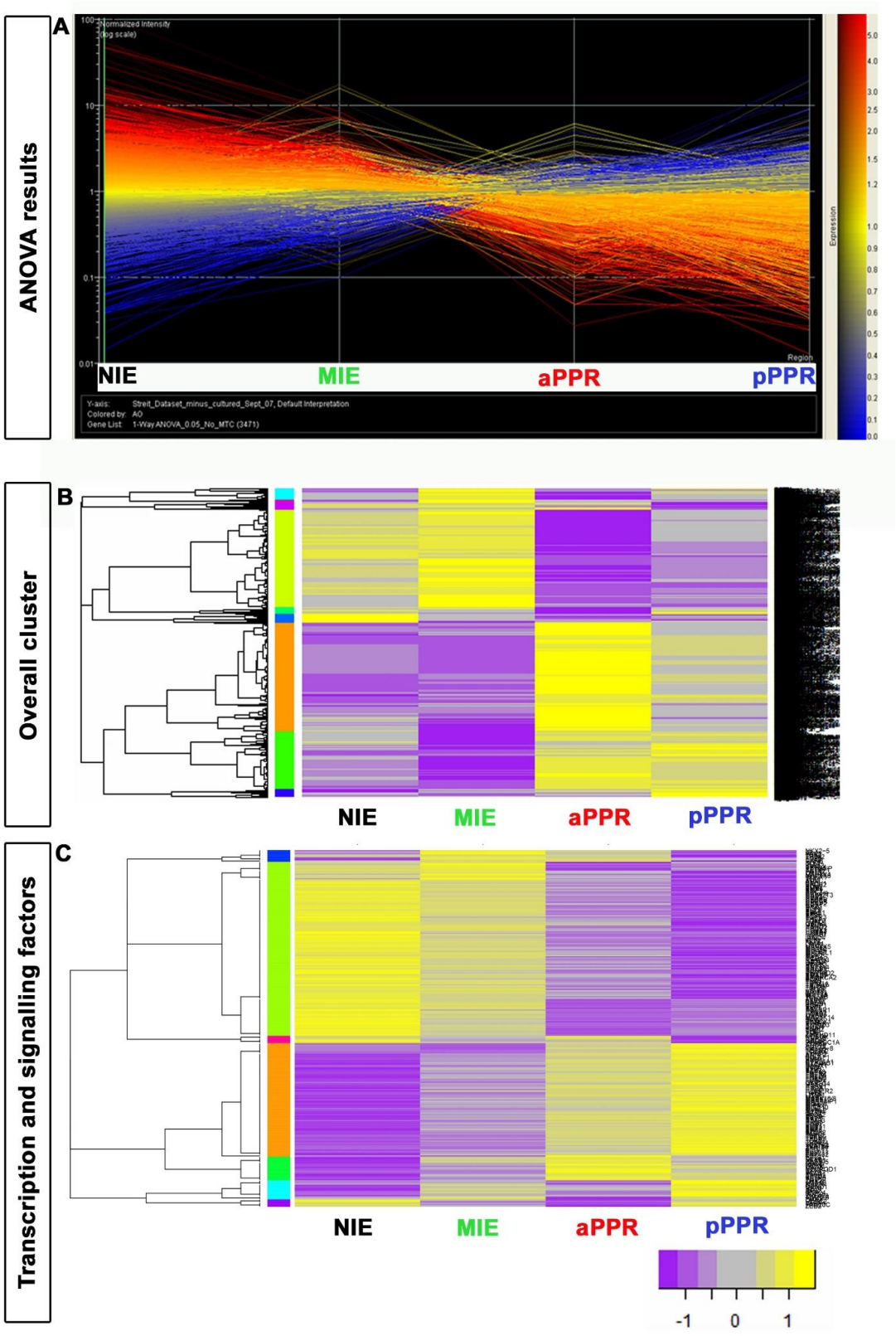


Figure 3.3: Microarray results

Figure 3.3 **Microarray results**

**A.** 3,741 transcripts were significantly different (p value <0.05) in at least one cell population; this diagram shows their expression profile across all four tissues. Coloured lines represent levels of expression in the area opaca; red is strongly expressed and blue is weakly expressed. **B.** 2,868 were unique transcripts; these were subsequently clustered based on expression profiles and segregate into 8 large clusters. Yellow represents highly enriched genes; purple indicates genes which are under enriched. Shown in key below heat maps **C.** Putative transcription factors and signalling pathway members were re-clustered producing distinct groups of genes in 7 clusters.

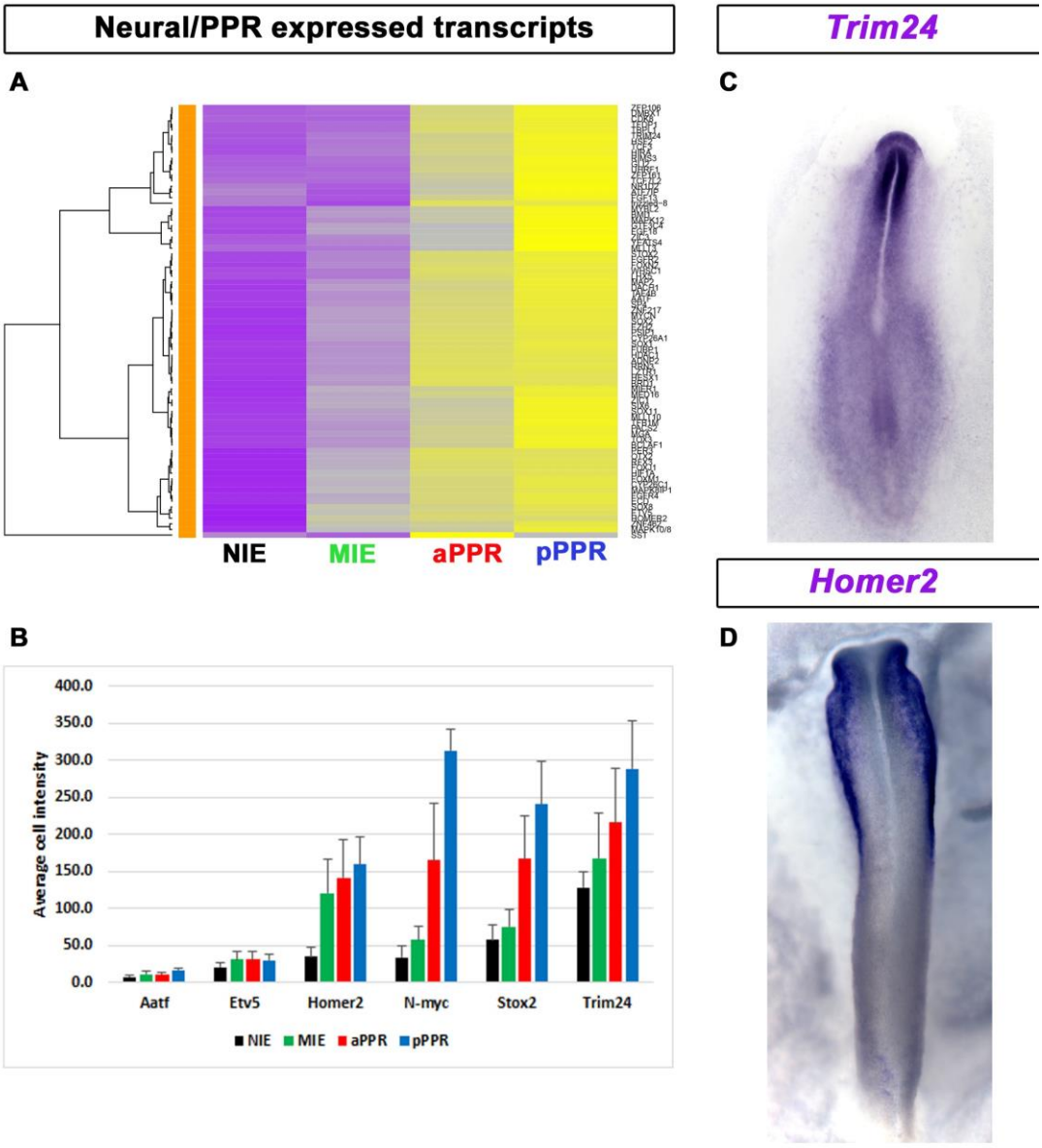


Figure 3.4: Neural/PPR cluster

**A**., A large cluster of transcripts prominently expressed in both the **aPPR** and **pPPR,** also being weakly induced by the mesoderm **(yellow = low expression, grey = no change, purple = high expression),**. **B,** average cell intensities plotted for genes in this cluster to validate the heatmap, genes are statically significant when compared to the **NIE. C-D**, in situ hybridisation showing expression of *Trim24* (**C**) and *Homer2*. Error bars represent SEM.

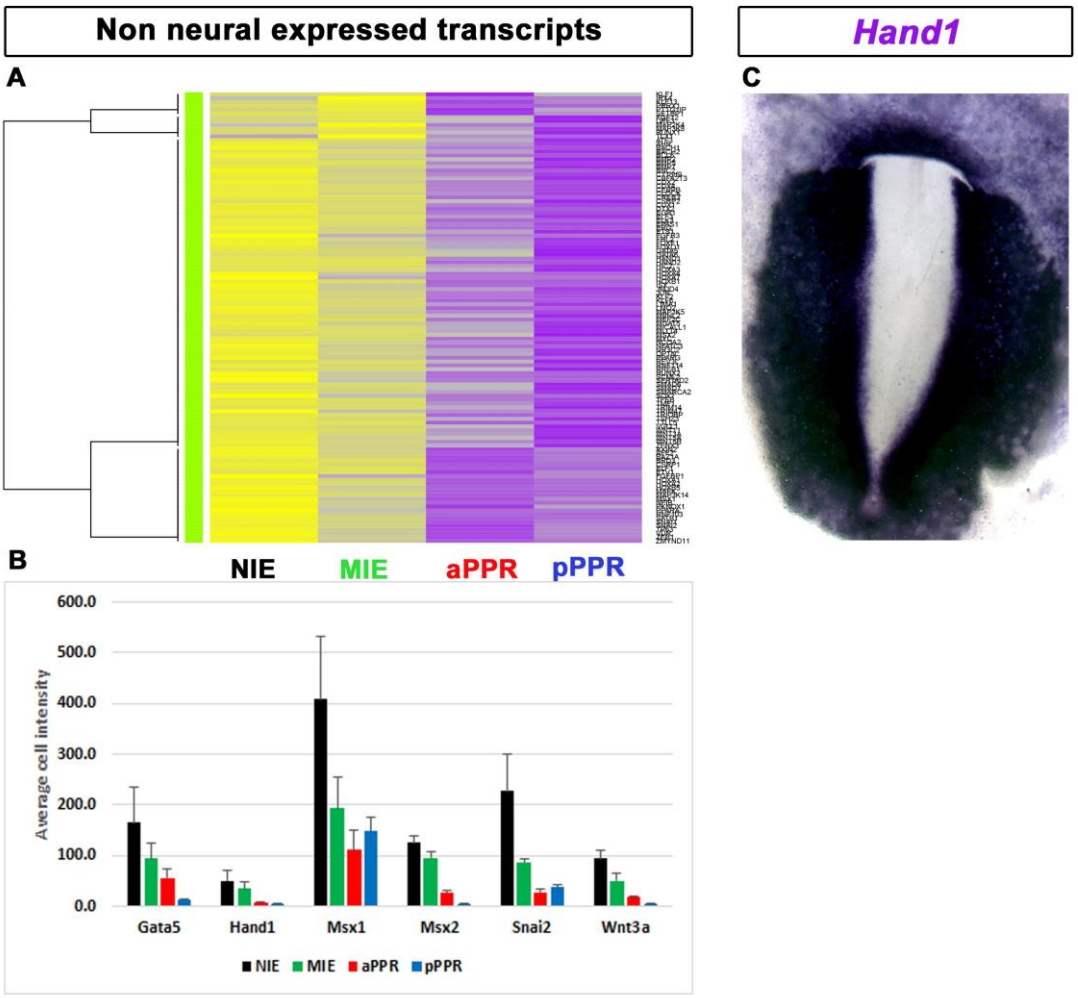


Figure 3.5: Non-neural ectoderm cluster

**A**, cluster of transcripts that are enriched in the non-neural ectoderm (**NIE**) and, weakly in the **aPPR**, **pPPR** and **MIE**. **(yellow = low expression, grey = no change, purple = high expression). B,** average cell intensities plotted for genes in this cluster to validate the heatmap, genes are statically significant when compared to the **NIE**.**C**, Expression profile of *Hand1* showing that it is restricted to the non-neural ectoderm and possibly the PPR.

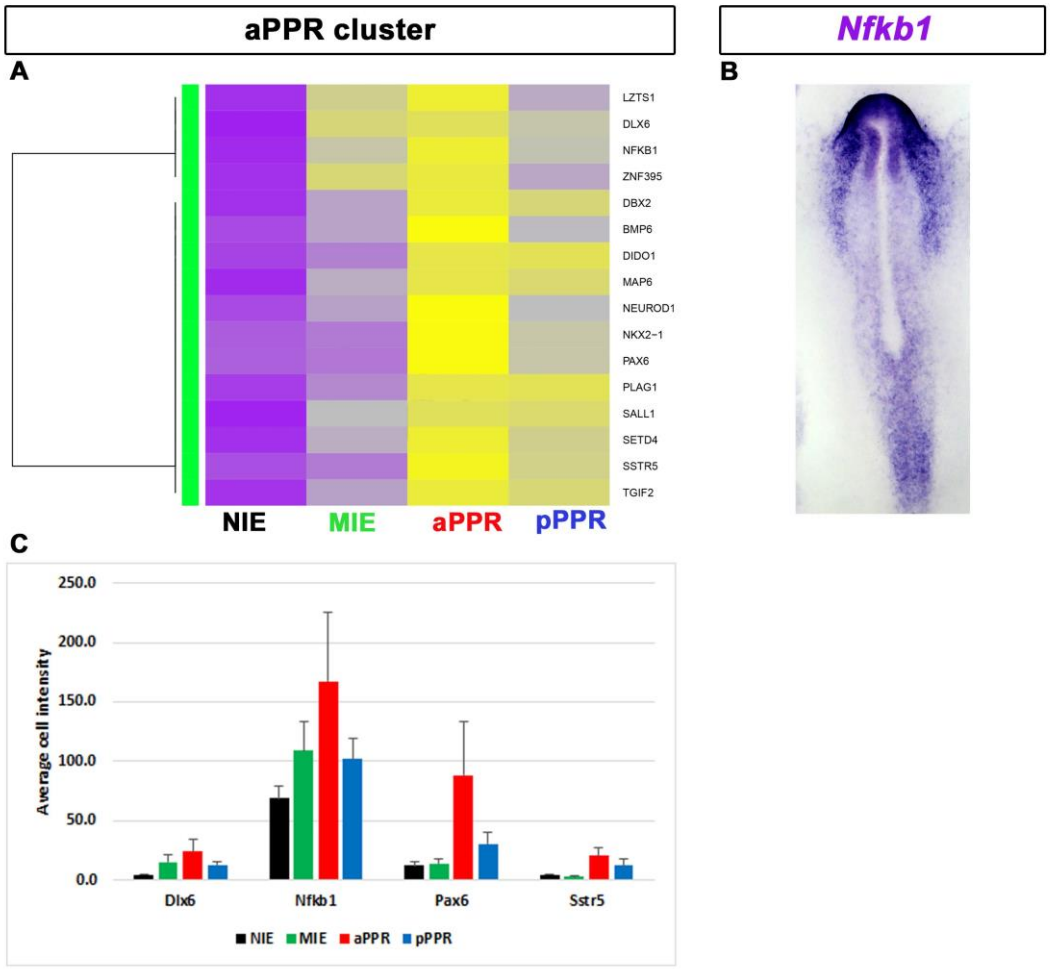


Figure 3.6: aPPR cluster

**A**, Anterior PPR enriched transcripts which are also induced by the lHM and are expressed lower in the pPPR and weakly in the NIE **(yellow = low expression, grey = no change, purple = high expression), B,** average cell intensities plotted for genes in this cluster to validate the heatmap, genes are statically significant when compared to the **NIE. C**, *Nfkb1* displays stronger expression in the aPPR region.

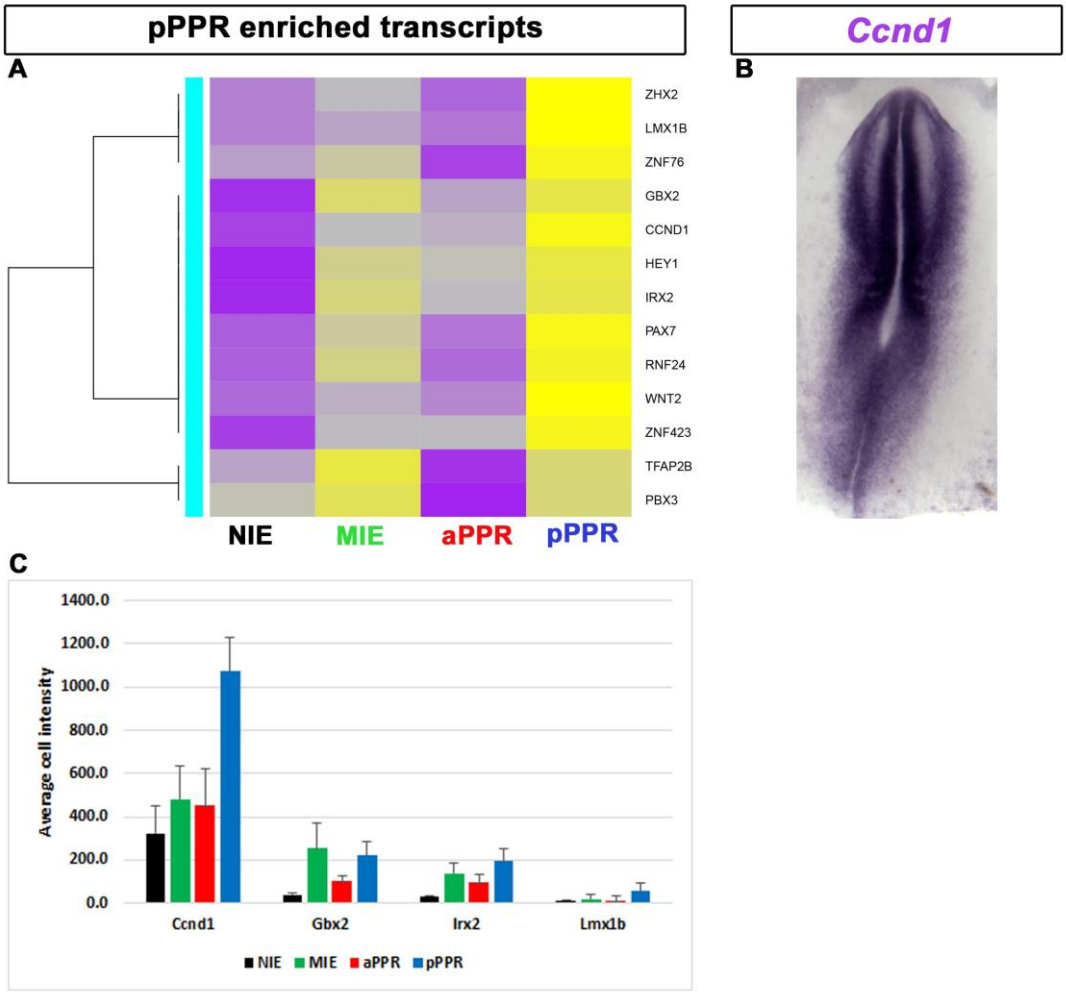


Figure 3.7: pPPR cluster

**A**, Cluster of genes enriched in the **pPPR** and may be induced by the lHM, they are absent or expressed at a lower value in the **NIE** and **aPPR (yellow = low expression, grey = no change, purple = high expression)**. **B,** average cell intensities plotted for genes in this cluster to validate the heatmap, genes are statically significant when compared to the **NIE C**, Ccnd1 is enriched the pPPR of a HH7$^{+}$ embryo (**C**).

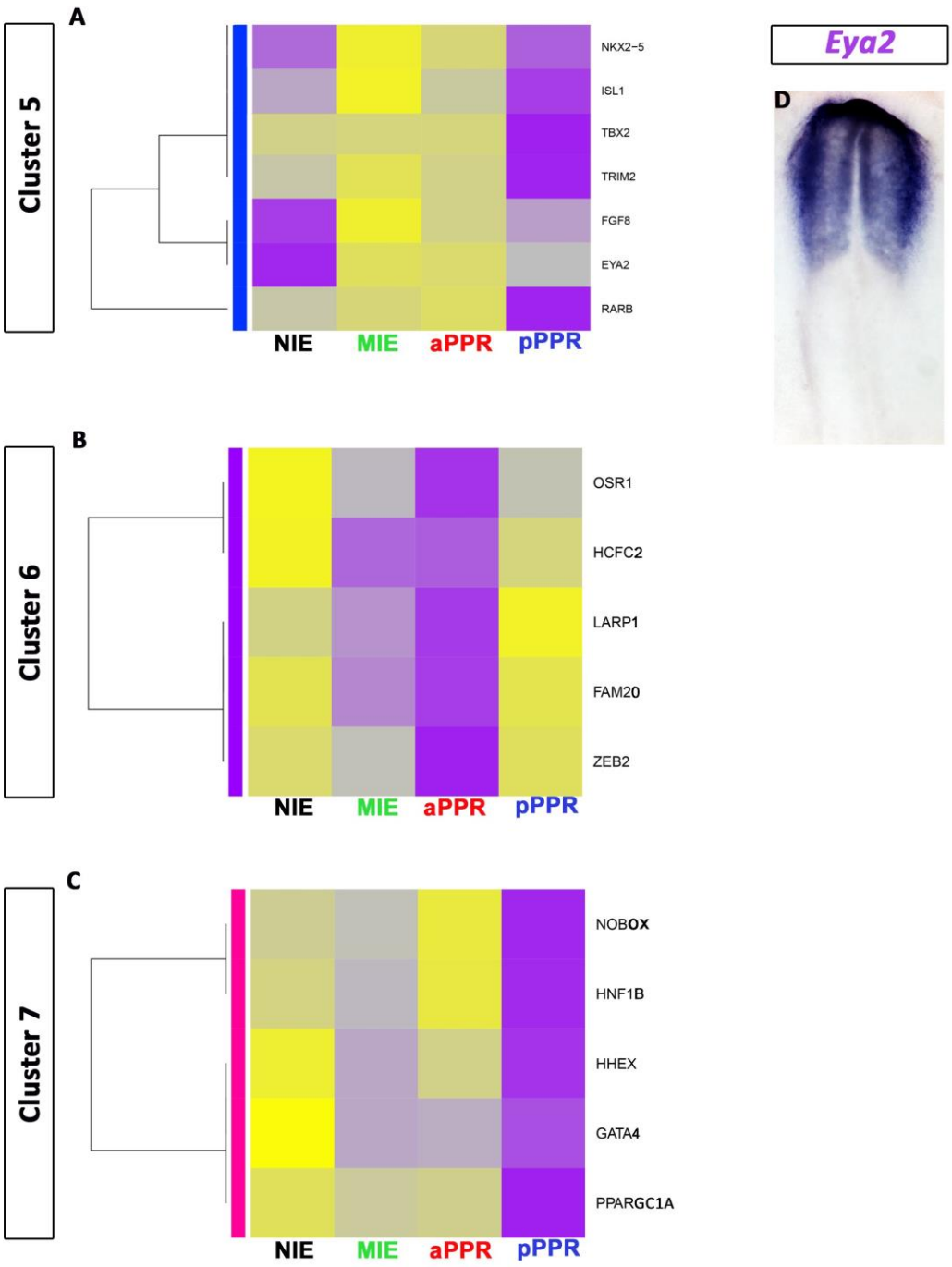


Figure 3.8: Eya2 cluster and small clusters of cardiac precursors

**A**, Eya 2 was clustered with a number of cardiac precursor cell markers: *Nkx2.5*, *Isl2*, and *Fgf8*, expressed in the underlying mesoderm however their spatial pattern did coincide with Eya2 (Lopez-Sanchez et al., 2009). **B**, Cluster 6 has genes that are expressed in the posterior and NIE, such as *Zeb2* (GEISHA) and *Osr1* another gene involved in heart development (Stricker et al., 2006). **C**, Cluster 7 contains cardiac cell precursors such as *Hhex* which is enriched in the anterior of the chick at HH6 (Lopez-Sanchez et al., 2009).

# 4 The role of mesoderm and neural tissues in PPR and placode induction.

## 4.1 Introduction

PPR induction is a complex process with different tissues having been implicated. Our current knowledge is largely based on classical embryology experiments using tissue grafting and ablation experiments in different species, as well as tissue recombination in vitro (1.4.3). Experiments in the newt *Taricha torosa* showed roles for various tissues in the induction of placodes including the heart mesoderm, endoderm and neural plate (Jacobson, 1963a; Jacobson, 1963b; Jacobson, 1963c; Jacobson, 1966). The hindbrain and lateral mesoderm have been implicated in induction and patterning of the otic placode (Alvarez et al., 2003; Gallagher et al., 1996; Hatch et al., 2007; Kil et al., 2005; Ladher et al., 2010; Schimmang, 2007; Waddington, 1936; Woo and Fraser, 1997; Wright and Mansour, 2003). The pharyngeal endoderm is in part responsible for the induction of the epibranchial placodes (Begbie et al., 1999; Nechiporuk et al., 2007) and signals from the neural tube appear to be responsible for trigeminal placode induction (Canning et al., 2008a; Stark et al., 1997). However, how these tissues cooperate, whether they induce specific placodes from the PPR or induce a PPR before induction of a placode is largely unknown.

There are few studies that investigate PPR induction and in particular the regulation of the PPR markers *Six1/4* and *Eya2*. In chick, the lHM is required for PPR formation and induces *Six1/4* and *Eya2* expression in the extra embryonic region after 12 hour's contact (Christophorou, 2008; Litsiou et al., 2005), while the pME is necessary for the induction of *Six1/Eya2* and *Pax6* in the aPPR (Lleras-Forero et al., 2013). Likewise, in Xenopus the cranial endomesoderm is necessary for PPR-specific expression of *Six1*. Thus, two different mesodermal populations have been implicated in PPR induction. Do both possess PPR inducing ability? Do they impart regional character? As the PPR forms it becomes already dived along the anterior-posterior axis based on the expression of genes such as *Otx2*, *Six3*, *Gbx2* and *Irx3* (Kobayashi et al., 2002; Steventon et al., 2014). This subdivision precedes the formation of mature cranial placodes. It is therefore possible that the lHM (posterior) and pME (anterior) induce PPR with distinct regional bias. To investigate the spatial subdivision of the PPR, experiments in this chapter will first establish if the pME acts as a PPR inducer and, if so, explore the differences and similarities between the response to lHM and pME signals.

The role of the neural plate in PPR induction remains controversial. In Xenopus, the anterior neural plate (aNP) can induce *Six1* ectopically in belly ectoderm (Ahrens and Schlosser, 2005). In contrast, in chick the neural plate does not have this ability (Litsiou et al., 2005), but does induce *Pax6* ectopically (Bailey, 2006). To resolve the question of whether the neural plate plays a role in PPR induction and how it cooperates with signals from the mesoderm, I will investigate the response of competent ectoderm to signals from the future fore- and hindbrain alone, and in combination with the mesoderm.

Induction of PPR markers takes a significant amount of time, in the case of the chick 12 hours exposure to lHM signals are required before a complete set of PPR genes is expressed (Christophorou, 2008). This suggests that there may be a cascade of events involving different transcriptional regulators controlling the induction of *Six1/4* and *Eya2*. Since in chick the extraembryonic region is competent to generate the PPR and sensory placodes (Litsiou et al., 2005) grafting inducing tissues into this region provides a useful tool to investigate putative regulators over time. Using this approach induction from time point zero can be investigated and time course experiments make it possible to create a temporal hierarchy of genes in response to different inducers.

In the previous chapter I described how the microarray screen identified different groups of genes related to PPR formation. Using these data I have now designed a NanoString probeset (Appendix9.3) to assess their expression changes in response to tissue grafts over time. This allows me to dissect the temporal hierarchy upstream of *Six1/4* and *Eya2* and to uncover the similarities and differences in response to signals from the mesoderm (lHM, pME) and neural plate (aNP, pNP), as well as combinations thereof.

## 4.2 A transcriptional hierarchy in response to mesoderm signals

### 4.2.1 Response to the lateral head mesoderm

To investigate the response of genes, suggested from the array screen and experimental evidence from the literature, to signals from the lHM, grafts were placed into the inner third of the extraembryonic region of primitive streak stage hosts (Figure 4.1, A). At this stage the extraembryonic epiblast is competent to form sensory placodes if exposed to appropriate signals (Litsiou et al., 2005) . After 3, 6, 12 or 24 hours the graft was removed and the underlying ectoderm was excised and analysed using the NanoString probe set containing known PPR and placode markers, newly identified transcripts (e.g. *Nfkb1*, *Trim24* and *Ccnd1*; see chapter 3) and genes specific to the neural crest and neural plate, as well as read outs to various signalling pathways. The induced ectoderm was compared to contralateral,

time matched, non-induced ectoderm (NIE) and transcripts with more than 1.2 fold change and a p-value less than 0.05 were considered significant. This analysis reveals changes in gene expression over time. Most transcript included in the NanoString probeset are expressed in different, partially overlapping domains during normal development. To interpret the meaning of a particular combination of genes at a given time point, I considered and compared their endogenous expression in the chick at pre-primitive streak (EGXI-XII; (Eyal-Giladi and Kochav, 1976)), primitive streak HH4$^{-}$/4; and head fold stages (HH6/7; PPR stage). This allowed me to determine to which embryonic territory the induced tissue corresponds.

Three hours after an lHM graft, there are a number of differentially regulated genes with *Bcl11a*, *Ccnd1*, *ERNI*, *Etv5*, *Mier1*, *N-myc*, *Otx2*, *Trim24* and *Zic3* being upregulated (P-value <0.05, Figure 4.1, C). The upregulation of *Trim24* was validated by in situ hybridisation; indeed, *Trim24* is expressed in the extraembryonic ectoderm overlying the grafted quail lHM (Figure 4.1, B, and B' (Due to the high level of expression of *ERNI* in the sample, *ERNI* values were removed from all graphs to allow easier visualisation. All significant *ERNI* values can be found in appendix 9.6)). At the same time, several transcripts are downregulated including *TfTfap2aa*, *Axin2*, *Dlx5*, *Eef1a1*, *Gata2* and *Kremen1* (P-value <0.05, Figure 4.1., D). Induced genes were then compared to their endogenous expression patterns, to find a relevant embryonic stage for the comparison the stage at which a majority of genes were first expressed was used. Therefore, if a set of genes which contained certain genes expressed at early stages and others at later stages, the later stage was used to find the region of expression overlap. Comparison of induction and expression patterns at 3 hours reveals that all upregulated genes, except *Bcl11a* (expression unknown), were expressed before primitive streak formation, e.g. *Trim24* (Figure 4.1, E). The expression of all upregulated transcripts overlaps in the central epiblast of the pre-streak embryo (Figure 4.1, F, Trevers 2015, Bally-Cuif et al., 1995; Streit et al., 2000). Conversely, downregulated genes were found to be expressed in the periphery of the pre-streak epiblast and are known non-neural ectoderm markers e.g. *Dlx5* and *Gata2*, (McLarren et al., 2003; Pera et al., 1999; Sheng and Stern, 1999; Trevers, 2015). Thus, the earliest response to lHM signals induces a domain that resembles the epiblast at very early stages of development.

At six hours after an lHM graft, a number of genes remain upregulated including *Ccnd1* and *Trim24*. In addition, several new genes are now induced among them *Cited2*, *Nfkb1*, *N-myc*, *Sall1*, *Sox3* and *Znf462* (Figure 4.2, B). *Sall1* induction was validated using quail grafts followed by in situ hybridisation (Figure 4.2, A-A'). At the 3 hrs time point, analysing the endogenous expression analysis of the upregulated genes suggests that the

induced domain is equivalent to the pre-streak epiblast as exemplified by the expression of *Sall1* (Figure 4.2, B, D). The downregulated genes now include the epidermal marker *Keratin19*, while *Axin2*, *Dlx5* and *Eef1a1* remain repressed by the lHM (Figure 4.2, C). These genes are expressed in the periphery of the pre-streak epiblast and mark NNE territory in the embryo at PPR stages (McLarren et al., 2003; Pera et al., 1999, Trevers 2015). Thus, the gene expression profile induced 6 hours after exposure to lHM signals continues to be equivalent to the epiblast prior to gastrulation.

By twelve hours exposure to an lHM graft, 28 genes are upregulated and the picture becomes increasingly complex. These include the PPR markers *Six1/4*, *Eya2*, the newly identified PPR marker *Homer2* and the *Six/Eya* co-factor *Dach1* (Figure 4.3, A). The *Six1* competence factor *Tfap2a* is also upregulated (Kwon et al., 2010) as are several genes involved in histone modification and DNA methylation such as *Ezh2*, *SetD2, Dnmt3b* and *Whsc1* (Figure 4.3, A). Interestingly, the pPPR markers *Foxi3* and *Gbx2* are present, as is the anterior marker *Otx2*. However, *Gbx2* is induced much stronger than *Otx2* (more than 3-fold over *Otx2*; Appendix 9.-9.5), while *Otx2* induction has declined as compared to the 3-hour time point. This finding suggests that after prolonged signalling, Gbx2 is the dominant factor of the mutually repressive pair (Katahira et al., 2000; Millet et al., 1999; Steventon et al., 2012; Tour et al., 2002). The induction of *Foxi3* was validated using quail grafts followed by in situ hybridisation (Figure 4.3, C-C'). Downregulated genes now include the neural crest and NNE markers *Msx1* and *BMP4*, both known to regulate *Six1* negatively at neural plate and PPR stages (Figure 4.3, B, (Ahrens and Schlosser, 2005; Chapman et al., 2002; Kwon et al., 2010; Litsiou et al., 2005; Sato et al., 2010).

Together, these results suggest that a region similar to the endogenous PPR has been induced in the extraembryonic epiblast. Several of the genes induced only begin to be expressed at HH5/6 in the normal embryo e.g. *Six1/4* and *Eya2* (Figure 4.3, D) and these are confined to the PPR itself. This indicates that the induced domain resembles the PPR. Other transcripts include factors that are initially expressed in the entire non-neural ectoderm, but by HH6/7 become restricted to or upregulated in the PPR for example *Gata3, Foxi3*, *Homer2 and Dlx6*. Several of these (*Dlx, Gata3*, *Foxi3*) are known to regulate the PPR markers *Six1* and *Eya2* (Ahrens and Schlosser, 2005; Esterberg and Fritz, 2009; Khatri et al., 2014; McLarren et al., 2003; Sato et al., 2010; Woda et al., 2003). In addition, there is still induction of *Otx2* and *Sall1*, which are generally confined to more anterior regions of the HH6 embryo. However, their endogenous expression overlaps with the anterior most portion of the pPPR, which is in turn marked by *Foxi3* and *Gbx2*. High levels of the latter

suggest that the induced territory has a transcriptional profile that closely resembles the pPPR.

At 24 hours there are relatively few genes induced and the earlier transcriptional profile is lost (Figure 4.4, A). This may indicate that the lHM does not have the ability to maintain PPR specific gene expression over time and requires additional signals to stabilise this fate, or that unknown signals in the area opaca overcome the initial induction. For example, it is possible that high levels of WNT signalling (Wilson et al., 2001) override PPR character, since Wnt antagonism is required for PPR formation, or have changed the properties of the inducing mesoderm.

In summary, the lHM induces a domain that resembles the most anterior portion of the pPPR with high levels of *Gbx2* and *Foxi3* suggesting a strong posterior bias. Over time, the induced tissue passes through different transcriptional states with the first resembling the gene expression profile of the pre-streak epiblast before progressing to a PPR-like state. Ultimately, the lHM seems to bias this PPR towards posterior character. Finally, these experiments have identified numerous genes, which are induced by the lHM before *Six1* and *Eya2* and are therefore possible upstream regulators.

### 4.2.2 aPPR induction by the prechordal mesendoderm

The pME is necessary for the induction of *Eya2* and *Pax6* and has been shown to impart anterior character to the central nervous system when grafted ectopically in the chick (Foley et al., 1997; Lleras-Forero et al., 2013; Pera and Kessel, 1997). These results make the pME a good candidate to control the aPPR formation. However, it is unknown if the pME is sufficient to induce the expression of *Six1* or *Eya2*. To investigate this the pME from HH5/6 Quail donors was grafted into the extraembryonic region of $HH3^{+}/4^{-}$ chick hosts and analysed after 16 hours by in situ hybridisation. 5/8 grafts (62%) induced *Six1* and 7/8 grafts (87%) induced *Eya2* after 16 hours (Figure 4.5, *Six1* n=8; A-A', *Eya2* n=8; B-B'). Once the inducing ability of pME was established, the response of the epiblast to pME grafts was assayed using the same parameters as in the lHM experiments.

At three hours a small number of genes are upregulated: *Ccnd1*, *Etv5, ERNI*, *Gbx2*, *Irx1*, *N-myc*, *Otx2*, *Trim24* and *Zic3* (Figure 4.6, A and B). This upregulation was validated by in situ hybridisation for *Ccnd1* after quail pME grafts (Figure 4.6, D-D'). Downregulated genes were *Tfap2a*, *Axin2*, *Eef1a1*, *and Gata2* (Figure 4.6, C). As for the lHM, when the endogenous expression for these genes was examined, it was found that they match the

central (upregulated transcripts) or peripheral (downregulated transcripts) epiblast of a pre-streak embryo, such as *Ccnd1* (Figure 4.6, E and F).

The number of genes induced at 6 hours increased to 25; the transcripts that remained upregulated included *Ccnd1*, *Etv5, ERNI N-myc*, *Otx2*, *Trim24* and *Zic3* (Figure 4.7 A). Newly induced transcripts comprised the PPR markers *Six1* and *Six4* and their co-factor *Dach1*, as well as *Cited2*, *Sall1*, *Sox3* and the Zinc finger proteins *Znf462* and *Znf423*. The induction of *Znf462* was validated by in situ hybridisation (Figure 4.7, C-C'). The genes downregulated at 3 hours remain repressed and are joined by *Dlx3/5* and *Msx1* (Figure 4.7, B). Unlike the three hour induced genes, whose expression in the normal embryo is initiated before gastrulation (see above), several of the new transcripts are first expressed only at late primitive streak stages. In particular, *Six1* and *-4* have a very weak expression in the neural plate, before being strongly expressed in the PPR (Esteve and Bovolenta, 1999; Sato et al., 2010). The overlapping expression of the induced genes thus matches a stage HH4/4$^{+}$ embryo in the anterior epiblast as shown by the expression of *Otx2*, *Sall1, Nfkb1* and *Six1* (Figure 4.7, D and E *Sall1*; Sato et al., 2012). Although there is expression of *Six1*, there is no expression of *Eya2* or *Homer2*, another PPR marker, suggesting that these cells have not yet fully reached a PPR-like state.

By twelve hours all PPR markers - *Six1*, *Eya2*, *Dach1* and *Homer2* - and anterior specific genes such as *Dlx6*, *pNOC*, *Sstr5* and *Six3* are upregulate in response to pME signals. While enriched genes *Otx2* and *Sall1* remain upregulated and NNE markers remain down regulated (Figure 4.8, B). In situ hybridisation confirms that indeed quail pME induces Otx2 (Figure 4.8, C-C'). The endogenous expression of these genes strongly suggests a domain resembling the aPPR has been induced. (Figure 4.8, A, D and E).

The 24 hour time point shows upregulation of a large number of genes indicating that. Unlike the lHM, the pME continues to signal and gene expression changes occur. Using the above inductions as a guide, it could be expected that the 24 hour time point might resemble a HH10-11 embryonic region. The transcripts now include *Sox10, Bmp4*, *Foxi3, Dlx3/5/6*, *Irx1/2/3*, the PPR markers *Six1, Eya2, Homer2*, retinoic acid regulator *Cyp26C1* and the anterior placode and forebrain marker *Pax6* (Figure 4.9, A). Only a small number of genes are downregulated and include the NNE marker *Hand1.* Although there is expression of *Pax6*, which may indicate that an anterior placode domain (lens, olfactory placode) has been induced, the results are not definitive as a large number of other markers are also induced and the comparison to endogenous expression suggests the presence of a mixed domain. There does not seem to be a single tissue that co-expresses all 24 hour induced

transcripts. *Sox10* is *normally* expressed in neural crest cells, but also in the otic placode. Other upregulated transcripts include genes expressed in the otic placode such as *Foxi3*, *BMP4, Irx1* and *Lmx1b*, but several are also present in other tissues including the neural tube and other placodes including the trigeminal and dorsal neural tube (Geisha (Abelló et al., 2010; Antin et al., 2007; Khatri and Groves, 2013; McKeown et al., 2005). *Cyp26C1* is normally expressed in the hindbrain, forebrain, retina and otic territory (Bothe and Dietrich, 2006; Reijntjes et al., 2004), while *Irx3* and *Gbx2* mark posterior neural tissue (Kobayashi et al., 2002; Shamim and Mason, 1999; Steventon et al., 2012). Although not significant *Pax2*, expressed in the mid-hindbrain boundary and the otic placode, displays a 262-fold increase over the NIE. Thus, it is difficult to interpret the identity of the tissue induced just considering the gene expression data. After 24 hours, it was often difficult to visualise and remove the pME graft, and it is therefore possible that graft tissue was included in the excised ectoderm thus contaminating the tissue. In addition, occasionally a vesicular structure was present in the grafted area (data not shown); together with the gene expression profiles this suggests that a nervous system-like territory may have been induced together with placodal structure.

In summary, the pME induces a PPR-like state by twelve hours and prior to this cells pass through stages that resemble the pre-streak epiblast and anterior neural plate border ectoderm. The induction of aPPR-specific genes indicate that the pME provides signals that bias the induced ectoderm to aPPR identity. Late response to a pME graft cannot be interpreted without additional experiments including careful study of gene expression by in situ hybridisation and host/donor labelling.

It is interesting to compare the response to lHM and pME signals. Three hours after grafting, the majority of transcription factors are common for both tissues (73%; Figure 4.10, A), with only *Mier1, Bcl11a* (lHM) and *Irx1* (pME) differentially induced. At six hours the similarity drops to 59% of all genes induced being identical (Figure 4.10, B), as the pME begins to initiate the expression of different factors such as *Six1*/4 and the induced domain starts to resemble an anterior neural plate border domain. By twelve hours only 43% of the transcripts are the same; the lHM-induced domain now has upregulated the pPPR markers *Foxi3* and *Gbx2*, while the pME induced territory now has an aPPR bias expressing *Six3*, *Sall1*, *Otx2*, and *Dlx6*. (Figure 4.10). These results suggest that the early steps in response to the pME and lHM are very similar and could reflect the induction of a "common state". Continued signalling subsequently imparts anterior-posterior bias onto the induced tissue reflecting the axial origin of the inducing tissue.

## 4.3 The neural plate induces a domain of mixed identity

As discussed above the lHM and pME can induce posterior and anterior biased PPR, respectively, in competent epiblast. However, neither tissue can directly induce full mature placodes (Ahrens and Schlosser, 2005; Christophorou, 2008; Litsiou et al., 2005) suggesting that other signals are required for the transition between PPR cells and placode cells. The neural plate has been proposed to provide signals that can induce PPR and placode markers although its precise contribution is still under discussion (Ahrens and Schlosser, 2005; Litsiou et al., 2005; Woo and Fraser, 1997). Therefore, the PPR inducing abilities of the future forebrain (anterior neural plate, aNP) and the future hindbrain (posterior neural plate, pNP) were investigated. The aNP or pNP from HH5/6 embryos was grafted into the extraembryonic region of a chick host at $HH3^{+}/4^{-}$ (aNP, Figure 4.11, A; pNP Figure 4.12, A). The ectoderm underneath was then excised at 3, 6, or 12 hours and analysed using NanoString; induction or repression of genes was compared to control NIE from the same time point.

Three hours after contact with the aNP only a small number of genes including *ERNI*, *Dlx5* and *Stox2* are induced in the overlying epiblast. These three genes are expressed at pre streak stages, however the other genes induced at this time point are not expressed pre-streak (*Bcl2* and *Chd7's* early expression is unknown). Therefore defining a related embryonic region at this stage is very difficult (Figure 4.11, C)

At six hours, a total of 15 genes are induced including *Etv5*, *Otx2, Sox3 and Sall1*. Many of these are also normally expressed in the epiblast at pre-streak stages (*Otx2, Sox3, Sall1, Etv5* and *Trim24*) while others are only turned on at neural plate stages (*Nfkb1*) (Figure 4.11, D). However, in addition the NNE gene *Foxi3* is also present, suggesting that the aNP may induce a mixed domain or a territory similar to the neural plate border, where both neural and non-neural genes overlap. By 12 hours, many more transcripts are initiated after neural plate grafts, however the identity of the domain induced is difficult to determine. Some induced genes are normally present in the neural plate of HH5/6 stage embryos such as *Sox2*, *Stox2*, *Znf462* and *Znf423*, while others do not overlap and are present in the NNE e.g. *Eya2*, *Gata3* and *Pax6* (Figure, 4.11,E) . It thus seems that an aNP graft induces a territory of mixed identity, although of overall anterior character with genes normally enriched anteriorly; *Otx2* and *Pax6* (Figure 4.11, B; 3-12hrs).

The pNP induces genes that also reflect its origin. At three hours there is induction of 14 transcripts and these include *Gbx2*, *Gata3*, *Irx1*/2, *Sox2* and *Zic3*. A number of genes

are expressed at pre-steak; *Etv5*, *Gbx2* and *Otx2*; while others are not induced until gastrulation; *Stox2* and *Irx1*/2; while *Sox2* is not present until HH5/6, suggesting that a mixed identity domain has been induced at 3 hours (Figure 4.12, C). At six hours the profile of genes induced changes with the expression of neural plate specific genes; *Sox2*, *Stox2*, *Znf423*, *Znf462*; neural plate border markers, *Etv5*, *Irx2/3* and *ERNI* and the down regulation of NNE genes *Gata2*, *Dlx3/5*, *Tfap2a* (Figure 4.12, D). At twelve hours a much larger cohort of genes is present and again includes a number of neural markers *Sox2*, *Stox2*, *Znf423*, *Znf462* but also genes absent from the neural plate at HH5/6 stages *Eya2*, *Lmx1b*, *Sox10*, *ERNI* (Figure 4.12, E). The presence of genes enriched in the posterior portion of the neural plate (*Ccnd1*, *Gbx2*, *Irx2* and *Lmx1b*) suggests that a domain of mixed identity has been induced but with a posterior bias (Figure 4.12, B; 3-12hrs).

In summary, the aNP and pNP induce domains of mixed identity in ectoderm competent to generate neural and placodal tissue. The induced territories seem to have an axial bias that resembles the origin of the inducing tissue.

Overall for all single grafts, at three hours the timing of induction and earliest onset of endogenous expression match a pre-streak state for the lHM and pME, the neural plate domains at this time point are difficult to define. At six hours the earliest point when the majority of genes are expressed is around the time of gastrulation $HH4^{-}$; and twelve hours matches a HH5/6 stage embryo.

## 4.4 Signals from the mesoderm and neural plate cooperate to subdivide the PPR.

The above results show that the lHM and pME provide cues to bias the induced ectoderm to a posterior or anterior PPR. Although the neural plate does not induce a definitive domain it does seem to impart positional information depending on its axial origin. A number of studies implicated signals from both tissues in placode induction (Ahrens and Schlosser, 2005; Ladher et al., 2000; Litsiou et al., 2005; Stark et al., 1997). However, it is unclear if the neural plate provides a generic signal or a region-specific signal. The aim of the next set of experiments was therefore to investigate if the combination of neural plate and mesoderm induces regionally defined placode domains and how the axial origin influences this process. Therefore, grafting experiments were carried out in which both tissues from the same (homotypic; lHM and pNP; pME and aNP) or different axial levels (heterotypic; lHM and aNP; pME and pNP) were combined. Grafts were placed into the extraembryonic region of $HH3^{+}/4^{-}$ and analysed by NanoString after 6 and 12 hours.

### 4.4.1 Otic/Epibranchial progenitor induction by the lHM and pNP

A combination graft of the lHM and pNP at six hours induces 29 transcripts which span the neural plate and posterior neural plate border domain; *Sox2*, *Stox2*, *Six1*, *Homer2*, *Foxi3* and *Gbx2* (Figure 4.13, A). These genes are consistent with a posterior neural plate border domain (Figure 4.13, B). Genes down regulated include the NNE markers *Gata2*, *Dlx3*, *Tfap2a* and *Msx1* (Figure 4.13, A). This is in contrast to the lHM and pNP single grafts at six hours; which induce a primitive streak or a neural plate border domain (section; 4.2.1, 4.3) respectively. At twelve hours there are now only 24 transcripts induced by the combination graft, with the induction of genes such as *Six1*, *Sox2* and *Stox2* lost. However a number of new transcripts have been induced, these include *Eya2*, *Gbx2*, *Lmx1b*, *Sox10* and *Pax2* (Figure 4.13, C). When analysing the overlapping regions for expression of known genes at the embryonic time point they are all expressed (HH8-10) at this time point 50% of the genes induced are expressed within the otic/epibranchial (Figure 4.13, D) and includes the definitive otic epibranchial progenitor (OEP) marker *Pax2* (Groves and Bronner-Fraser, 2000; Padanad and Riley, 2011). This is in contrast to the lHM and pNP single grafts at 12 hours which only have 37% and 31% of genes expressed in OEP's respectively and neither up regulates *Pax2*. Overall the combination of the lHM and pNP initially at 6 hours creates a posterior neural plate border like domain and by 12 hours the cells have a resemblance to OEPS.

### 4.4.2 pME and aNP combination grafts may induced a nested domain similar to the LOP

The combination of a pME and an aNP, when grafted at 6 hours leads to the up regulation of 20 transcripts; including Gbx*2, Otx2, Irx1/2* and *Stox2* (Figure 4.14, A). NNE markers are down regulated by the combination graft (Figure 4.14, A). The induction of these markers when compared to the overlapping expression domain in the early embryo, resembles the neural plate border at the boundary of anterior and posterior (Figure 4.4.3, B). At twelve hours, the combination graft now leads to the upregulation of many more genes (53 transcripts) such as, *Dlx6, Sstr5*, *Sall1*, *Six1*, *Six3, Pdlim4* and *Pax6* (Figure 4,14, C). Around a third of the genes (29%) are expressed in lens and olfactory progenitors (LOP), this is only slightly higher than the pME (22%) and the aNP (21%) single graft, suggesting the combination only marginally improves the ability to induce LOPs. There is also a low level induction of otic and epibranchial genes; *Irx1*, *Lmx1b* and *Sox10*. Although these genes are

expressed in the OEPD, it should be noted that they are expressed in different tissues. *Lmx1b* and *Irx1* are expressed in the forebrain at later stages (HH12+), it is possible that the pME and aNP creates conditions that induce a forebrain state. It is important to note that only the combination provides induction of *Pax6* and *Six3* together, with other lens markers such as *Gata3*, *Dlx6*, *Pdlim4* and *Sox2*; olfactory markers *Dach1* and *Hesx1* and the PPR markers *Six1* and *Eya2*. This may indicate a nested domain of cells that more closely resembles LOPs has been induced by the combination. This may be part of a larger induction of a forebrain like-state, explaining the induction of genes that have varying expression patterns e.g. *Lmx1b* and the *Zic* genes. Although further analysis using more definitive markers (such as *l-maf*) is be required to determine if this nested domain contains LOP cells.

### 4.4.3 Axial heterotypic grafts fail to induce PPR or placode markers

To investigate if the neural plate can override the axial bias provided by the mesoderm or if the neural plate signal was generic axial heterotypic co-grafts were carried out (lHM/aNP and pME/pNP). These grafts were once again analysed at 6 and 12 hours and compared to endogenous domains of expression. Heterotypic combination of tissues did not induce a PPR or a placode state at 6 hours, the same was true for 12 hours (figure 4.15, A-B). However, the addition of the heterotypic neural plate graft alongside a mesoderm graft (lHM/aNP and pME/pNP) although not sufficient to fully override the mesoderm's initial axial bias on induction; the heterotypic neural plate suppressed the axial markers induced by the mesoderm. *Foxi3* and *Gbx2* induced by the lHM, were no longer induced when an aNP was grafted alongside the lHM, pME and pNP combination grafts followed a similar pattern (Figure 4.15, A-B), with a reduction in genes such as *Six3* and *Sall1*. Therefore, it is possible that only grafts where the axial origins are similar will induce PPR and subsequent placode progenitors.

## 4.5 Discussion

The induction of the PPR is mediated by surrounding tissues and can be measured by the presence of *Six1*/4 and *Eya2*. The tissues that have been implicated in PPR induction include the lateral head mesoderm and the neural plate (Ahrens and Schlosser, 2005; Litsiou et al., 2005). Here I have identified the pME as a new source of signals which will induce the PPR markers *Six1* and *Eya2*; the neural plate does not have PPR inducing capabilities. I have also

showed that the lHM and pME will induce a regionally biased ectopic PPR that is related to the axial location of the lHM and pME (posterior, anterior). Furthermore, when combined in an axial heterotypic manner the neural plate will reinforce the signals from the lHM or pME and promote the induction of placode progenitors. Finally the results from this study can be used to define a genetic hierarchy upstream of Six and Eya.

### 4.5.1 Hierarchy in response to mesoderm tissues

The majority of genes which are induced at three hours by the lHM and pME are expressed in the pre streak stage embryo such as *Etv5*, *ERNI*, *Otx2*, *Trim24* and *Zic3*. This raises the possibility that the induced ectoderm is equivalent to a pre streak epiblast domain. Interestingly, some of these early genes are induced by the hypoblast , which underlies the epiblast, these include *ERNI* and *Otx2* (Albazerchi and Stern, 2007). It is possible that the other genes induced at 3 hours (*Etv5*, *Trim24* and *Zic3*) may also be induced by the hypoblast, although further experiments are needed to confirm this. In support of a similarity between induction by the lHM/pME and the hypoblast; they are all sources of FGF signalling and WNT and BMP antagonism (Albazerchi and Stern, 2007; Litsiou et al., 2005).

At six hours the genes induced by the lHM include *Cited2*, *Nfkb1*, *Sall1*, *Sox3* and *Znf462*, the majority of these new genes and the ones that have remained up regulated from earlier (*Trim24*) are still mainly expressed at the pre-streak stage (Trevers, 2015) suggesting that although the number of genes have increased the overall embryonic identity of the domain has not changed. In contrast the pME induces genes that only become expressed at neural plate stages, these include *Six1/4* and *Znf423*. Although *Six1* and *4* are PPR markers, they are first expressed at gastrula stages (Esteve and Bovolenta, 1999; Sato et al., 2012) surrounding the neural plate border and In the absence of other PPR markers, *Eya2* and *Homer2*, the induced region appears to resemble the neural plate border. This region also appears to be biased towards the anterior epiblast, shown by the induction of genes such as *Otx2*, *Sall1* and *Nfkb1* which are all enriched in the anterior portion of the epiblast. Therefore the lHM at 6 hours is equivalent a pre-streak embryo, while the pME induces a domain that matches the anterior neural plate border.

By twelve hours in both conditions there is upregulation of *Eya2* and *Six1*; plus other PPR genes including the new PPR marker *Homer2* (Tambalo, 2014) suggesting that a PPR has been induced. The onset of various markers suggests the lHM has induced a posterior biased PPR (*Foxi3*, *Gbx2*); whereas the pME has induced an anterior biased PPR (*Six3*, *Dlx6*, *and Otx2*). In support of these finding, the endogenous expression of *ERNI* persists in the

anterior portion of the embryo which is consistent with the result that *ERNI* is still expressed in the pME induction at 12 hours and not in the 12 hour lHM induction (Streit et al., 2000 A.Streit personal communication) Can the anterior and posterior markers, *Otx2* and *Gbx2*, be used to further support the idea that the lHM and pME induce axial biased. *Otx2* and *Gbx2* are mutually repressive (Katahira et al., 2000; Millet et al., 1999; Steventon et al., 2012) therefore you would expect *Gbx2* to be dominant in a posterior biased domain and *Otx2* to be dominant in an anterior biased domain. Indeed in the lHM induced PPR *Gbx2* is 3 fold higher than *Otx2* and conversely in the pME induced domain *Otx2* is 9 fold higher than *Gbx2*. These results suggests that by 12 hours there is induction of an axially biased PPR at 12 hours and that the origin of the mesoderm tissue is the defining factor in initiating this bias.

At 24 hours the lHM has lost all of the earlier induction, indicating that the lHM may be susceptible to fate changes or lack the ability to induce maintenance factors to stabilise the induction. In contrast the pME by 24 hours the domain induced appears to resemble a nervous system like structure. The genes induced span various nervous system tissues, there is also up regulation of *Pax6* which may suggest an anterior placode domain has been induced. However, there is also a strong upregulation of *Pax2* (although not significant) which may indicate that a posterior placode domain may be present. In contrast to the lHM graft which is easily visualised and removed at 24 hours the pME graft has fused to the extra embryonic ectoderm to the point where complete removal is almost impossible. This fusion and induction of genes spanning various embryonic domains makes interpretation very difficult and indirect induction cannot be ruled out.

In conclusion the lHM and pME both induce a PPR state that passes through stages that match early embryonic development and are eventually biased to either an anterior or posterior fate. Interestingly, induction from the lHM and the pME at the early time point is similar to the induction from the Node (Trevers, 2015, data not shown). This may suggest that the early steps in neural and PPR induction are similar, although further experiments are needed to investigate this.

### 4.5.2 Similarities and differences in response to the lHM and pME

When the response of the lHM and pME are compared against each other at 3 hours the majority of genes are similar with only two genes unique to the lHM (*Mier1* and *Bcl11a*) and one (*Irx1*) to the pME. It is difficult to conclude what the differences mean at this early time point of induction and further experiments are necessary. The pME seems to be stronger/faster at inducing genes, this can be seen by the induction of *Six1* at six hours,

whereas the lHM only induces *Six1* by 12 hours. Although analysis of the raw data, comparing mean expression values does not support a stronger level of induction, suggesting unknown factors may be involved from the pME. It is possible that the pME may induce the same set of genes as the lHM but at an earlier time point but this would require further experiments.

### 4.5.3 Putative upstream regulators of six1/4 and eya2

The results of these experiments can be used to identify putative regulators of the PPR markers *Six1* and *Eya2*.it has already been shown that the factors *Tfap2a/c*, *Foxi1* and *Gata3* are required for placodal competence (Kwon et al., 2010). However, might these factors also directly regulate PPR markers? In the lHM induction *Tfap2a* is first down regulated at 3 and 6 hour before being up regulated at the same time as *Six1* and *Eya2* at 12 hours. Conversely, *Tfap2a* is not up regulated at any point when *Six1* is induced by the pME, therefore there might be a role for *Tfap2a* in the direct regulation of *Six1* but this may depend on the tissue involved in PPR induction. Another of the factors that has been shown to be a competence factor for *Six1* and *Eya2*, *Gata3*, is upregulated in both the pME and lHM inductions at the same time as *Six1* and *Eya2* are both present at 12 hours and therefore may be involved in the direct regulation of these markers. It is possible that *Tfap2a* and *Gata3* are involved in creating a domain of competence for the PPR but also in the direct regulation of the PPR markers as they are regulated at the same time as *Six1*.

Recent evidence has shown that the homeodomain transcription factors *Dlx5* and *Msx1* are involved in the direct regulation of *Six1* (Sato et al., 2010). *Msx1* is a negative regulator of *Six1* and in the lHM induction of *Six1* it is down regulated at 12 hours, the time point at which *Six1* is positively regulated. Interestingly, *Msx1* is down regulated at 6 hours by the pME and Six1 is upregulated at 6 hours, this is earlier than the lHM. Therefore the down regulation of *Msx1* is clearly responsible for the induction of *Six1* to occur. *Dlx5* is not positively upregulated when *Six1* or *Eya2* are positively regulated, suggesting that it although it can regulate PPR markers in a positive manner it is not required for their induction.

*Nfkb1* is upregulated at six hours in the pME condition when *Six1* is present and is upregulated before the onset of *Six1* in the lHM condition. *Nfkb1* knockout mice have accelerated hearing loss and auditory nerve degeneration, suggesting a role in sensory formation and maintenance (Lang et al., 2006) and therefore possibly in the regulation of *Six1* or *Eya2*. A better candidate for regulation of *Six1* is *Sall1*, it is up regulated at 6 hours in both conditions and is expressed earlier in embryonic development than both *Six1* and

*Eya2*. *Sall1*, is normally thought of as a transcriptional repressor but can act as a transcriptional activator and the aPPR *Six1*-14 enhancer has numerous *Sall1* binding sites present (Chapter 6, Yamamoto et al., 2010). *Sall1* mutations in humans have been shown to be present in BOR syndromic patients, BOR is associated with mutations in *Six1* and *Eya2* (Abdelhak et al., 1997; Engels et al., 2000; Just et al., 2003; Ruf et al., 2004). Although *Six1* and *Eya2* have been shown to activate expression of *Sall1* in kidney development (Chai et al., 2006) *Sall1's* earlier expression in the neural plate border and earlier onset of expression in the grafting assays suggest it is good candidate to investigate further as a *Six1*/*Eya2* PPR regulator.

Overall, a number of factors (*Tfap2a*, *Gata3*) previously shown to be involved in setting up a competence domain for the PPR may also be involved in the direct regulation of *Six1* and *Eya2*. While the down regulation of *Msx1* is necessary for the induction of *Six1*. There are also a number of new candidates that may be putative regulators of *Six1* and *Eya2*, such as *Sall1* and *Nfkb1* that require further investigation to determine their role in direct regulation.

### 4.5.4 Does the neural plate induce PPR?

The neural plate has been shown to induce the PPR marker *Six1* in xenopus and chick (Ahrens and Schlosser, 2005; Litsiou et al., 2005), and this was thought to indicate the induction of a PPR cell fate. However, the evidence from chick shows that only a small percentage of neural plate grafts induce *Six1* in the host epiblast and that *Six4* and *Eya2* are never induced (Litsiou et al., 2005). Therefore I looked to confirm if either the anterior or posterior neural plate could induce *Six1/4* or *Eya2* and if this induction resembled a PPR state. The results showed that *Six1* and *4* were never induced by either neural plate, only *Eya2* was induced at 12 hours by both the aNP and pNP. There was also the absence of other PPR genes such as *Dach1* and *Homer2*. Although the neural plate can induce *Eya2* the domain never resembles a PPR and therefore the neural plate is not directly responsible for inducing the PPR. However, neural plate grafts induce a mixed identity domain which has both neural plate markers (*Sox2*) and NNE makers (*Gata3* and *Keratin19*). These domains are also biased axially and this depends on the axial origin of the neural plate graft. Therefore the neural plate may provide numerous signals, homeogenetic signals where it induces a domain that is similar to its own; but also axial signals that can provide positional identity to a domain.

### 4.5.5 Combining neural plate and mesoderm grafts promotes placode progenitor identity

Recent evidence has shown that combined signalling from the neural tube and mesoderm can induce the otic placode marker *Pax2* (Ladher et al., 2000). Therefore I looked at if combining mesoderm and neural plate tissue in an axial homotypic and axial heterotypic combinations would lead to the induction of ectopic placode progenitor domains. Combiinng the lHM with the pNP did lead to the promotion of otic placode progenitor identity, with 50% of the genes induced at 12 hours being expressed in the otic/epibranchial region (*Pax2, Sox10, Lmx1b, Foxi3, Gbx2, Eya2* and *Pea3*). When the lHM was grafted with the aNP, there was no induction of PPR markers or placode identity, this indicates that the signals provided by the pNP are specific for the correct axial domain to be induced. In the lHM/pNP condition there is an upregulation of the WNT response gene *Lef1* (Eastman and Grosschedl, 1999), this is not present in the lHM alone condition and suggests the addition of a neural plate has added the WNT signal required to shift the induced fate from a PPR to an Otic fate. Which has been showed to be sufficient when combined with FGF to induce *Pax2*. Another factor, *Lmx1b* is upregulated at the same time as *Pax2* and there is experimental evidence that the neural plate is required to maintain *Lmx1* in the otic placode (Giraldez, 1998) A combination of the pME and aNP marginally promotes the induction of lens and olfactory progenitors, while again the heterotypic combination does not induce a PPR or a LOP domain. The combination of the aNP and pME is seemingly necessary to get the combined expression of *Pax6* and *Six3* in the same induction, two genes important for the development of the lens, although further markers (Such as *l-maf* and crystallin genes) and single cell analysis would further elucidate this process. However, a number of otic genes are also induced in the aNP and pME such as *Hey1, Irx1* and other genes overlap in their expression in the otic, olfactory and lens placode (*Dach1, Lef1* and *Hesx1*). This raises the possibility that the combination of factors is vital and creates nested domains of expression that will generate specific progenitors and that not one factor is definitively responsible for

Therefore, the following model is proposed. First a common domain is induced, this domain is subsequently axially biased depending on the axial origin of the tissue imparting the signal. Second to create the correctly positioned domain “local inductors” combine to impart signals which induce mature axial domains, such as placodes. However, this tissue combination must be co-incident. Therefore co-incident local organisers pattern the

nervous systems after an induction of a common domain. In chicken this model may explain the process of induction by the hypoblast and then regionalisation by tissues such as the node, lHM and pME (Figure 7.1).

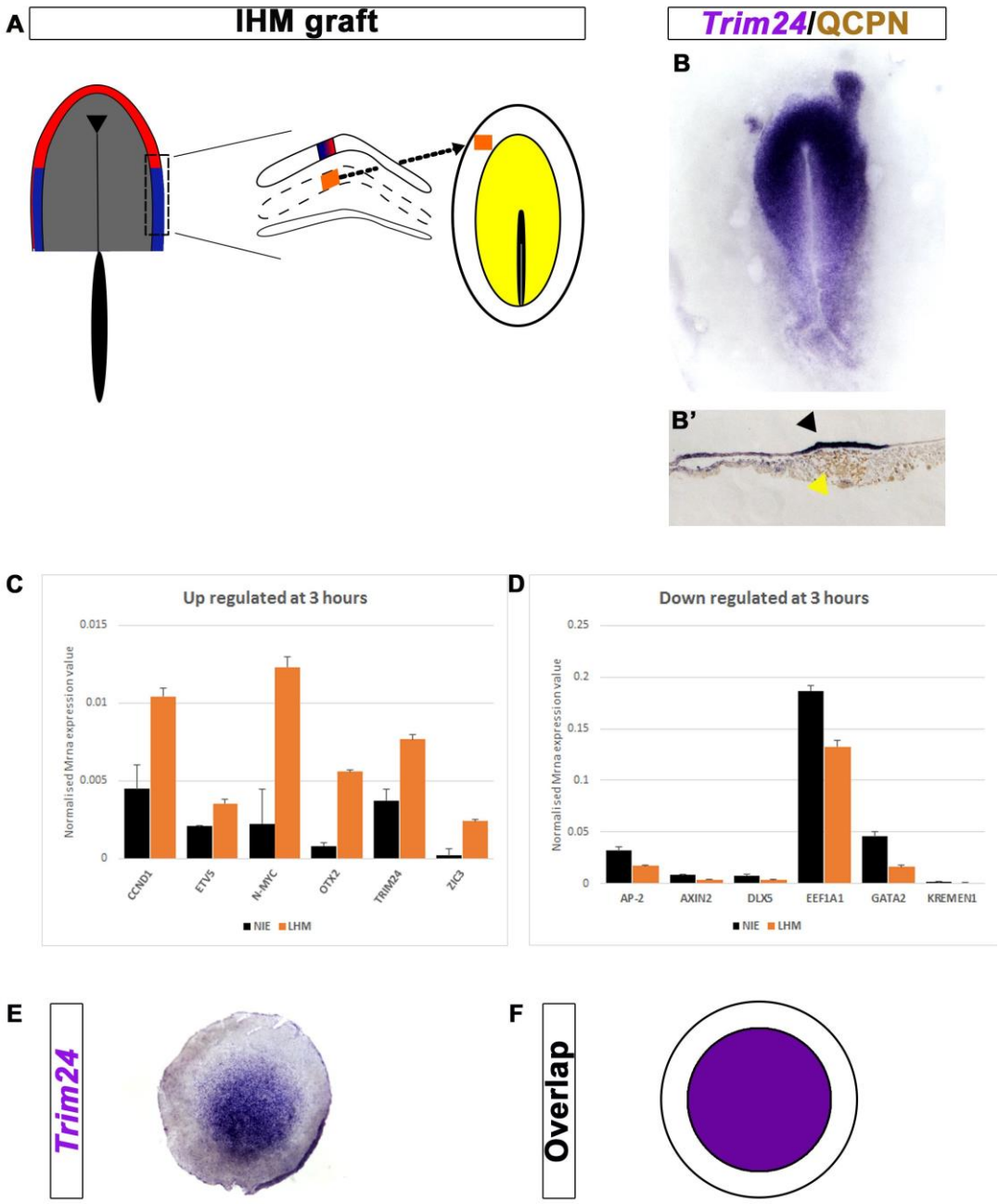


Figure 4.1: Response to lHM graft at 3 hrs

**A.** Diagrammatic representation of the experiment. The lHM underlying the PPR (dotted box) was grafted into the extraembryonic region of a $HH3^{+}/4^{-}$ chick host; after 3 hrs the ectoderm in contact with the graft was isolated and analysed by NanoString. **B, B'**. *Trim24* is induced by the lHM; quail lHM is labelled by immunostaining using quail specific antibodies QCPN marked by yellow arrow (brown; **B-B'**) and *Trim24* mRNA is detected by in situ hybridisation (blue) in the overlying ectoderm marked by black arrow. **C.** Bar chart showing transcripts that are upregulated significantly (p-value <0.05) by an lHM graft (orange) as compared to non-induced ectoderm (black). Error bars represent standard error of the mean (SEM) **D**. Bar chart showing transcripts that are downregulated significantly (p-value <0.05) by an lHM graft (orange) as compared to non-induced ectoderm (black). Error bars represent SEM **E.** *Trim24* is expressed in the pre-streak epiblast similar to all other upregulated genes. **F**. Diagram summarising the earliest overlapping expression pattern of all induced genes.

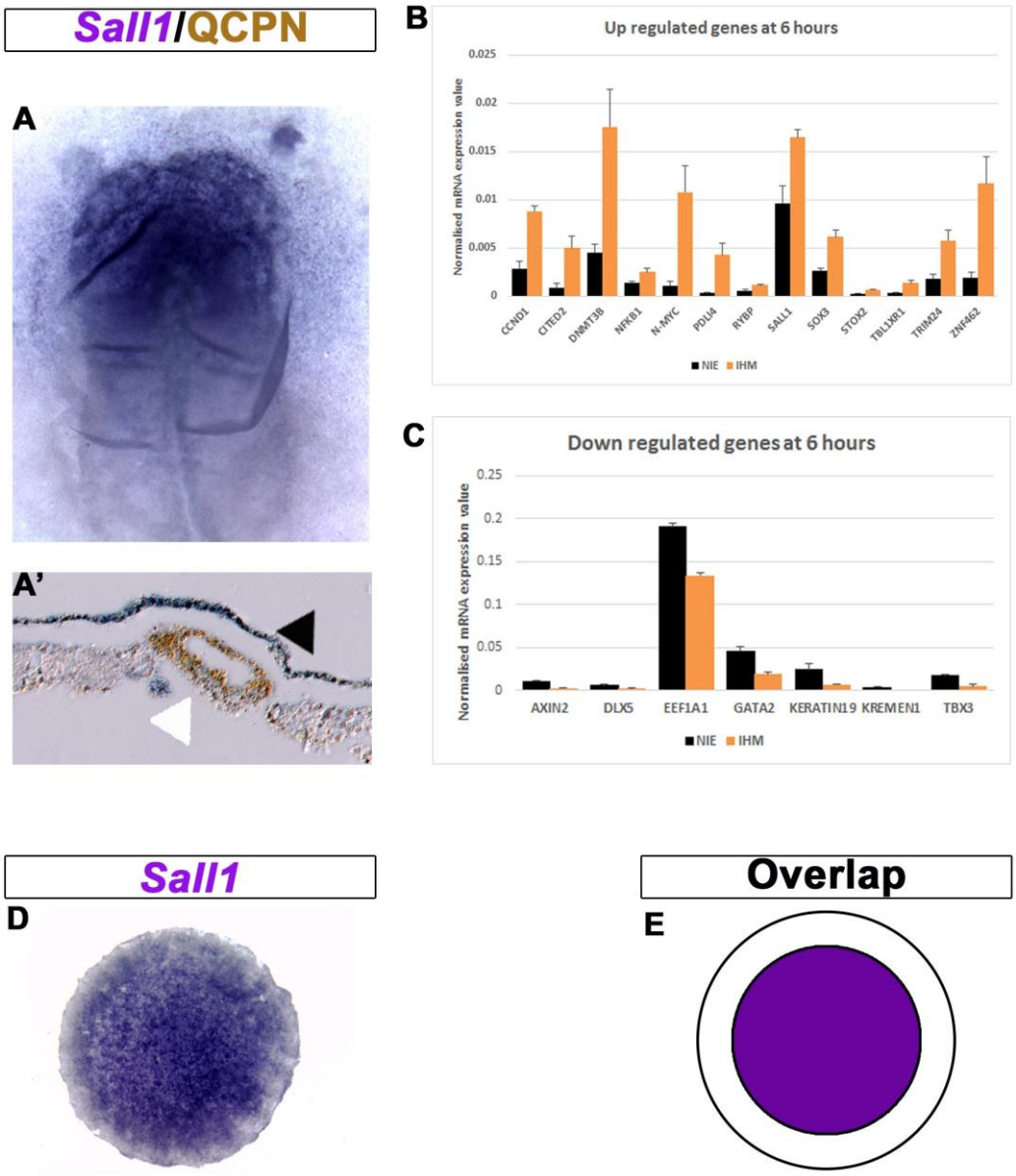


Figure 4.2: Response to lHM graft at 6hrs

**A- A'.** Grafts of lHM were made into the extra embryonic ectoderm, after 6 hours *Sall1* is induced by the lHM; quail tissue is labelled by immunostaining using quail specific antibodies QCPN marked by white arrow (brown; **A-A'**) and *Sall1* mRNA is detected by in situ hybridisation (blue) in the overlying ectoderm marked by black arrow. **B.** Bar chart showing transcripts that are upregulated significantly (p-value <0.05) by an lHM graft (orange) as compared to non-induced ectoderm (black). Error bars represent SEM. **C** Bar chart showing transcripts that are downregulated significantly (p-value <0.05) by an lHM graft (orange) as compared to non-induced ectoderm (black). Error bars represent SEM **D.** *Sall1* is expressed in the pre-streak epiblast similar to the majority of other upregulated genes. **E**. Diagram summarising the earliest overlapping expression pattern of all induced genes.

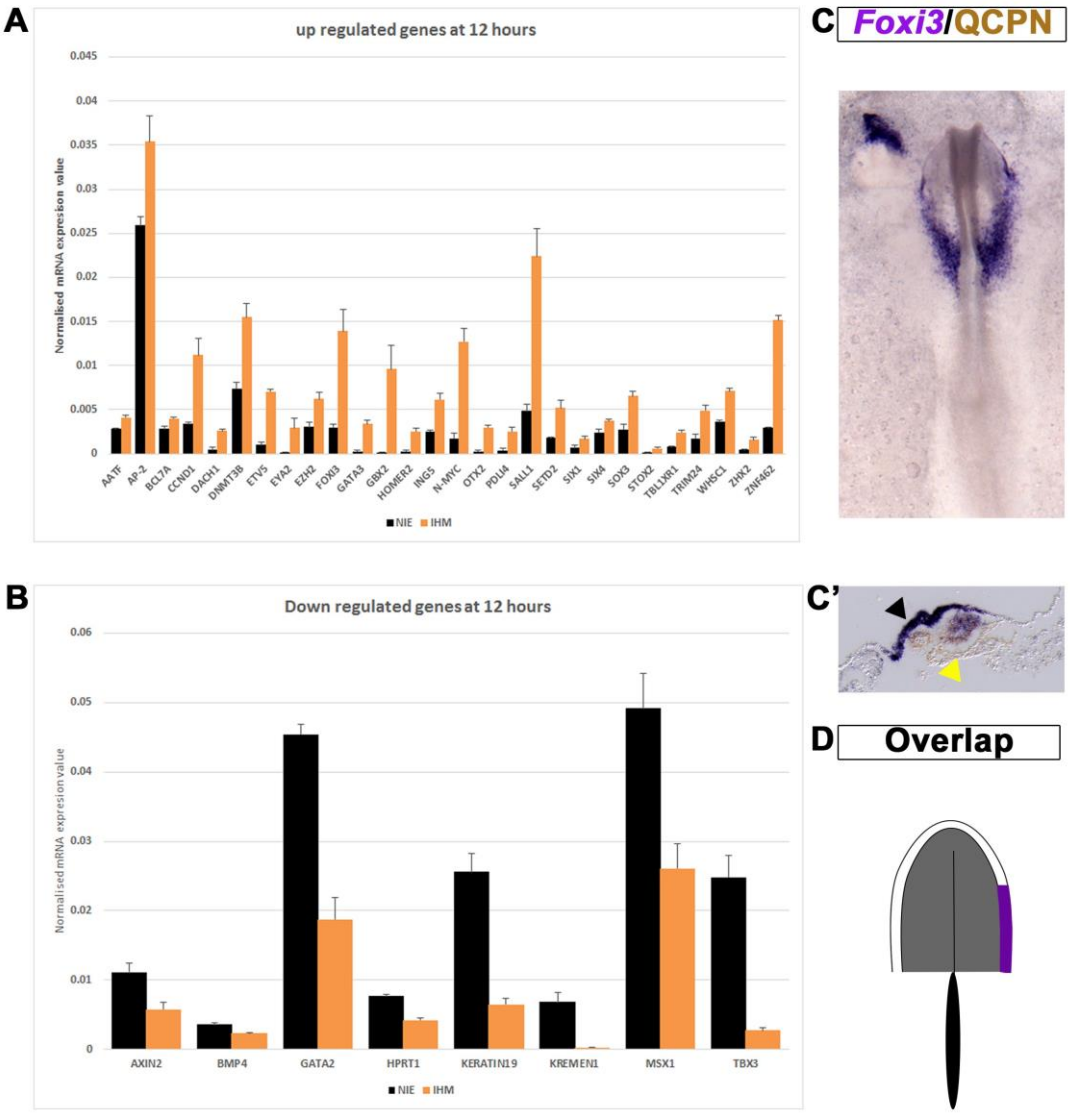


Figure 4.3: Response to lHM at 12hrs

**A.** Bar chart showing transcripts that are upregulated significantly at 12 hours (p-value <0.05) by an lHM graft (orange) as compared to non-induced ectoderm (black). Error bars represent standard error of the mean (SEM) **B**. Bar chart showing transcripts that are downregulated significantly (p-value <0.05) by an lHM graft (orange) as compared to non-induced ectoderm (black). Error bars represent SEM. **C-C'**. *Foxi3* is induced by the lHM after 12 hours; quail lHM is labelled by immunostaining using quail specific antibodies QCPN marked by white arrow (brown; **C-C'**) and *Foxi3* mRNA is detected by in situ hybridisation (blue) in the overlying ectoderm marked by black arrow. **D**. Diagram summarising the earliest overlapping expression pattern of all induced genes. As indicated by *Foxi3* expression in **C.**

**A**

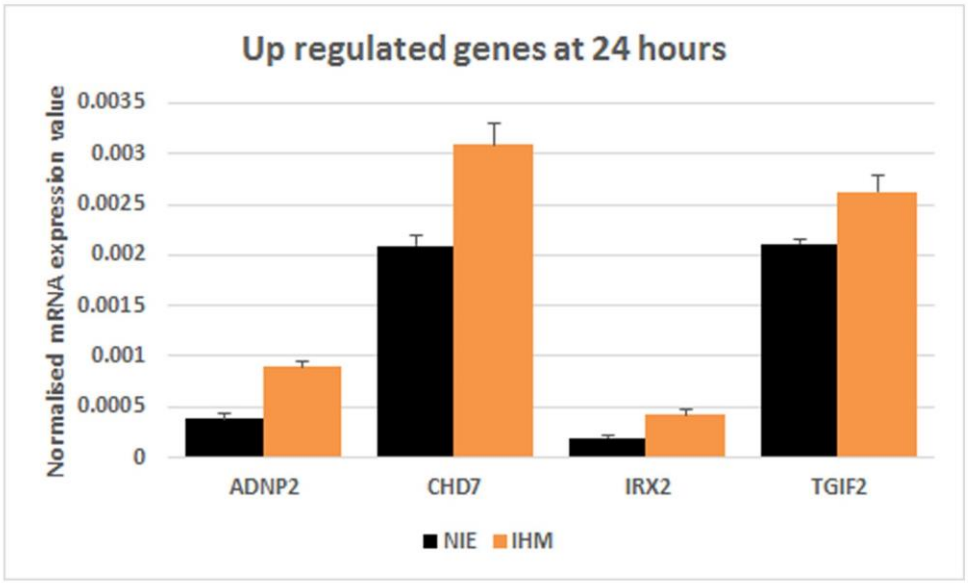


Figure 4.4: Response to lHM at 12hrs

**A.** Bar charts representing the genes that are upregulated significantly (P-value <0.05) by the lHM (orange) at 24 hours when compared to time matched non-induced ectoderm (black). Error bars represent SEM.

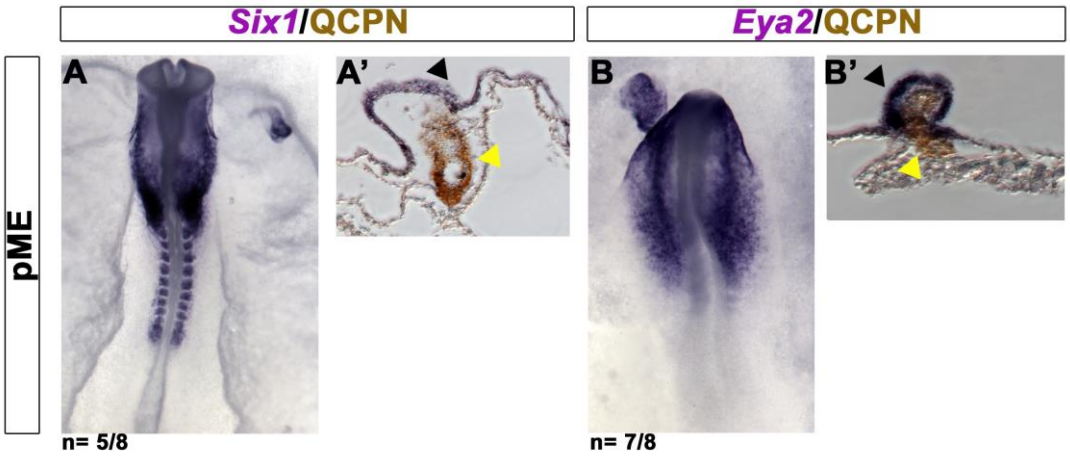


Figure 4.5: The prechordal mesendoderm can induce PPR markers

**A-A'.** Grafts of quail derived pME into the extraembryonic ectoderm were analysed by immunostaining using quail specific antibodies QCPN (Brown, marked by white arrows) and insitu hybridisation to detect mRNA (Blue) after 16 hours**.** After 16 hours *Six1* is upregulated in the overlying ectoderm in 5 out of 8 grafts marked by black arrow (62%, Blue). QCPN stained tissue (Brown) is marked by a yellow arrow. **B-B'.** After 16 hours *Eya2* is upregulated in the overlying ectoderm in 7 out of 8 grafts marked by black arrow (87%, Blue). QCPN stained tissue (Brown) is marked by a yellow arrow.

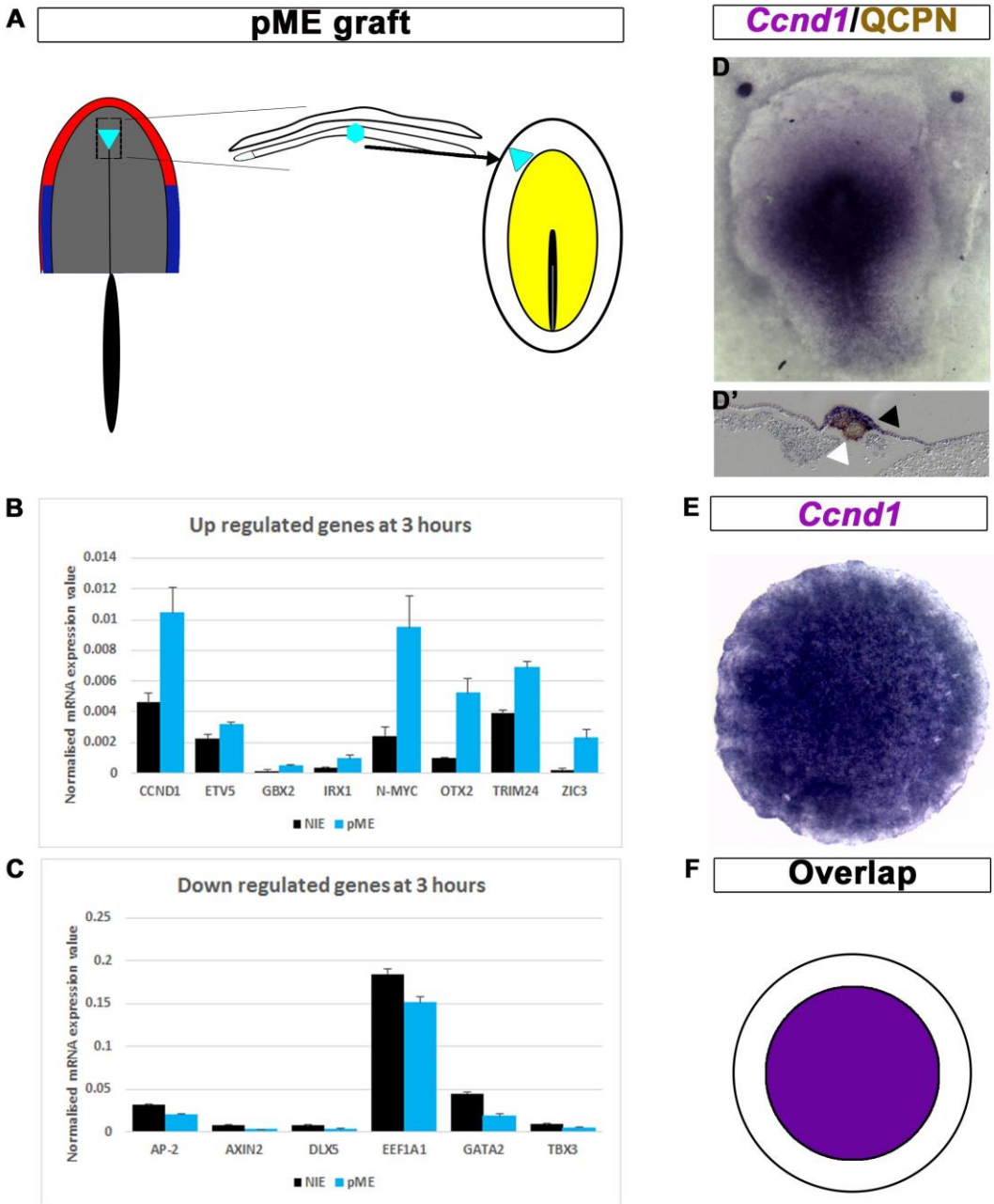


Figure 4.6: Response to pME graft at 3hrs

**Figure 4.6: Response to pME graft at 3hrs**

**A.** Diagrammatic representation of the experiment. The pME which lies in from of the developing notochord and under the ectoderm of the anterior epiblast (Sky blue region dotted box) was grafted into the extraembryonic region of a $HH3^{+}/4^{-}$ chick host; after 3 hrs the ectoderm in contact with the graft was isolated and analysed by NanoString. **B.** Bar chart showing transcripts that are upregulated significantly at 3 hours (p-value <0.05) by a pME graft (Sky blue) as compared to non-induced ectoderm (black). Error bars represent standard error of the mean (SEM) **C**. Bar chart showing transcripts that are downregulated significantly at 3 hours (p-value <0.05) by an lHM graft (Sky blue) as compared to non-induced ectoderm (black). Error bars represent SEM **D, D'**. *Ccnd1* is induced by the pME; quail lHM is labelled by immunostaining using quail specific antibodies QCPN marked by white arrow (brown; **D-D'**) and *Ccnd1* mRNA is detected by in situ hybridisation (blue) in the overlying ectoderm marked by black arrow**. E.** *Ccnd1* is expressed in the pre-streak epiblast similar to all other upregulated genes. **F**. Diagram summarising the earliest

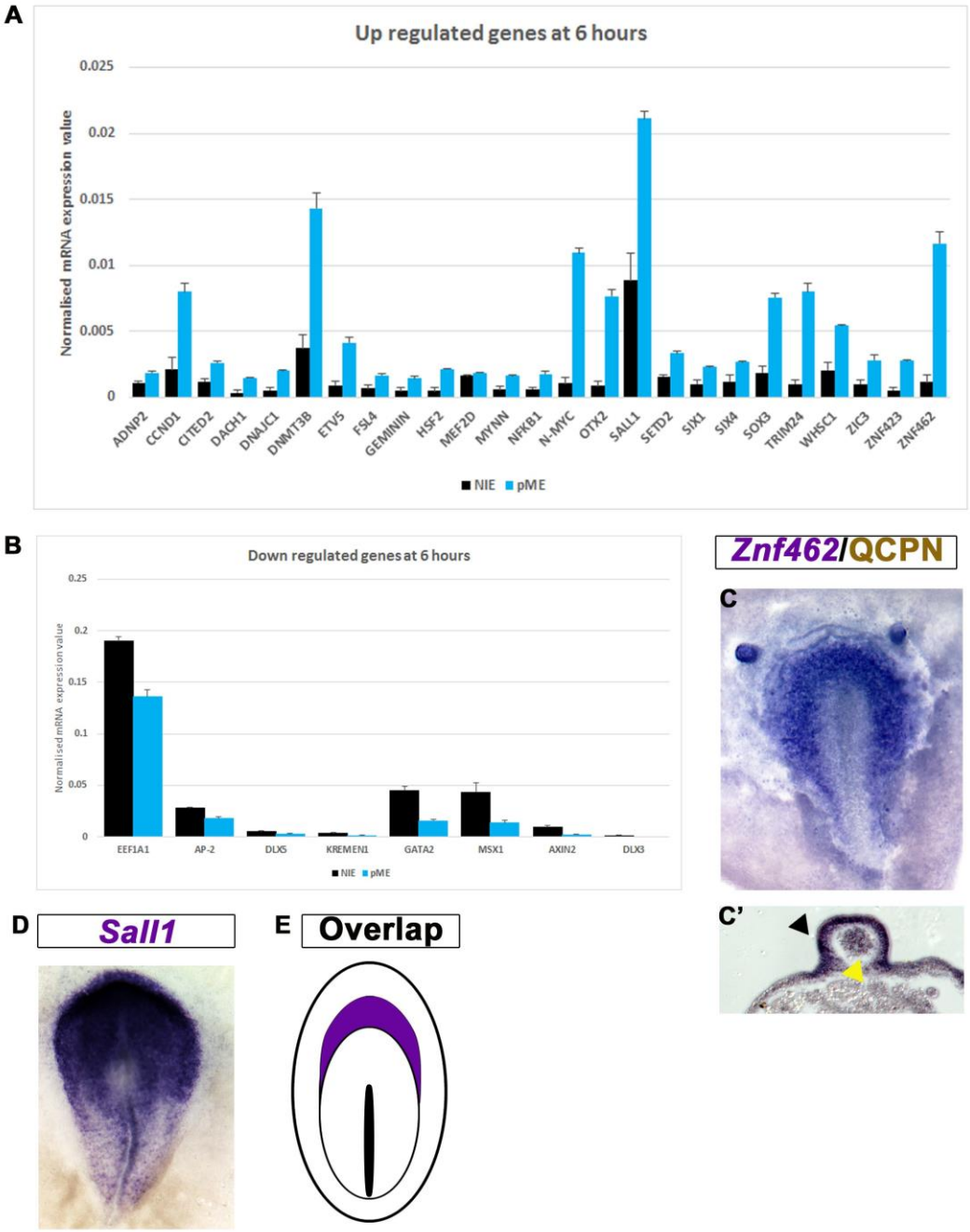


Figure 4.7: Response to pME graft at 6hrs

**A.** Bar chart showing transcripts that are upregulated significantly after 6 hours (p-value <0.05) by a pME graft (Sky blue) as compared to non-induced ectoderm (black). Error bars represent standard error of the mean (SEM) **B**. Bar chart showing transcripts that are downregulated significantly after 6 hours (p-value <0.05) by an lHM graft (Sky blue) as compared to non-induced ectoderm (black). Error bars represent SEM **C, C'**. *Znf462* is induced by the pME; quail lHM is labelled by immunostaining using quail specific antibodies QCPN marked by white arrow (brown; **D-D'**) and *Znf462* mRNA is detected by in situ hybridisation (blue) in the overlying ectoderm marked by black arrow. **D.** *Sall1* is expressed in the pre-neural plate with an anterior enrichment, similar to all other upregulated genes. **E**. Diagram summarising the earliest overlapping expression pattern of all induced genes, in the anterior neural plate.

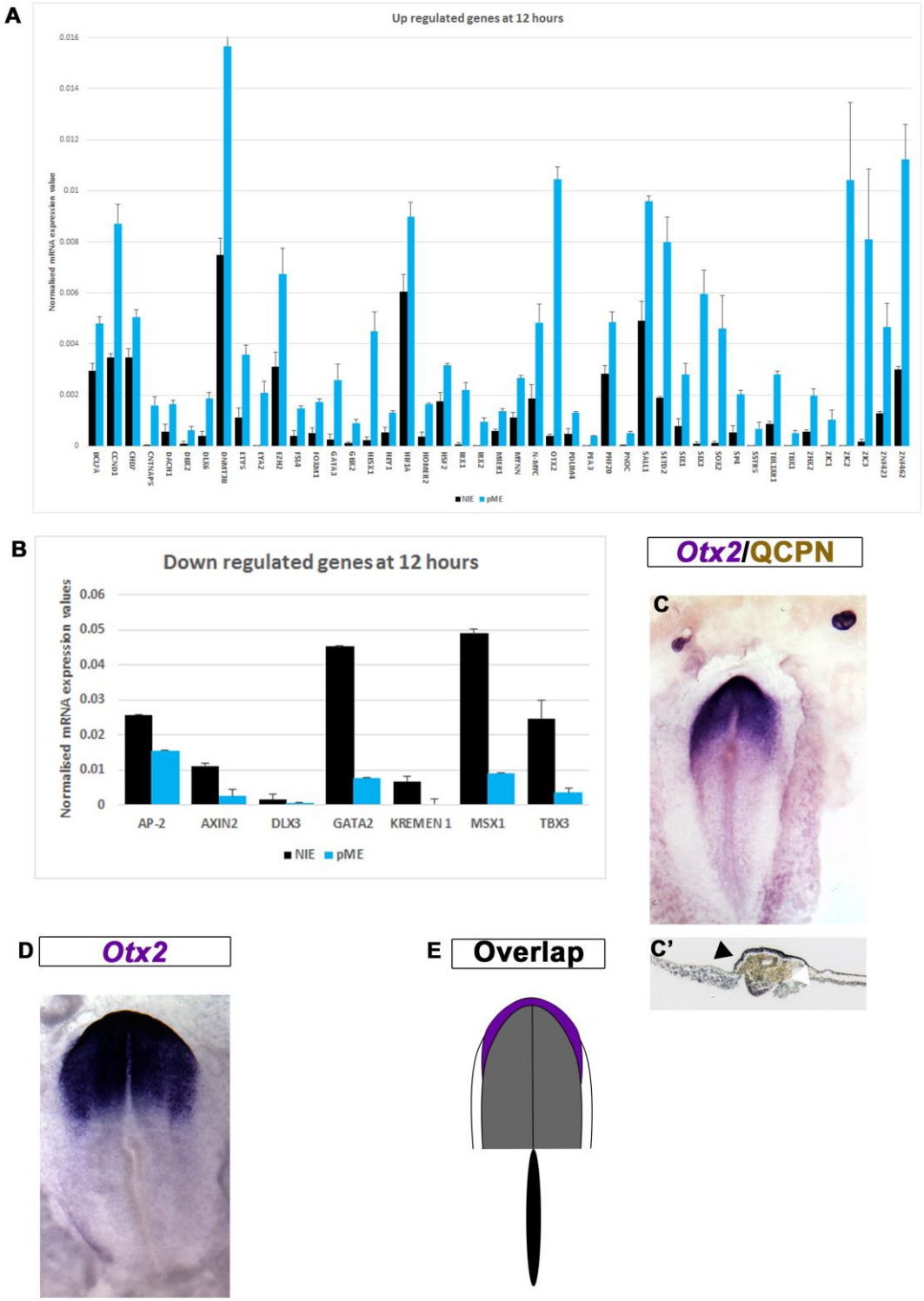


Figure 4.8: Response to pME graft at 12hrs

**Figure 4.8: Response to a pME graft at 12 hours**

**A.** Bar chart showing transcripts that are upregulated significantly after 12 hours (p-value <0.05) by a pME graft (Sky blue) as compared to non-induced ectoderm (black). Error bars represent standard error of the mean (SEM) **B**. Bar chart showing transcripts that are downregulated significantly after 12 hours (p-value <0.05) by an lHM graft (Sky blue) as compared to non-induced ectoderm (black). Error bars represent SEM **C, C'**. *Otx2* is induced by the pME; quail lHM is labelled by immunostaining using quail specific antibodies QCPN marked by white arrow (brown; **D-D'**) and *Otx2* mRNA is detected by in situ hybridisation (blue) in the overlying ectoderm marked by black arrow. **D.** *Otx2* is expressed in the anterior neural plate and aPPR, similar the majority of upregulated genes. **E**. Diagram summarising the earliest overlapping expression pattern of all induced genes, which matched the anterior pre-placodal region.

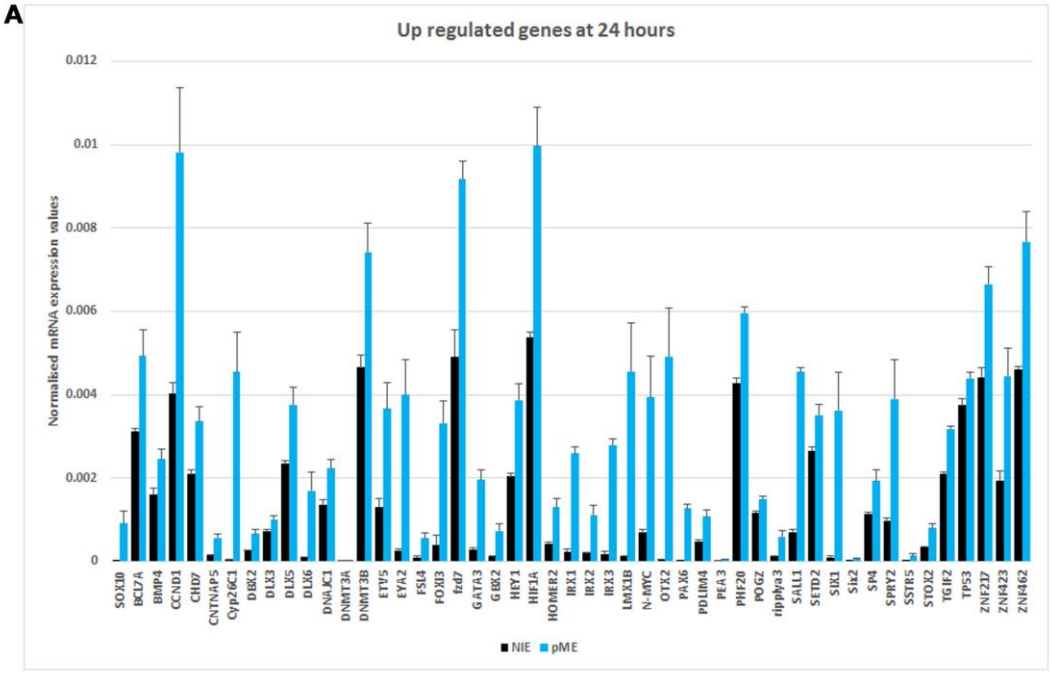


Figure 4.9: Response to pME at 24hrs

**A.** Bar chart showing transcripts that are upregulated significantly after 24 hours (p-value <0.05) by a pME graft (Sky blue) as compared to non-induced ectoderm (black). Error bars represent standard error of the mean (SEM)

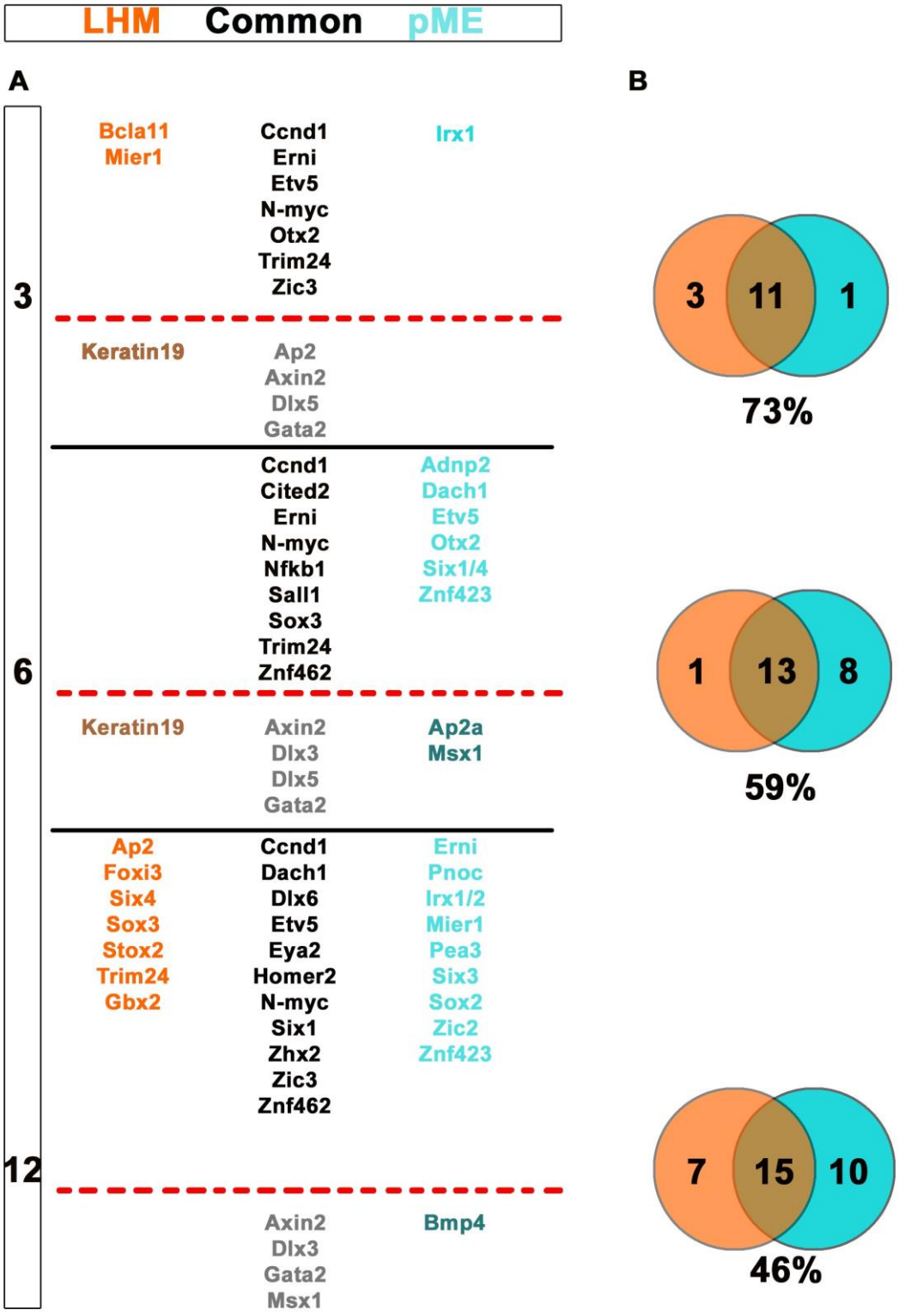


Figure 4.10: Comparison of response to lHM and pME grafts

**Figure 4.10: Comparison of response to lHM and pME grafts**

**A,** The upregulated genes from the lHM (Orange) were compared to the pME (Sky blue) at 3, 6 and 12 hours. Time points are separated by black lines. Red dotted line separates up (above the line) and down (below the line) regulated genes. Up regulated genes unique to the lHM are in Orange, down regulated in brown. Common up regulated genes are in black, common down regulated genes are in light grey. Up regulated genes unique to the pME condition are in Sky blue. Down regulated genes unique to the pME are in dark blue. **B,** Venn diagrams displaying the number of genes unique and in common to each condition; lHM orange; pME Blue.

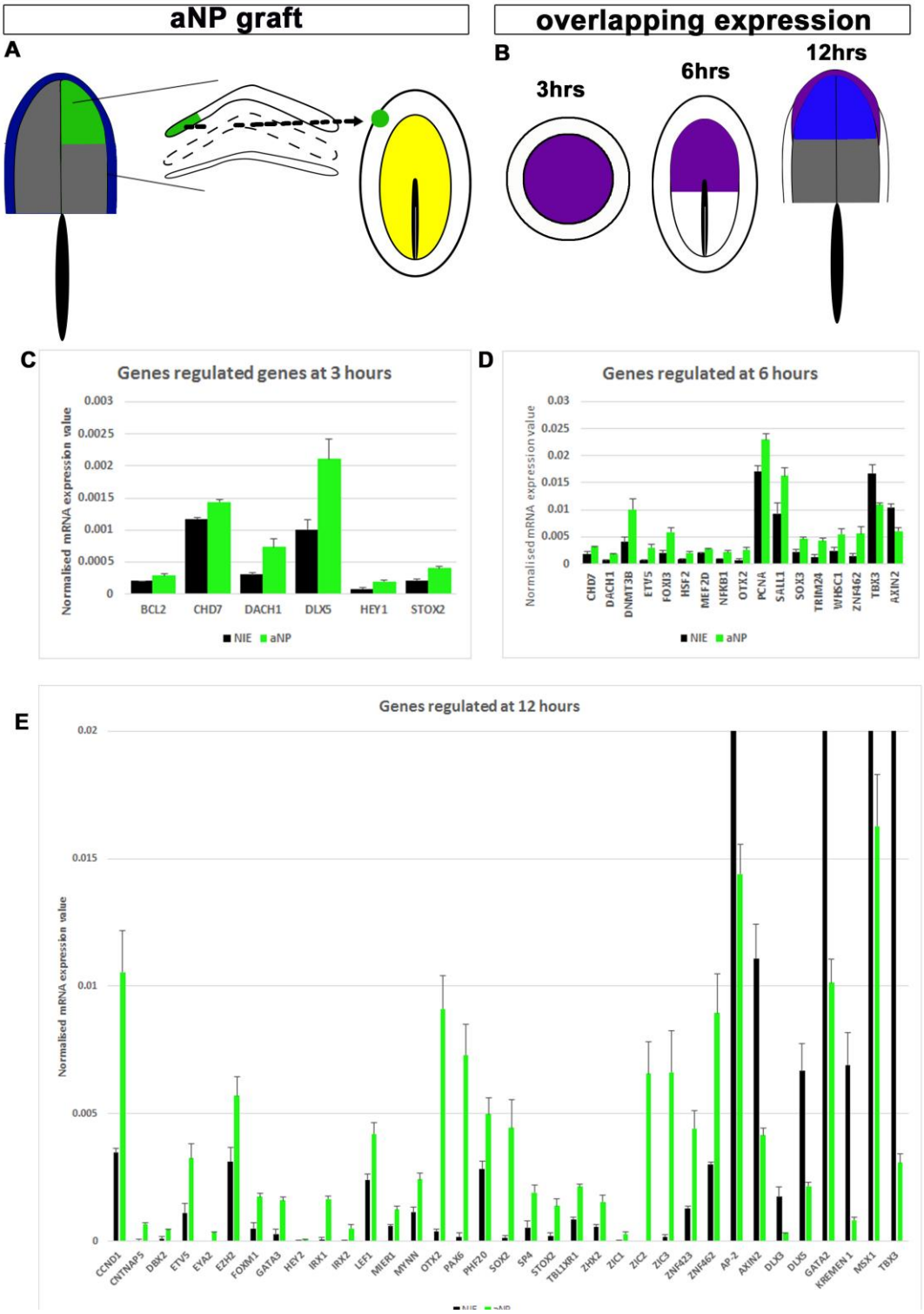


Figure 4.11: Response to an anterior neural plate graft at 3, 6 and 12 hrs.

**Figure 4.11: Response to an anterior neural plate graft at 3, 6 and 12 hours**

**A.** Diagrammatic representation of the experiment. The anterior neural plate (green region) was grafted into the extraembryonic region of a $HH3^{+}/4^{-}$ chick host; after 3, 6 or 12 hrs the ectoderm in contact with the graft was isolated and analysed by NanoString. **B.** Diagrams summarising the earliest expression patterns of all induced genes by the aNP at 3, 6 and 12 hrs. At 12 hours the expression patterns of all induced genes did not overlap in one single domain but marked two adjacent exclusive domains; the anterior neural plate (Blue) and the aPPR (Purple). **C.** Bar chart showing transcripts that are upregulated significantly at 3 hrs (p-value <0.05) by an aNP graft (Green) as compared to non-induced ectoderm (black). Error bars represent standard error of the mean (SEM) **D**. Bar chart showing transcripts that are upregulated significantly at 6 hrs (p-value <0.05) by an aNP graft (Green) as compared to non-induced ectoderm (black). Error bars represent SEM. **E**. Bar chart showing transcripts that are regulated significantly at 12 hrs (p-value <0.05) by an aNP graft (Green) as compared to non-induced ectoderm (black). In the case of a number of genes the NIE value is so high as to be off the scale. Error bars represent SEM

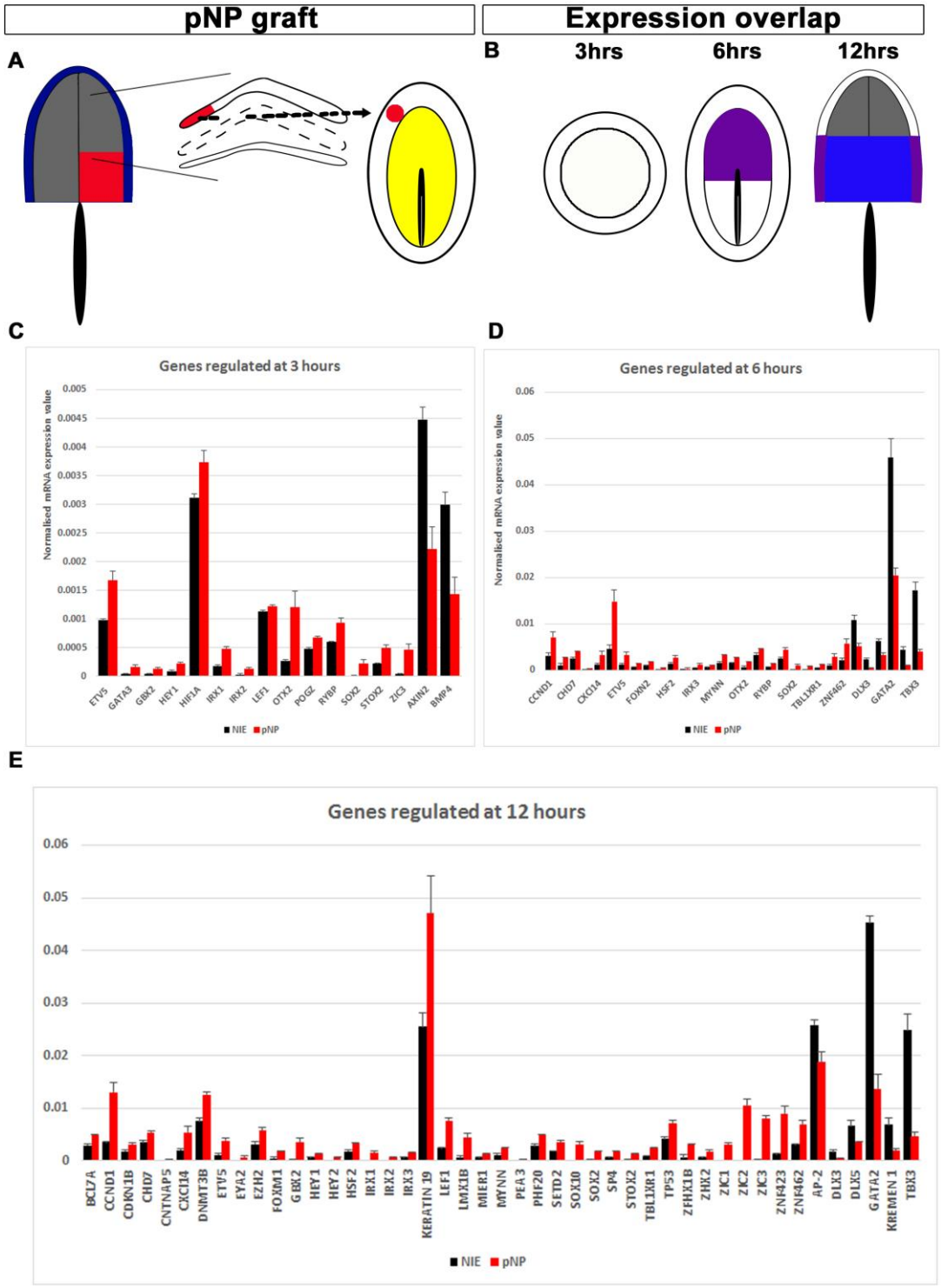


Figure 4.12: Response to a posterior neural plate graft at 3, 6 and 12 hours

**Figure 4.12: Response to a posterior neural plate graft at 3, 6 and 12 hours.**

**A.** Diagrammatic representation of the experiment. The posterior neural plate (Red region) was grafted into the extraembryonic region of a $HH3^{+}/4^{-}$ chick host; after 3, 6 or 12 hrs the ectoderm in contact with the graft was isolated and analysed by NanoString. **B.** Diagrams summarising the earliest expression patterns of all induced genes by the pNP at 3, 6 and 12 hrs. At 12 hours the expression patterns of all induced genes did not overlap in one single domain but marked two adjacent exclusive domains; the posterior neural plate (Blue) and the aPPR (Purple). **C.** Bar chart showing transcripts that are upregulated significantly at 3 hrs (p-value <0.05) by an pNP graft (Red) as compared to non-induced ectoderm (black). Error bars represent standard error of the mean (SEM) **D**. Bar chart showing transcripts that are upregulated significantly at 6 hrs (p-value <0.05) by an pNP graft (Red) as compared to non-induced ectoderm (black). Error bars represent SEM. **E**. Bar chart showing transcripts that are regulated significantly at 12 hrs (p-value <0.05) by an aNP graft (Red) as compared to non-induced ectoderm (black). Error bars represent SEM

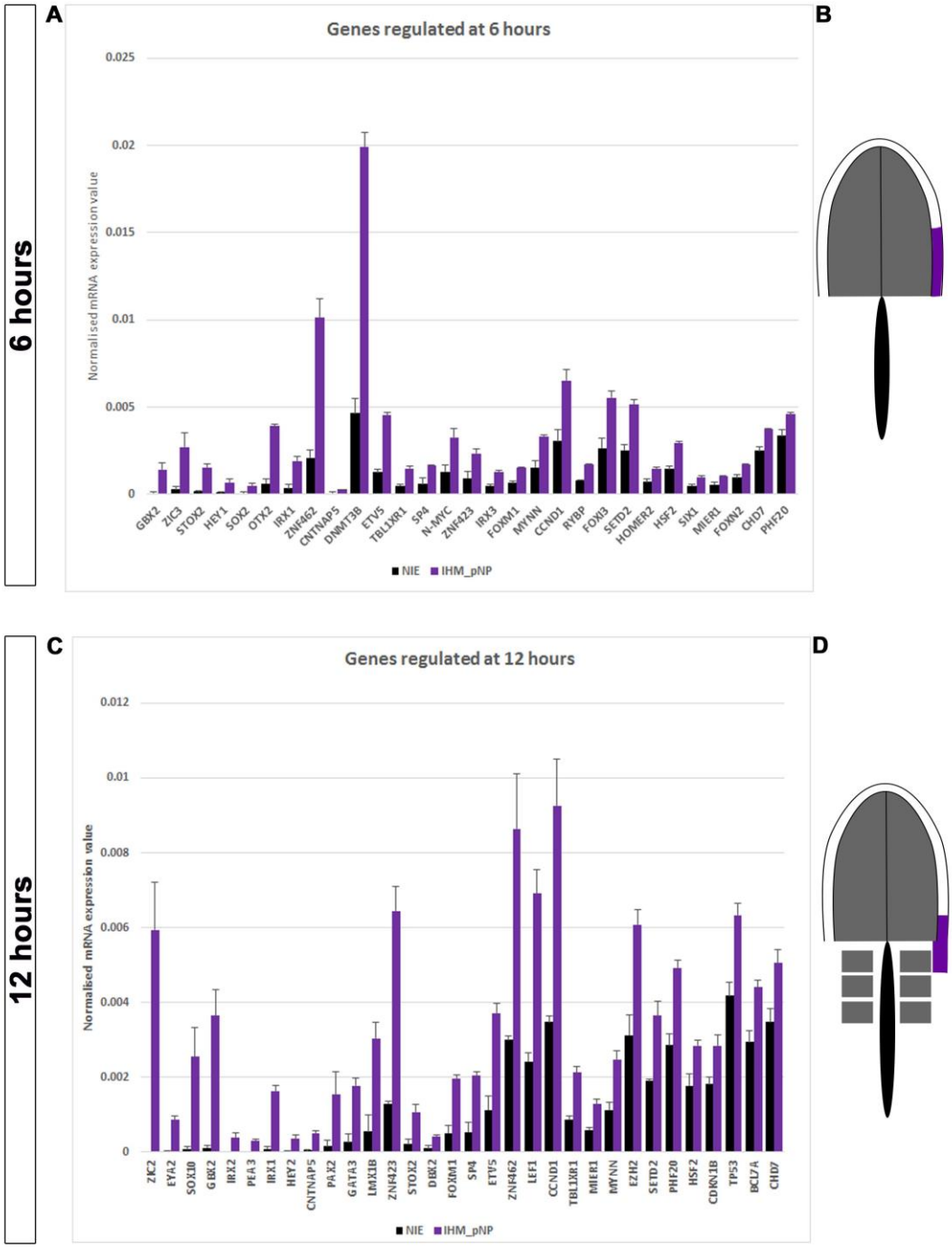


Figure 4.13: Response to lHM and pNP combination grafts at 6 and 12hrs

**Figure 4.13: Response to lHM and pNP combination grafts at 6 and 12hrs**

**A.** Axial homotypic combination grafts of lHM and pNP were made in to the extraembryonic region of a $HH3^{+}/4^{-}$ chick host; after 6 or 12 hrs the ectoderm in contact with the graft was isolated and analysed by NanoString Bar chart showing transcripts that are upregulated significantly at 6 hrs (p-value <0.05) by an lHM and pNP graft (Purple) as compared to non-induced ectoderm (black). Error bars represent standard error of the mean (SEM). **B.** Summary diagram displaying earliest overlapping region of expression patterns. **C.** Bar chart showing transcripts that are upregulated significantly at 12 hrs (p-value <0.05) by an lHM and pNP graft (Purple) as compared to non-induced ectoderm (black). Error bars represent standard error of the mean (SEM). **D.** Summary diagram displaying earliest overlapping region of expression patterns, that corresponds to the OEPD.

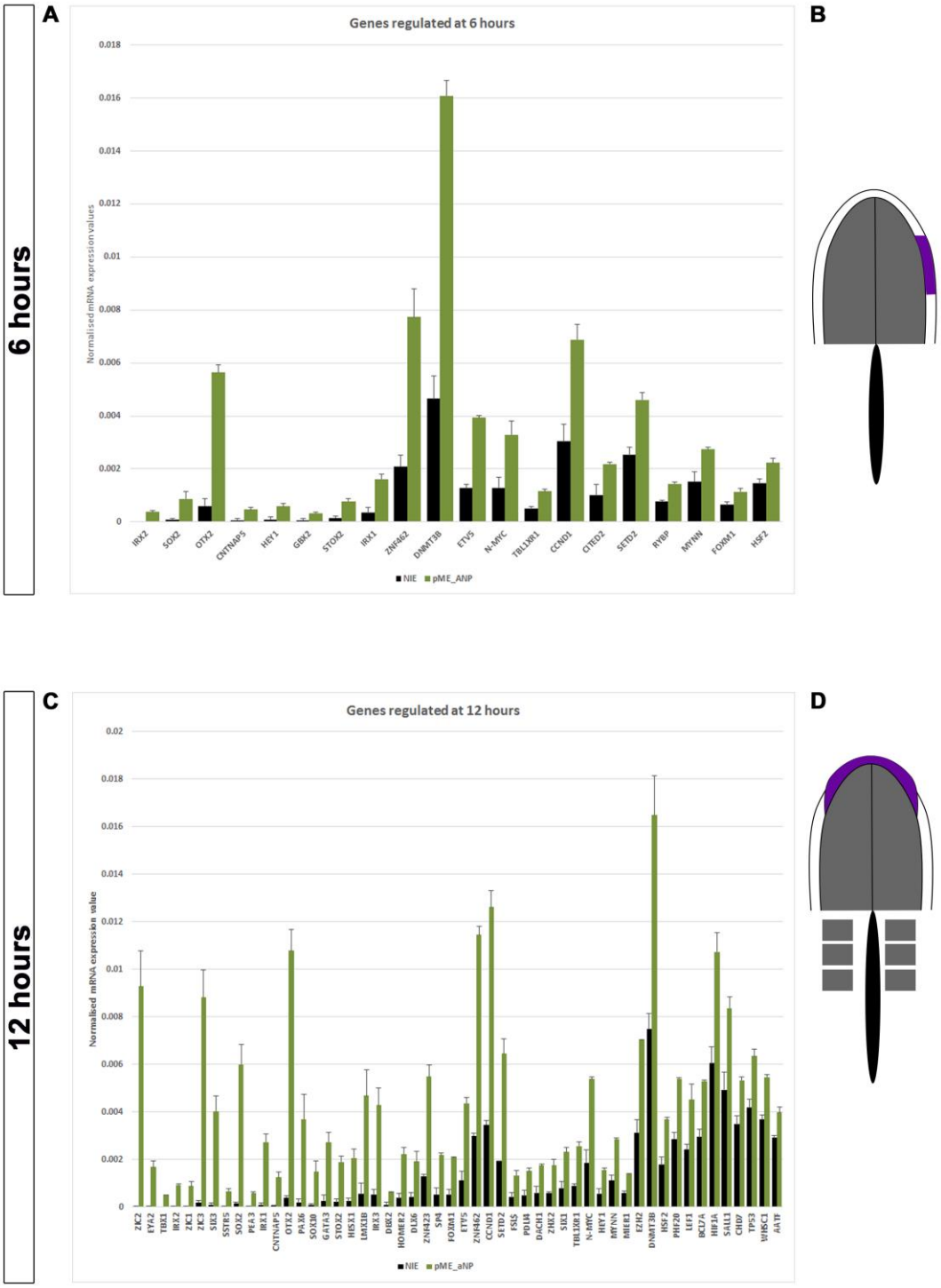


Figure 4.14: Response to pME and aNP combination grafts at 6 and 12hrs

Figure 4.14: Response to pME and aNP combination grafts at 6 and 12hrs

**A**. Axial homotypic combination grafts of pME and aNP were made in to the extraembryonic region of a $HH3^{+}/4^{-}$ chick host; after 6 or 12 hrs the ectoderm in contact with the graft was isolated and analysed by NanoString. Bar chart showing transcripts that are upregulated significantly at 6 hrs (p-value <0.05) by an lHM and pNP graft (Khaki green) as compared to non-induced ectoderm (black). Error bars represent standard error of the mean (SEM). **B.** Summary diagram displaying earliest overlapping region of expression patterns. **C.** Bar chart showing transcripts that are upregulated significantly at 12 hrs (p-value <0.05) by a pME and aNP graft (Khaki green) as compared to non-induced ectoderm (black). Error bars represent standard error of the mean (SEM). **D.** Summary diagram displaying earliest overlapping region of expression patterns, this contains a region that corresponds to LOP cells.

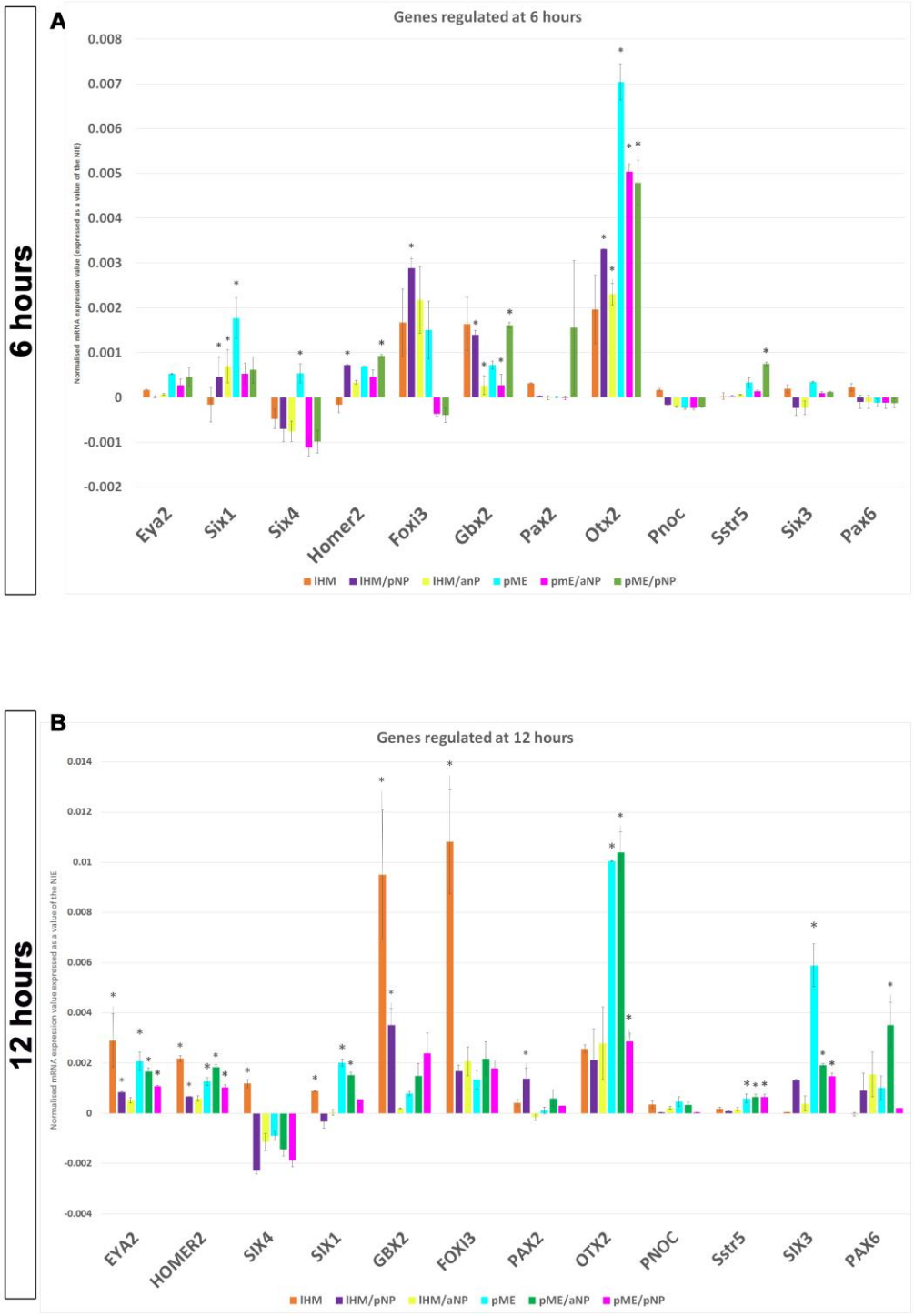


Figure 4.15: Axial heterotypic grafts compared to single and homotypic combination grafts at 6 and 12 hours

**Figure 4.15: Axial heterotypic grafts compared to single and homotypic grafts at 6 and 12 hours**

Axial heterotypic grafts of lHM and aNP (Yellow) or pME and pNP (Pink) were made in to the extraembryonic region of a $HH3^{+}/4^{-}$ chick host; after 6 or 12 hrs the ectoderm in contact with the graft was isolated and analysed by NanoString

. **A.** Bar char displaying the regulation of genes at 6 hours in the following conditions; lHM (Orange), lHM/pNP (Purple), lHM/aNP (Yellow), pME (Sky blue), pME/aNP (Khaki green) and pME/pNP (Pink). Mean expression values are expressed as a value of the control NIE value. Therefore, a negative value on the graph merely represents that the value in the experimental condition is lower than the control and is not an indication of repression. Significantly regulated genes are marker by * and have a P-value <0.05.

**B.** Bar char displaying the regulation of genes at 6 hours in the following conditions; lHM (Orange), lHM/pNP (Purple), lHM/aNP (Yellow), pME (Sky blue), pME/aNP (Khaki green) and pME/pNP (Pink). Mean expression values are expressed as a value of the control NIE value. Therefore, a negative value on the graph merely represents that the value in the experimental condition is lower than the control and is not an indication of repression. Significantly regulated genes are marker by * and have a P-value <0.05

# 5. Signalling during PPR induction

The previous chapter investigated the temporal response to signals from the lHM and pME, specifically pointing to sets of transcripts induced prior to the Six/Eya cassette. These results showed that different targets are under the control of each tissue. The lHM is a source of FGF and antagonists of the WNT and BMP families (Chapman et al., 2002; Litsiou et al., 2005; Lunn et al., 2007; Ogita et al., 2001; Rodríguez Esteban et al., 1999) and these signalling factors can indeed induce *Six4* in competent epiblast after 16 hours (Litsiou et al., 2005). In addition, while FGF signalling is required within the first 4 hours of induction, after this time period it is dispensable and PPR markers are induced even when FGF is blocked at the 4 hour mark (Litsiou et al., 2005). Therefore, this chapter will investigate the sufficiency and necessity of individual signals (FGF, WNT antagonists and BMP antagonists) for the induction of PPR-specific genes and their potential upstream regulators from both the lHM and pME.

FGF signalling seems to play an important role during early ectodermal patterning. During neural induction, FGF is responsible for the expression of 'pre-neural' genes including *ERNI* and *Sox3* (Streit et al., 2000), which are both expressed before gastrulation and remain expressed in the neural plate and its border at primitive streak stages (section 1.3.1). FGF can also repress NNE and neural crest factors (*Msx1* and BMP4; (Stuhlmiller and García-Castro, 2012). Although FGF4 can induce ectopic neural crest markers (*Pax7*, *Msx1* and *Snail2*) without inducing mesoderm, this happens in the presence of a neural promoting media, whose effects were not determined. Also within this experiment the incidence of neural crest marker induction was very low. Suggesting, variable extrinsic influences not investigate played a role in this induction (Yardley and García-Castro, 2012). Therefore, FGF can initiate the early neural induction sequence, the neural crest program and is part of the signalling cascade responsible for the induction of PPR markers.

WNT signalling is also important in positioning the neural plate border and the PPR (Sections, 1.3.2, 1.4.3). The canonical WNT pathway promotes neural crest fate at the cost of PPR and neural plate territories (Basch et al., 2006; Brugmann et al., 2004; Chang and Hemmati-Brivanlou, 1998; García-Castro et al., 2002; LaBonne and Bronner-Fraser, 1998; McLarren et al., 2003), and indeed needs to be inhibited for early steps in neural development to occur, this inhibition Is mediated by FGF signalling (Gunhaga et al., 2003; Wilson et al., 2000; Wilson et al., 2001) At the very early stages of development WNT positions the posterior marginal zone at the border of the area pellucida and allows *Vg1* to initiate axis induction (Skromne and Stern, 2001). The lHM is a source of WNT antagonists

and their miss-expression expands PPR markers but does not induced them ectopically (Brugmann et al., 2004; Litsiou et al., 2005). Consequently, WNT and its attenuation is involved in PPR induction, although the direct targets and temporal necessity has not been investigated.

The role of BMP signalling in ectodermal patterning has been widely investigated due to the initial theory that BMP inhibition alone is sufficient for neural induction in *Xenopus* (Wilson and Hemmati-Brivanlou, 1995, For review see: De Robertis and Kuroda, 2004; Harland, 2000; Weinstein and Hemmati-Brivanlou, 1999). In the context of PPR formation, ectopic expression of BMP antagonists leads to its expansion inducing expression of the PPR markers *Six4* and *Eya2* (Litsiou et al., 2005). However, there is also a role for BMP signalling at an earlier point in development. BMP activity is responsible for the induction of a number of factors such as *Tfap2a*, *Foxi1, Dlx3* and *Gata2/3*, which are in turn required for setting up a domain of competence for PPR induction (Kwon et al., 2010; Pieper et al., 2011). However, the role of BMP attenuation has not been thoroughly investigated to determine which targets are controlled by the inhibition of BMP signalling in PPR development.

To investigate the role of FGF, WNT and BMP signalling in PPR induction, gain- and loss-of-function approaches were carried out combined with tissue grafting experiments using the induction assay in the chick extraembryonic region. To ask which lHM- or pME-induce transcripts require FGF signalling, BMP and WNT antagonism each tissue was grafted together with appropriate inhibitors. For gain-of-function experiments, FGF8-coated beads were grafted into the extraembryonic region of $HH4^{-}$ hosts, while BMP attenuation was achieved by exposing the embryo to Dorsomorphin (a BMP inhibitor). For all experiments the exposed extraembryonic ectoderm was dissected at various time points (3, 6 or 12 (12 hours is only applicable to loss of FGF from lHM experiment)) and analysed by NanoString using the same probe set used in previous experiments.

## 5.1 The sufficiency and necessity of FGF signalling in PPR induction

To investigate FGF sufficiency, heparin beads coated in 50mg/ml of mouse recombinant FGF8b were grafted into the extraembryonic region of a HH stage $3^{+}/4^{-}$ chick embryo (Figure, 5.1a, A). The underlying ectoderm was then dissected after 3 or 6 hours, the response of a wide range of transcripts was then analysed using NanoString. The time points of 3 and 6 hours were chosen to match the time points of tissue grafts. Later time points

were not investigated as the response may represent the combination of FGF targets and secondary effects downstream.

The appropriate FGF8b concentration was determined using *Sox3* as a positive control, which is known to be induced by FGF (Streit et al., 2000). After 3 hours *Sox3* was indeed induced in the presence of beads coated in 50mg/ml of FGF8b (Figure 5.1a, B). When assayed by NanoString, after 3 hours a small number of genes was induced, *Trim2*4, *Sall4*, *Etv5* and *ERNI*. A number of these genes are known to be FGF responsive, for example *ERNI*, or the FGF mediator *Etv5*; another factor in the FGF pathway *Pea3* is also on the cusp of induction with 3-fold change, but a p-value of only 0.06 (Figure 5.1a, D; Lunn et al., 2007; Streit et al., 2000). In addition, FGF is also sufficient to reduce the level of several NNE genes *Tfap2a*, *Axin2*, *Dlx5* and *Gata2*. When compared to the endogenous expression of the induced genes several initially found in the pre-streak epiblast (*ERNI* (Streit et al., 2000; *Trim24* (Figure, 4.1) *Etv5*, (Trevers, 2015), while *Sall4* is expressed in the pre-neural plate epiblast (Barembaum and Bronner-Fraser, 2007) although its expression at pre-streak stages has not been investigated. Induction of *Trim24* by an FGF8 bead after 3 hours was validated using in situ hybridisation (Figure 5.1a, C). In contrast, FGF-repressed transcripts are initially restricted to the peripherally epiblast at primitive streak stages (e.g. *Dlx5* and *Gata2* (Pera and Kessel, 1997; Sheng and Stern, 1999) and later confined to the non-neural ectoderm. The induction of these early factors and their endogenous expression patterns suggests that FGF generates cells, whose transcriptional profile is similar to the early pre-streak embryo.

How does the response to FGF signalling compare to the response to tissue grafts (Figure 5.1.1, F). Similar to the lHM and pME, at 3 hours FGF8 initiates the expression of *Ccnd1*, *ERNI*, *Etv5* and *Trim24* and suppresses *Tfap2a*, *Axin2*, *Dlx5* and *Gata2* (Figure 5.1b F-G). Although not quite significant *N-myc*, a gene induced by the lHM and pME, has a trend towards being induced by FGF, with a 4-fold increase and a p-value of 0.06. *Cxcl14* induction is only observed with FGF8, but not with the lHM. Finally, it should be pointed out that unlike the results obtained by in situ hybridisation, *Sox3* was not induced in the NanoString analysis. A possible reason for this is that the short oligonucleotide is not able to bind to the target sequence with a high affinity. Overall, 50% of the genes regulated by each tissue are in common with those controlled by FGF signalling (Figure 5.1b, F). However, each tissue also induces factors that are not regulated by FGF. These results suggest that at 3 hours FGF regulates a large proportion of the genes that are also induced by both the lHM and pME. Considering endogenous expression domains of these transcripts, suggests that the FGF–inducted tissue matches the transcriptional profile of the pre-streak stage epiblast.

At 6 hours, FGF8 has now up regulated 15 factors, a number of which were already induced at 3 hours (*Ccnd1, Etv5* and *Trim2*4). Among the novel transcripts are *Cited2*, *Dmnt3b*, *Mier1*, *Morc2*, *Nfkb1, Rybp*, *Tbl1xr1*, *Zhx2*, *Znf423* and *Znf462* (Figure 5.1a, E). Surprisingly, one of the fastest genes to respond to FGF, *ERNI*, is no longer upregulated at 6 hours; this may reflect its dynamic expression in the embryo being lost from the forming neural plate and later from the PPR (Streit et al., 2000; Streit, 2002). The NNE genes downregulated by FGF at 3 hour remain repressed, with the exception of *TFap2a*, which now is no longer repressed but is not upregulated either. The genes that are upregulated are mainly expressed in the neural plate and border at HH stage $4^+$ e.g. *Cited2*, *Mier1* and *Znf462*.

The comparison of 6hr FGF-regulated and lHM- or pME-controlled transcripts (Figure 5.1.1, G) reveals that 48% of genes are in common between lHM and FGF, but only 38% when comparing pME and FGF (Figure 5.1b, G-G'). FGF promotes the expression of several genes, not induced by lHM or pME (*Mier1*, *Morc2* and *Zhx2*) and vice versa (lHM; *Sall1*, *Stox2* and *Pdlim4*; pME; *Fsl4*, *Hsf2* and *Zic3*). Importantly, for example while *Six1* is expressed in response to the pME, this is not apparent with FGF. Thus, while a similar set of transcripts is initiated after a short period of tissue or FGF exposure, the downstream events diverge later.

A complementary set of experiments was designed to assess which genes induced by the lHM or pME require FGF signalling. To do this each tissue was grafted into the extraembryonic region of a HH stage $3^+/4^-$ chick embryo together with three Ag1x2 beads coated with the FGF receptor inhibitor SU5402 (Figure 5.2, A; (Mohammadi et al., 1997)). The effective SU5402 concentration (25mM) was determined in previous experiments, where SU5402 beads were combined with organiser grafts (Streit et al., 2000). As before, the tissue underneath the graft was removed and analysed by NanoString at various time points (lHM 3, 6 and 12 hours; pME 3 and 6 hours). This was then compared to the lHM in the presence of DMSO condition.

As discussed above FGF8 beads rapidly induce the expression of *Cxcl14*, which is never initiated by the lHM and therefore not considered further. Of the remaining genes, *Etv5* and *Trim24*, which do respond to the lHM, the FGF-mediator *Etv5* was significantly lower along with *Otx2* while *Ccnd1, Trim24* and Zic3 were all lower in the presence of SU5402 (Figure 5.2, B) but not quite below the 0.05 significance threshold. Thus, these genes may depend on FGF input and FGF8 is sufficient to induce them. In contrast, *N-myc* which was lower was not significant at all and *ERNI* continued to be expressed in the

absence of FGF signalling, suggesting that while FGF8 can induce its expression, FGF signalling is not required, and that other factors within the lHM have *ERNI*-inducing ability.

A number of gene upregulated in response to the lHM grafts continue to be expressed when FGF signalling is compromised namely, *ERNI*, *N-myc*, *Otx2* and *Zic3* (Figure 5.2, B). This finding proposes that FGF is not required for a number lHM-induced transcripts. Interestingly, the attenuation of FGF signalling leads to the induction a new gene *Irx1* suggesting that FGF from the lHM may prevent its induction while other signals promote it (Figure 5. 2, B; 3 hours).

As discussed above, lHM grafts repress the expression of *Axin2*, *Dlx3/5*, *EEf1a1*, *Gata2*, *Kertain19* and *Kremen1* and of those *Axin2*, *Dlx3/5* and *Gata2* are also repressed by FGF8 alone. The majority of these transcripts continue to be repressed even in the absence of FGF signalling, suggesting that while FGF8 can suppress their expression it is not required to do so and other signals in the lHM can compensate for the loss of FGF signalling (Figure 5.2, B; 3 hours).

At Six hours' genes when the lHM and lHM/SU Combination are compared genes significantly lower in the presence of SU5402 include; *Ccnd1, Nfkb1*, *Dnmt3b* and *Sox3*, (Figure 5.2, C). While genes that are lower but not significant include, *N-myc*, *Pdli4, Sall1* and *Stox2.* There was no change in ERNI, ETV5 and Znf462 (Figure 5.2, C). *Etv5* and *ERNI* remains upregulated even when FGF signalling is attenuated, it is possible that they respond to other signals. Another possibility exists, the inhibitor is coated on to fine glass beads (AGX12) and it cannot be determined that the rate and concentration with which the inhibitor is released by the beads is consistent, therefore there may still be residual FGF signalling.

The 12-hour comparison reveals that *N-myc*, *Etv5*, *Sall1,* and *Znf462* are all significantly lower, suggesting these genes depending on FGF signalling (Figure 5.2, C). Genes that may be influenced by a lack of FGF signalling but may not depend on FGF, as they are lower but not significant when compared to the lHM alone condition, are; Gbx2, Ccnd1 and Foxi3. Genes that don't change suggesting an independence of FGF include *Trim24*, *Znf462*, *N-myc*, *Otx2*, *Homer2*, *Eya2*, *Gata3*, *Dach1* and *Six1*. Interestingly these include the PPR genes *Six1* and *Eya2*.

The dependence of the FGF signalling from the pME was investigated at 3 and 6 hours. The decision to omit the 12-hour time point was taken for the reason that the long term effects on the grafted tissue of signalling inhibitors were not known. Experiments

which will be discussed in the section below using a WNT activator (BIO) lead to loss of *Six1/Eya2* in the graft after 12 hours, suggesting the graft had changed fate.

At 3 hours the pME/SU combination when compared to the pME/DMSO induction showed *N-myc* and *Trim24* to be significantly lower suggesting their induction depends on FGF from the pME at 3 hours. Another gene significantly changed was *Keratin19* which was now significantly higher in the pME/SU condition, indicating the repression of this gene is dependent on FGF (Figure 5.3, B). A number of genes were slightly lower, e.g. Otx2 but these were not significant (Figure 5.3, B), while others induced by the pME alone were not changed at all.

At 6 hours the comparisons of SU treated grafts and DMSO treated grafts showed that a large number of genes were significantly lower in the pME/SU condition; *Ccnd1*, *Cited2*, *Six1*, *Six4*, *Irx2*, *Otx2*, *Zic2*, *Sall1*, Trim24 and *Znf423* (Figure 5.3, B). This lower set of genes now includes *Six1* and *4* genes, suggesting that at this time point they depend on FGF for the induction from the pME.

In conclusion the attenuation of FGF signalling from both the lHM and pME leads to the loss of a number of genes, this loss is greater for the pME. Suggesting that the pME is more sensitive to the loss of FGF in PPR induction.

## 5.2 The role of WNT signalling in PPR induction

PPR induction requires the inhibition of canonical WNT signalling (Brugmann et al., 2004; Litsiou et al., 2005) and both the lHM and pME are the source of different WNT antagonists. To establish which lHM- and pME-response genes require WNT inhibition, either tissue was grafted into the extraembryonic region of a stage $HH3^{+}/4^{-}$ chick embryo surrounded by AG1X2 beads coated with the WNT activator BIO ((2'Z, 3'E)-6-Bromoindirubin-3'-oxime).

First, an effective concentration needed to be established. WNT signalling is involved in patterning the neural plate with high levels of WNT imparting posterior character to rostral tissue (Nordström et al., 2002). These findings were exploited to determine a suitable BIO concentration and its effect on *Otx2* expression in the forebrain was assessed (Figure 5.4). Beads were grafted into the anterior neural plate of a HH stage $4^{-}$ chick; these were left to grow for 12 hours. At a concentration of 2.5µM *Otx2* was found to be disrupted when compared to control beads, which had been soaked in 1:1000 DMSO (Figure 5.4; A-B). Although a larger down regulation of *Otx2* was expected than what was

achieved, the bead appeared to move as development proceeded, suggesting that tissue was not exposed for long enough to achieve a full down regulation of *Otx2*. As the extra embryonic region of the chick remains relatively flat during the experimental time period, a large movement of the bead was not anticipated. Also the distance of the bead to the graft could be assessed easily grafts where the bead had moved further than half a width of a bead away were not used for subsequent NanoString analysis. However, there were obvious morphological defects to the neural tube at this concentration. Therefore, 2.5µM was used as the concentration to attenuate WNT signalling in the extraembryonic region.

To assess which lHM-induced genes require WNT antagonism, lHM grafts were placed next to competent epiblast surrounded by BIO-coated beads or beads incubated in vehicle alone (DMSO 1:1000; Figure 5.5, A). The ectoderm adjacent to the grafts was analysed after 3 and 6 hours using NanoString. Longer incubation times were not assessed because WNT signalling may influence the graft itself, as it is known to pattern the mesoderm (Eisenberg et al., 1997; Hoppler and Moon, 1998). At 3 hours, the lHM surrounded by BIO-coated beads has caused an increase in a number of genes, which are normally not expressed in response to the lHM. These include *Lef1*, *Hsf2* and *Tbl1xr1* , shown to be regulated in cells by WNT (Lef1 is shown for validation in Figure 5.5, B; (Choi et al., 2011; Huber et al., 1996; Kavak et al., 2010), suggesting that there is a level of effectiveness of WNT activation by BIO.

Comparison of the original lHM experiment and the lHM/BIO combination that *Otx2* was significantly lower than the original induction and that *Trim24* was lower but not significant. Suggesting these two genes may depend on the inactivation of WNT in the induction assay (Figure 5.7, B). Other genes remained unchanged. However, it should be noted that there was a large amount of variability within this experiment suggesting the results should be met with some caution as to their reliability (seen in standard error bars, Figure 5.5, B). However, the significant lowering of *Otx2* does correlate with the control experiment, suggesting the BIO is indeed active (Figure 5.5, A; Figure 5.5, B).

At 6 hours' genes that were significantly changed included *Sall1*, *Sox3* and *Trim24*, while *N-myc* and *Znf462* were lower neither was statistically significant. Suggesting that these genes all require WNT antagonism to be expressed. There is very little effect on genes originally down regulated by the lHM

The above results show that a number of transcripts normally induced by lHM grafts depend on WNT inhibition suggesting that WNT antagonism may be required at early stages of PPR induction. To investigate the timing of this requirement in more detail lHM grafts

were combined with BIO-coated beads at different time points during the induction assay. All grafts were analysed after 16 hrs, when the lHM normally induces the PPR markers *Eya2* and *Six1*

The lHM was grafted alone (control; lHM 16 hrs) or together with Bio-coated beads (lHM+BIO, 16 hrs). To assess whether a pulse of activation is sufficient to interfere with the induction of PPR markers, lHM was grafted together with BIO beads and the beads were removed after 5 hrs, while the embryos were grown for another 11 hours (lHM+ 5hrs BIO). To assess whether WNT activation interferes with PPR induction at late stages of the process, the lHM was grafted and BIO-coated beads were added either 5 (lHM+BIO after 5hrs) or 12 hours (lHM + BIO after 12 hrs) later. All experiments were analysed using *Eya2* in situ hybridisation, while "lHM+BIO after 5 hrs" was also analysed by *Six1* in situ hybridisation. In all conditions containing BIO *Eya2* and *Six1* induction was lost or reduced in the graft and host (Figure 5.6, A-F). These results suggest that unlike FGF signalling, which is required for the first 5 hours of induction (Litsiou et al., 2005), WNT antagonism may be required throughout PPR induction.

Similar experiments were carried out to assess how overriding WNT antagonism affects the response to pME grafts. As above, the pME was grafted into HH3+/4- hosts together with Ag1x2 beads coated in 2.5µM of BIO or 1:1000 DMSO (Figure 5.6, A). The ectoderm in contact with the grafts was dissected and analysed by NanoString.

At 3 hours, the pME induces *Ccnd1*, *ERNI*, *Etv5*, *Gbx2*, *Irx1*, N-*myc*, *Otx2*, *Trim24* and *Zic3* (Figure 4.6; Chapter 4); most of these continue to be induced when WNT is activated and only a small number of genes significantly different: *Gbx2*, *N-myc* and *Trim2*4 (Figure 5.10, B) indicating that their induction requires attenuation of WNT signalling. Of the genes normally downregulated by the pME; *Tfap2a*, *Axin2*, *Dlx5* , *Gata2* and *Dlx5*. The down regulation of *Eef1a1* is lost on the activation of WNT and *Dlx3* and *Kremen1* are now down regulated when they were not in the pME alone condition (Figure 5.7, B). Thus, few changes are observed 3 hrs after pME and BIO-bead grafts.

By 6 hours in response to a and pME/BIO graft the induction of the PPR markers *Six1/4* is significantly lower, alongside *Sall1*, *Trim24* and *N-myc*. *Otx2* is lower but not significant. These results indicate that WNT antagonism from the pME is vital in PPR induction and may play an early role in the induction of the PPR.

## 5.3 The role of BMP antagonism in PPR induction

The induction of the PPR requires the attenuation of BMP signalling (Litsiou et al., 2005) and the lHM and pME are both sources of BMP antagonists (GEISHA: Antin et al., 2007; Ogita et al., 2001; Rodríguez Esteban et al., 1999). To establish the targets that require BMP inhibition from lHM- and pME- either tissue was grafted into the extra embryonic region of the chick and surrounded by heparin beads coated in Recombinant mouse BMP4 (R&D Systems). To assess which transcripts BMP inhibition is sufficient to induce Dorsomorphin dihydrochloride (6-[4-[2-(1-Piperidinyl) ethoxy] phenyl]-3-(4-pyridinyl)-pyrazolo [1, 5-a] pyrimidine dihydrochloride, Tocris Bioscience) was grafted into the extra embryonic region. In both experiments the underlying ectoderm was removed after 3 or 6 hours and analysed by NanoString (Figure 5.9, A).

The working concentration of BMP4 was established by grafting BMP4-coated heparin beads into the border of the neural plate of a 4$^{-}$ chick embryo. After 8 hours, the expression of the neural marker *Sox2* was assessed as previous experiments established that activation of BMP signalling narrows the neural plate (Linker and Stern, 2004). At 1µg/ml of BMP4, there was a loss of *Sox2* in the neural plate when compared to the control side of the embryo (Figure 5.8, white v yellow bar). Therefore, this concentration was used in all further experiments.

A three hours the lHM induces genes *Bcl11a*, *Ccnd1*, *ERNI*, *Etv5*, *Mier1*, *N-myc*, *Otx2*, *Trim24* and *Zic3* (Figure 4.1; Chapter 4). Genes that are unaffected in the lHM/BMP condition are; *Etv5*, *ERNI*. However, *Otx2* and *Ccnd1* normally upregulated in the lHM condition are significantly lower when BMP is activated (Figure 5.9, B). *Trim24*, N-myc and Zic3 are lower in the presence of BMP but not significantly (Figure 5.13, B). While *Dlx5* which is normally repressed in the presence of the lHM alone is now upregulated when BMP is activated (Figure 5.9, B).

At 6 hours there are only 3 genes are significantly effected in the lHM/BMP condition, Including *Ccnd1* and *ERNI* (Figure 5.9, C). While the addition of BMP no longer leads to the down regulation of *Dlx5* (Figure 5.9, C). These results show a number of genes require the inhibition of BMP and that overriding BMP will lead to a loss of factors in PPR development.

The necessity of BMP signalling in the pME was analysed in the same way as the lHM. At 3 hours the pME induces *Ccnd1*, *ERNI*, *Etv5*, *Gbx2*, *Irx1*, *N-myc*, *Otx2*, *Trim24* and *Zic3* (Figure 4.3, Chapter 4); and in the pME/BMP condition only *Trim24* is significantly lower

in the presence of BMP, while *N-myc* and *Ccnd1* are lower but not to a significant degree. Suggesting only *Trim24* is effected by the addition of BMP (Figure 5.10, B).

At 6 hours, the response that the pME usually generates has changed on the addition of BMP4, with Six1/4, trim24, Sox3 and N-myc all significantly lower (Figure 5.10, B). Suggesting these genes all require the inhibition of BMP to be induced in the PPR induction cascade.

Complementary experiments were carried out to assess whether BMP antagonism is sufficient to induce any genes in the PPR induction cascade. Dorsomorphin, an established BMP antagonist (Hao et al., 2008) was added to the albumen in which the embryo was cultured. To establish a suitable concentration, the effect of Dorsomorphin on somite development was tested as BMP signalling mediates medio-lateral patterning of the mesoderm with high levels of BMP promoting lateral plate mesoderm and low or no BMP signalling favouring somite development. Stage HH $4^-$ chick embryos were cultured for 12 hours with different concentrations of Dorsomorphin; at 10µM of Dorsomorphin somites were expanded into the lateral plate mesoderm consistent with findings that beads of noggin will convert the lateral plate mesoderm into extra somites (Figure 5.11 A and B, n = 3, (Tonegawa and Takahashi, 1998).

Consequently, Dorsomorphin was added to the albumen on which HH stage $3^+/4^-$ chick embryo was cultured, after 3 or 6 hours extra embryonic ectoderm was excised along with time matched control (1:1000 DMSO added to albumin) ectoderm and analysed by NanoString.

The lHM induces *Bcl11a*, *Ccnd1*, *ERNI*, *Etv5*, *Mier1*, *N-myc*, *Otx2*, *Trim24* and *Zic3* at three hours (Figure 4.1; chapter 4). While At 3 hours Dorsomorphin upregulates *Dach1*, *Sall1*, *Irx1* and *Nfkb1* (Figure 5.12, A). Comparatively, none of the genes induced by Dorsomorphin are induced by the lHM at 3 hours (Figure 5.12, A). Suggesting, that BMP inhibition is not sufficient to induce any factors that the lHM induces at 3 hours. Although at 6 hours in the lHM only condition Nfkb1 and *Sall1* are upregulated, these genes are upregulated by Dorsomorphin at 3 hours (Figure 5.12, A). This may suggest that BMP inhibition plays a role in the positive regulation of these genes. At 6 hours Dorsomorphin only induces *Zhx2*, this gene is not regulated by the lHM (Appendix 9.7).

The pME induces *Ccnd1*, *ERNI*, *Etv5*, *Gbx2*, *Irx1*, N-*myc*, *Otx2*, *Trim24* and *Zic3* at 3 hours, While Dorsomorphin only induces Irx1 of this cohort of genes (Figure 5.12, A). Suggesting that BMP inhibition is sufficient for the induction of *Irx1*. *Irx1*, is also lost on the application of BMP to the PME, indicating that BMP inhibition is not only sufficient for Irx1 induction

but also necessary. Again at 6 hours Dorsomorphin induces no factors that the pME induces (Appendix 9.7).

These results show that the attenuation of BMP is necessary for the induction of targets involved in the temporal hierarchy upstream of the Six/Eya cassette. It is also necessary for the induction of Irx1 which is normally induced by the pME at 3 hours in PPR induction.

## 5.4 A model of signalling during PPR initiation

The previous sections analysed the role of FGF, BMP and WNT signalling during the earliest phases of PPR induction and defined the signalling inputs required for many of the factors induced by the pME and lHM. The next step requires the integration of these results into a comprehensive model to understand how each target in the PPR induction cascade is controlled by different signals. To do this all results were collated and compared to create models of the response to signals from the lHM and pME at 3 and 6 hours. The above effect of each signalling factor was used to determine the signalling input for each gene. The results were visualised using BioTapestry (Longabaugh et al., 2005)

At 3 hours, the lHM induced only 9 genes namely *Bcl11a*, *Ccnd1*, *ERNI*, *Etv5*, *Mier1*, *N-myc*, *Otx2*, *Trim24* and *Zic3* and represses *Tfap2a, Axin2, Dlx5, Gata2* and *Kremen1*. Most of these are under the control of FGF signalling (induction; *ERNI*, *Etv5*, and *Trim2*4; repression: *Tfap2a*, *Axin2*, *Dlx5* and *Gata2*). Activation of the FGF pathway is both required and sufficient to induce *Etv5* and *Ccnd1*, the FGF pathway also controls *Otx2.* BMP antagonism is possibly necessary for *Zic3 1* induction, while a number of genes need combined input from different pathways. *Ccnd1* induction and *Dlx5* repression are regulated by both FGF and BMP antagonism, while *Zic3* is the only gene under the control of BMP and WNT antagonism and *Otx2* induction needs input from all three signalling pathways FGF together with inhibition of BMP and WNT. The regulation of one gene cannot be determined: *Bcl11a* induction is not affected under any condition suggesting an unknown signalling factor to be responsible for induction (Figure 5.13).

Three hours of pME signalling induced a similar set of transcripts than the lHM (See chapter 4, section 4.2) the majority of which are initiated by FGF signalling, similar to lHM-induced genes. The repression of Keratin19 requires FGF, while *Gbx2* induction depends on WNT antagonism. *Ccnd1* requires the presence of both WNT and BMP antagonism. Two genes, *N-myc* and *Trim24*, require all three signals for induction. Only a single transcript, *Irx1* is induced by BMP signalling alone: BMP inhibition can induce its expression. The vast majority of genes appear to require input from both pathways for their induction, FGF activation and

BMP antagonism (*ERNI*, *Ccnd1*, *N-myc*, *Trim2*4; Figure 5.21) While, *Zic3* and *Otx2* induction can't be explained by these experiments in relation to their induction by the pME (Figure 5.14). This may be due to the levels of signalling factors being different from the lHM in the pME and thus not being overridden by the addition of SU5402, BMP4 or BIO.

Overall the above results show the dependency of each target induced by the lHM and pME on FGF, WNT antagonists and BMP antagonists. The large number of genes that show regulation in some part (Sufficient or required) by FGF coincides with the result that FGF is required only for the first 5 hours in PPR induction (Litsiou et al., 2005). Together, this suggests that FGF is key to initiate the first response in cells on their way to become PPR, as BMP antagonism can only induce Irx1 at 3hrs. However, WNT antagonism sufficiency remains to be tested.

## 5.5 A model of signalling at 6 hours in PPR development

6 hours of lHM signalling induces a larger set of genes, but represses only one additional transcript *Keratin19*, when compared to 3 hours LHM exposure. FGF is sufficient for Most downregulated transcripts (*Axin2*, *Dlx3*/*5* and *Gata2*). FGF is required for the genes *Nfkb1* and Dmnt3b. Wnt antagonism is required for *Sall1*, *N-myc* and also influences *Znf462*. BMP antagonism is required for *Dlx5* repression and *ERNI*. Combined signalling of FGF and WNT antagonism is necessary for *Sox3*; while FGF an BMP antagonism is necessary for *Ccnd1* (Figure 5.15). While *Stox2* and *Nfkb1* are not effected by any signalling factor loss, suggesting an untested signalling factor regulates these two.

6 hours after exposure to the pME Ccnd1, Cited2, Irx2, Zic2 and Znf423 depend on FGF signalling. Sall1 depends on WNT antagonism, with Sox3 induction depending on BMP antagonism. The combined signalling of FGF and WNT antagonism is necessary for the induction of Sall1 and Otx2 and BMP and WNT antagonism is necessary for N-myc signalling. The PPR genes Six1/4 depend on the presence of all three signalling pathways for their induction at 6 hours by the pME. (Figure 5.16). A small number of genes signalling dependence remains to be accounted for (Figure 5.16)

Overall at early time points for both the lHM and pME induced genes there is a large role for FGF signalling, there is role for BMP antagonism. While, at later time points the role for all three is important to PPR induction. One difference between the lHM and pME is the role of *Irx1* at 3 hours, induced by the pME and under the control of BMP antagonism, it is absent from lHM inductions. It is possible that as in previous experiments in early

development there is an important role for FGF early and subsequently WNT signalling at a later time point (Gunhaga et al., 2003; Wilson et al., 2000; Wilson et al., 2001)

## 5.6 Discussion

Chapter 4 described the temporal hierarchy of gene expression in response to signals from the PPR-inducing tissues, the lHM and pME. Experiments in the current chapter aimed to unravel the downstream targets of FGF activation, BMP and WNT antagonism, three pathways that cooperate to induce placode progenitor next to the neural plate. A combination of these signals can also induce ectopic PPR-like cells in competent ectoderm and this assay was therefore used to disentangle the contribution of each pathway to PPR initiation. I find that although the lHM and pME induce different sets of genes at each time point, many of the earliest responses to both tissues are in part initiated or controlled by are dependent on FGF signalling alone or in combination with BMP antagonism. WNT inhibition seems to be required slightly later, when many up- and downregulated genes are dependent on input from all three pathways. Together, these experiments suggest that FGF may trigger the earliest response and start PPR induction in accordance with published data (Litsiou et al., 2005) while BMP and WNT inhibition is important at a slightly later point.

### 5.6.1 FGF signalling: a mediator for PPR initiation?

Among the earliest responses to FGF activation is the induction of the known FGF-target *Etv5*, which is known to mediate many FGF responses (Roehl and Nüsslein-Volhard, 2001). The finding that FGF is sufficient and required for *Etv5* expression validates both gain- and loss-of-function approaches demonstrating successful activation and inhibition of the pathway. In comparison to *Etv5*, *ERNI* is also regulated by FGF signalling (Streit et al., 2000) although FGF requirement could not be demonstrated. This is different from earlier results which showed that *ERNI* is induced by the organiser, Hensen's node, but this fails when FGF is inhibited. One possible explanation for this discrepancy is that *ERNI* induction occurs rapidly, after only one hour. Unlike in previous experiments (Streit et al., 2000), the embryos were not pre-incubated with FGF inhibitor, but beads and tissue grafts were placed at the same time raising the possibility that an initial wave of FGF may initiate *ERNI* before signalling can be blocked efficiently. In support of this, experiments (data not included) showed that *Trim24*, whose induction I show requires FGF signalling, takes much longer to be induced: it is only weakly upregulated by the lHM at 2 hours and fully induced by 3 hours. Therefore, *Trim2*4 may require sustained FGF signalling and can be blocked efficiently in the

assay used. Thus, the initial response to FGF, the lHM and pME is likely to be a hierarchy with *ERNI* being initiated first and *Trim2*4 appearing later together with *Etv5*.

In both 3 hour signalling models one gene for which regulation cannot be accounted for is *Otx2*, it has previously been shown that FGF cannot induce *Otx2* alone (Albazerchi and Stern, 2007) but that a low level of FGF with WNT and BMP antagonists can induce *Otx2* (Albazerchi and Stern, 2007). Therefore, it may be a case that the inhibition of the signalling molecules only lowers the level of signalling and does not abolish it and thus it cannot abolish *Otx2* induction.

Analysing how different pathway antagonists/agonists alter the response to pME and lHM derived signals reveals subtle differences in signalling from each tissue. Although a few genes rely on WNT and BMP antagonism, in the early period of PPR induction the vast majority of genes are under the control of FGF in particular lHM-induced transcripts. Indeed FGF is only required for the first 5 hours of PPR induction (Litsiou et al., 2005) supporting the idea that FGF is important early during this process. Further analysis of early FGF response genes reveals that all (*Ccnd1*, *ERNI*, *Etv5* and *Trim24*) begin to be expressed at pre-primitive streak stages in the normal embryo before gastrulation (Bally-Cuif et al., 1995; Millet et al., 1999; Streit et al., 2000; Tour et al., 2002) and FGF input is required or sufficient from the grafted lHM or pME. However, these mesodermal tissues have not yet formed at pre-streak stages, suggesting that another source of FGF regulates their expression at this time. A good candidate is the hypoblast, an extraembryonic layer underlying the pre-streak epiblast, which has already been shown to induce *ERNI* and *Otx2* (Streit et al., 2000) and is a source of FGF signalling. These observations suggest that the initial step in response to signals from the lHM and pME resembles a pre-streak epiblast and that cells in the area opaca recapitulate the sequence of events ultimately leading to PPR formation, beginning from the early embryo. Interestingly, some lHM and pME response genes are also induced in response to a graft of Hensen's node (Streit et al., 2000; Trevers, 2015) suggesting that neural and placodal induction may share the earliest steps. FGF signalling may thus be one of the signals initiating both neural and placodal induction before both fates separate.

Overall the early induction of targets relies heavily on FGF with WNT and BMP antagonists playing a small role, most likely in maintaining these genes rather than inducing them, as shown by a BMP antagonist not being able to induce targets involved in PPR induction. The hypoblast has been shown to be able to induce a number of the factors that are expressed early in neural development (*ERNI*, *Otx2*) and further experiments should seek to understand if the hypoblast induces all the genes that FGF alone can as well, which

would provide evidence that FGF does induce a ground state akin to early neural/PPR and neural crest development.

Experiments conducted on early pre-streak embryos, show that blocking FGF signalling leads to the up regulation of BMP and WNT targets and that FGF prevents WNT signalling in the pre-streak epiblast fated to become neural, neural crest and PPR (Wilson et al., 2001). Within these results there is a reliance on FGF signalling early but by 6 hours of induction there is a greater reliance on the repression of WNT and BMP signalling that FGF signalling. This fits with experimental evidence that at PPR stages gain- or loss-of-function of WNT and BMP will lead to a reduction or expansion of the PPR respectively (Brugmann et al., 2004; Litsiou et al., 2005). This may also fit with FGF being responsible for the early embryonic epiblast where it has been shown to repress WNT and BMP (Wilson et al., 2001)

In addition, there seems to be a difference between the role of BMP antagonism from the lHM and pME. At early stages more genes in the pME induction are lost upon the addition of BMP than compared to the lHM induction. One possibility is that is the pME expresses lower levels of BMP antagonism, for example *Chordin* and *Noggin* are expressed in the notochord right up the pME but are absent from the pME (Chapman et al., 2002; Streit and Stern, 1999). While *Follistatin* is expressed in the lHM underlying the pPPR but not in the pME (Chapman et al., 2002). Suggesting that smaller shifts in BMP concentration will create larger effects.

### 5.6.2Signalling: "a co-ordinate like system of information"

A co-ordinate system is the use of one or more numbers to uniquely describe a position in geometric or Euclidean space (Weisstein, 2002). This could be equated to a biological system, whereby the numbers of the co-ordinate system are actually the level (concentration or absence/presence of different signals) of signalling that a cell receives at a particular point in the tissue of an embryo. More precisely the cellular read out of this signalling changes/biases the fate of the cell, which is therefore determined by its position. In this system there are two tissues the lHM and pME which bias the PPR to either a posterior or anterior axial position (chapter4). Subtle differences in regulation by signalling molecules of targets that respond to these tissues may play a role in this bias. The two tissues have different signalling molecules present within their makeup. Signalling molecules present within the lHM include FGF19, The WNT antagonist Dan and the BMP antagonists Cerberus and Follistatin (Chapman et al., 2002; Ladher et al., 2000; Ogita et al., 2001). There are also readouts of FGF signalling (pERK, *Etv5* and *Pea3* (Lunn et al., 2007; Roehl and Nüsslein-Volhard, 2001) and BMP signalling (pSMAD2/5/8 (Faure et al., 2002;

Stuhlmiller and García-Castro, 2012)) present within the overlying ectoderm. While, the pME has low levels or an absence of BMP antagonists such as Chordin, Noggin and Follistatin (Chapman et al., 2002; Streit and Stern, 1999). The pME shows expression of the FGF readout *Pea3,* suggesting the presence of FGF signalling (Lunn et al., 2007; Roehl and Nüsslein-Volhard, 2001). There is also expression of the WNT antagonists from the secreted frizzled and DKK families in the pME (Chapman et al., 2002). The results from this study show that the pME is more sensitive to a loss of FGF and BMP antagonism than the lHM. This sensitivity may be due to the lower level of BMP antagonists and FGF's expressed with in the pME. However, this sensitivity might reveal the subtle differences in levels of signalling that lead to the induction of different genes that will provide the distinction in spatial position. Indeed experiments in Xenopus after gastrulation show that increasing activation of FGF signalling can promote neural crest genes over PPR genes and shift the boundaries of the PPR (Brugmann et al., 2004). While, gain- and loss-of-function of the WNT pathway has been shown to shift the anterior and posterior position of genes such as *Otx2* and *Gbx2* and the boundaries of the PPR (Brugmann et al., 2004; Nordström et al., 2002). This together with the different sensitivities suggests that the level of signalling can create differences at particular points and thus could be suggested to be 'co-ordinate like system'.

Overall the signalling information provides level of information that sets up domains of expression, which subsequently become refined by cross activation and repressive interactions of induced transcription factors into defined regions of identity. While, future work should look to investigate if the genes that are suggested to be under the control of each signal are direct targets. Furthermore, recent evidence has implicated a role for neuropeptide signalling in aPPR induction (Lleras-Forero et al., 2013) and retinoic acid signalling in the induction of *Six1* in the PPR (Jaurena et al., 2015). Therefore, it would be useful to understand which genes they control in the hierarchy of genes proposed in this study.

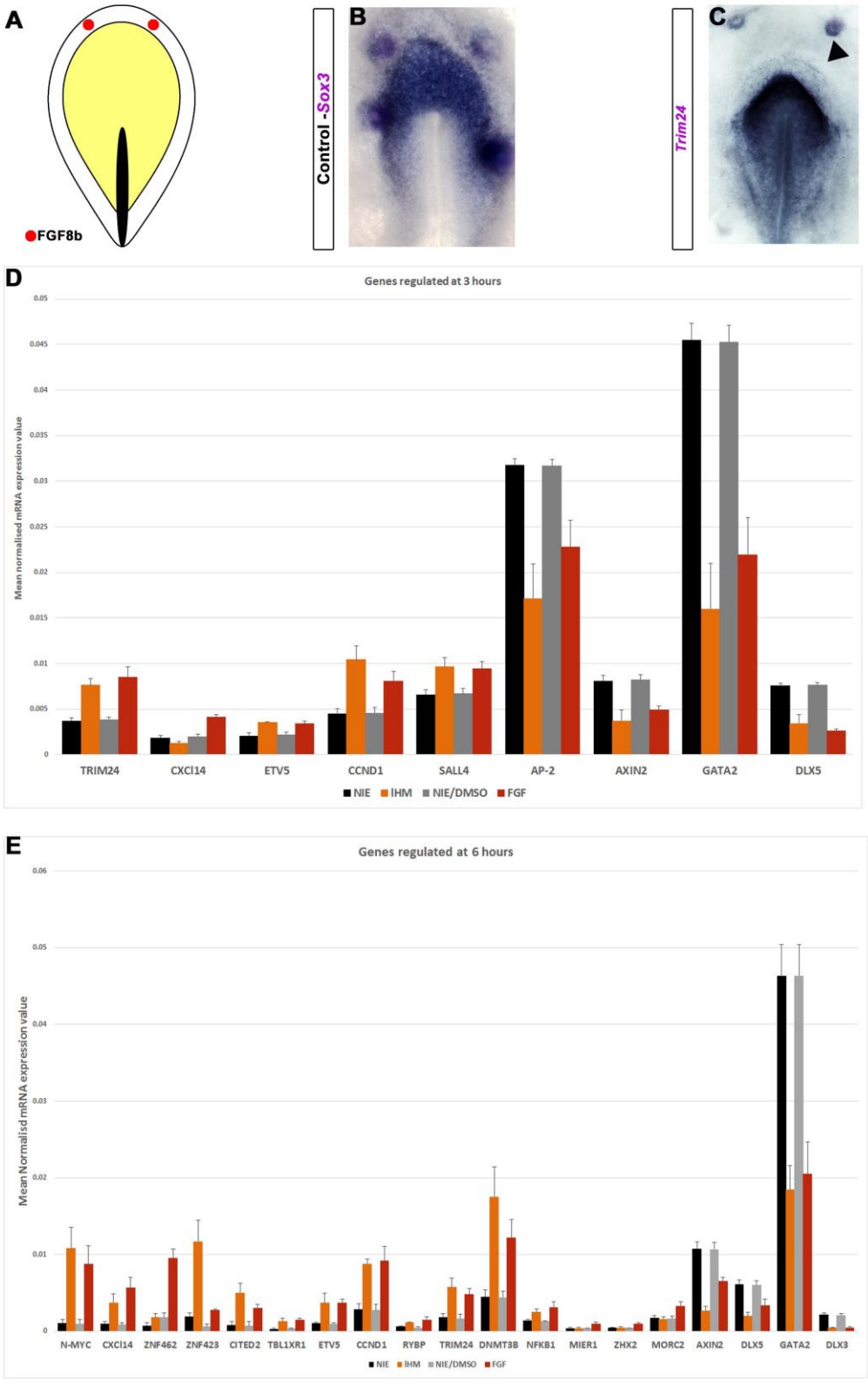


Figure 5.1a: Response to FGF at 3 and 6hrs

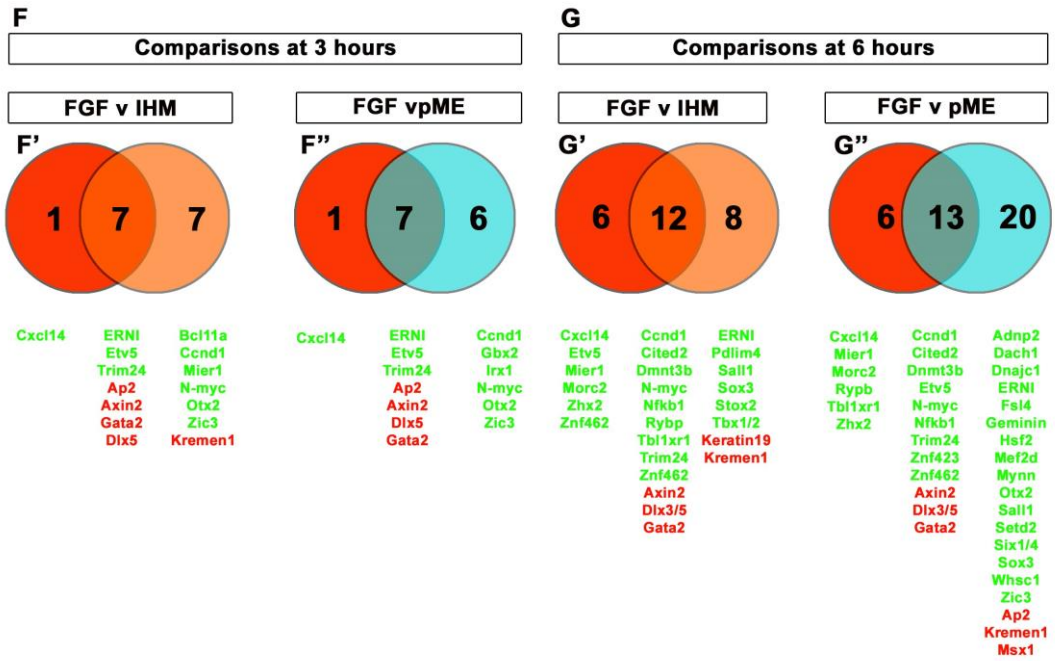


Figure 5.1b: Response to FGF at 3 and 6hrs

**A.** Diagram showing the position of FGF8-coated heparin beads grafted into the extra embryonic region at HH stage 4$^{-}$. **B.** The concentration of FGF8 was determined using *Sox3* as a positive control. **C.** Fgf8 induces *Trim2*4. **D.** Bar charts showing the response of gene expression to 3 hrs FGF8 exposure as evaluated by NanoString. Only genes that show statistically significant changes in the FGF8 are shown (p-value <0.05), compared to the values from the lHM (orange) and pME (Sky blue). Y-axis indicates normalised expression values. **E**. Bar charts showing the response of gene expression to 6 hrs FGF8 exposure as evaluated by NanoString. Only genes that show statistically significant changes in the FGF8 are shown (p-value <0.05), compared to the values from the lHM (orange) and pME (Sky blue). Y-axis indicates normalised expression values. **F**. Comparison of genes induced after 3 hours by FGF and lHM or pME; genes in green are up regulated and those in red are downregulated. **G.** Comparison of genes induced after 6 hours by FGF and lHM or pME; genes in green are up regulated and those in red are downregulated.

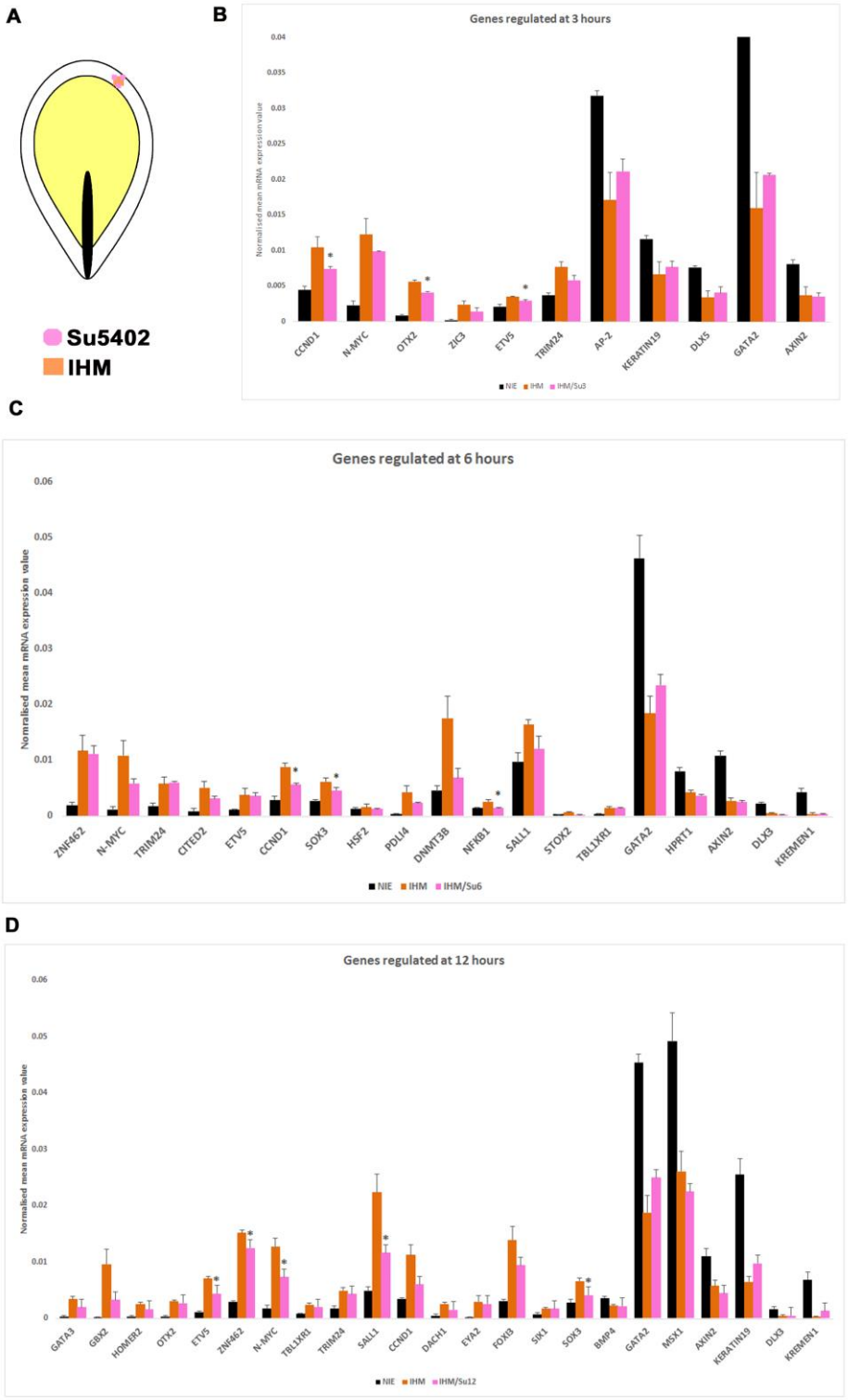


Figure 5.2: Effects of FGF knockdown by SU5402 on IHM response at 3, 6 and 12 hrs

**Figure 5.2: Effects of FGF knockdown by SU5402 on lHM response at 3, 6 and 12 hours**

**A** Diagrammatic representation of the lHM graft surrounded by Agx12 beads coated in 25mM SU5402. Grafts were left in contact with the ectoderm for 3, 6 or 12 hours. Following this the ectoderm underlying the graft was removed an analysed by NanoString. **B.** Bar charts showing the response of gene expression to 3 hrs lHM/SU5402 (Pink) exposure as evaluated by NanoString. * indicates statistical significance between lHM and lHM/SU5402 (p-value <0.05), alongside the values from the lHM (orange)and NIE (black) Y-axis indicates normalised expression values. **C.** Bar charts showing the response of gene expression to 6 hrs lHM/SU5402 (Pink) exposure as evaluated by NanoString. * indicates statistical significance between lHM and lHM/SU5402 (p-value <0.05), alongside the values from the lHM (orange)and NIE (black) Y-axis indicates normalised expression values. **D** Bar charts showing the response of gene expression to 3 hrs lHM/SU5402 (Pink) exposure as evaluated by NanoString). * indicates statistical significance between lHM and lHM/SU5402 (p-value <0.05) Y-axis indicates normalised expression values. All Error bars in above graphs are SEM

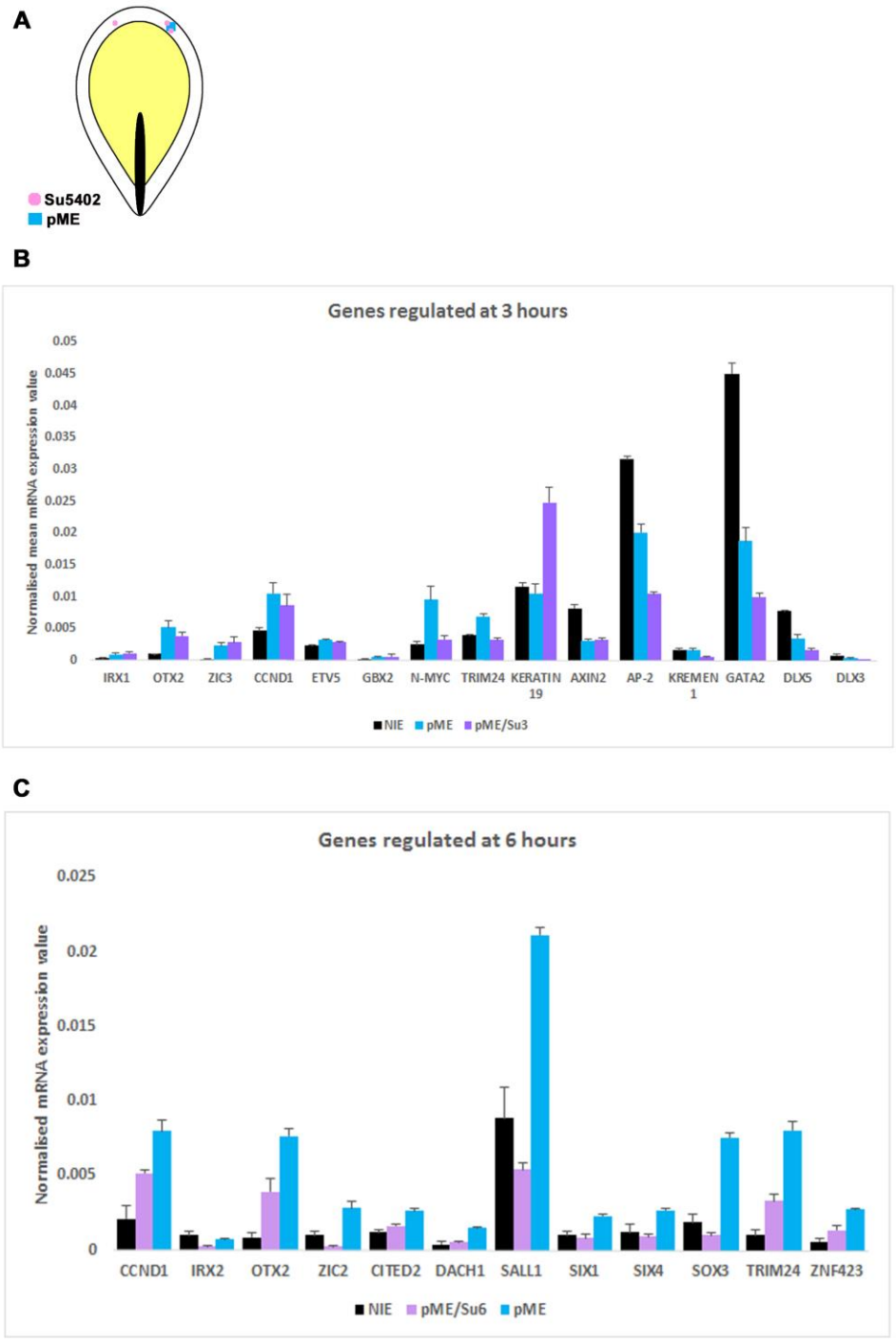


Figure 5.3: Effects of FGF knockdown by SU5402 on pME response at 3 and 6hrs

**Figure 5.3: Effects of FGF knockdown by SU5402 on pME response at 3 and 6hrs**

**A** Diagrammatic representation of the pME graft surrounded by Agx12 beads coated in 25mM SU5402. Grafts were left in contact with the ectoderm for 3, 6 or 12 hours. Following this the ectoderm underlying the graft was removed an analysed by NanoString. **B.** Bar charts showing the response of gene expression to 3 hrs pME/SU5402 (Violet) exposure as evaluated by NanoString. * indicates statistical significance between pME and pME/SU5402 (p-value <0.05), the values from the pME (sky blue)and NIE (black) Y-axis indicates normalised expression values. **C.** Bar charts showing the response of gene expression to 6 hrs pME/SU5402 (Violet) exposure as evaluated by NanoString. * indicates statistical significance between lHM and lHM/SU5402 (p-value <0.05). Y-axis indicates normalised expression value.

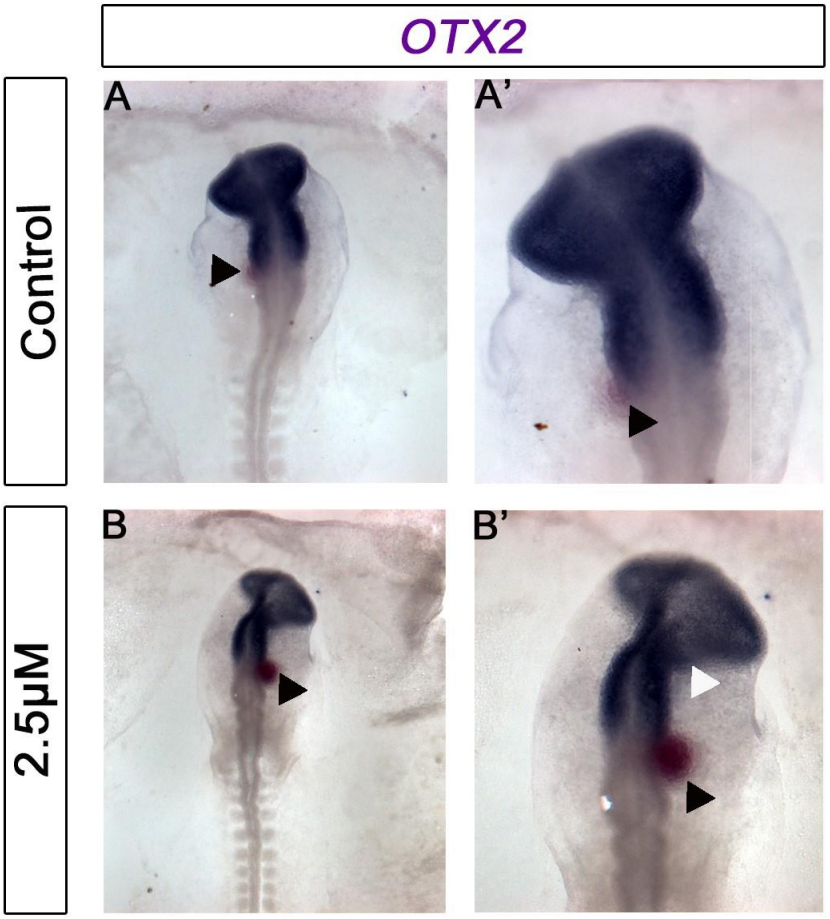


Figure 5.4: Effects of BIO on *Otx2* expression

**A**, Control experiment, Agx12 beads were coated in 1:1000 DMSO (in PBS) and placed in the anterior neural plate of HH stage 4 embryos which were then incubated for 12 hours. No effect on *Otx2* expression was observed (n = 4). **A'** Close up of area in which the bead was grafts. **B** and **B'**, following the same assay as above Agx12 beads were coated in 2.5µM of BIO (Wnt antagonist), the embryos ere incubated for 12 hours and a reduction in *Otx2* compared to the wild type was observed (n= 4).A complete reduction was not observed as expected, this may be due to the bead moving in development and therefore underlying tissue was not exposed for long enough to achieve a complete abolishment of *Otx2.* However, in B' there are also defects of the neural tube which were not present in the DMSO control, suggesting that at this concentration BIO is having an effect on morphology.

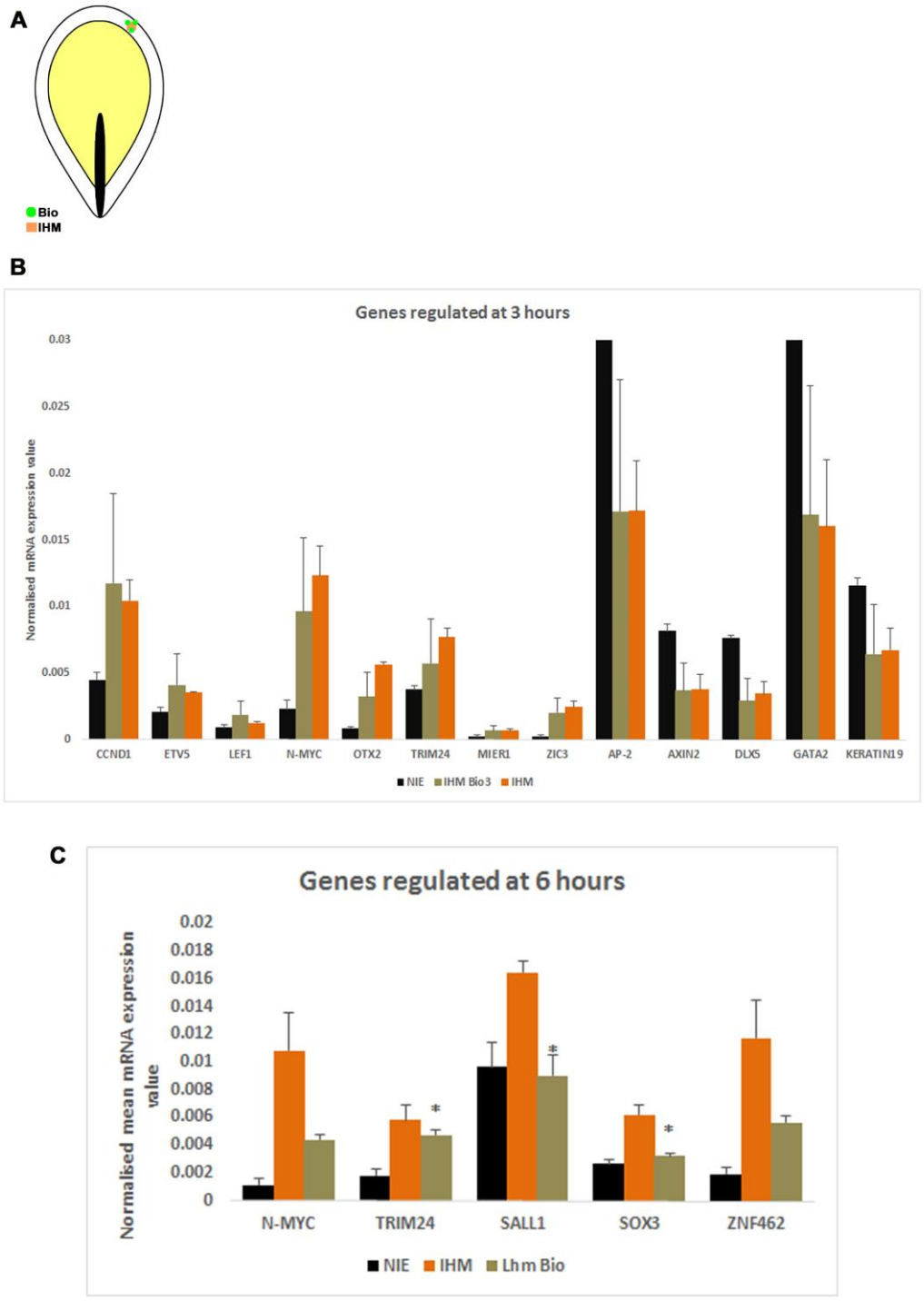


Figure 5.5: Effects of BIO on lHM response at 3 and 6hrs

**Figure 5.5: Effects of BIO on lHM response at 3 and 6hrs**

**A** Diagrammatic representation of the lHM graft surrounded by Agx12 beads coated in 2.5µM BIO. Grafts were left in contact with the ectoderm for 3, 6 or 12 hours. Following this the ectoderm underlying the graft was removed an analysed by NanoString. **B.** Bar charts showing the response of gene expression to 3 hrs lHM/BIO (Olive green) exposure as evaluated by NanoString. * indicates statistical significance between lHM and lHM/BIO (p-value <0.05), alongside the values from the lHM (orange)and NIE (black) Y-axis indicates normalised expression values. **C.** Bar charts showing the response of gene expression to 6 hrs lHM/BIO (Olive green) exposure as evaluated by NanoString. * indicates statistical significance between lHM and lHM/BIO (p-value <0.05), alongside the values from the lHM (orange) and NIE (black) Y-axis indicates normalised expression value. All error bars represent SEM

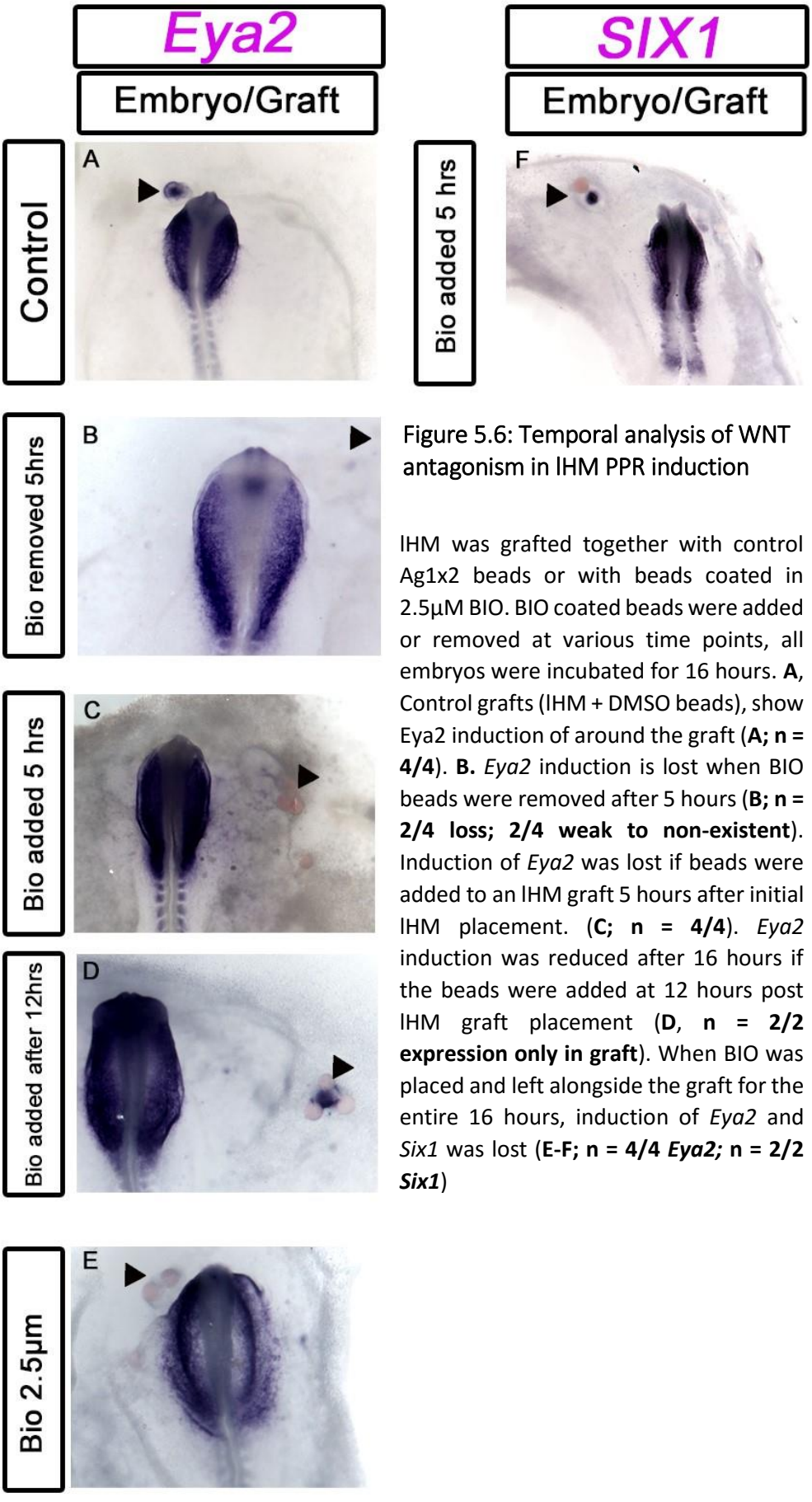


Figure 5.6: Temporal analysis of WNT antagonism in lHM PPR induction

lHM was grafted together with control Ag1x2 beads or with beads coated in 2.5µM BIO. BIO coated beads were added or removed at various time points, all embryos were incubated for 16 hours. **A**, Control grafts (lHM + DMSO beads), show Eya2 induction of around the graft (**A; n = 4/4**). **B.** *Eya2* induction is lost when BIO beads were removed after 5 hours (**B; n = 2/4 loss; 2/4 weak to non-existent**). Induction of *Eya2* was lost if beads were added to an lHM graft 5 hours after initial lHM placement. (**C; n = 4/4**). *Eya2* induction was reduced after 16 hours if the beads were added at 12 hours post lHM graft placement (**D**, **n = 2/2 expression only in graft**). When BIO was placed and left alongside the graft for the entire 16 hours, induction of *Eya2* and *Six1* was lost (**E-F; n = 4/4 *Eya2;* n = 2/2 *Six1***)

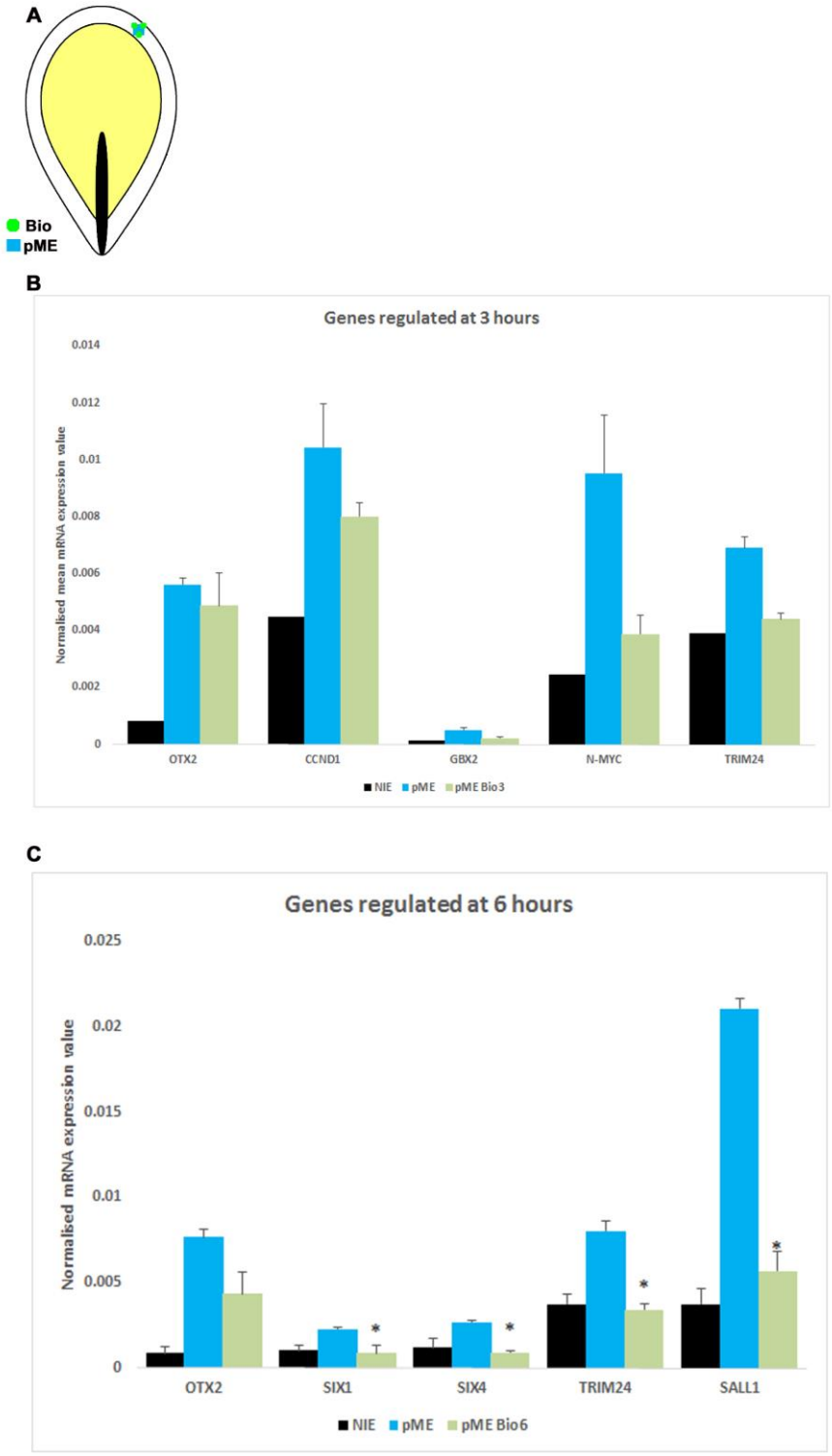


Figure 5.7: response to pME/BIO at 3 and 6hrs

Figure 5.7: Response to pME/BIO at 3 and 6 hours

**A** Diagrammatic representation of the pME graft surrounded by Agx12 beads coated in 2.5µM BIO. Grafts were left in contact with the ectoderm for 3, 6 or 12 hours. Following this the ectoderm underlying the graft was removed an analysed by NanoString. **B.** Bar charts showing the response of gene expression to 3 hrs pME/BIO (light green) exposure as evaluated by NanoString. * indicates statistical significance between pME and pME/SU5402 (p-value <0.05), alongside the values from the pME (sky blue)and NIE (black) Y-axis indicates normalised expression values. **C.** Bar charts showing the response of gene expression to 6 hrs pME/BIO (light green) exposure as evaluated by NanoString. * indicates statistical significance between pME and pME/BIO (p-value <0.05), alongside the values from the pME (sky blue) and NIE (black) Y-axis indicates normalised expression value.

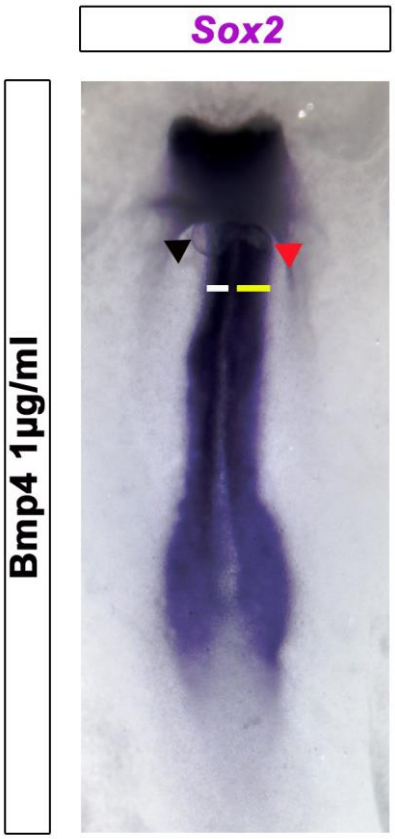


Figure 5.8: Effects of BMP4 on *Sox2* expression

To find a concentration of BMP4 that would disrupt gene regulation in embryonic development, grafts of BMP4 beads were made into the neural plate of a HH stage 4 embryo and left to develop for 8 to 10 hours. At 1µg/ml *Sox2* in the neural plate was found to be narrower (white line) under the BMP4 bead, marked by the black arrow when compared to the control bead (yellow line),(1:1000 DMSO); marked by red arrow **n= 2.**

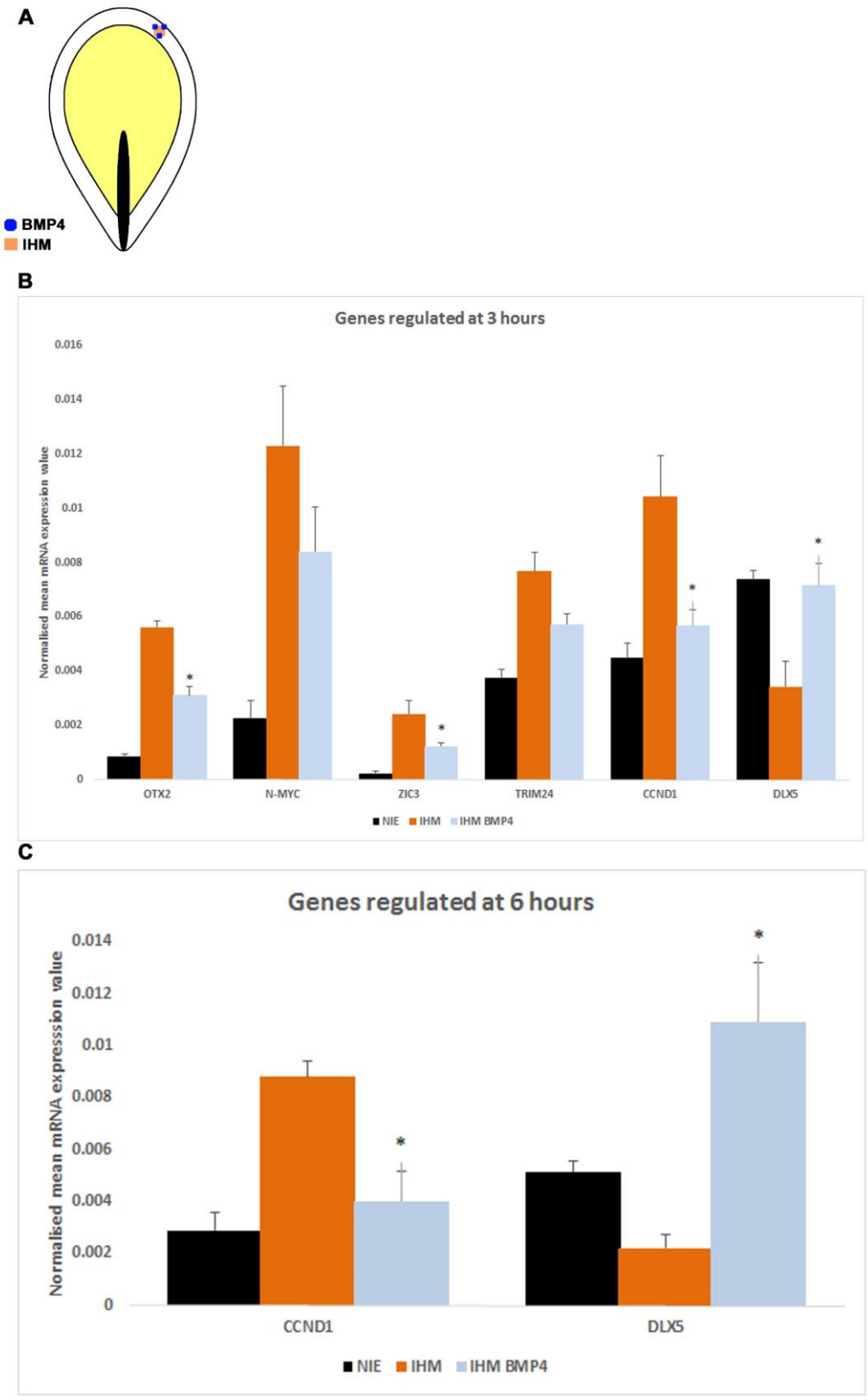


Figure 5.9: response to lHM at 3 and 6hrs in the presence of BMP4

**Figure 5.9: Response to lHM at 3 and 6 hours in the presence of BMP4**

**A** Diagrammatic representation of the lHM graft surrounded by heparin beads coated in 1µg/ml of BMP4. Grafts were left in contact with the ectoderm for 3,6 or 12 hours. Following this the ectoderm underlying the graft was removed an analysed by NanoString. **B.** Bar charts showing the response of gene expression to 3 hrs lHM/BMP4 (Light blue) exposure as evaluated by NanoString. * indicates statistical significance between lHM and lHM/BMP4 (p-value <0.05), alongside the values from the lHM (orange)and NIE (black) Y-axis indicates normalised expression values. **C.** Bar charts showing the response of gene expression to 6 hrs lHM/BMP4 (Light blue) exposure as evaluated by NanoString. * indicates statistical significance between lHM and lHM/BMP4 (p-value <0.05), alongside the values from the lHM (orange)and NIE (black) Y-axis indicates normalised expression values. All error bars represent SEM

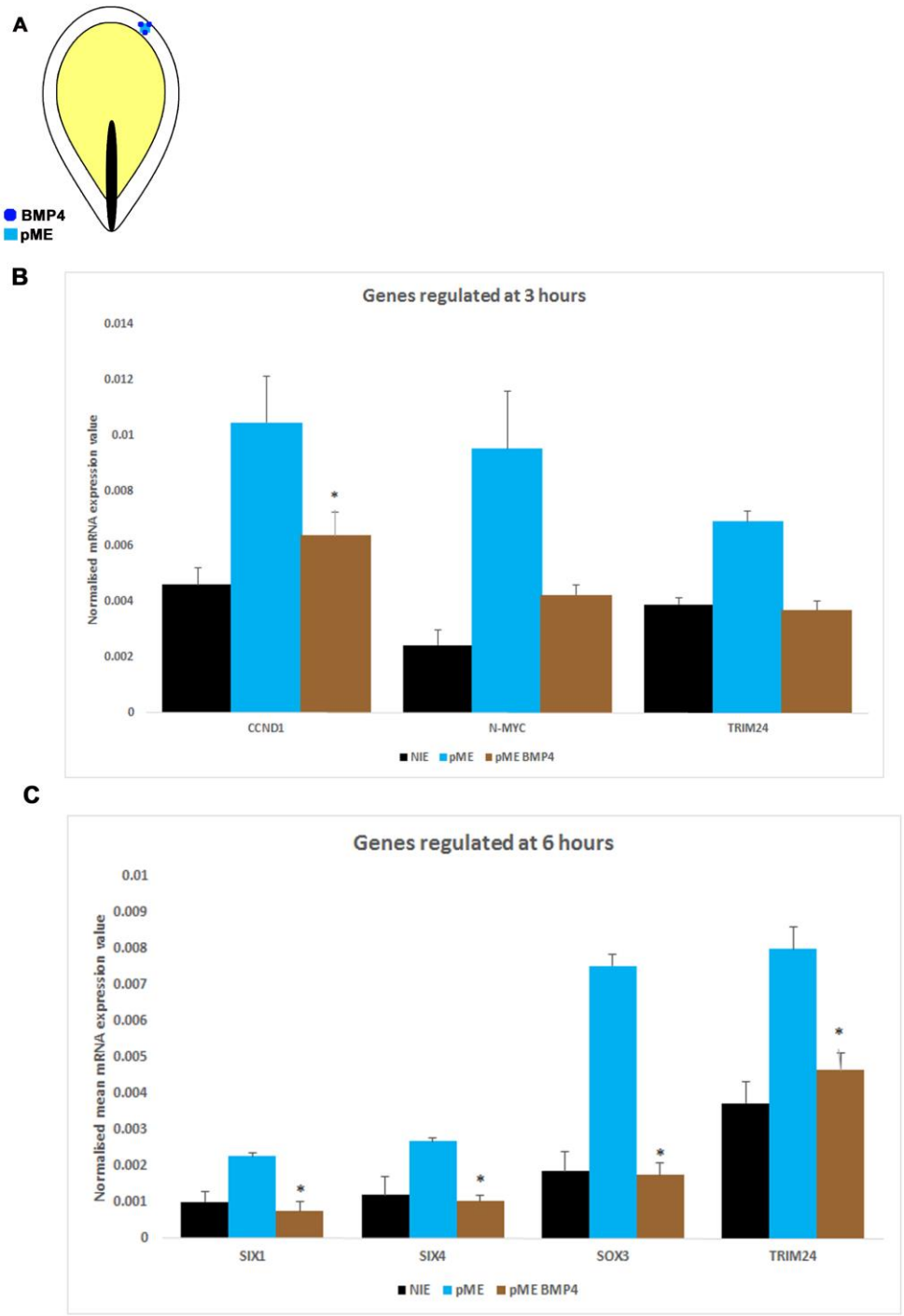


Figure 5.10: Response to pME at 3 and 6 hours in the presence of BMP4

**Figure 5.10: Response to pME at 3 and 6 hours in the presence of BMP4**

**A** Diagrammatic representation of the pME graft surrounded by heparin beads coated in 1μg/ml of BMP4. Grafts were left in contact with the ectoderm for 3, 6 or 12 hours. Following this the ectoderm underlying the graft was removed an analysed by NanoString. **B.** Bar charts showing the response of gene expression to 3 hrs pME/BMP4 (Brown) exposure as evaluated by NanoString.) * indicates statistical significance between pME and pME/BMP4 (p-value <0.05), alongside the values from the pME (sky blue) and NIE (black) Y-axis indicates normalised expression values. **C.** Bar charts showing the response of gene expression to 6 hrs pME/BMP4 (Brown) exposure as evaluated by NanoString. * indicates statistical significance between pME and pME/BMP4 (p-value <0.05), alongside the values from the pME (sky blue) and NIE (black) Y-axis indicates normalised expression value. All error bars represent SEM.

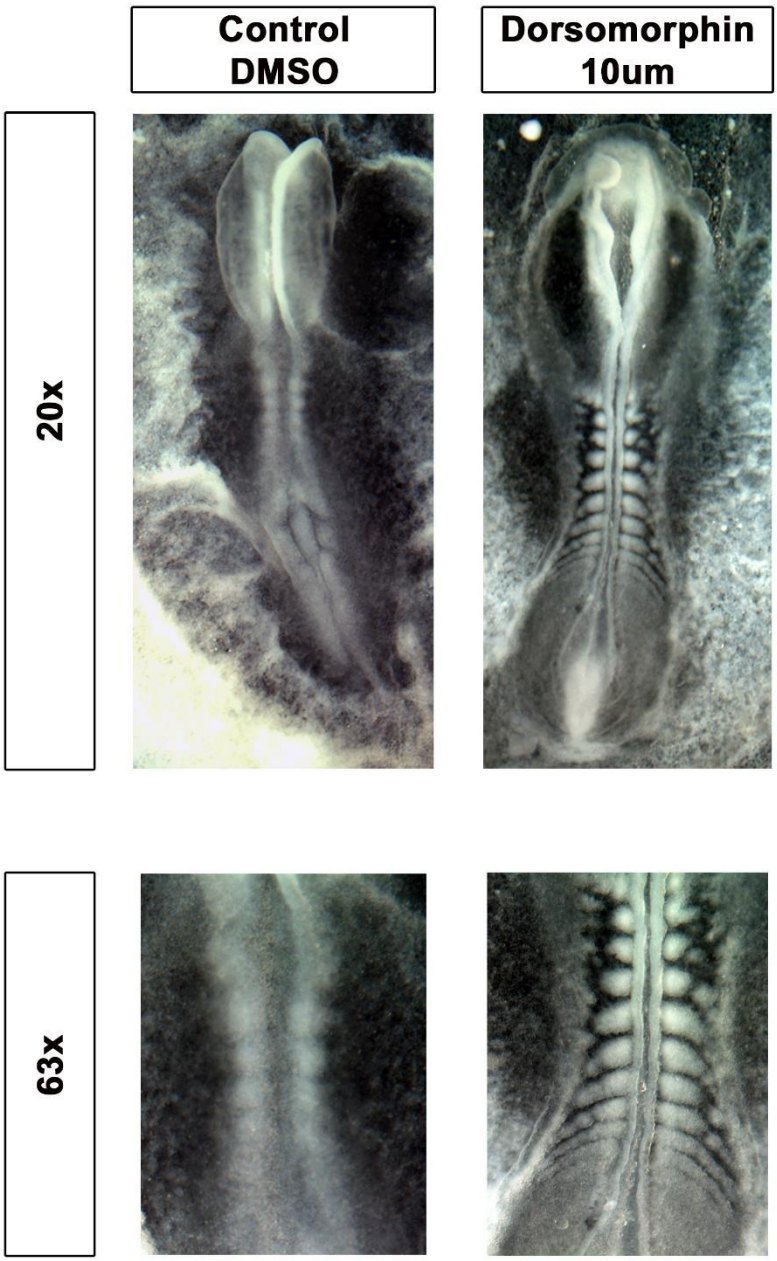


Figure 5.11: Effects of Dorsomorphin on somite development

To find the correct concentration of Dorsomorphin a BMP antagonist was added to the albumin on which the embryos were cultured. Embryos were placed on the albumin at HH stage 4 and incubated for 12 hours. The concentration of 10 µM was found to disrupt somite formation consistent with previous findings for BMP antagonists (n = 3). Control experiments used 1:1000 DMSO added to the albumen.

A

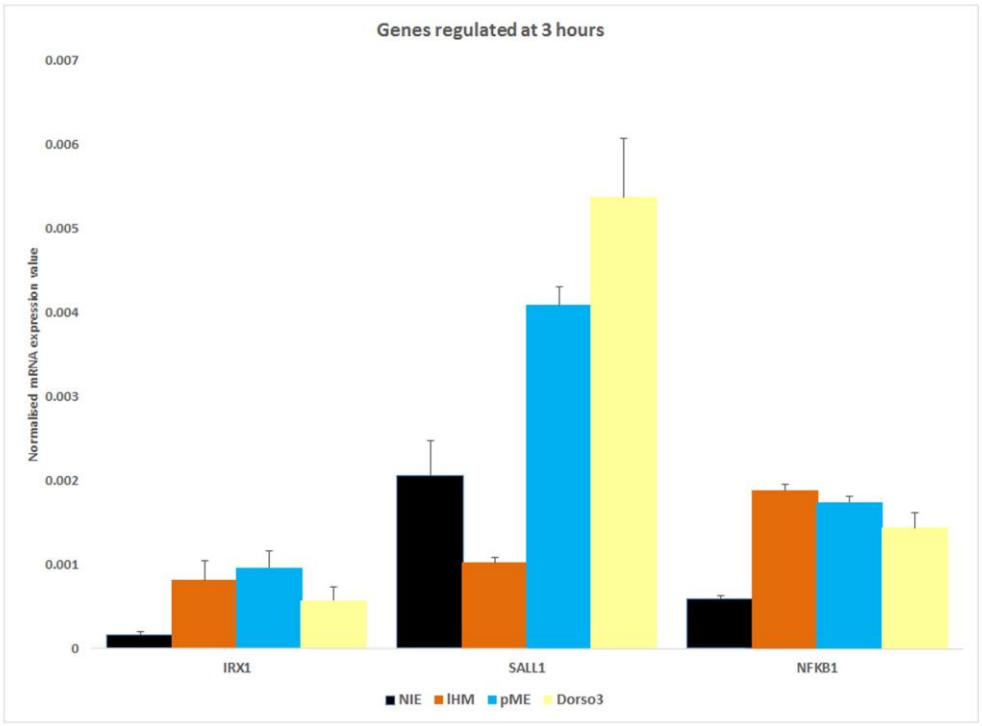


Figure 5.12: Response to Dorsomorphin at 3 hrs compared to lHM and pME

**A.** Beads coated in the BMP antagonist Dorsomorphin were added to the extra embryonic region of a $HH3^{+}/4^{-}$ embryo, beads were left in contact with the ectoderm for 3 or 6 hours. Following this the ectoderm underlying the graft was removed an analysed by NanoString; Bar charts showing the response of gene expression to 3 hrs Dorsomorphin (yellow) exposure as evaluated by NanoString. Only genes that show statistically significant changes in Dorsomorphin are shown (p-value <0.05) against the NIE/DMSO control (grey), alongside the values from the, lHM (orange) pME (sky blue) and NIE (black) Y-axis indicates normalised expression values .**B,C;.** Gene's upregulated by Dorsomorphin at 3hrs (yellow) were compared to the time matched lHM (orange) or pME (Sky blue) experiment. Venn diagrams display the number of genes in common; gene lists display upregulated genes in green and down regulated in red; position of the gene corresponds to the condition they are regulated or both.

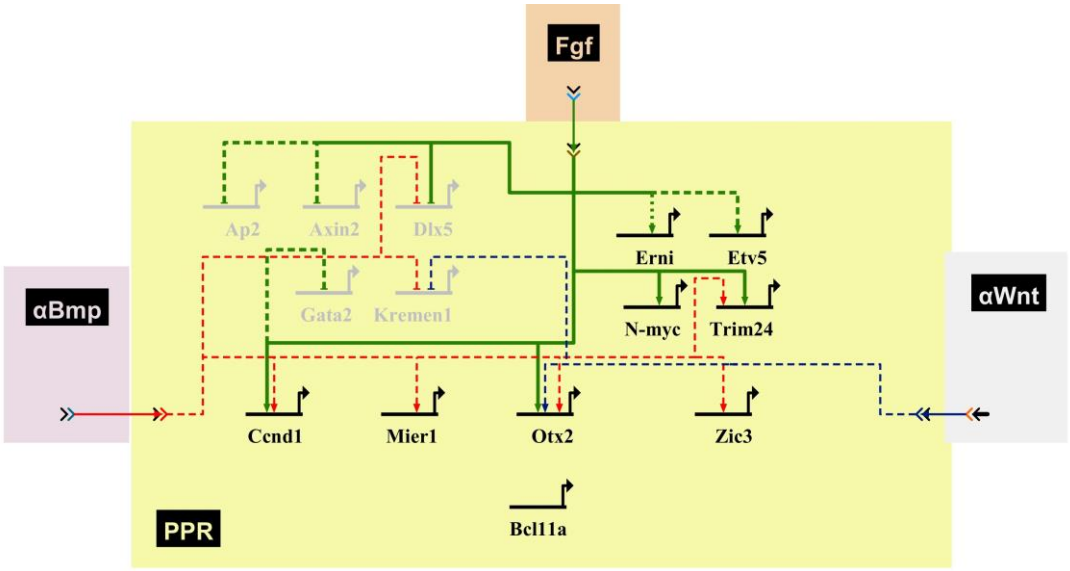


Figure 5.13: model of 3 hours signalling from the lHM

The sufficiency and necessity of each target at 3 hours on the signals from the lHM was determined and displayed using the BioTapestry software. Lines indicate regulation from FGF (green), WNT antagonists (Blue) and BMP antagonists (Red). Solid lines indicate sufficiency and necessity of a signal to induce the target (e.g. *Trim24*); dashed lines indicate that the signal is necessary (e.g. *Etv5*); Dotted lines indicate a signal is sufficient but not necessary for the induction of a target (e.g. *ERNI*).

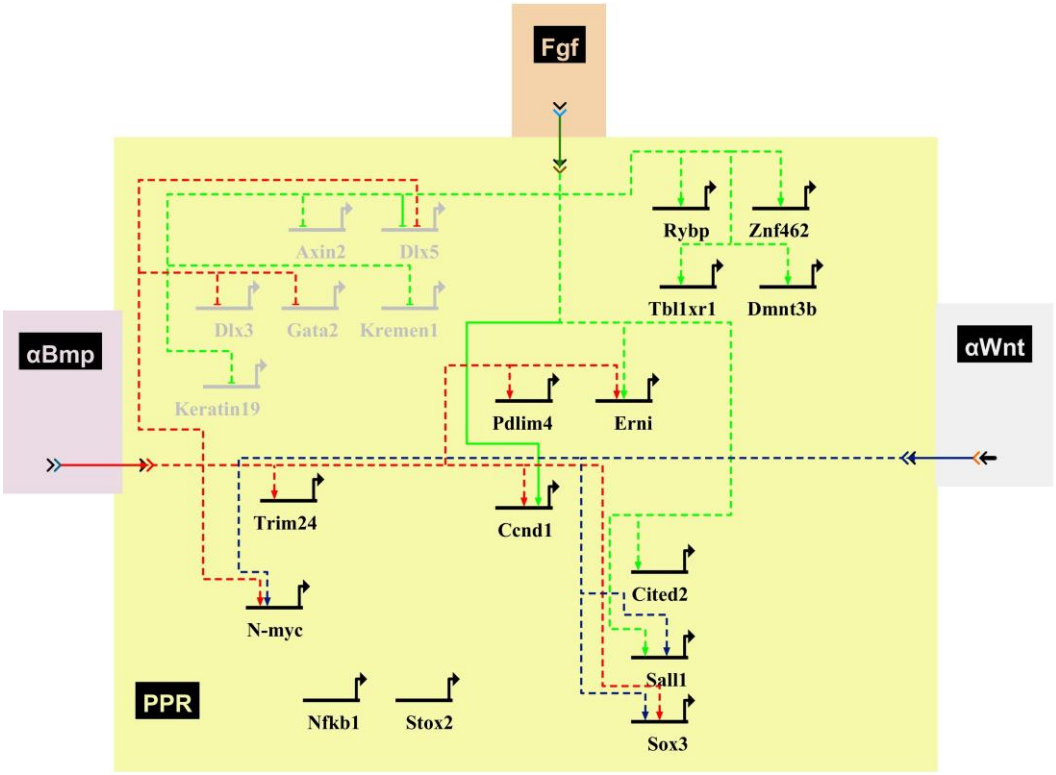


Figure 5.14: Model of signalling from the lHM at 6hrs

The sufficiency and necessity of each target at 6 hours on the signals from the lHM was determined and displayed using the BioTapestry software. Lines indicate regulation from FGF (green), WNT antagonists (Blue) and BMP antagonists (Red). Solid lines indicate necessity and sufficiency of a signal to induce the target; dashed lines indicate that the signal is necessary for the targets expression; Dotted lines indicate a signal is sufficient but not necessary for the induction of a target.

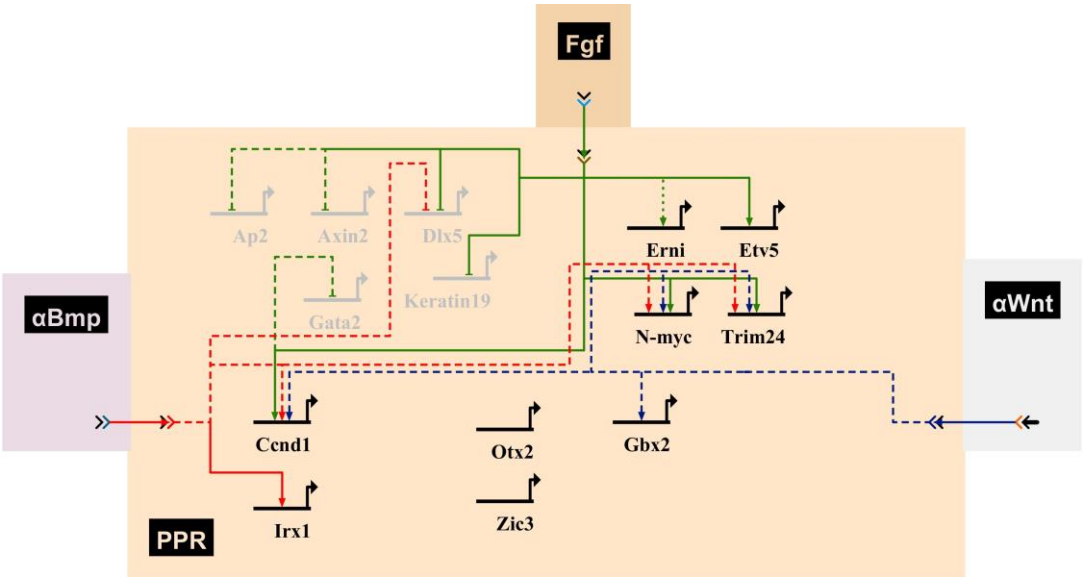


Figure 5.15: Model of signalling from the pME at 3 hours

The sufficiency and necessity of each target at 3 hours on the signals from the pME was determined and displayed using the BioTapestry software. Lines indicate regulation from FGF (green), WNT antagonists (Blue) and BMP antagonists (Red). Solid lines indicate sufficiency of a signal to induce the target; dashed lines indicate that the signal is necessary for targets expression; dotted lines indicate a signal is sufficient but not necessary for the induction of a target.

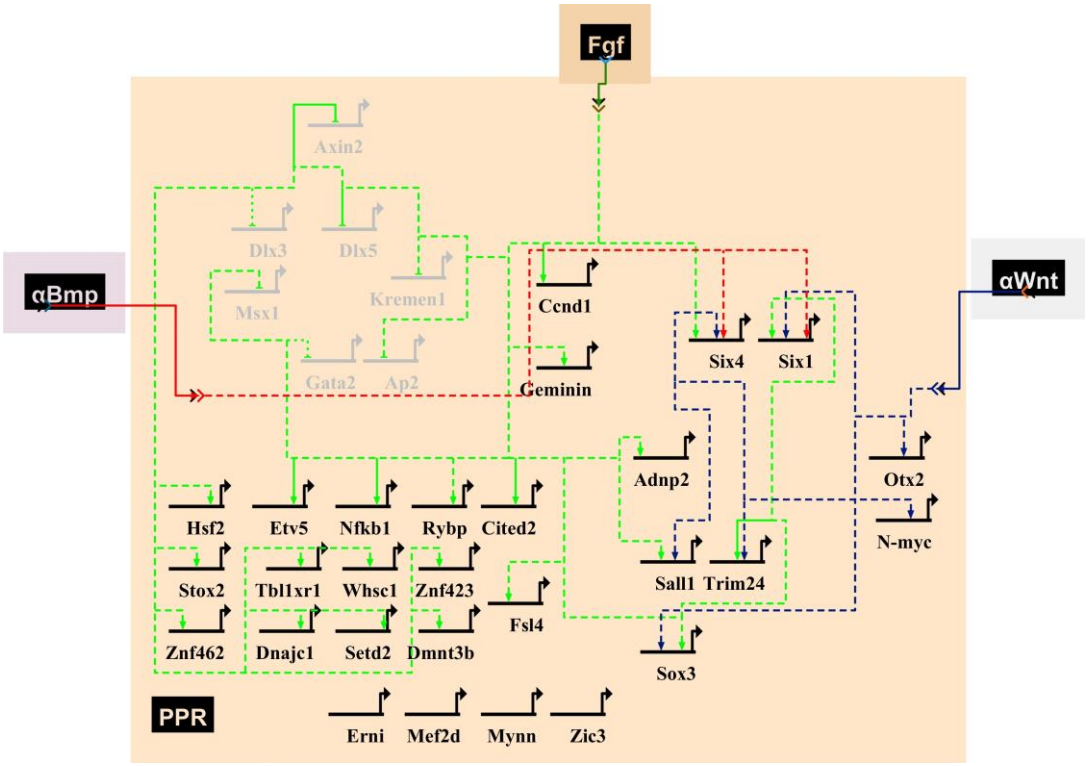


Figure 5.15: Model of signalling from the pME at 6hrs

The sufficiency and necessity of each target at 6 hours on the signals from the pME was determined and displayed using the BioTapestry software. Lines indicate regulation from FGF (green), WNT antagonists (Blue) and BMP antagonists (Red). Solid lines indicate sufficiency of a signal to induce the target; dashed lines indicate that the signal is necessary for the targets expression; Dotted lines indicate a signal is sufficient but not necessary for the induction of a target.

# 6 Bioinformatics prediction of Six/Eya and Pax genes regulators

## 6.1 Introduction

The experiments in chapter 4 provide a temporal hierarchy of genes during the induction of *Six1*/*Eya*2. Transcripts that are induced or repressed prior to *Six1*/*Eya*2 may be novel regulators of these genes. An aPPR enhancer Six1-14 was identified upstream of the transcription start site of Six1 and is located in the intergenic region between Six1 and Six4 (Sato et al., 2010). The enhancer is conserved in human, mouse, opossum, chick and *Xenopus* and is active in the chick aPPR from HH5 onwards consistent with the expression of Six1, before being confined to the very anterior tip of the embryo, possibly the olfactory region (Sato et al., 2010). Analysis of the transcription factor binding sites in Six1-14 revealed the presence and location of homeodomain, Sox, Gata and E-box binding sites. The homeodomain transcription factors Dlx5 and Msx1 were subsequently shown to regulate enhancer activity positively and negatively, respectively, and both factors bind directly to the enhancer (Sato et al., 2010). However, no further analysis has been performed and therefore other transcription factors binding sites need to be predicted or experimentally verified to identify possible *Six1* upstream regulators. To investigate this the Six1-14 enhancer was analysed using a transcription factor binding site motif analyser against a large library. This analysis was then compared to the data from chapter 4.

Gene regulatory networks comprise the interactions and regulation of genes and can be derived from direct experimental evidence of the interactions (Stathopoulos and Levine, 2005). However, interactions can also be inferred from large data sets using statistical analysis. An inferred network while disadvantageous as it does not have direct empirical evidence of interaction; is advantageous as large data sets can be screened for potential interactions which can be followed up experimentally. This advantage can decrease the time in which new interactions can be found. Another advantage is that it may identify interactions that were not easily discoverable by previous statistical methods. GENIE3 is an algorithm that predicts interactions using random forests, a tree-based ensemble method, in which the expression profile of each gene is predicted using the profiles of all other genes and a pattern of interactions is built up (Huynh-Thu et al., 2010). These interactions can then be used to create a network that has directionality and regulatory interactions among network components can be inferred and subsequently tested. The large amount of data generated in chapter 4, allows for an inference-based

method of network prediction to be used to generate a GRN. This GRN can then be analysed to highlight genes, which may be regulators of the PPR factors *Six1* and *Eya2*, as well as placode specific genes, *Pax2* and *Pax6*.

## 6.2 Results

### 6.2.1 Analysis of the aPPR Six1 enhancer

Previously, the Six1-14 enhancer was analysed using rVISTA and only transcription factor binding sites for transcription factor super families were identified using an alignment method (Loots and Ovcharenko, 2004; Sato et al., 2010). However, binding sites for individual transcription factors was not investigated and further potential interacting factors were not discovered. Therefore, here I aim to determine a full set of transcription factor binding sites for Six1-14. The Cis-eLement OVERrepresentation (CLOVER) tool analyses a DNA sequence for transcription factor binding motifs and compares this to a library of known transcription factor binding sites which have been identified, to find any motifs which are statistically overrepresented (Frith et al., 2004). The aPPR Six1-14 (747bp) enhancer was processed using CLOVER against a reference library comprised of the combined Jaspar and Transfac vertebrate transcription factor binding site libraries (Portales-Casamar et al., 2009; Wingender et al., 2000). Transcription factor binding sites were classed as enriched if they were significantly overrepresented (p-value <0.05) when compared to the same sequence shuffled 1000 times randomly.

The analysis picked up a number of binding sites which had been identified previously in Sato's analysis (Sato et al., 2010), these included Dlx-, Gata-, Msx- and Sox-family binding sites, which provides validation for the analysis carried out here. Overall, the new analysis highlighted 186 unique transcription factor binding sites, with several being present multiple times and the total number of binding sites being 219. The transcription factor binding sites were then compared to genes that were present in the NanoString probe set. This comparison highlighted a number of genes of which were regulated before or concomitantly with *Six1*. For example, a Sall1 binding site was discovered within the enhancer (Figure 6.1, B), *Sall1* is upregulated before the onset of *Six1* (6 hours). Therefore, it may have a role in the direct regulation of *Six1* through binding to the aPPR enhancer. *Sall1* is also enriched in the aPPR and has been shown to work as both a transcriptional repressor and activator (de Celis and Barrio, 2009; Yamamoto et al., 2010). Genes that are regulated concomitantly with Six1 include *Lmx1a/b* and *Gbx2*. These genes have binding sites within the aPPR enhancer (Figure 1A) and therefore may play a role in *Six1* regulation.

Another factor, Hsf2 also has a binding site in the aPPR enhancer and is expressed from HH4 in the early neural plate, where it continues to be expressed at PPR stages (Tambalo, 2014), suggesting it may be a putative negative regulator of *Six1-14*.

Within the Six1-14 enhancer there are also binding sites for Pax2 and Pax6 (Figure 6.1, B). Although these genes are expressed after the onset of *Six1* in the embryo (Bhattacharyya et al., 2004; Streit, 2002), it is possible that these factors influence the expression of this enhancer. The aPPR enhancer is maintained in the olfactory placode (Sato et al., 2010), where *Pax6* is expressed (Bhattacharyya et al., 2004) and thus Pax6 may regulate the aPPR enhancer. In contrast, Pax2 is expressed in the otic placode (Streit, 2002), a region from which the aPPR enhancer activity is absent it may therefore act as a repressor.

Overall a number of binding sites previously not described has been uncovered (Sall, Lmx, Gbx, Hox and Pax); the corresponding transcription factors are known to be involved in the development of the PPR or the placodes arising from it and therefore may play a role in the direct regulation of the aPPR enhancer.

### 6.2.2 Network prediction highlights new potential regulators of PPR and placode specific genes

To identify new candidate regulators of PPR and placode fate and to prioritise them for further investigation, I generated a network from the expression data derived from the tissue grafting experiments using GENIE3 (Huynh-Thu et al., 2010).

The data from all tissue grafting experiments analysed by NanoString were used as input for GENIE3. As a cut off the interactions were ranked based on their importance measure and only the top 1000 were used for the following analysis. The network can also be treated as directed, due to the algorithm using input and target genes, through predicting the behaviour of the target gene from the expression data from all other genes (input genes). A network for the top 1000 interactions was visualised using Cytoscape with the following parameters: organisation is based on the interaction matrix, node size is based on the number of inputs (High value of indegree = Large size node) and the width of the connections between genes is based on the interaction matrix (Appendix 9.10, full network). To investigate genes which may have an important function in the PPR, the first neighbours (putative regulators and targets) of Six1, Eya2, Pax2 and Pax6 were highlighted and small networks were created. This allows any genes which may directly regulate the above genes to be viewed, as well as their potential targets.

The inferred network predicts that Six1 is regulated by a small number of genes. The co-factors Eya2 and Dach1 are present as first neighbours suggesting the network replicates previously described interactions where Six1, Eya2 and Dach1 form a complex to regulate the transcription of target genes (Chen et al., 1997; Kawakami et al., 1996b). Thus, these predictions seem to replicate known experimental data reliably. Furthermore, three other genes Ezh2, Hesx1 and Irx3 are predicted to regulate Six1 directly. The network also predicts Six1 as a regulator of a number of genes including its cofactors Eya2 and Dach1, as well as Irx2, Hif1a, Hey1, Pnoc and Nfkb1 (Figure 6.2, A). Eya2 is regulated by several genes including Hey2, Gata3, Dlx3, Hesx1, Ezh2, Hif1a, Zhx2 and Six1 (Figure 6.2, B).

The network describing possible factors upstream of Pax2 includes genes already known to regulate Pax2 such as Gbx2, Dlx3 and Gata3 (Esterberg and Fritz, 2009; Pieper et al., 2012; Steventon et al., 2012). However, it also provides a number of novel interactions; for example lef1 is predicted to regulate Pax2 and is a known WNT effector (Eastman and Grosschedl, 1999) consistent with the fact that WNT signalling is required for otic placode formation. *Lmx1b* is predicted to be a regulator of Pax2 (Figure 6.3, A). Pax6 is a in a large network of first neighbours and is predicted to be regulated by numerous genes, these include the anterior enriched transcripts *Otx2* and *Nfkb1*, as well as the neural transcript *Zic3* (Figure 6.3, B). Pax6 is also regulated by *Dlx5*, consistent with the findings that Pax6 and Dlx5 are involved in promoting the lens placode or olfactory placodes respectively. Thus, the interaction of Dlx5 to Pax6 may be direct (Bhattacharyya and Bronner-Fraser, 2008).

These predicted networks suggest new putative regulators of PPR and placode specific transcription fact that were previously not described, in conjunction with the temporal hierarchy, and they provide useful targets for future investigation of the regulation and induction of the PPR.

## 6.3 Discussion

In this chapter I explored potential regulators of *Six1* and other PPR specific genes using transcription factor binding site analysis of a known Six1 enhancer, as well as network inference approaches. This analysis reveals that, as expected (Sato et al., 2010) Dlx3/5, Gata2/3 and Msx binding sites were found to be enriched in the Six1 enhancer (Six1-14). The analysis also uncovered further previously unidentified binding sites which were overrepresented in *Six1-14.* These include sites for transcription factors that are induced by mesoderm grafts prior to or at the same time as the Six1 such as Gbx2 and Sall1 suggesting

that they may play a role in directly regulating Six1. Although direct interactions have so far not been reported for Sall1, it is enriched in the aPPR (Section 3.2) as compared to the pPPR, an up regulated before Six1 by the lHM and pME (Section 4.2), as well as being expressed before *Six1* in normal development. Interestingly, mutations in *Sall1* have been shown to cause BOR syndrome, which is also caused by mutations in Eya2 and Six1. This may suggest a level of interaction, they have also been shown to interact in the Kidney (Chai et al., 2006; Just et al., 2003). Together these observations suggests that Sall1 may directly regulate *Six1*. However, as it works as both an activator and repressor(de Celis and Barrio, 2009 review; Yamamoto et al., 2010) it is difficult to predict how Sall1 would affect the aPPR six1-14 enhancer.

In addition, *Six1-14* harbours binding sites for Lmx1a/b and Pax2. However, these genes are not upregulated prior to *Six1* in any tissue grafting experiment and are normally expressed after the onset of Six1. It is therefore unlikely that they play a role in initiating Six1 expression. However both are transcriptional activators and repressors (Goode and Elgar, 2009; Hoekstra et al., 2013), and therefore may be involved in the maintenance of Six1, or repression of the anterior enhancers activity in the posterior PPR. Another factor, Gbx2 normally expressed in the pPPR and required for otic specification (Grocott et al., 2012 review; Steventon et al., 2012) also has a binding site and may prevent the Six1-14 enhancer from being active in this region. A large number of binding sites for Hox family members were also predicted in Six1-14; since Six1-14 is inactive in the posterior PPR this may indicate that posterior factors are involved in the repression of Six1-14, thus confining its activity anteriorly. Although the Hox binding site is a homeobox binding sequence ATTA, which all homeodomain proteins (e.g. Dlx, Msx, Gbx) have, it is possible these are unique binding sites for each of these genes. The library of transcription factor binding sites also includes the identity of surrounding bases and the frequency at which they occur. This change in base identity around a binding site can influence the affinity with which transcription factors bind (Liberzon et al., 2004). However, another possibility exists, it can be suggested that instead of regulation at the sequence level, a generic binding site would leave regulation to the combination of factors that are present in the cellular environment and not rely on the presence of specific factors that can or cannot bind to Six1-14.

There are also binding sites for the transcription factor Pax6, consistent with its expression in the aPPR. Although *Pax6* is expressed after *Six1* in the embryo, the presence of a biding site in Sxi1-14 suggests a role for Pax6 in maintaining its expression, e.g. in the olfactory placode (Sato et al., 2010). Conversely, it may also indicate a repressive role, Pax6 is expressed in the lens and eventually Six1 is excluded from the lens forming region, as is

the aPPR enhancer (Sato et al., 2010). Pax6 can act as a repressor or activator, therefore further investigation into its precise role in on the aPPR enhancer is required. Although high levels of Pax6 in the lens show it acts more as a repressor, the exclusion of Six1-14 may also indicate this (Duncan et al., 1998; Hill and Hanson, 1992).

The uncovering of these transcription factor binding sites and the relationship between their behaviour and Six1 in the above experiments serves as a good first indication of their direct involvement in Six1 regulation in the PPR. Combining this with the network analysis may possibly lead to easier identification of regulators. For example, Sall1 has a binding site in the aPPR enhancer and is a first neighbour in the GENIE3 predicted network making it a likely candidate for Six1 regulation.

A number of other *Six1* enhancers that are conserved between mouse and chick have been identified and show various expression profiles. These enhancers are found to be specific for different placodes and early embryonic structures such as the olfactory, otic, somites, notochord and mesoderm have been identified (Sato et al., 2010; Sato et al., 2012). However, a pPPR enhancer for *Six1* remains elusive, there may be a number of reasons for this; there may be a difference in conservation between species in a potential pPPR enhancer region; or the pPPR enhancer may be located a long distance from the *Six1* start site and thus falls outside the analysed regions.

Network inference from expression data is a valuable tool to discover new potential interactions and to indicate which genes in large data sets may be useful to investigate further. Here, genes which regulate Six1, Eya2 and Pax2/6 were of particular interest. The GENIE3 algorithm was used to predict and infer a network from all the experimental results obtain in the tissue experiment (Chapter 4). When isolated the core PPR genes Six1, Eya2 and Dach1, which form a transcription factor complex (Chen et al., 1997), are shown to interact suggesting that the network can predict already validated interactions. The first neighbours of Six1 include Ezh2, Hesx1 and Irx3 as potential *Six1* regulators. Although Hesx1 is not differentially regulated at any point in the tissue experiments, Ezh2 and Irx3 are upregulated at various time points and often together with Six1. *Hesx1*, a transcriptional repressor (Carvalho et al., 2003) is expressed in the anterior neural plate at early stages, but only weakly in the PPR (GEISHA: Antin et al., 2007; Chapman et al., 2003) and may thus restrict *Six1* to its normal territory. Ezh2 and Irx3 are both upregulated in the tissue grafting experiments when Six1 is upregulated and therefore may be good candidates for further investigation. Irx1 has already been shown to have a role in the induction of Six1 in the PPR (Glavic et al., 2004), while Irx3 is involved in the early steps of neural specification. Since Irx

genes 1/2 and 3 are not highly similar in sequence (Bellefroid et al., 1998) it may indicate they have different roles in PPR and neural specification. Irx3 is expressed in the posterior region of the PPR and is also a homeodomain protein (GESHIA Antin et al., 2007; Bellefroid et al., 1998). The aPPR enhancer as described above has a large region in which homeodomain proteins can bind, these predictions together make Irx3 a highly viable candidate for further investigation, in a role as a regulator of Six1. Ezh2 is predicted to regulate both Six1 and Eya2, Ezh2 is part of the polycomb repressor complex PRC2 which acts as a transcriptional repressor (Tan et al., 2013); however, Ezh2 has also been shown to act independent of the PRC2 complex as a transcription activator (Lee et al., 2011; Tan et al., 2013). The expression pattern of Ezh2 shows it is expressed in the early neural plate and may overlap with expression in the neural plate border and subsequent PPR (Tambalo, 2014). Ezh2 relies on a number of factors for the correct function of the PRC2 complex (EED, SUZ12, JARID2, AEBP2, RbAp46/48, and PCL) (Margueron and Reinberg, 2011) Although the expression of Ezh2 is known at early chick stages, the only other member of the Prc2 complex with an available expression pattern was PCL. *PCL* was expressed in the early primitive streak only partially overlapping with *Ezh2* and not in the neural plate border. Therefore, Ezh2 may act in PPR development by repressing factors as part of the PRC2 complex, allowing Six1 and Eya2 to be expressed, although it is unlikely due to the absence of other factors. Or it may act directly as a transcriptional activator promoting Six1 and Eya2. However, as only the expression patterns of Ezh2 and PCL can be looked at for early chick stage, it is not possible to fully evaluate a possible involvement of the PRC2 complex in Six1 and Eya2 regulation.

Lef1 is a first neighbour of Pax2 and in tissue grafting experiments is up regulated prior to *Pax2*. Lef1 is a mediator of canonical Wnt signalling (Eastman and Grosschedl, 1999), and the Wnt pathway is necessary for the development of the otic placode and *Pax2* expression (Ohyama et al., 2007), therefore Lef1 may be a key regulator of *Pax2*. An enhancer for Pax2 and 8 in xenopus, has binding sites for the transcription factors Gata, Gbx and Foxi (Ochi et al., 2012), all three of these factors are predicted regulators of Pax2 within this network and all upregulated at the same time as Pax2 in the tissue experiments. Suggesting, that they are good candidates for further investigation in future experiments. While loss of *Foxi3* has been shown to abolish *Pax2* expression in the otic (Khatri et al., 2014)

The presumptive lens ectoderm enhancer for Pax6 (Dimanlig et al., 2001; Kammandel et al., 1999; Williams et al., 1998) contains homeobox binding sites, this may suggest that factors such as Otx2, Dlx5 and , a predicted regulator, can bind and promote the expression of Pax6 through this enhancer.

It is difficult to assess if the genes which are predicted to be regulators of Eya2 are putative regulators, there have been no enhancers identified for the control of Eya2 expression in PPR. However a number of these genes, Hey2, Gata3, Dlx3 and Six1, do have overlapping expression patterns with Eya2, indicating they are expressed at the right time to be regulators.

Overall these predicted networks only serve to highlight genes that may have a role in the regulation of the genes involved in PPR development. However, they are a useful tool to identify genes which may have not stood out previously as good candidates for further investigation. Candidates which are of most interest are Sall1, predicted by binding sites analysis, overlapping gene expression in the aPPR and inference prediction. The second is Irx3, it is a homeodomain transcription factor and expressed in the right time and place to be involved in *Six1* regulation. While Ezh2 is a candidate that could regulate both Eya2 and Six1.

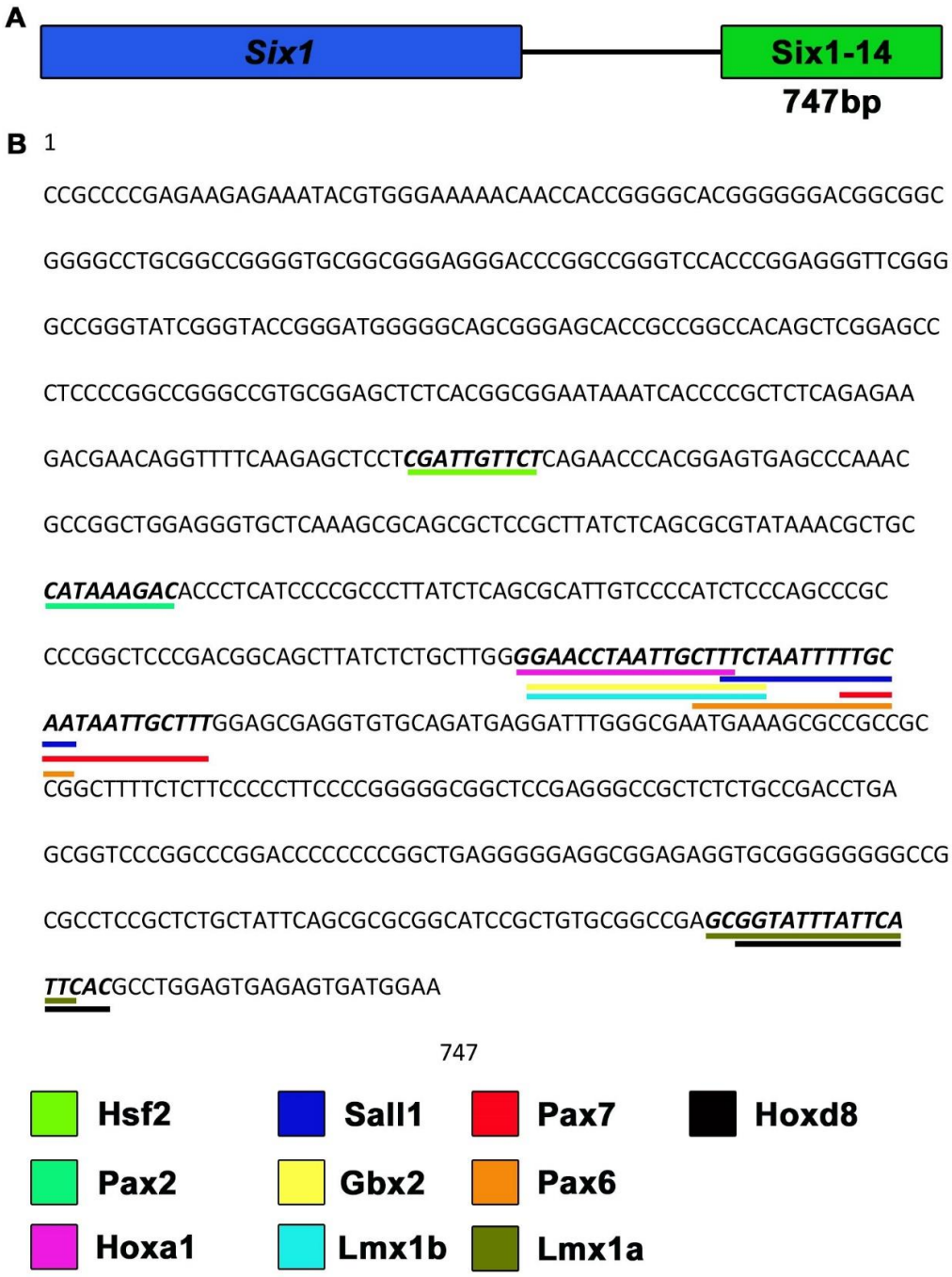


Figure 6.1: Transcription factor binding site analysis of the Six1-14 aPPR enhancer

**A**. The 747bp (chromosome:WASHUC2:5:56961322:56962068:1) aPPR Six1-14 (Green) enhancer was identified upstream of *Six1* (blue) and is active in aPPR in chick, xenopus and mouse (Sato et al., 2010). **B**, Clover analysis of the Six1-14 enhancer region uncovered a large number of previously unidentified binding sites (Full list- Appendix 9.10), genes relevant to this study were extracted and their position is marked under the sequence by coloured rectangles. Colours correspond to key under the sequence.

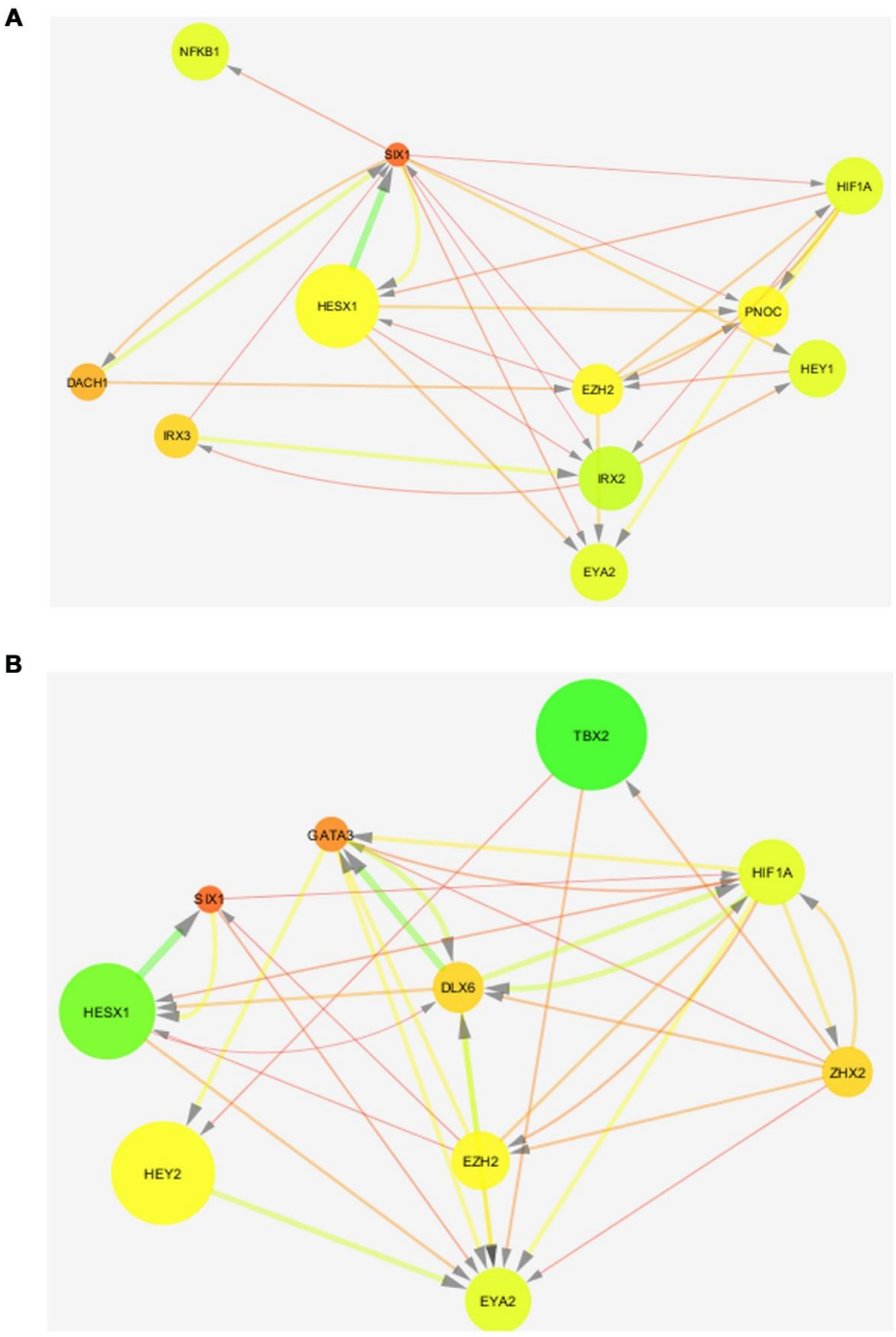


Figure 6.2: Predicted networks for regulation of Six1 and Eya2

**A**, Six1 was isolated from the overall network (Appendix 9.10) along with its first neighbours (genes with a direct input into or from Six1). Large nodes/bright colours = a large amount of in degree, The network was inferred from all expression data in chapter 4, directionality of interaction is inferred from the importance of the expression values of one gene in the data set to explain the behaviour of the target gene; in this case Six1. **B**, The first neighbours of Eya2, analysed and extracted in the same manner as Six1.

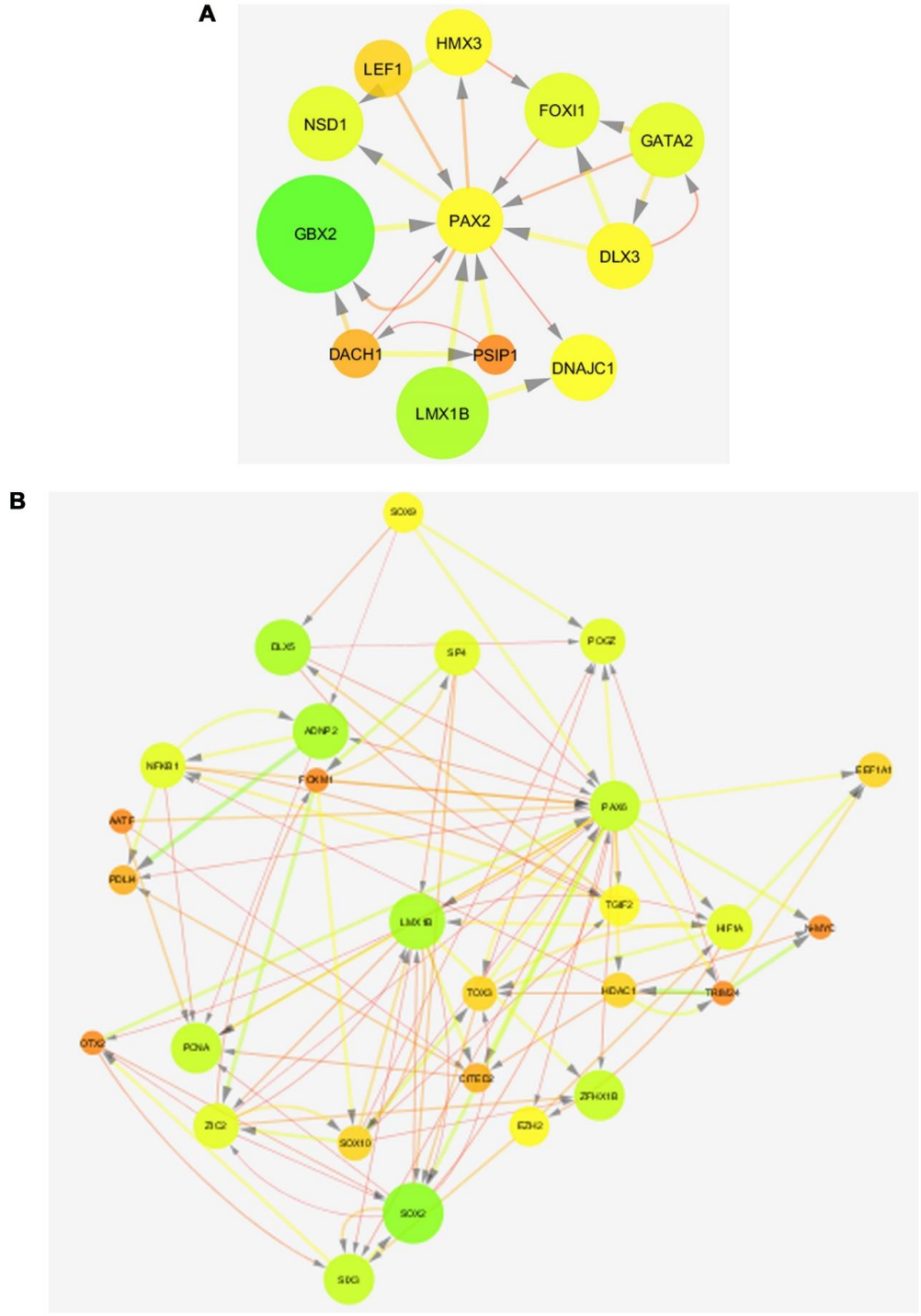


Figure 6.3: Predicted networks for Pax2 and Pax6 regulation

**A**, Pax2 was isolated from the overall network (Appendix 9.10) along with its first neighbours (genes with a direct input into or from Six1). Large nodes/bright colours = a large amount of in degree, The network was inferred from all expression data in chapter 4, directionality of interaction is inferred from the importance of the expression values of one gene in the data set to explain the behaviour of the target gene; in this case Pax2. **B**, The first neighbours of Eya6, analysed and extracted in the same manner as Pax2.

# 7. Discussion

The overall goal of this research was to dissect the events that specify sensory placode progenitors in the cranial ectoderm. Using the nuclear factors *Six1* and *Eya2* as PPR markers the project assessed the response to PPR-inducing tissues and signals over time and thus defined the transcriptional hierarchy as cells acquire PPR identity. The PPR forms from the neural plate border, a region characterised by overlapping expression of early neural and non-neural ectoderm transcripts (Dickinson et al., 1995; LaBonne and Bronner-Fraser, 1998; Liem et al., 1995; Selleck and Bronner-Fraser, 1995; Streit and Stern, 1999; For review see: Grocott et al., 2012; Ohyama and Groves, 2004). Border and PPR genes are both promoted and restricted by signals from the underlying mesoderm and the adjacent neural plate (Ahrens and Schlosser, 2005; Dickinson et al., 1995; Jacobson, 1963a; Jacobson, 1963b; Jacobson, 1963c; LaBonne and Bronner-Fraser, 2000; Liem et al., 1995; Litsiou et al., 2005; Lleras-Forero et al., 2013; Mancilla and Mayor, 1996; Moury and Jacobson, 1990; Selleck and Bronner-Fraser, 1995; Streit and Stern, 1999; Streit et al., 2000). These tissues provide FGFs, WNT antagonists and BMP antagonists, which are necessary and sufficient for the induction of *Six1/4* and *Eya1/2* (Ahrens and Schlosser, 2005; Litsiou et al., 2005; Ohyama et al., 2006). Subsequently, the PPR becomes subdivided into discrete domains along its anterior and posterior axis to generate placode progenitors of more restricted potential, which are marked by the expression of *Pax*2, *-3* and *-6* (Bhattacharyya et al., 2004; Steventon et al., 2012; Streit, 2002; Wakamatsu, 2011: For review see: Grocott et al., 2012; Schlosser, 2010). These progenitor cells will eventually separate and form distinct cranial placodes, which form essential parts of the sensory ganglia and organs in the vertebrate head.

This thesis has identified a new source of PPR-inducing signals, the prechordal mesendoderm, and demonstrated that different mesodermal cell populations induce a PPR with regional bias. This finding suggests that anterior-posterior PPR character is established at the time of or shortly after induction. In addition, I have dissected the contribution of each mesoderm and of the neural plate to PPR induction and subdivision. Finally, these experiments have allowed me to propose a transcriptional hierarchy upstream of *Six1/4* and *Eya2*, as well as the role of different signals in this hierarchy.

## 7.1 A ‘common state’ for neural, neural crest and placode progenitors?

The formation of the PPR and subsequent placodes has been investigated extensively since early experiments identified a morphologically distinct region of ectoderm competent to

form all placodes (Jacobson, 1963a). Recently, two apparently opposing models for the induction of PPR and neural crest cells have been put forward: the neural plate border model and the binary competence model (for review: Schlosser, 2010)

The neural plate border is a region between the neural plate and NNE, where a number of genes from each domain overlap such as the neural plate transcripts *Sox3* and *ERNI* and the NNE genes *Dlx5* and *Gata3* (McLarren et al., 2003; Pera et al., 1999; Sheng and Stern, 1999; Streit, 2002; Streit and Stern, 1999). Fate maps have shown that this domain contains cells that will form the neural plate, neural crest and PPR (Pieper et al., 2011; Selleck and Bronner-Fraser, 1995; Streit, 2002; Xu et al., 2008) suggesting either that border cells are multipotent or that the border is a territory of mixed progenitors.

Recent experiments in *Xenopus* show that neural crest cells only come from the neural plate ectoderm and PPR cells only come from NNE (Ahrens and Schlosser, 2005; Pieper et al., 2012). However, this is in contrast to evidence from older experiments in amphibians and chick, which show that PPR and neural crest cells can come from both neural plate tissue and NNE (Glavic et al., 2004; Litsiou et al., 2005; Mancilla and Mayor, 1996; Moury and Jacobson, 1990; Selleck and Bronner-Fraser, 1995; Streit and Stern, 1999). Reviewing recent data more carefully suggests that considering timing of cell fate allocation resolves this apparent controversy. While in *Xenopus* grafts of the neural plate from post-gastrulation stages have lost the ability to initiate PPR gene expression when confronted with future epidermis, younger neural plates show competence to express *Six1* and *Foxd3*, markers for PPR and neural crest cell fate respectively (Pieper et al., 2012). The same is true for NNE ectoderm: early NNE ectoderm is competent to generate both neural crest and PPR, but as gastrulation continues neural crest competence is lost (Pieper et al., 2012). These changes in competence reflect the refinement of gene expression such as *Dlx3* and *Gata2* to the NNE (Pieper et al., 2012). It is therefore likely that the discrepancy between both models can be explained by differences in the timing when these experiments are done. In agreement with this early neural and NNE gene expression patterns resolve over time into defined regions, going from the neural plate border to the sharply defined neural plate, neural crest, PPR and NNE (Dickinson et al., 1995; Liem et al., 1995; Pieper et al., 2012; Selleck and Bronner-Fraser, 1995; Streit and Stern, 1999)For review see: Grocott et al., 2012). These changes correlate with the segregation of cell fates into refined domains. Thus, considering the temporal changes of gene expression and progenitor distribution resolves the apparent discrepancies between the border and binary competence models.

Do the tissue grafting experiments provide more evidence for a 'common state' shared between neural, neural crest and PPR induction and an entry into defining it molecularly? Hensen's node when grafted into the NNE in chick induces neural fate, marked by *Sox2* after 9-12 hours (Streit and Stern, 1999; Streit et al., 2000; Trevers 2014). However, prior to the induction of definitive neural markers other 'pre-neural genes are induced including *Sox3*, *Erni*, *Churchill* and many others that have been identified in a recent screen (Streit et al., 2000; Sheng et al., 2003; Trevers, 2014). PPR inducing signals emanate from the lateral head mesoderm (Litsiou et al., 2004) and from the pre-chordal mesendoderm (this study), and time course experiments presented here reveal that many of the genes induced early by these tissues are the same as those induced by a node graft. Unfortunately, similar time course experiments have not been performed for neural crest induction, although mesodermal signals are also relevant. Thus, the induction assays reveal that indeed neural and PPR induction may share initial steps before they separate to follow different routes. Interestingly, all early node and mesoderm response genes so far tested are expressed prior to gastrulation in pre-streak embryos suggesting that this 'common state' resembles pre-streak epiblast.

What are the signalling events that induce these set of genes and initiate the process? FGF signalling has already been implicated in the induction of *ERNI*, *Sox3*, *Churchill* and many others (Pinho et al., 2011; Streit and Stern, 1999; Streit et al., 2000). Likewise, FGF signalling is required during the early phase of PPR induction (Litsiou et al., 2004). Here I show that many genes that are induced at 3 hours by the lHM and pME are also induced by FGF at 3 hours and depend on FGF signalling. Together these observations indicate that FGF might be the signal that induces the 'common state'. Interestingly, at pre-streak stages the hypoblast also induces genes that make up the 'common state' within three hours and is a source of FGF8 (Albazerchi and Stern, 2007). Therefore, it is possible that a 'common state' exists in the pre-streak epiblast possibly induced by the hypoblast and that this state persists at the neural plate border before cells differentiate into placode and neural crest. Recent evidence from *Xenopus* has shown that genes expressed at blastula stages remain expressed in neural crest cells until they differentiate, suggesting a pluripotent or early state has persisted allowing them to retain their differentiation potential (Buitrago-Delgado et al., 2015). These genes are comparable to a persistence of the border genes in the PPR, suggesting that PPR cells may also maintain this state.

## 7.2 Regionalisation of the PPR

### 7.2.1 Conferring anterior-posterior bias to PPR cells

Although there is some degree of intermingling of different cell fates within the PPR (Kozlowski et al., 1997; Pieper et al., 2011; Streit, 2002; Xu et al., 2008) precursors for the most anterior and posterior placodes are well separated. How is the PPR subdivided into anterior and posterior domains? Here I show that although the initial steps in the response to the lHM and pME are very similar, cells are rapidly biased towards the rostral and caudal identity. Evidence of a regional bias is also evident from the analysis of gene expression in the early embryo. *Otx2* and *Gbx2* initially overlap but form mutually opposing domains in the anterior and posterior PPR, respectively (Steventon et al., 2012). A number of other genes further refine these territories among them *Six3* and *Irx3* (Kobayashi et al., 2002). However, their functional significance in relation to PPR patterning and placode formation has yet to be investigated. Specific genes expressed in the pPPR are required for the formation of otic placode, such as *Foxi3* ((Khatri and Groves, 2013; Khatri et al., 2014; Nissen, 2003; Solomon, 2003) while a pNoc and somatostatin signalling loop is required aPPR formation and lens/olfactory specification (Lleras-Forero et al., 2013). Furthermore, the apparently homogenous domain of *Six1* expression controlled by different enhancers (Sato et al., 2010) suggesting that the gene regulatory controls differ in the a- and p-PPR. The microarray screen conducted in this study identified novel genes that were restricted within the PPR, e.g. *Sall1* and *Nfkb1* (aPPR) and *Ccnd1* (pPPR). These are novel candidates for providing regional restriction to the PPR and require further investigation to determine their function.

### 7.2.2 Establishing anterior, intermediate and posterior placodal domains

Following the division of the PPR into anterior and posterior domains there is further refinement into progenitor domains that precede the cranial placodes, marked by *Pax* gene expression (Grocott et al., 2012; Martin and Groves, 2006; Schlosser, 2010; Streit, 2002; Wakamatsu, 2011). The lHM and pME can induce a PPR but cannot induce ectopic placodes (Christophorou, 2008; Litsiou et al., 2005, this study) suggesting that additional tissues are required. Classical embryological experiments provide evidence for the involvement of the neural plate in the determination of various placodes (Jacobson, 1963a; Jacobson, 1963c;

Model et al., 1981; Waddington, 1936), although it is unclear if this role is in initial induction of the placode territory or later patterning (Ahrens and Schlosser, 2005; Litsiou et al., 2005).

In *Taricha Torosa* combining presumptive placode territory with the neural plate leads to the induction of otic and lens placodes (Jacobson, 1963a). When the neural plate was rotated along the anterior posterior axis, otic and lens placodes are lost (Jacobson, 1963c). Likewise, preventing signalling between the neural plate and placode ectoderm prevents trigeminal placode formation (Stark et al., 1997). Grafting experiments in *Xenopus* showed that the neural plate induces *Six1* and in 50% of cases *Eya1* (Ahrens and Schlosser, 2005), while in chick only *Six1* induction is observed in a few cases after a long time (Litsiou et al., 2005) and never in experiments in this study. Taken together, these results suggest that the neural plate may mediate some aspect of PPR induction, but on its own is not capable of inducing a complete PPR. Here I provide evidence that the neural plate cooperates with the mesoderm to provide regional identity. OEP cells are induced by a combination of lHM and pNP signalling, while the combination of pME and aNP promotes lens-olfactory character. Conversely, heterotopic combinations of mesoderm and neural pate show that the NP does not impose a-p character but seems to 'neutralise' the anterior-posterior bias imparted by different mesodermal populations. Taken together current evidence does not support a major role for the neural plate in PPR induction, but suggests a role in regionalisation.

This leads to the following model of PPR induction. PPR induction initially follows similar steps as neural induction, and this may be induced by FGF from the hypoblast. This transcriptional 'state' is maintained at the border of the neural plate and as lHM and pME emerge during gastrulation they induce and locally bias the PPR to impart anterior and posterior PPR identity. This local bias is then enhanced by signalling from adjacent neural plate to promote LOPs, OEPs or trigeminal precursors. (Figure 7.1)

## 7.3 The transcriptional hierarchy controlling the Six and Eya cassette

The PPR is marked by members of the *Six* transcription factor family and the transcription co-factor *Eya* (*Eya1* in *Xenopus*, *Eya2* in chick; (Esteve and Bovolenta, 1999; Ishihara et al., 2008a; Pieper et al., 2011; Sato et al., 2010). Little is known about the transcriptional inputs that control the expression of these genes in the PPR.

Briefly, a number of factors are positive regulators of *Six1*. In zebrafish, these are four factors *Tfap2a/c*, *Foxi1* and *Gata3*, which act as competence factors that cross activate

and maintain each other in the presence of BMP signalling (Kwon et al., 2010). *Six1* and *Eya1* expression is observed only in the presence of these factors. Similar experiments have been carried out in *Xenopus* where *Gata2* has also been implicated as a competence factor for *Six1* and *Eya1* (Pieper et al., 2012). There is a large amount of evidence for the involvement of *Dlx* genes in the formation of the border region and promotion PPR cell fate (Bhattacharyya et al., 2004; Esterberg and Fritz, 2009; McLarren et al., 2003; Pera et al., 1999; Pieper et al., 2012; Solomon and Fritz, 2002; Woda et al., 2003). These experiments include overexpression, loss-of-function and mutant analysis to show that *Dlx* genes positively promote *Six1*. Indeed, Dlx5 activates the aPPR enhancer for *Six1* (Six1-14) directly (Sato et al., 2010). In medaka, ectopic Sox3 expression promotes *Eya1* placing the early neural/neural plate border gene upstream of PPR transcripts (Köster et al., 2000). Finally, in *Xenopus* Zic1 and Irx1 also enhance *Six1* expression, although it is unclear whether this is through direct interaction with a Six1 regulatory element (Glavic et al., 2004; Hong and Saint-Jeannet, 2007; Jaurena et al., 2015).

In addition, there is also evidence for factors that negatively regulate *Six1* and *Eya2* in the PPR. A number of these are implicated in the promotion of neural crest cells such as *Pax3/7*, which when overexpressed lead to the loss *Six1* and a reduction in the PPR (Hong and Saint-Jeannet, 2007; Sato et al., 2010) with *Pax7* postulated to regulate the aPPR enhancer *Six1*-14 directly (Sato et al., 2010). Although *Msx1* early on promotes border fate it later represses *Six1* while favouring the neural crest lineage by directly repressing the aPPR enhancer Six1-14 (Phillips et al., 2006; Sato et al., 2010; Streit and Stern, 1999; Suzuki et al., 1997). Here I have established a temporal hierarchy of transcription factors upstream of the Six and Eya network. At the top of this hierarchy, most likely in response to FGF, is set of genes including *Ccnd1, ERNI, N-myc, Otx2* and *Trim24*. This is followed by a cohort of genes that include *Nfkb1, Sall1* and *Stox2*. With genes not identified in PPR regulation before such as *Trim24, Stox2* and *Nfkb1* occurring before *Six1* and *Eya2*, this makes them interesting candidates to follow up in future experiments. While multiple lines of evidence, from network predictions, transcription factor binding site analysis, position in the temporal hierarchy and overlapping gene expression in the NPB/aPPR, suggest that *Sall1* that is a good candidate to further investigate for PPR regulation.

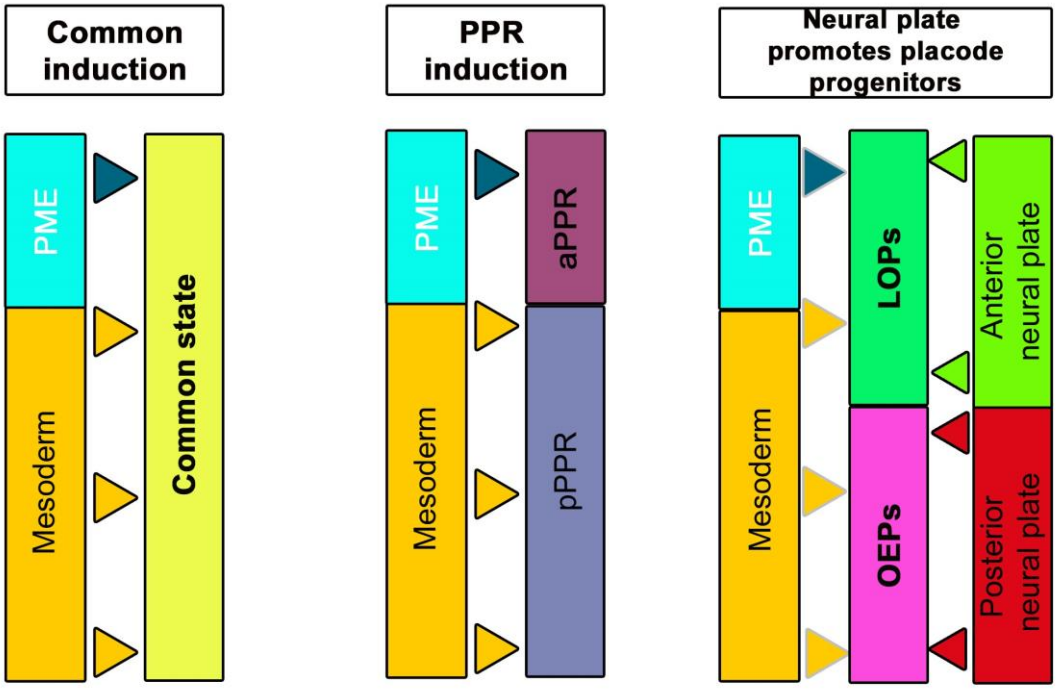


Figure 7.1: Model for PPR and placode progenitor induction from a 'common state'

Initially the lHM (orange) and pME (Sky blue) induce a common domain (yellow), this is initiated mainly by FGF signalling with BMP antagonists playing a small role from the pME. This domain rapidly diverges towards either a pPPR fate (blue) or an aPPR (purple). At this point there is a larger role for FGF, WNT antagonists and BMP antagonists in maintaining and initiating targets. Following this the neural plate promotes the formation of placode precursors in and axial homotypic fashion. The lHM and pNP (red) promote OEPS (Pink). While the pME and aNP (green) promotes the formation LOPs

# Biblography


**Abdelhak, S., Kalatzis, V., Heilig, R., Compain, S., Samson, D., Vincent, C., Weil, D., Cruaud, C., Sahly, I., Leibovici, M., et al.** (1997). A human homologue of the Drosophila eyes absent gene underlies branchio-oto-renal (BOR) syndrome and identifies a novel gene family. *Nat. Genet.* **15**, 157–164.

**Abelló, G., Khatri, S., Radosevic, M., Scotting, P. J., Giráldez, F. and Alsina, B.** (2010). Independent regulation of Sox3 and Lmx1b by FGF and BMP signaling influences the neurogenic and non-neurogenic domains in the chick otic placode. *Dev. Biol.* **339**, 166–178.

**Abu-Elmagd, M., Ishii, Y., Cheung, M., Rex, M., Le Rouëdec, D. and Scotting, P. J.** (2001). cSox3 expression and neurogenesis in the epibranchial placodes. *Dev. Biol.* **237**, 258–269.

**Adelmann, H. B.** (1922). The significance of the prechordal plate: an interpretative study. *Am. J. Anat.* **31**, 55–101.

**Ahrens, K. and Schlosser, G.** (2005). Tissues and signals involved in the induction of placodal Six1 expression in Xenopus laevis. *Dev. Biol.* **288**, 40–59.

**Albazerchi, A. and Stern, C. D.** (2007). A role for the hypoblast (AVE) in the initiation of neural induction, independent of its ability to position the primitive streak. *Dev. Biol.* **301**, 489–503.

**Alvarez, Y., Alonso, M. T., Vendrell, V., Zelarayan, L. C., Chamero, P., Theil, T., Bösl, M. R., Kato, S., Maconochie, M., Riethmacher, D., et al.** (2003). Requirements for FGF3 and FGF10 during inner ear formation. *Development* **130**, 6329–6338.

**Anderson, A. M., Weasner, B. M., Weasner, B. P. and Kumar, J. P.** (2012). Dual transcriptional activities of SIX proteins define their roles in normal and ectopic eye development. *Development* **139**, 991–1000.

**Antin, P. B., Kaur, S., Stanislaw, S., Davey, S., Konieczka, J. H., Yatskievych, T. a and Darnell, D. K.** (2007). Gallus expression in situ hybridization analysis: a chicken embryo gene expression database. *Poult. Sci.* **86**, 1472–1477.

**Bachvarova, R. F., Skromne, I. and Stern, C. D.** (1998). Induction of primitive streak and Hensen's node by the posterior marginal zone in the early chick embryo. *Development* **125**, 3521–3534.

**Bailey, A. P., Bhattacharyya, S., Bronner-Fraser, M. and Streit, A.** (2006). Lens specification is the ground state of all sensory placodes, from which FGF promotes olfactory identity. *Dev. Cell* **11**, 505–17.

**Baker, C. V and Bronner-Fraser, M.** (2000). Establishing neuronal identity in vertebrate neurogenic placodes. *Development* **127**, 3045–3056.

**Baker, C. V and Bronner-Fraser, M.** (2001). Vertebrate cranial placodes I. Embryonic induction. *Dev. Biol.* **232**, 1–61.

**Baker, C. V, Stark, M. R., Marcelle, C. and Bronner-Fraser, M.** (1999). Competence, specification and induction of Pax-3 in the trigeminal placode. *Development* **126**, 147–156.

**Bally-Cuif, L., Gulisano, M., Broccoli, V. and Boncinelli, E.** (1995). C-Otx2 Is Expressed in Two Different Phases of Gastrulation and Is Sensitive To Retinoic Acid Treatment in Chick Embryo. *Mech. Dev.* **49**, 49–63.

**Barembaum, M. and Bronner-Fraser, M.** (2007). Spalt4 mediates invagination and otic placode gene expression in cranial ectoderm. *Development* **134**, 3805–14.

**Basch, M. L., Bronner-Fraser, M. and García-Castro, M. I.** (2006). Specification of the neural crest occurs during gastrulation and requires Pax7. *Nature* **441**, 218–222.

**Begbie, J., Brunet, J. F., Rubenstein, J. L. and Graham, a** (1999). Induction of the epibranchial placodes. *Development* **126**, 895–902.

**Bellairs, R.** (1993). Fertilization and early embryonic development in poultry. *Poult. Sci.* **72**, 874–881.

**Bellairs, R., Lorenz, F. W. and Dunlap, T.** (1978). Cleavage in the chick embryo. *J. Embryol. Exp. Morphol.* **43**, 55–69.

**Bellefroid, E. J., Kobbe, A., Gruss, P., Pieler, T., Gurdon, J. B. and Papalopulu, N.** (1998). Xiro3 encodes a xenopus homolog of the Drosophila Iroquois genes and functions in neural specification. *EMBO J.* **17**, 191–203.

**Bessarab, D. a., Chong, S. W. and Korzh, V.** (2004). Expression of zebrafish six1 during sensory organ development and myogenesis. *Dev. Dyn.* **230**, 781–786.

**Betancur, P., Bronner-Fraser, M. and Sauka-Spengler, T.** (2010). Assembling neural crest regulatory circuits into a gene regulatory network. *Annu. Rev. Cell Dev. Biol.* **26**, 581–603.

**Bhasin, N., Maynard, T. M., Gallagher, P. a. and LaMantia, a. S.** (2003). Mesenchymal/epithelial regulation of retinoic acid signaling in the olfactory placode. *Dev. Biol.* **261**, 82–98.

**Bhat, N., Kwon, H.-J. and Riley, B. B.** (2013). A gene network that coordinates preplacodal competence and neural crest specification in zebrafish. *Dev. Biol.* **373**, 107–17.

**Bhattacharyya, S. and Bronner-Fraser, M.** (2008). Competence, specification and commitment to an olfactory placode fate. *Development* **135**, 4165–4177.

**Bhattacharyya, S., Bailey, A. P., Bronner-Fraser, M. and Streit, A.** (2004). Segregation of lens and olfactory precursors from a common territory: cell sorting and reciprocity of Dlx5 and Pax6 expression. *Dev. Biol.* **271**, 403–14.

**Bok, J., Bronner-Fraser, M. and Wu, D. K.** (2005). Role of the hindbrain in dorsoventral but not anteroposterior axial specification of the inner ear. *Development* **132**, 2115–2124.

**Bonini, N. M., Leiserson, W. M. and Senzer, S.** (1993). The eyes absent Gene : Genetic Control of Cell Survival and Differentiation in the Developping Drosophila Eye. *Cell* **72**, 379–395.

**Bonini, N. M., Bui, Q. T., Gray-Board, G. L. and Warrick, J. M.** (1997). The Drosophila eyes absent gene directs ectopic eye formation in a pathway conserved between flies and vertebrates. *Development* **124**, 4819–26.

**Bothe, I. and Dietrich, S.** (2006). The molecular setup of the avian head mesoderm and its implication for craniofacial myogenesis. *Dev. Dyn.* **235**, 2845–2860.

**Boucher, C. a, Carey, N., Edwards, Y. H., Siciliano, M. J. and Johnson, K. J.** (1996). Cloning of the human SIX1 gene and its assignment to chromosome 14. *Genomics* **33**, 140–142.

**Bovolenta, P., Mallamaci, A., Puelles, L. and Boncinelli, E.** (1998). Expression pattern of cSix3, a member of the Six/sine oculis family of transcription factors. *Mech. Dev.* **70**, 201–203.

**Brown, S. T., Wang, J. and Groves, A. K.** (2005). Dlx gene expression during chick inner ear development. *J. Comp. Neurol.* **483**, 48–65.

**Brugmann, S. a and Moody, S. a** (2005). Induction and specification of the vertebrate ectodermal placodes: precursors of the cranial sensory organs. *Biol. Cell* **97**, 303–19.

**Brugmann, S. a, Pandur, P. D., Kenyon, K. L., Pignoni, F. and Moody, S. a** (2004). Six1 promotes a placodal fate within the lateral neurogenic ectoderm by functioning as both a transcriptional activator and repressor. *Development* **131**, 5871–81.

**Buck, L. B.** (2000). The molecular architecture of odor and pheromone sensing in mammals. *Cell* **100**, 611–618.

**Buitrago-Delgado, E., Nordin, K., Rao, a., Geary, L. and LaBonne, C.** (2015). Shared regulatory programs suggest retention of blastula-stage potential in neural crest cells. *Science (80-. ).*

**Canning, C. a, Lee, L., Luo, S. X., Graham, A. and Jones, C. M.** (2008a). Neural tube derived Wnt signals cooperate with FGF signaling in the formation and differentiation of the trigeminal placodes. *Neural Dev.* **3**, 35.

**Canning, C. a, Lee, L., Luo, S. X., Graham, A. and Jones, C. M.** (2008b). Neural tube derived Wnt signals cooperate with FGF signaling in the formation and differentiation of the trigeminal placodes. *Neural Dev.* **3**, 35.

**Carvalho, L. R., Woods, K. S., Mendonca, B. B., Marcal, N., Zamparini, A. L., Stifani, S., Brickman, J. M., Arnhold, I. J. P. and Dattani, M. T.** (2003). A homozygous mutation in HESX1 is associated with evolving hypopituitarism due to impaired repressor-corepressor interaction. *J. Clin. Invest.* **112**, 1192–1201.

**Chai, L., Yang, J., Di, C., Cui, W., Kawakami, K., Lai, R. and Ma, Y.** (2006). Transcriptional activation of the SALL1 by the human SIX1 homeodomain during kidney development. *J. Biol. Chem.* **281**, 18918–26.

**Chambers, D. and Lumsden, A.** (2009). Profiling Gene Transcription in the Developing Embryo. In *Molecular Embryology SE - 42* (ed. Sharpe, P. and Mason, I.), pp. 631–655. Humana Press.

**Chang, C. and Hemmati-Brivanlou, a** (1998). Neural crest induction by Xwnt7B in Xenopus. *Dev. Biol.* **194**, 129–134.

**Chapman, S. C., Collignon, J., Schoenwolf, G. C. and Lumsden, A.** (2001). Improved method for chick whole-embryo culture using a filter paper carrier. *Dev. Dyn.* **220**, 284–289.

**Chapman, S. C., Schubert, F. R., Schoenwolf, G. C. and Lumsden, A.** (2002). Analysis of spatial and temporal gene expression patterns in blastula and gastrula stage chick embryos. *Dev. Biol.* **245**, 187–199.

**Chapman, S. C., Schubert, F. R., Schoenwolf, G. C. and Lumsden, A.** (2003). Anterior identity is established in chick epiblast by hypoblast and anterior definitive endoderm. *Development* **130**, 5091–5101.

**Charles, M. a, Suh, H., Hjalt, T. a, Drouin, J., Camper, S. a and Gage, P. J.** (2005). PITX genes are required for cell survival and Lhx3 activation. *Mol. Endocrinol.* **19**, 1893–1903.

**Chen, R., Amoui, M., Zhang, Z. and Mardon, G.** (1997). Dachshund and eyes absent proteins form a complex and function synergistically to induce ectopic eye development in Drosophila. *Cell* **91**, 893–903.

**Chen, B., Kim, E. H. and Xu, P. X.** (2009). Initiation of olfactory placode development and neurogenesis is blocked in mice lacking both Six1 and Six4. *Dev. Biol.* **326**, 75–85.

**Cheyette, B. N., Green, P. J., Martin, K., Garren, H., Hartenstein, V. and Zipursky, S. L.** (1994). The Drosophila sine oculis locus encodes a homeodomain-containing protein required for the development of the entire visual system. *Neuron* **12**, 977–996.

**Choi, H. K., Choi, K. C., Yoo, J. Y., Song, M., Ko, S. J., Kim, C. H., Ahn, J. H., Chun, K. H., Yook, J. I. and Yoon, H. G.** (2011). Reversible SUMOylation of TBL1-TBLR1 Regulates β-Catenin-Mediated Wnt Signaling. *Mol. Cell* **43**, 203–216.

**Chow, R. L., Altmann, C. R., Lang, R. a and Hemmati-Brivanlou, a** (1999). Pax6 induces ectopic eyes in a vertebrate. *Development* **126**, 4213–4222.

**Christ, S., Biebel, U. W., Hoidis, S., Friedrichsen, S., Bauer, K. and Smolders, J. W. T.** (2004). Hearing Loss in Athyroid Pax8 Knockout Mice and Effects of Thyroxine Substitution. *Audiol. Neurotol.* **9**, 88–106.

**Christophorou, N. a D.** (2008). The role of Eya2 and Six1 in early placode development. A thesis submitted to the King's College London's Higher Degree Office in partial fulfilment for the Degree of Doctor of Philosophy.

**Christophorou, N. a D., Bailey, A. P., Hanson, S. and Streit, A.** (2009). Activation of Six1 target genes is required for sensory placode formation. *Dev. Biol.* **336**, 327–36.

**Christophorou, N. a D., Mende, M., Lleras-Forero, L., Grocott, T. and Streit, A.** (2010). Pax2 coordinates epithelial morphogenesis and cell fate in the inner ear. *Dev. Biol.* **345**, 180–190.

**Clark, W. M. and Fowler, I.** (1960). The inhibition of lens-inducing capacity of the optic vesicle with adult lens antisera. *Dev. Biol.* **2**, 155–172.

**Collinson, J. M., Hill, R. E. and West, J. D.** (2000). Different roles for Pax6 in the optic vesicle and facial epithelium mediate early morphogenesis of the murine eye. *Development* **127**, 945–956.

**Cooper, S. T. and Hanson, I. M.** (2005). A screen for proteins that interact with PAX6: C-terminal mutations disrupt interaction with HOMER3, DNCL1 and TRIM11. *BMC Genet.* **6**, 43.

**COULOMBRE, J. L. and COULOMBRE, A. J.** (1963). LENS DEVELOPMENT: FIBER ELONGATION AND LENS ORIENTATION. *Science* **142**, 1489–1490.

**Couly, G. F. and Le Douarin, N. M.** (1985). Mapping of the early neural primordium in quail-chick chimeras. I. Developmental relationships between placodes, facial ectoderm, and prosencephalon. *Dev. Biol.* **110**, 422–439.

**Couly, G. F., Coltey, P. M. and Le Douarin, N. M.** (1992). The developmental fate of the cephalic mesoderm in quail-chick chimeras. *Development* **114**, 1–15.

**Cvekl, A. and Piatigorsky, J.** (1996). Lens development and crystallin gene expression: many roles for Pax-6. *Bioessays* **18**, 621–630.

**D'Amico-Martel, A. and Noden, D. M.** (1983). Contributions of placodal and neural crest cells to avian cranial peripheral ganglia. *Am. J. Anat.* **166**, 445–468.

**De Celis, J. F. and Barrio, R.** (2009). Regulation and function of Spalt proteins during animal development. *Int. J. Dev. Biol.* **53**, 1385–98.

**De Moerlooze, L., Spencer-Dene, B., Revest, J. M., Hajihosseini, M., Rosewell, I. and Dickson, C.** (2000). An important role for the IIIb isoform of fibroblast growth factor receptor 2 (FGFR2) in mesenchymal-epithelial signalling during mouse organogenesis. *Development* **127**, 483–492.

**De Robertis, E. M. and Kuroda, H.** (2004). Dorsal-ventral patterning and neural induction in Xenopus embryos. *Annu. Rev. Cell Dev. Biol.* **20**, 285–308.

**DeHaan, R. L.** (1963). Migration patterns of the precardiac mesoderm in the early chick embryo. *Exp. Cell Res.* **29**, 544–560.

**Dickinson, M. E., Selleck, M. a, McMahon, a P. and Bronner-Fraser, M.** (1995). Dorsalization of the neural tube by the non-neural ectoderm. *Development* **121**, 2099–2106.

**Dimanlig, P. V, Faber, S. C., Auerbach, W., Makarenkova, H. P. and Lang, R. a** (2001). The upstream ectoderm enhancer in Pax6 has an important role in lens induction. *Development* **128**, 4415–4424.

**Dude, C. M., Kuan, C.-Y. K., Bradshaw, J. R., Greene, N. D. E., Relaix, F., Stark, M. R. and Baker, C. V. H.** (2009). Activation of Pax3 target genes is necessary but not sufficient for neurogenesis in the ophthalmic trigeminal placode. *Dev. Biol.* **326**, 314–326.

**Duggan, C. D., DeMaria, S., Baudhuin, A., Stafford, D. and Ngai, J.** (2008). Foxg1 is required for development of the vertebrate olfactory system. *J. Neurosci.* **28**, 5229–5239.

**Duncan, M. K., Haynes, J. I., Cvekl, a and Piatigorsky, J.** (1998). Dual roles for Pax-6: a transcriptional repressor of lens fiber cell-specific beta-crystallin genes. *Mol. Cell. Biol.* **18**, 5579–5586.

**Dutta, S., Dietrich, J.-E., Aspöck, G., Burdine, R. D., Schier, A., Westerfield, M. and Varga, Z. M.** (2005). Pitx3 Defines an Equivalence Domain for Lens and Anterior Pituitary Placode. *Development* **132**, 1579–1590.

**Eastman, Q. and Grosschedl, R.** (1999). Regulation of LEF-1/TCF transcription factors by Wnt and other signals. *Curr. Opin. Cell Biol.* **11**, 233–240.

**Eccles, M. R. and Schimmenti, L. a** (1999). Renal-coloboma syndrome: a multi-system developmental disorder caused by PAX2 mutations. *Clin. Genet.* **56**, 1–9.

**Ehrman, L. a and Yutzey, K. E.** (1999). Lack of regulation in the heart forming region of avian embryos. *Dev. Biol.* **207**, 163–175.

**Eisenberg, C. a, Gourdie, R. G. and Eisenberg, L. M.** (1997). Wnt-11 is expressed in early avian mesoderm and required for the differentiation of the quail mesoderm cell line QCE-6. *Development* **124**, 525–536.

**elAmraoui, A. and Dubois, P. M.** (1993). Experimental evidence for the early commitment of the presumptive adenohypophysis. *Neuroendocrinology* **58**, 609–615.

**Engels, S., Kohlhase, J. and McGaughran, J.** (2000). A SALL1 mutation causes a branchio-oto-renal syndrome-like phenotype. *J. Med. Genet.* **37**, 458–460.

**Esterberg, R. and Fritz, A.** (2009). dlx3b/4b are required for the formation of the preplacodal region and otic placode through local modulation of BMP activity. *Dev. Biol.* **325**, 189–199.

**Esteve, P. and Bovolenta, P.** (1999). cSix4, a member of the six gene family of transcription factors, is expressed during placode and somite development. *Mech. Dev.* **85**, 161–165.

**Eyal-Giladi, H. and Fabian, B. C.** (1980). Axis determination in uterine chick blastodiscs under changing spatial positions during the sensitive period for polarity. *Dev. Biol.* **77**, 228–232.

**Eyal-Giladi, H. and Kochav, S.** (1976). From cleavage to primitive streak formation: a complementary normal table and a new look at the first stages of the development of the chick. I. General morphology. *Dev. Biol.* **49**, 321–37.

**Faber, S. C., Dimanlig, P., Makarenkova, H. P., Shirke, S., Ko, K. and Lang, R. a** (2001). Fgf receptor signaling plays a role in lens induction. *Development* **128**, 4425–4438.

**Fabian, B. and Eyal-Giladi, H.** (1981). A SEM study of cell shedding during the formation of the area pellucida in the chick embryo. *J. Embryol. Exp. Morphol.* **64**, 11–22.

**Fainsod, a, Steinbeisser, H. and De Robertis, E. M.** (1994). On the function of BMP-4 in patterning the marginal zone of the Xenopus embryo. *EMBO J.* **13**, 5015–5025.

**Faure, S., de Santa Barbara, P., Roberts, D. J. and Whitman, M.** (2002). Endogenous patterns of BMP signaling during early chick development. *Dev. Biol.* **244**, 44–65.

**Favor, J., Sandulache, R., Neuhäuser-Klaus, a, Pretsch, W., Chatterjee, B., Senft, E., Wurst, W., Blanquet, V., Grimes, P., Spörle, R., et al.** (1996). The mouse Pax2(1Neu) mutation is identical to a human PAX2 mutation in a family with renal-coloboma syndrome and results in developmental defects of the brain, ear, eye, and kidney. *Proc. Natl. Acad. Sci. U. S. A.* **93**, 13870–13875.

**Fernández-Garre, P., Rodríguez-Gallardo, L., Gallego-Díaz, V., Alvarez, I. S. and Puelles, L.** (2002). Fate map of the chicken neural plate at stage 4. *Development* **129**, 2807–22.

**Foley, a C., Storey, K. G. and Stern, C. D.** (1997). The prechordal region lacks neural inducing ability, but can confer anterior character to more posterior neuroepithelium. *Development* **124**, 2983–96.

**Fortina, P. and Surrey, S.** (2008). Digital mRNA profiling. *Nat. Biotechnol.* **26**, 293–4.

**Freter, S., Muta, Y., Mak, S.-S., Rinkwitz, S. and Ladher, R. K.** (2008). Progressive restriction of otic fate: the role of FGF and Wnt in resolving inner ear potential. *Development* **135**, 3415–3424.

**Frith, M. C., Fu, Y., Yu, L., Chen, J. F., Hansen, U. and Weng, Z.** (2004). Detection of functional DNA motifs via statistical over-representation. *Nucleic Acids Res.* **32**, 1372–1381.

**Fujiwara, M., Uchida, T., Osumi-Yamashita, N. and Eto, K.** (1994). Uchida rat (rSey): a new mutant rat with craniofacial abnormalities resembling those of the mouse Sey mutant. *Differentiation.* **57**, 31–38.

**Furuta, Y. and Hogan, B. L. M.** (1998). BMP4 is essential for lens induction in the mouse embryo. *Genes Dev.* **12**, 3764–3775.

**Gallagher, B. C., Henry, J. J. and Grainger, R. M.** (1996). Inductive processes leading to inner ear formation during Xenopus development. *Dev. Biol.* **175**, 95–107.

**Gallardo, M. E., Lopez-Rios, J., Fernaud-Espinosa, I., Granadino, B., Sanz, R., Ramos, C., Ayuso, C., Seller, M. J., Brunner, H. G., Bovolenta, P., et al.** (1999). Genomic cloning and characterization of the human homeobox gene SIX6 reveals a cluster of SIX genes in chromosome 14 and associates SIX6 hemizygosity with bilateral anophthalmia and pituitary anomalies. *Genomics* **61**, 82–91.

**García-Castro, M. I., Marcelle, C. and Bronner-Fraser, M.** (2002). Ectodermal Wnt function as a neural crest inducer. *Science* **297**, 848–851.

**Garcia-Martinez, V., Alvarez, I. S. and Schoenwolf, G. C.** (1993). Locations of the ectodermal and nonectodermal subdivisions of the epiblast at stages 3 and 4 of avian gastrulation and neurulation. *J. Exp. Zool.* **267**, 431–446.

**Gaston-Massuet, C., Andoniadou, C. L., Signore, M., Sajedi, E., Bird, S., Turner, J. M. A. and Martinez-Barbera, J. P.** (2008). Genetic interaction between the homeobox transcription factors HESX1 and SIX3 is required for normal pituitary development. *Dev. Biol.* **324**, 322–333.

**Geiss, G. K., Bumgarner, R. E., Birditt, B., Dahl, T., Dowidar, N., Dunaway, D. L., Fell, H. P., Ferree, S., George, R. D., Grogan, T., et al.** (2008). Direct multiplexed measurement of gene expression with color-coded probe pairs. *Nat. Biotechnol.* **26**, 317–325.

**Ghanbari, H., Seo, H. C., Fjose, a and Brändli, a W.** (2001). Molecular cloning and embryonic expression of Xenopus Six homeobox genes. *Mech. Dev.* **101**, 271–7.

**Giot, L., Bader, J. S., Brouwer, C., Chaudhuri, a, Kuang, B., Li, Y., Hao, Y. L., Ooi, C. E., Godwin, B., Vitols, E., et al.** (2003). A protein interaction map of Drosophila melanogaster. *Science* **302**, 1727–1736.

**Giraldez, F.** (1998). Regionalized organizing activity of the neural tube revealed by the regulation of lmx1 in the otic vesicle. *Dev. Biol.* **203**, 189–200.

**Glavic, A., Gómez-Skarmeta, J. L. and Mayor, R.** (2002). The homeoprotein Xiro1 is required for midbrain-hindbrain boundary formation. *Development* **129**, 1609–1621.

**Glavic, A., Honoré, S. M., Feijóo, C. G., Bastidas, F., Allende, M. L. and Mayor, R.** (2004). Role of BMP signaling and the homeoprotein iroquois in the specification of the cranial placodal field. *Dev. Biol.* **272**, 89–103.

**Gleiberman, a S., Fedtsova, N. G. and Rosenfeld, M. G.** (1999). Tissue interactions in the induction of anterior pituitary: role of the ventral diencephalon, mesenchyme, and notochord. *Dev. Biol.* **213**, 340–353.

**Goode, D. K. and Elgar, G.** (2009). The PAX258 gene subfamily: A comparative perspective. *Dev. Dyn.* **238**, 2951–2974.

**Goriely, A., Diez Del Corral, R. and Storey, K. G.** (1999). c-Irx2 expression reveals an early subdivision of the neural plate in the chick embryo. *Mech. Dev.* **87**, 203–206.

**Gotoh, N., Ito, M., Yamamoto, S., Yoshino, I., Song, N., Wang, Y., Lax, I., Schlessinger, J., Shibuya, M. and Lang, R. a** (2004). Tyrosine phosphorylation sites on FRS2alpha responsible for Shp2 recruitment are critical for induction of lens and retina. *Proc. Natl. Acad. Sci. U. S. A.* **101**, 17144–17149.

**Grainger, R. M., Herry, J. J. and Henderson, R. a** (1988). Reinvestigation of the role of the optic vesicle in embryonic lens induction. *Development* **102**, 517–526.

**Gray, H. and Leonard, C. H.** (1983). *The concise Gray's anatomy*. Secaucus, N.J.: Chartwell Books.

**Grocott, T., Johnson, S., Bailey, A. P. and Streit, A.** (2011). Neural crest cells organize the eye via TGF-β and canonical Wnt signalling. *Nat. Commun.* **2**, 265.

**Grocott, T., Tambalo, M. and Streit, A.** (2012). The peripheral sensory nervous system in the vertebrate head: a gene regulatory perspective. *Dev. Biol.* **370**, 3–23.

**Groves, a K. and Bronner-Fraser, M.** (2000). Competence, specification and commitment in otic placode induction. *Development* **127**, 3489–99.

**Groves, A. K. and Labonne, C.** (2014). Setting appropriate boundaries: Fate, patterning and competence at the neural plate border. *Dev. Biol.* **389**, 2–12.

**Gunhaga, L., Marklund, M., Sjödal, M., Hsieh, J.-C., Jessell, T. M. and Edlund, T.** (2003). Specification of dorsal telencephalic character by sequential Wnt and FGF signaling. *Nat. Neurosci.* **6**, 701–707.

**Haddon, C. and Lewis, J.** (1996). Early ear development in the embryo of the zebrafish, Danio rerio. *J. Comp. Neurol.* **365**, 113–128.

**Halder, G., Callaerts, P., Flister, S., Walldorf, U., Kloter, U. and Gehring, W. J.** (1998). Eyeless initiates the expression of both sine oculis and eyes absent during Drosophila compound eye development. *Development* **125**, 2181–2191.

**Hamburger, V. and Hamilton, H.** (1951). A series of normal stages in the development of the chick embryo. *J. Morphol.* **88**,.

**Hao, J., Daleo, M. a, Murphy, C. K., Yu, P. B., Ho, J. N., Hu, J., Peterson, R. T., Hatzopoulos, A. K. and Hong, C. C.** (2008). Dorsomorphin, a selective small molecule inhibitor of BMP signaling, promotes cardiomyogenesis in embryonic stem cells. *PLoS One* **3**, e2904.

**Hara, K.** (1961). Regional neural differentiation induced by prechordal and presumptive chordal mesoderm in the chick embryo: PhD Thesis.

**Harland, R.** (2000). Neural induction. *Curr. Opin. Genet. Dev.* **10**, 357–362.

**Hatada, Y. and Stern, C. D.** (1994). A fate map of the epiblast of the early chick embryo. *Development* **120**, 2879–89.

**Hatch, E. P., Noyes, C. A., Wang, X., Wright, T. J. and Mansour, S. L.** (2007). Fgf3 is required for dorsal patterning and morphogenesis of the inner ear epithelium. *Development* **134**, 3615–3625.

**Heeg-Truesdell, E. and LaBonne, C.** (2006). Neural induction in Xenopus requires inhibition of Wnt-β-catenin signaling. *Dev. Biol.* **298**, 71–86.

**Heller, N. and Brandli, A. W.** (1997). Xenopus Pax-2 displays multiple splice forms during embryogenesis and pronephric kidney development. *Mech. Dev.* **69**, 83–104.

**Hill, R. E. and Hanson, I. M.** (1992). Molecular genetics of the Pax gene family. *Curr. Opin. Cell Biol.* **4**, 967–972.

**Hoekstra, E. J., Mesman, S., de Munnik, W. a. and Smidt, M. P.** (2013). LMX1B Is Part of a Transcriptional Complex with PSPC1 and PSF. *PLoS One* **8**, 1–13.

**Hoijman, E., Rubbini, D., Colombelli, J. and Alsina, B.** (2015). Mitotic cell rounding and epithelial thinning regulate lumen growth and shape. *Nat. Commun.* **6**, 7355.

**Hong, C. and Saint-Jeannet, J.** (2007). The activity of Pax3 and Zic1 regulates three distinct cell fates at the neural plate border. *Mol. Biol. Cell* **18**, 2192–2202.

**Hoppler, S. and Moon, R. T.** (1998). BMP-2/-4 and Wnt-8 cooperatively pattern the Xenopus mesoderm. *Mech. Dev.* **71**, 119–129.

**Huang, X., Hong, C. and Donnell, M. O.** (2005). for Neurogenesis in the Olfactory System. **102**, 11349–11354.

**Huber, O., Korn, R., McLaughlin, J., Ohsugi, M., Herrmann, B. G. and Kemler, R.** (1996). Nuclear localization of beta-catenin by interaction with transcription factor LEF-1. *Mech. Dev.* **59**, 3–10.

**Huynh-Thu, V. A., Irrthum, A., Wehenkel, L. and Geurts, P.** (2010). Inferring regulatory networks from expression data using tree-based methods. *PLoS One* **5**, 1–10.

**Ikeda, K., Watanabe, Y., Ohto, H. and Kawakami, K.** (2002). Molecular interaction and synergistic activation of a promoter by Six, Eya, and Dach proteins mediated through CREB binding protein. *Mol. Cell. Biol.* **22**, 6759–6766.

**Ikeda, K., Ookawara, S., Sato, S., Ando, Z. I., Kageyama, R. and Kawakami, K.** (2007). Six1 is essential for early neurogenesis in the development of olfactory epithelium. *Dev. Biol.* **311**, 53–68.

**Ishihara, T., Ikeda, K., Sato, S., Yajima, H. and Kawakami, K.** (2008a). Differential expression of Eya1 and Eya2 during chick early embryonic development. *Gene Expr. Patterns* **8**, 357–367.

**Ishihara, T., Sato, S., Ikeda, K., Yajima, H. and Kawakami, K.** (2008b). Multiple evolutionarily conserved enhancers control expression of Eya1. *Dev. Dyn.* **237**, 3142–3156.

**Jacobson, A. G.** (1963a). The determination and positioning of the nose, lens and ear. I. Interactions within the ectoderm, and between the ectoderm and underlying tissues. *J. Exp. Zool.* **154**, 273–283.

**Jacobson, A. G.** (1963b). Determination and positioning of the nose, lens and ear. II. The role of the endoderm. *J. Exp. Zool.* **154**, 285–291.

**Jacobson, A. G.** (1963c). The determination and positioning of the nose, lens and ear. III. Effects of reversing the antero-posterior axis of epidermis, neural plate and neural fold. *J. Exp. Zool.* **154**, 293–303.

**Jacobson, A. G.** (1966). Inductive processes in embryonic development. *Science* **152**, 25–34.

**Jaurena, M. B., Juraver-Geslin, H., Devotta, A. and Saint-Jeannet, J.-P.** (2015). Zic1 controls placode progenitor formation non-cell autonomously by regulating retinoic acid production and transport. *Nat. Commun.* **6**, 7476.

**Jemc, J. and Rebay, I.** (2007). The eyes absent family of phosphotyrosine phosphatases: properties and roles in developmental regulation of transcription. *Annu. Rev. Biochem.* **76**, 513–538.

**Jorquera, B., Goicoechea, O. and Molinari, E.** (1989). [Differentiation of the crystalline lens in explants of the chicken embryo in the absence of the hypoblast and optical vesicle]. *Anat. Histol. Embryol.* **18**, 32–44.

**Jung, S.-K., Jeong, D. G., Chung, S. J., Kim, J. H., Park, B. C., Tonks, N. K., Ryu, S. E. and Kim, S. J.** (2010). Crystal structure of ED-Eya2: insight into dual roles as a protein tyrosine phosphatase and a transcription factor. *FASEB J.* **24**, 560–9.

**Just, W., Trautmann, T., Baumstark, A. and Müller, D.** (2003). Exclusion of the SALL1 gene as a cause of branchio-oculo-facial syndrome. *Am. J. Med. Genet. A* **117A**, 196–198.

**Kaji, T. and Artinger, B.** (2004). dlx3b and dlx4b function in the development of Rohon-Beard sensory neurons and trigeminal placode in the zebrafish neurula. *Dev. Biol.* **276**, 523–540.

**Kalcheim, C. and Le Douarin, N. M.** (1986). Requirement of a neural tube signal for the differentiation of neural crest cells into dorsal root ganglia. *Dev. Biol.* **116**, 451–466.

**Kamachi, Y., Sockanathan, S., Liu, Q., Breitman, M., Lovell-Badge, R. and Kondoh, H.** (1995). Involvement of SOX proteins in lens-specific activation of crystallin genes. *EMBO J.* **14**, 3510–3519.

**Kamachi, Y., Uchikawa, M., Collignon, J., Lovell-Badge, R. and Kondoh, H.** (1998). Involvement of Sox1, 2 and 3 in the early and subsequent molecular events of lens induction. *Development* **125**, 2521–2532.

**Kammandel, B., Chowdhury, K., Stoykova, a, Aparicio, S., Brenner, S. and Gruss, P.** (1999). Distinct cis-essential modules direct the time-space pattern of the Pax6 gene activity. *Dev. Biol.* **205**, 79–97.

**Kang, Y., Lin, Y., Li, X., Wu, Q., Huang, L., Li, Q. and Hu, Q.** (2012). Mutation analysis of PAX6 in inherited and sporadic aniridia from northeastern China. *Mol. Vis.* **18**, 1750–4.

**Karkinen-Jääskeläinen, M.** (1978). Permissive and directive interactions in lens induction. *J. Embryol. Exp. Morphol.* **44**, 167–179.

**Katahira, T., Sato, T., Sugiyama, S., Okafuji, T., Araki, I., Funahashi, J. I. and Nakamura, H.** (2000). Interaction between Otx2 and Gbx2 defines the organizing center for the optic tectum. *Mech. Dev.* **91**, 43–52.

**Kavak, E., Najafov, A., Ozturk, N., Seker, T., Cavusoglu, K., Aslan, T., Duru, A. D., Saygili, T., Hoxhaj, G., Hiz, M. C., et al.** (2010). Analysis of the Wnt/B-catenin/TCF4 pathway using SAGE, genome-wide microarray and promoter analysis: Identification of BRI3 and HSF2 as novel targets. *Cell. Signal.* **22**, 1523–1535.

**Kawakami, K., Ohto, H., Takizawa, T. and Saito, T.** (1996a). Identification and expression of six family genes in mouse retina. *FEBS Lett.* **393**, 259–263.

**Kawakami, K., Ohto, H., Ikeda, K. and Roeder, R. G.** (1996b). Structure, function and expression of a murine homeobox protein AREC3, a homologue of Drosophila sine oculis gene product, and implication in development. *Nucleic Acids Res.* **24**, 303–10.

**Kawakami, K., Sato, S., Ozaki, H. and Ikeda, K.** (2000). Six family genes--structure and function as transcription factors and their roles in development. *Bioessays* **22**, 616–26.

**Kawamura, K., Kouki, T., Kawahara, G. and Kikuyama, S.** (2002). Hypophyseal development in vertebrates from amphibians to mammals. *Gen. Comp. Endocrinol.* **126**, 130–135.

**Kawauchi, S., Shou, J., Santos, R., Hébert, J. M., McConnell, S. K., Mason, I. and Calof, A. L.** (2005). Fgf8 expression defines a morphogenetic center required for olfactory neurogenesis and nasal cavity development in the mouse. *Development* **132**, 5211–5223.

**Keller, R. E.** (1976). Vital dye mapping of the gastrula and neurula of Xenopus laevis. II. Prospective areas and morphogenetic movements of the deep layer. *Dev. Biol.* **51**, 118–137.

**Kever, L., Colleye, O., Herrel, a., Romans, P. and Parmentier, E.** (2014). Hearing capacities and otolith size in two ophidiiform species (Ophidion rochei and Carapus acus). *J. Exp. Biol.* **217**, 2517–2525.

**Khatri, S. B. and Groves, A. K.** (2013). Expression of the Foxi2 and Foxi3 transcription factors during development of chicken sensory placodes and pharyngeal arches. *Gene Expr. Patterns* **13**, 38–42.

**Khatri, S. B., Edlund, R. K. and Groves, A. K.** (2014). Foxi3 is necessary for the induction of the chick otic placode in response to FGF signaling. *Dev. Biol.* **391**, 158–169.

**Khudyakov, J. and Bronner-Fraser, M.** (2009). Comprehensive spatiotemporal analysis of early chick neural crest network genes. *Dev. Dyn.* **238**, 716–723.

**Kil, S. H., Streit, A., Brown, S. T., Agrawal, N., Collazo, A., Zile, M. H. and Groves, A. K.** (2005). Distinct roles for hindbrain and paraxial mesoderm in the induction and patterning of the inner ear revealed by a study of vitamin-A-deficient quail. *Dev. Biol.* **285**, 252–271.

**Kimura-Yoshida, C., Mochida, K., Ellwanger, K., Niehrs, C. and Matsuo, I.** (2015). Fate Specification of Neural Plate Border by Canonical Wnt Signaling and Grhl3 is Crucial for Neural Tube Closure. *EBioMedicine* **2**, 513–527.

**King, H. D.** (1904). Experimental studies on the eye of the frog embryo. **19** ,.

**Kioussi, C., O'Connell, S., St-Onge, L., Treier, M., Gleiberman, a S., Gruss, P. and Rosenfeld, M. G.** (1999). Pax6 is essential for establishing ventral-dorsal cell boundaries in pituitary gland development. *Proc. Natl. Acad. Sci. U. S. A.* **96**, 14378–14382.

**Kirby, R. J., Hamilton, G. M., Finnegan, D. J., Johnson, K. J. and Jarman, A. P.** (2001). Drosophila homolog of the myotonic dystrophy-associated gene, SIX5, is required for muscle and gonad development. *Curr. Biol.* **11**, 1044–1049.

**Knouff, R. A.** (1935). The developmental pattern of ectodermal placodes in Rana Pipiens. *J. Comp. Neurol.* **62**, 17–71.

**Kobayashi, M., Toyama, R., Takeda, H., Dawid, I. B. and Kawakami, K.** (1998). Overexpression of the forebrain-specific homeobox gene six3 induces rostral forebrain enlargement in zebrafish. *Development* **125**, 2973–2982.

**Kobayashi, M., Nishikawa, K., Suzuki, T. and Yamamoto, M.** (2001). The homeobox protein Six3 interacts with the Groucho corepressor and acts as a transcriptional repressor in eye and forebrain formation. *Dev. Biol.* **232**, 315–26.

**Kobayashi, D., Kobayashi, M., Matsumoto, K., Ogura, T., Nakafuku, M. and Shimamura, K.** (2002). Early subdivisions in the neural plate define distinct competence for inductive signals. *Development* **129**, 83–93.

**Kochav, S. and Eyal-Giladi, H.** (1971). Bilateral symmetry in chick embryo determination by gravity. *Science* **171**, 1027–1029.

**Köster, R. W., Kühnlein, R. P. and Wittbrodt, J.** (2000). Ectopic Sox3 activity elicits sensory placode formation. *Mech. Dev.* **95**, 175–87.

**Kouki, T., Imai, H., Aoto, K., Eto, K., Shioda, S., Kawamura, K. and Kikuyama, S.** (2001). Developmental origin of the rat adenohypophysis prior to the formation of Rathke's pouch. *Development* **128**, 959–963.

**Kozlowski, D. J., Murakami, T., Ho, R. K. and Weinberg, E. S.** (1997). Regional cell movement and tissue patterning in the zebrafish embryo revealed by fate mapping with caged fluorescein. *Biochem. Cell Biol.* **75**, 551–562.

**Kozlowski, D. J., Whitfield, T. T., Hukriede, N. a., Lam, W. K. and Weinberg, E. S.** (2005). The zebrafish dog-eared mutation disrupts eya1, a gene required for cell survival and differentiation in the inner ear and lateral line. *Dev. Biol.* **277**, 27–41.

**Kroeber, M., Davis, N., Holzmann, S., Kritzenberger, M., Shelah-Goraly, M., Ofri, R., Ashery-Padan, R. and Tamm, E. R.** (2010). Reduced expression of Pax6 in lens and cornea of mutant mice leads to failure of chamber angle development and juvenile glaucoma. *Hum. Mol. Genet.* **19**, 3332–3342.

**Kwon, H. J. and Riley, B. B.** (2009). Mesendodermal signals required for otic induction: Bmp-antagonists cooperate with Fgf and can facilitate formation of ectopic otic tissue. *Dev. Dyn.* **238**, 1582–1594.

**Kwon, H. J., Bhat, N., Sweet, E. M., Cornell, R. a. and Riley, B. B.** (2010). Identification of early requirements for preplacodal ectoderm and sensory organ development. *PLoS Genet.* **6**,.

**LaBonne, C. and Bronner-Fraser, M.** (1998). Neural crest induction in Xenopus: evidence for a two-signal model. *Development* **125**, 2403–2414.

**LaBonne, C. and Bronner-Fraser, M.** (2000). Snail-related transcriptional repressors are required in Xenopus for both the induction of the neural crest and its subsequent migration. *Dev. Biol.* **221**, 195–205.

**Ladher, R. K., Anakwe, K. U., Gurney, a L., Schoenwolf, G. C. and Francis-West, P. H.** (2000). Identification of synergistic signals initiating inner ear development. *Science* **290**, 1965–1967.

**Ladher, R. K., O'Neill, P. and Begbie, J.** (2010). From shared lineage to distinct functions: the development of the inner ear and epibranchial placodes. *Development* **137**, 1777–1785.

**LaMantia, a S., Bhasin, N., Rhodes, K. and Heemskerk, J.** (2000). Mesenchymal/epithelial induction mediates olfactory pathway formation. *Neuron* **28**, 411–425.

**Lang, R. a.** (2004). Pathways regulating lens induction in the mouse. *Int. J. Dev. Biol.* **48**, 783–791.

**Lang, H., Schulte, B. a, Zhou, D., Smythe, N., Spicer, S. S. and Schmiedt, R. a** (2006). Nuclear factor kappaB deficiency is associated with auditory nerve degeneration and increased noise-induced hearing loss. *J. Neurosci.* **26**, 3541–3550.

**Lassiter, R. N. T., Dude, C., Reynolds, S. B., Winters, N. I., Baker, C. V. H. and Stark, M. R.** (2007). Canonical Wnt Signaling is Required for Ophthalmic Trigeminal Placode Cell Fate Determination and Maintenance. *Dev. Biol.* **308**, 392–406.

**Lassiter, R. N. T., Reynolds., S. B., Marin, K. D., Mayo, T. F. and Stark, M. R.** (2009). FGF signaling is essential for ophthalmic trigeminal placode cell delamination and differentiation. *Dev. Dyn.* **238**, 1073–1082.

**Lee, S. T., Li, Z., Wu, Z., Aau, M., Guan, P., Karuturi, R. K. M., Liou, Y. C. and Yu, Q.** (2011). Context-Specific Regulation of NF-??B Target Gene Expression by EZH2 in Breast Cancers. *Mol. Cell* **43**, 798–810.

**Léger, S. and Brand, M.** (2002). Fgf8 and Fgf3 are required for zebrafish ear placode induction, maintenance and inner ear patterning. *Mech. Dev.* **119**, 91–108.

**Lewis W H** (1901). Experimental studies on the development of the eye in amphibia. I. On the origin of the lens. *Am. J. Anat.* **111**,.

**Li, H. S., Yang, J. M., Jacobson, R. D., Pasko, D. and Sundin, O.** (1994). Pax-6 is first expressed in a region of ectoderm anterior to the early neural plate: implications for stepwise determination of the lens. *Dev. Biol.* **162**, 181–194.

**Li, X., Oghi, K. a, Zhang, J., Krones, A., Bush, K. T., Glass, C. K., Nigam, S. K., Aggarwal, A. K., Maas, R., Rose, D. W., et al.** (2003). Eya protein phosphatase activity regulates Six1-Dach-Eya transcriptional effects in mammalian organogenesis. *Nature* **426**, 247–254.

**Liberzon, A., Ridner, G. and Walker, M. D.** (2004). Role of intrinsic DNA binding specificity in defining target genes of the mammalian transcription factor PDX1. *Nucleic Acids Res.* **32**, 54–64.

**Liem, K. F., Tremml, G., Roelink, H. and Jessell, T. M.** (1995). Dorsal differentiation of neural plate cells induced by BMP-mediated signals from epidermal ectoderm. *Cell* **82**, 969–979.

**Linker, C. and Stern, C. D.** (2004). Neural induction requires BMP inhibition only as a late step, and involves signals other than FGF and Wnt antagonists. *Development* **131**, 5671–81.

**Linker, C., De Almeida, I., Papanayotou, C., Stower, M., Sabado, V., Ghorani, E., Streit, A., Mayor, R. and Stern, C. D.** (2009). Cell communication with the neural plate is required for induction of neural markers by BMP inhibition: evidence for homeogenetic induction and implications for Xenopus animal cap and chick explant assays. *Dev. Biol.* **327**, 478–486.

**Litsiou, A., Hanson, S. and Streit, A.** (2005). A balance of FGF, BMP and WNT signalling positions the future placode territory in the head. *Development* **132**, 4051–62.

**Liu, W., Lagutin, O. V, Mende, M., Streit, A. and Oliver, G.** (2006). Six3 activation of Pax6 expression is essential for mammalian lens induction and specification. *EMBO J.* **25**, 5383–5395.

**Lleras-Forero, L., Tambalo, M., Christophorou, N., Chambers, D., Houart, C. and Streit, A.** (2013). Neuropeptides: developmental signals in placode progenitor formation. *Dev. Cell* **26**, 195–203.

**Lombardo, A. and Slack, J. M. W.** (1998). Postgastrulation effects of fibroblast growth factor on \textit{Xenopus} development. *Dev. Dyn.* **212**, 75–85.

**Longabaugh, W. J. R., Davidson, E. H. and Bolouri, H.** (2005). Computational representation of developmental genetic regulatory networks. **283**, 1–16.

**Loosli, F., Winkler, S. and Wittbrodt, J.** (1999). Six3 overexpression initiates the formation of ectopic retina. *Genes Dev.* **13**, 649–654.

**Loots, G. G. and Ovcharenko, I.** (2004). rVISTA 2.0: Evolutionary analysis of transcription factor binding sites. *Nucleic Acids Res.* **32**, 217–221.

**Lopez-Sanchez, C., Garcia-Masa, N., Gañan, C. M. and Garcia-Martinez, V.** (2009). Movement and commitment of primitive streak precardiac cells during cardiogenesis. *Int. J. Dev. Biol.* **53**, 1445–1455.

**Lunn, J. S., Fishwick, K. J., Halley, P. a and Storey, K. G.** (2007). A spatial and temporal map of FGF / Erk1 / 2 activity and response repertoires in the early chick embryo. *Dev. Biol.* **302**, 536 – 552.

**Luo, T., Matsuo-Takasaki, M., Lim, J. H. and Sargent, T. D.** (2001). Differential regulation of Dlx gene expression by a BMP morphogenetic gradient. *Int. J. Dev. Biol.* **45**, 681–4.

**M.Hanson, I., Seawright, A., Hardman, K., Hodgson, S., Zaletayev, D., Fekete, G. and Heyningen, V. van** (1993). PAX6 mutations in aniridia. *Hum. Mol. Genet.* **2** , 915–920.

**Mackereth, M. D., Kwak, S.-J., Fritz, A. and Riley, B. B.** (2005). Zebrafish pax8 is required for otic placode induction and plays a redundant role with Pax2 genes in the maintenance of the otic placode. *Development* **132**, 371–82.

**Mahmood, R., Kiefer, P., Guthrie, S., Dickson, C. and Mason, I.** (1995). Multiple roles for FGF-3 during cranial neural development in the chicken. *Development* **121**, 1399–1410.

**Mahmood, R., Mason, I. J. and Morriss-Kay, G. M.** (1996). Expression of Fgf-3 in relation to hindbrain segmentation, otic pit position and pharyngeal arch morphology in normal and retinoic acid-exposed mouse embryos. *Anat. Embryol. (Berl).* **194**, 13–22.

**Maier, E., Nord, H., von Hofsten, J. and Gunhaga, L.** (2011). A balance of BMP and notch activity regulates neurogenesis and olfactory nerve formation. *PLoS One* **6**,.

**Mancilla, a and Mayor, R.** (1996). Neural crest formation in Xenopus laevis: mechanisms of Xslug induction. *Dev. Biol.* **177**, 580–589.

**Mansour, S. L., Goddard, J. M. and Capecchi, M. R.** (1993). Mice homozygous for a targeted disruption of the proto-oncogene int-2 have developmental defects in the tail and inner ear. *Development* **117**, 13–28.

**Margueron, R. and Reinberg, D.** (2011). The Polycomb Complex PRC2 and its Mark in Life. *Nature* **469**, 343–349.

**Maroon, H., Walshe, J., Mahmood, R., Kiefer, P., Dickson, C. and Mason, I.** (2002). Fgf3 and Fgf8 are required together for formation of the otic placode and vesicle. *Development* **129**, 2099–2108.

**Martin, K. and Groves, A. K.** (2006). Competence of cranial ectoderm to respond to Fgf signaling suggests a two-step model of otic placode induction. *Development* **133**, 877–87.

**Mathers, P. H., Grinberg, a, Mahon, K. a and Jamrich, M.** (1997). The Rx homeobox gene is essential for vertebrate eye development. *Nature* **387**, 603–607.

**Matsuo-Takasaki, M., Matsumura, M. and Sasai, Y.** (2005). An essential role of Xenopus Foxi1a for ventral specification of the cephalic ectoderm during gastrulation. *Development* **132**, 3885–3894.

**McCabe, K. L. and Bronner, M.** (2011). Tetraspanin, CD151, is required for maintenance of trigeminal placode identity. *J. Neurochem.* **117**, 221–230.

**McCabe, K. L., Shiau, C. E. and Bronner-Fraser, M.** (2007). Identification of candidate secreted factors involved in trigeminal placode induction. *Dev. Dyn.* **236**, 2925–2935.

**McCabe, K. L., Sechrist, J. W. and Bronner-Fraser, M.** (2009). Birth of ophthalmic trigeminal neurons initiates early in the placodal ectoderm. *J. Comp. Neurol.* **514**, 161–173.

**McCarroll, M. N. and Nechiporuk, A. V.** (2013). Fgf3 and Fgf10a work in concert to promote maturation of the epibranchial placodes in Zebrafish. *PLoS One* **8**, 1–13.

**McCarroll, M. N., Lewis, Z. R., Culbertson, M. D., Martin, B. L., Kimelman, D. and Nechiporuk, a. V.** (2012). Graded levels of Pax2a and Pax8 regulate cell differentiation during sensory placode formation. *Development* **139**, 2740–2750.

**McKeown, S. J., Lee, V. M., Bronner-Fraser, M., Newgreen, D. F. and Farlie, P. G.** (2005). Sox10 overexpression induces neural crest-like cells from all dorsoventral levels of the neural tube but inhibits differentiation. *Dev. Dyn.* **233**, 430–44.

**McLarren, K. W., Litsiou, A. and Streit, A.** (2003). DLX5 positions the neural crest and preplacode region at the border of the neural plate. *Dev. Biol.* **259**, 34–47.

**Meier, S.** (1981). Development of the chick embryo mesoblast: morphogenesis of the prechordal plate and cranial segments. *Dev. Biol.* **83**, 49–61.

**Mendonsa, E. S. and Riley, B. B.** (1999). Genetic analysis of tissue interactions required for otic placode induction in the zebrafish. *Dev. Biol.* **206**, 100–112.

**Millet, S., Campbell, K., Epstein, D. J., Losos, K., Harris, E. and Joyner, a L.** (1999). A role for Gbx2 in repression of Otx2 and positioning the mid/hindbrain organizer. *Nature* **401**, 161–164.

**Miyake, T., Von Herbing, I. H. and Hall, B. K.** (1997). Neural ectoderm, neural crest, and placodes: Contribution of the otic placode to the ectodermal lining of the embryonic opercular cavity in Atlantic Cod (Teleostei). *J. Morphol.* **231**, 231–252.

**Model, P. G., Jarrett, L. S. and Bonazzoli, R.** (1981). Cellular contacts between hindbrain and prospective ear during inductive interaction in the axolotl embryo. *J. Embryol. Exp. Morphol.* **66**, 27–41.

**Modrell, M. S. and Baker, C. V. H.** (2012). Evolution of electrosensory ampullary organs: Conservation of Eya4 expression during lateral line development in jawed vertebrates. *Evol. Dev.* **14**, 277–285.

**Mohammadi, M., McMahon, G., Sun, L., Tang, C., Hirth, P., Yeh, B. K., Hubbard, S. R. and Schlessinger, J.** (1997). Structures of the tyrosine kinase domain of fibroblast growth factor receptor in complex with inhibitors. *Science* **276**, 955–960.

**Monsoro-Burq, A. H., Wang, E. and Harland, R.** (2005). Msx1 and Pax3 cooperate to mediate FGF8 and WNT signals during Xenopus neural crest induction. *Dev. Cell* **8**, 167–178.

**Mortensen, a. H., Schade, V., Lamonerie, T. and Camper, S. a.** (2014). Deletion of OTX2 in neural ectoderm delays anterior pituitary development. *Hum. Mol. Genet.* **24**, 939–953.

**Moury, J. D. and Jacobson, a G.** (1990). The origins of neural crest cells in the axolotl. *Dev. Biol.* **141**, 243–253.

**Nechiporuk, A., Linbo, T., Poss, K. D. and Raible, D. W.** (2007). Specification of epibranchial placodes in zebrafish. *Development* **134**, 611–623.

**New, D.** (1955). A new technique for the cultivation of the chick embryo in vitro. *J. Embryol. Exp. Morphol.* **3**,.

**Nica, G., Herzog, W., Sonntag, C., Nowak, M., Schwarz, H., Zapata, A. G. and Hammerschmidt, M.** (2006). Eya1 is required for lineage-specific differentiation, but not for cell survival in the zebrafish adenohypophysis. *Dev. Biol.* **292**, 189–204.

**Nieuwkoop, P. D.** (1977). Chapter 4 Origin and Establishment of Embryonic Polar Axes in Amphibian Development. In (ed. Biology, A. A. M. and A. M. B. T.-C. T. in D.), pp. 115–132. Academic Press.

**Nissen, R. M.** (2003). Zebrafish foxi one modulates cellular responses to Fgf signaling required for the integrity of ear and jaw patterning. *Development* **130**, 2543–2554.

**Noden, D. M.** (1988). Interactions and fates of avian craniofacial mesenchyme. *Development* **103 Suppl**, 121–140.

**Noden, D. M. and Francis-West, P.** (2006). The differentiation and morphogenesis of craniofacial muscles. *Dev. Dyn.* **235**, 1194–1218.

**Noramly, S. and Grainger, R. M.** (2002). Determination of the embryonic inner ear. *J. Neurobiol.* **53**, 100–128.

**Nordström, U., Jessell, T. M. and Edlund, T.** (2002). Progressive induction of caudal neural character by graded Wnt signaling. *Nat. Neurosci.* **5**, 525–32.

**Northcutt, R. G. and Brandle, K.** (1995). Development of branchiomeric and lateral line nerves in the axolotl. *J. Comp. Neurol.* **355**, 427–454.

**Ochi, H., Tamai, T., Nagano, H., Kawaguchi, A., Sudou, N. and Ogino, H.** (2012). Evolution of a tissue-specific silencer underlies divergence in the expression of pax2 and pax8 paralogues. *Nat. Commun.* **3**, 848.

**Ogita, J., Isogai, E., Sudo, H., Sakiyama, S., Nakagawara, A. and Koseki, H.** (2001). Expression of the Dan gene during chicken embryonic development. *Mech. Dev.* **109**, 363–365.

**Ohto, H., Kamada, S., Tago, K., Tominaga, S. I., Ozaki, H., Sato, S. and Kawakami, K.** (1999). Cooperation of six and eya in activation of their target genes through nuclear translocation of Eya. *Mol. Cell. Biol.* **19**, 6815–6824.

**Ohyama, T. and Groves, A. K.** (2004). Generation of Pax2-Cre mice by modification of a Pax2 bacterial artificial chromosome. *Genesis* **38**, 195–9.

**Ohyama, T., Mohamed, O. a, Taketo, M. M., Dufort, D. and Groves, A. K.** (2006). Wnt signals mediate a fate decision between otic placode and epidermis. *Development* **133**, 865–75.

**Ohyama, T., Groves, A. K. and Martin, K.** (2007). The first steps towards hearing: mechanisms of otic placode induction. *Int. J. Dev. Biol.* **51**, 463–72.

**Oliver, G., Wehr, R., Jenkins, N. a, Copeland, N. G., Cheyette, B. N., Hartenstein, V., Zipursky, S. L. and Gruss, P.** (1995a). Homeobox genes and connective tissue patterning. *Development* **121**, 693–705.

**Oliver, G., Mailhos, A., Wehr, R., Copeland, N. G., Jenkins, N. A. and Gruss, P.** (1995b). Six3, a murine homologue of the sine oculis gene, demarcates the most anterior border of the developing neural plate and is expressed during eye development. *Development* **121**, 4045–4055.

**Padanad, M. S. and Riley, B. B.** (2011). Pax2/8 proteins coordinate sequential induction of otic and epibranchial placodes through differential regulation of foxi1, sox3 and fgf24. *Dev. Biol.* **351**, 90–98.

**Palmeirim, I., Henrique, D., Ish-Horowicz, D. and Pourquié, O.** (1997). Avian hairy gene expression identifies a molecular clock linked to vertebrate segmentation and somitogenesis. *Cell* **91**, 639–648.

**Pandur, P. D. and Moody, S. a** (2000). Xenopus Six1 gene is expressed in neurogenic cranial placodes and maintained in the differentiating lateral lines. *Mech. Dev.* **96**, 253–7.

**Parlier, D., Moers, V., Van Campenhout, C., Preillon, J., Leclère, L., Saulnier, A., Sirakov, M., Busengdal, H., Kricha, S., Marine, J. C., et al.** (2013). The Xenopus doublesex-related gene Dmrt5 is required for olfactory placode neurogenesis. *Dev. Biol.* **373**, 39–52.

**Patthey, C., Gunhaga, L. and Edlund, T.** (2008). Early development of the central and peripheral nervous systems is coordinated by Wnt and BMP signals. *PLoS One* **3**, 2–11.

**Paxton, C. N., Bleyl, S. B., Chapman, S. C. and Schoenwolf, G. C.** (2010). Identification of differentially expressed genes in early inner ear development. *Gene Expr. Patterns* **10**, 31–43.

**Pera, E. M. and Kessel, M.** (1997). Patterning of the chick forebrain anlage by the prechordal plate. *Development* **124**, 4153–62.

**Pera, E., Stein, S. and Kessel, M.** (1999). Ectodermal patterning in the avian embryo: epidermis versus neural plate. *Development* **126**, 63–73.

**Phillips, B. T., Bolding, K. and Riley, B. B.** (2001). Zebrafish fgf3 and fgf8 encode redundant functions required for otic placode induction. *Dev. Biol.* **235**, 351–365.

**Phillips, B. T., Storch, E. M., Lekven, A. C. and Riley, B. B.** (2004). A direct role for Fgf but not Wnt in otic placode induction. *Development* **131**, 923–931.

**Phillips, B. T., Kwon, H. J., Melton, C., Houghtaling, P., Fritz, A. and Riley, B. B.** (2006). Zebrafish msxB, msxC and msxE function together to refine the neural-nonneural border and regulate cranial placodes and neural crest development. *Dev. Biol.* **294**, 376–390.

**Piatigorsky, J.** (1998). Gene sharing in lens and cornea: Facts and implications. *Prog. Retin. Eye Res.* **17**, 145–174.

**Pieper, M., Eagleson, G. W., Wosniok, W. and Schlosser, G.** (2011). Origin and segregation of cranial placodes in Xenopus laevis. *Dev. Biol.* **360**, 257–75.

**Pieper, M., Ahrens, K., Rink, E., Peter, A. and Schlosser, G.** (2012). Differential distribution of competence for panplacodal and neural crest induction to non-neural and neural ectoderm. *Development* **139**, 1175–87.

**Pignoni, F., Hu, B., Zavitz, K. H., Xiao, J., Garrity, P. a and Zipursky, S. L.** (1997). The eye-specification proteins So and Eya form a complex and regulate multiple steps in Drosophila eye development. *Cell* **91**, 881–91.

**Pinho, S., Simonsson, P. R., Trevers, K. E., Stower, M. J., Sherlock, W. T., Khan, M., Streit, A., Sheng, G. and Stern, C. D.** (2011). Distinct steps of neural induction revealed by Asterix, Obelix and TrKC, genes induced by different signals from the organizer. *PLoS One* **6**,.

**Piotrowski, T. and Baker, C. V. H.** (2014). The development of lateral line placodes: Taking a broader view. *Dev. Biol.* **389**, 68–81.

**Popper, A. N., Ramcharitar, J. and Campana, S. E.** (2005). Why otoliths? Insights from inner ear physiology and fisheries biology. *Mar. Freshw. Res.* **56** , 497–504.

**Portales-Casamar, E., Thongjuea, S., Kwon, A. T., Arenillas, D., Zhao, X., Valen, E., Yusuf, D., Lenhard, B., Wasserman, W. W. and Sandelin, A.** (2009). JASPAR 2010: The greatly expanded open-access database of transcription factor binding profiles. *Nucleic Acids Res.* **38**, 105–110.

**Porter, F. D., Drago, J., Xu, Y., Cheema, S. S., Wassif, C., Huang, S. P., Lee, E., Grinberg, a, Massalas, J. S., Bodine, D., et al.** (1997). Lhx2, a LIM homeobox gene, is required for eye, forebrain, and definitive erythrocyte development. *Development* **124**, 2935–2944.

**Psychoyos, D. and Stern, C. D.** (1996). Fates and migratory routes of primitive streak cells in the chick embryo. *Development* **122**, 1523–1534.

**Quackenbush, J.** (2001). Quackenbush 2001. **2**, 418–427.

**Quinn, J. C., West, J. D. and Hill, R. E.** (1996). Multiple functions for Pax6 in mouse eye and nasal development. *Genes Dev.* **10**, 435–446.

**Redkar, a, Montgomery, M. and Litvin, J.** (2001). Fate map of early avian cardiac progenitor cells. *Development* **128**, 2269–2279.

**Reijntjes, S., Gale, E. and Maden, M.** (2004). Generating gradients of retinoic acid in the chick embryo: Cyp26C1 expression and a comparative analysis of the Cyp26 enzymes. *Dev. Dyn.* **230**, 509–517.

**Rex, M., Orme, A., Uwanogho, D., Tointon, K., Wigmore, P. M., Sharpe, P. T. and Scotting, P. J.** (1997). Dynamic expression of chicken Sox2 and Sox3 genes in ectoderm induced to form neural tissue. *Dev. Dyn.* **209**, 323–332.

**Rodríguez Esteban, C., Capdevila, J., Economides, a N., Pascual, J., Ortiz, a and Izpisúa Belmonte, J. C.** (1999). The novel Cer-like protein Caronte mediates the establishment of embryonic left-right asymmetry. *Nature* **401**, 243–251.

**Roehl, H. and Nüsslein-Volhard, C.** (2001). Zebrafish pea3 and erm are general targets of FGF8 signaling. *Curr. Biol.* **11**, 503–507.

**Rogers, C. D., Jayasena, C. S., Nie, S. and Bronner, M. E.** (2012). Neural crest specification: tissues, signals, and transcription factors. *Wiley Interdiscip. Rev. Dev. Biol.* **1**, 52–68.

**Ruben, R. J.** (1973). Development and cell kinetics of the kreisler (kr/kr) mouse. *Laryngoscope* **83**, 1440–1468.

**Rudnick, D.** (1935). Regional restriction of potencies in the chick during embryogenesis. *J. Exp. Zool.* **71**, 83–99.

**Ruf, R. G., Xu, P.-X., Silvius, D., Otto, E. a, Beekmann, F., Muerb, U. T., Kumar, S., Neuhaus, T. J., Kemper, M. J., Raymond, R. M., et al.** (2004). SIX1 mutations cause branchio-oto-renal syndrome by disruption of EYA1-SIX1-DNA complexes. *Proc. Natl. Acad. Sci. U. S. A.* **101**, 8090–5.

**Sabado, V., Barraud, P., Baker, C. V. H. and Streit, A.** (2012). Specification of GnRH-1 neurons by antagonistic FGF and retinoic acid signaling. *Dev. Biol.* **362**, 254–262.

**Sadl, V. S., Sing, A., Mar, L., Jin, F. and Cordes, S. P.** (2003). Analysis of hindbrain patterning defects caused by the kreislerenu mutation reveals multiple roles of Kreisler in hindbrain segmentation. *Dev. Dyn.* **227**, 134–142.

**Sahly, I., Andermann, P. and Petit, C.** (1999). The zebrafish eya1 gene and its expression pattern during embryogenesis. *Dev. Genes Evol.* **209**, 399–410.

**Sanchez-Arrones, L., Stern, C. D., Bovolenta, P. and Puelles, L.** (2012). Sharpening of the anterior neural border in the chick by rostral endoderm signalling. *Development* **139**, 1034–44.

**Sater, a K. and Jacobson, a G.** (1989). The specification of heart mesoderm occurs during gastrulation in Xenopus laevis. *Development* **105**, 821–830.

**Sato, S., Ikeda, K., Shioi, G., Ochi, H., Ogino, H., Yajima, H. and Kawakami, K.** (2010). Conserved expression of mouse Six1 in the pre-placodal region (PPR) and identification of an enhancer for the rostral PPR. *Dev. Biol.* **344**, 158–71.

**Sato, S., Ikeda, K., Shioi, G., Nakao, K., Yajima, H. and Kawakami, K.** (2012). Regulation of Six1 expression by evolutionarily conserved enhancers in tetrapods. *Dev. Biol.* **368**, 95–108.

**Schimmang, T.** (2007). Expression and functions of FGF ligands during early otic development. *Int. J. Dev. Biol.* **51**, 473–481.

**Schlosser, G.** (2003). Hypobranchial placodes in Xenopus laevis give rise to hypobranchial ganglia, a novel type of cranial ganglia. *Cell Tissue Res.* **312**, 21–29.

**Schlosser, G.** (2006). Induction and specification of cranial placodes. *Dev. Biol.* **294**, 303–51.

**Schlosser, G.** (2010). *Making senses development of vertebrate cranial placodes.* 1st ed. Elsevier Inc.

**Schlosser, G. and Ahrens, K.** (2004). Molecular anatomy of placode development in Xenopus laevis. *Dev. Biol.* **271**, 439–466.

**Schlosser, G. and Northcutt, R. G.** (2000). Development of neurogenic placodes in Xenopus laevis. *J. Comp. Neurol.* **418**, 121–146.

**Schlosser, G., Awtry, T., Brugmann, S. a, Jensen, E. D., Neilson, K., Ruan, G., Stammler, A., Voelker, D., Yan, B., Zhang, C., et al.** (2008). Eya1 and Six1 promote neurogenesis in the cranial placodes in a SoxB1-dependent fashion. *Dev. Biol.* **320**, 199–214.

**Schoenwolf, G. C., Garcia-Martinez, V. and Dias, M. S.** (1992). Mesoderm movement and fate during avian gastrulation and neurulation. *Dev. Dyn.* **193**, 235–48.

**Schonberger, J., Wang, L., Shin, J. T., Kim, S. Do, Depreux, F. F. S., Zhu, H., Zon, L., Pizard, A., Kim, J. B., MacRae, C. A., et al.** (2005). Mutation in the transcriptional coactivator EYA4 causes dilated cardiomyopathy and sensorineural hearing loss. *Nat Genet* **37**, 418–422.

**Seifert, R., Jacob, M. and Jacob, H. J.** (1993). The avian prechordal head region: a morphological study. *J. Anat.* **183 ( Pt 1**, 75–89.

**Seimiya, M. and Gehring, W. J.** (2000). The Drosophila homeobox gene optix is capable of inducing ectopic eyes by an eyeless-independent mechanism. *Development* **127**, 1879–1886.

**Selleck, M. a and Bronner-Fraser, M.** (1995). Origins of the avian neural crest: the role of neural plate-epidermal interactions. *Development* **121**, 525–38.

**Selleck, M. a J. and Stern, C. D.** (1992). Commitment of mesoderm cells in Hensen's node of the to notochord and somite. *Development* **114**, 403–415.

**Seo, H. C., Drivenes, Ø., Ellingsen, S. and Fjose, A.** (1998a). Expression of two zebrafish homologues of the murine Six3 gene demarcates the initial eye primordia. *Mech. Dev.* **73**, 45–57.

**Seo, H. C., Drivenes, O., Ellingsen, S. and Fjose, A.** (1998b). Transient expression of a novel Six3-related zebrafish gene during gastrulation and eye formation. *Gene* **216**, 39–46.

**Seo, H. C., Curtiss, J., Mlodzik, M. and Fjose, A.** (1999). Six class homeobox genes in Drosophila belong to three distinct families and are involved in head development. *Mech. Dev.* **83**, 127–139.

**Servetnick, M. and Grainger, R. M.** (1991). Changes in neural and lens competence in Xenopus ectoderm: evidence for an autonomous developmental timer. *Development* **112**, 177–188.

**Shamim, H. and Mason, I.** (1999). Expression of Gbx2 during early development of the chick embryo. *Mech. Dev.* **85**, 189–192.

**Sheng, G. and Stern, C. D.** (1999). Gata2 and Gata3: novel markers for early embryonic polarity and for non-neural ectoderm in the chick embryo. *Mech. Dev.* **87**, 213–6.

**Shou, J., Murray, R. C., Rim, P. C. and Calof, a L.** (2000). Opposing effects of bone morphogenetic proteins on neuron production and survival in the olfactory receptor neuron lineage. *Development* **127**, 5403–5413.

**Silver, S. J., Davies, E. L., Doyon, L. and Rebay, I.** (2003). Functional Dissection of Eyes absent Reveals New Modes of Regulation within the Retinal Determination Gene Network Functional Dissection of Eyes absent Reveals New Modes of Regulation within the Retinal Determination Gene Network. *Mol. Cell. Biol.* **23**, 5989–5999.

**Simeone, a, Acampora, D., Gulisano, M., Stornaiuolo, a and Boncinelli, E.** (1992). Nested expression domains of four homeobox genes in developing rostral brain. *Nature* **358**, 687–690.

**Simpson, A., Moss, D. and Slingsby, C.** (1995). The avian eye lens protein delta-crystallin shows a novel packing arrangement of tetramers in a supramolecular helix. *Structure* **3**, 403–412.

**Simrick, S., Lickert, H. and Basson, M. A.** (2011). Sprouty genes are essential for the normal development of epibranchial ganglia in the mouse embryo. *Dev. Biol.* **358**, 147–155.

**Sjödal, M., Edlund, T. and Gunhaga, L.** (2007). Time of Exposure to BMP Signals Plays a Key Role in the Specification of the Olfactory and Lens Placodes Ex Vivo. *Dev. Cell* **13**, 141–149.

**Skromne, I. and Stern, C. D.** (2001). Interactions between Wnt and Vg1 signalling pathways initiate primitive streak formation in the chick embryo. *Development* **128**, 2915–2927.

**Smith, A. N., Miller, L. A. D., Song, N., Taketo, M. M. and Lang, R. a.** (2005). The duality of β-catenin function: A requirement in lens morphogenesis and signaling suppression of lens fate in periocular ectoderm. *Dev. Biol.* **285**, 477–489.

**Smith, A. N., Radice, G. and Lang, R. a.** (2010). Which FGF ligands are involved in lens induction? *Dev. Biol.* **337**, 195–198.

**Solomon, K. S.** (2003). Zebrafish foxi1 mediates otic placode formation and jaw development. *Development* **130**, 929–940.

**Solomon, K. S. and Fritz, A.** (2002). Concerted action of two dlx paralogs in sensory placode formation. *Development* **129**, 3127–3136.

**Spemann, H.** (1901). Uber Korrelationen in der Entwicklung des Auges.

**Stark, M. R., Sechrist, J., Bronner-Fraser, M. and Marcelle, C.** (1997). Neural tube-ectoderm interactions are required for trigeminal placode formation. *Development* **124**, 4287–4295.

**Stathopoulos, A. and Levine, M.** (2005). Genomic regulatory networks and animal development. *Dev. Cell* **9**, 449–462.

**Stern, C. D.** (1990). The marginal zone and its contribution to the hypoblast and primitive streak of the chick embryo. *Development* **109**, 667–682.

**Stern, C. and Downs, K.** (2012). The hypoblast (visceral endoderm): an evo-devo perspective. **1069**, 1059–1069.

**Stern, C. D. and Ireland, G. W.** (1981). An integrated experimental study of endoderm formation in avian embryos. *Anat. Embryol. (Berl).* **163**, 245–263.

**Steventon, B., Mayor, R. and Streit, A.** (2012). Mutual repression between Gbx2 and Otx2 in sensory placodes reveals a general mechanism for ectodermal patterning. *Dev. Biol.* **367**, 55–65.

**Steventon, B., Mayor, R. and Streit, A.** (2014). Neural crest and placode interaction during the development of the cranial sensory system. *Dev. Biol.* **389**, 28–38.

**Stone, L. S.** (1924). Experiments on the transplantation of placodes of the cranial ganglia in the amphibian embryo. I. Heterotopic transplantations of the ophthalmic placode upon the head of Amblystoma punctatum. *J. Comp. Neurol.* **38**, 73–105.

**Stone, L. S.** (1928). Experiments on the transplantation of placodes of the cranial ganglia in the amphibian embryo. II. Heterotopic transplantations of the ophthalmic placode upon the head and body of amblystoma punctatum. *J. Comp. Neurol.* **47**, 91–116.

**Stone, L. S.** (1931). Induction of the ear by medulla and its relation to experiments on the lateralis system in amphibia. Scienc. *Science (80-. ).* **74**, 577.

**Streit, A.** (2002). Extensive Cell Movements Accompany Formation of the Otic Placode. *Dev. Biol.* **249**, 237–254.

**Streit, A.** (2004). Early development of the cranial sensory nervous system: from a common field to individual placodes. *Dev. Biol.* **276**, 1–15.

**Streit, A.** (2007). The preplacodal region: an ectodermal domain with multipotential progenitors that contribute to sense organs and cranial sensory ganglia. *Int. J. Dev. Biol.* **51**, 447–61.

**Streit, a and Stern, C. D.** (1999). Establishment and maintenance of the border of the neural plate in the chick: involvement of FGF and BMP activity. *Mech. Dev.* **82**, 51–66.

**Streit, A., Sockanathan, S., Pérez, L., Rex, M., Scotting, P. J., Sharpe, P. T., Lovell-badge, R. and Stern, C. D.** (1997). Preventing the loss of competence for neural induction : HGF / SF , L5 and Sox-2. **1202**, 1191–1202.

**Streit, a, Lee, K. J., Woo, I., Roberts, C., Jessell, T. M. and Stern, C. D.** (1998). Chordin regulates primitive streak development and the stability of induced neural cells, but is not sufficient for neural induction in the chick embryo. *Development* **125**, 507–19.

**Streit, a, Berliner, a J., Papanayotou, C., Sirulnik, a and Stern, C. D.** (2000). Initiation of neural induction by FGF signalling before gastrulation. *Nature* **406**, 74–78.

**Stricker, S., Brieske, N., Haupt, J. and Mundlos, S.** (2006). Comparative expression pattern of Odd-skipped related genes Osr1 and Osr2 in chick embryonic development. *Gene Expr. Patterns* **6**, 826–834.

**Stuhlmiller, T. J. and García-Castro, M. I.** (2012). FGF/MAPK signaling is required in the gastrula epiblast for avian neural crest induction. *Development* **139**, 289–300.

**Sun, S. K., Dee, C. T., Tripathi, V. B., Rengifo, A., Hirst, C. S. and Scotting, P. J.** (2007). Epibranchial and otic placodes are induced by a common Fgf signal, but their subsequent development is independent. *Dev. Biol.* **303**, 675–686.

**Suzuki, a, Ueno, N. and Hemmati-Brivanlou, a** (1997). Xenopus msx1 mediates epidermal induction and neural inhibition by BMP4. *Development* **124**, 3037–3044.

**Szeto, D. P., Rodriguez-Esteban, C., Ryan, A. K., O'Connell, S. M., Liu, F., Kioussi, C., Gleiberman, A. S., Izpisúa-Belmonte, J. C. and Rosenfeld, M. G.** (1999). Role of the Bicoid-related homeodomain factor Pitx1 in specifying hindlimb morphogenesis and pituitary development. *Genes Dev.* **13**, 484–494.

**Tadjuidje, E. and Hegde, R. S.** (2013). The Eyes Absent proteins in development and disease. *Cell. Mol. Life Sci.* **70**, 1897–913.

**Tambalo, M.** (2014). Towards a gene regulatory network for otic and epibranchial specification. *KCL (King's Coll. London)*.

**Tan, J., Yan, Y., Wang, X., Jiang, Y. and Xu, H. E.** (2013). EZH2: biology, disease, and structure-based drug discovery. *Acta Pharmacol. Sin.* **35**, 161–174.

**Tang, H. K., Chao, L. Y. and Saunders, G. F.** (1997). Functional analysis of paired box missense mutations in the PAX6 gene. *Hum. Mol. Genet.* **6**, 381–386.

**Tomarev, S. I. and Piatigorsky, J.** (1996). Lens crystallins of invertebrates--diversity and recruitment from detoxification enzymes and novel proteins. *Eur. J. Biochem.* **235**, 449–465.

**Tonegawa, a and Takahashi, Y.** (1998). Somitogenesis controlled by Noggin. *Dev. Biol.* **202**, 172–182.

**Tootle, T. L., Silver, S. J., Davies, E. L., Newman, V., Latek, R. R., Mills, I. A., Selengut, J. D., Parlikar, B. E. W. and Rebay, I.** (2003). The transcription factor Eyes absent is a protein tyrosine phosphatase. *Nature* **426**, 299–302.

**Torres, M. and Giráldez, F.** (1998). The development of the vertebrate inner ear. *Mech. Dev.* **71**, 5–21.

**Torres, M., Gómez-Pardo, E. and Gruss, P.** (1996). Pax2 contributes to inner ear patterning and optic nerve trajectory. *Development* **122**, 3381–3391.

**Tour, E., Pillemer, G., Gruenbaum, Y. and Fainsod, A.** (2002). Gbx2 interacts with Otx2 and patterns the anterior-posterior axis during gastrulation in Xenopus. *Mech. Dev.* **112**, 141–151.

**Toy, J., Yang, J. M., Leppert, G. S. and Sundin, O. H.** (1998). The optx2 homeobox gene is expressed in early precursors of the eye and activates retina-specific genes. *Proc. Natl. Acad. Sci. U. S. A.* **95**, 10643–10648.

**Trainor, P. a** (2003). Making headway: the roles of Hox genes and neural crest cells in craniofacial development. *ScientificWorldJournal.* **3**, 240–264.

**Trevers, K. E.** (2015). A Cascade of Molecular Events During Neural Induction. *UCl (University Coll. London)*.

**Vendrell, V., Carnicero, E., Giraldez, F., Alonso, M. T. and Schimmang, T.** (2000). Induction of inner ear fate by FGF3. *Development* **127**, 2011–2019.

**Verwoerd, C. D. and van Oostrom, C. G.** (1979). Cephalic neural crest and placodes. *Adv. Anat. Embryol. Cell Biol.* **58**, 1–75.

**Villanueva, S., Glavic, A., Ruiz, P. and Mayor, R.** (2002). Posteriorization by FGF, Wnt, and retinoic acid is required for neural crest induction. *Dev. Biol.* **241**, 289–301.

**Vogel, K. S. and Davies, a M.** (1993). Heterotopic transplantation of presumptive placodal ectoderm changes the fate of sensory neuron precursors. *Development* **119**, 263–276.

**Waddington, C. C. a** (1936). Experiments on the development of the head of the chick embryo. *J. Exp. Biol.* **13**, 219–236.

**Waddington, C. H.** (1937). The determination of the auditory placode in the chick. *J. Exp. Biol.* 232–239.

**Wakamatsu, Y.** (2011). Mutual repression between Pax3 and Pax6 is involved in the positioning of ophthalmic trigeminal placode in avian embryo. *Dev. Growth Differ.* **53**, 994–1003.

**Wawersik, S., Purcell, P., Rauchman, M., Dudley, a T., Robertson, E. J. and Maas, R.** (1999). BMP7 acts in murine lens placode development. *Dev. Biol.* **207**, 176–188.

**Wawersik, S., Evola, C. and Whitman, M.** (2005). Conditional BMP inhibition in Xenopus reveals stage-specific roles for BMPs in neural and neural crest induction. *Dev. Biol.* **277**, 425–442.

**Wayne, S., Robertson, N. G., DeClau, F., Chen, N., Verhoeven, K., Prasad, S., Tranebjärg, L., Morton, C. C., Ryan, a F., Van Camp, G., et al.** (2001). Mutations in the transcriptional activator EYA4 cause late-onset deafness at the DFNA10 locus. *Hum. Mol. Genet.* **10**, 195–200.

**Weasner, B., Salzer, C. and Kumar, J. P.** (2007). Sine oculis, a member of the SIX family of transcription factors, directs eye formation. *Dev. Biol.* **303**, 756–771.

**Webb, J. F. and Noden, D. M.** (1993). Ectodermal Placodes Contributions to the Development of the Vertebrate Head. *Integr. Comp. Biol.* **33**, 434–447.

**Weinstein, D. C. and Hemmati-Brivanlou, A.** (1999). Neural induction. *Annu. Rev. Cell Dev. Biol.* **15**, 411–433.

**Weisstein, E. W.** (2002). *CRC concise encyclopedia of mathematics*. CRC press.

**Williams, S. C., Altmann, C. R., Chow, R. L., Hemmati-Brivanlou, A. and Lang, R. a.** (1998). A highly conserved lens transcriptional control element from the Pax-6 gene. *Mech. Dev.* **73**, 225–229.

**Wilson, P. a and Hemmati-Brivanlou, a** (1995). Induction of epidermis and inhibition of neural fate by Bmp-4. *Nature* **376**, 331–333.

**Wilson, P. a, Lagna, G., Suzuki, a and Hemmati-Brivanlou, a** (1997). Concentration-dependent patterning of the Xenopus ectoderm by BMP4 and its signal transducer Smad1. *Development* **124**, 3177–3184.

**Wilson, S. I., Graziano, E., Harland, R., Jessell, T. M. and Edlund, T.** (2000). An early requirement for FGF signalling in the acquisition of neural cell fate in the chick embryo. *Curr. Biol.* **10**, 421–429.

**Wilson, S. I., Rydström, a, Trimborn, T., Willert, K., Nusse, R., Jessell, T. M. and Edlund, T.** (2001). The status of Wnt signalling regulates neural and epidermal fates in the chick embryo. *Nature* **411**, 325–330.

**Winchester, C. L., Ferrier, R. K., Sermoni, a, Clark, B. J. and Johnson, K. J.** (1999). Characterization of the expression of DMPK and SIX5 in the human eye and implications for pathogenesis in myotonic dystrophy. *Hum. Mol. Genet.* **8**, 481–492.

**Wingender, E., Chen, X., Hehl, R., Karas, H., Liebich, I., Matys, V., Meinhardt, T., Prüss, M., Reuter, I. and Schacherer, F.** (2000). TRANSFAC: an integrated system for gene expression regulation. *Nucleic Acids Res.* **28**, 316–319.

**Woda, J. M., Pastagia, J., Mercola, M. and Artinger, K. B.** (2003). Dlx proteins position the neural plate border and determine adjacent cell fates. *Development* **130**, 331–342.

**Woo, K. and Fraser, S. E.** (1997). Specification of the zebrafish nervous system by nonaxial signals. *Science* **277**, 254–257.

**Wright, T. J. and Mansour, S. L.** (2003). Fgf3 and Fgf10 are required for mouse otic placode induction. *Development* **130**, 3379–3390.

**Xu, P. X., Woo, I., Her, H., Beier, D. R. and Maas, R. L.** (1997). Mouse Eya homologues of the Drosophila eyes absent gene require Pax6 for expression in lens and nasal placode. *Development* **124**, 219–231.

**Xu, P. X., Adams, J., Peters, H., Brown, M. C., Heaney, S. and Maas, R.** (1999). Eya1-deficient mice lack ears and kidneys and show abnormal apoptosis of organ primordia. *Nat. Genet.* **23**, 113–117.

**Xu, P.-X., Zheng, W., Huang, L., Maire, P., Laclef, C. and Silvius, D.** (2003). Six1 is required for the early organogenesis of mammalian kidney. *Development* **130**, 3085–3094.

**Xu, H., Dude, C. M. and Baker, C. V. H.** (2008). Fine-grained fate maps for the ophthalmic and maxillomandibular trigeminal placodes in the chick embryo. *Dev. Biol.* **317**, 174–86.

**Yamada, M., Revelli, J. P., Eichele, G., Barron, M. and Schwartz, R. J.** (2000). Expression of chick Tbx-2, Tbx-3, and Tbx-5 genes during early heart development: evidence for BMP2 induction of Tbx2. *Dev. Biol.* **228**, 95–105.

**Yamamoto, C., Fukuda, N., Matsumoto, T., Higuchi, T., Ueno, T. and Matsumoto, K.** (2010). Zinc-finger transcriptional factor Sall1 induces angiogenesis by activation of the gene for VEGF-A. *Hypertens. Res.* **33**, 143–148.

**Yardley, N. and García-Castro, M. I.** (2012). FGF signaling transforms non-neural ectoderm into neural crest. *Dev. Biol.* **372**, 166–177.

**Yuan, S. and Schoenwolf, G. C.** (2000). Islet-1 marks the early heart rudiments and is asymmetrically expressed during early rotation of the foregut in the chick embryo. *Anat. Rec.* **260**, 204–207.

**Zheng, W., Huang, L., Wei, Z.-B., Silvius, D., Tang, B. and Xu, P.-X.** (2003). The role of Six1 in mammalian auditory system development. *Development* **130**, 3989–4000.

**Zou, D., Silvius, D., Fritzsch, B. and Xu, P.-X.** (2004). Eya1 and Six1 are essential for early steps of sensory neurogenesis in mammalian cranial placodes. *Development* **131**, 5561–5572.

**Zou, D., Silvius, D., Rodrigo-Blomqvist, S., Enerbäck, S. and Xu, P.-X.** (2006). Eya1 regulates the growth of otic epithelium and interacts with Pax2 during the development of all sensory areas in the inner ear. *Dev. Biol.* **298**, 10.1016/j.ydbio.2006.06.049.

**Zuber, M. E., Perron, M., Philpott, A., Bang, A. and Harris, W. a.** (1999). Giant eyes in Xenopus laevis by overexpression of XOptx2. *Cell* **98**, 341–352.

**Zygar, C. a, Cook, T. L. and Grainger, R. M.** (1998). Gene activation during early stages of lens induction in Xenopus. *Development* **125**, 3509–3519.

# 9 Appendix

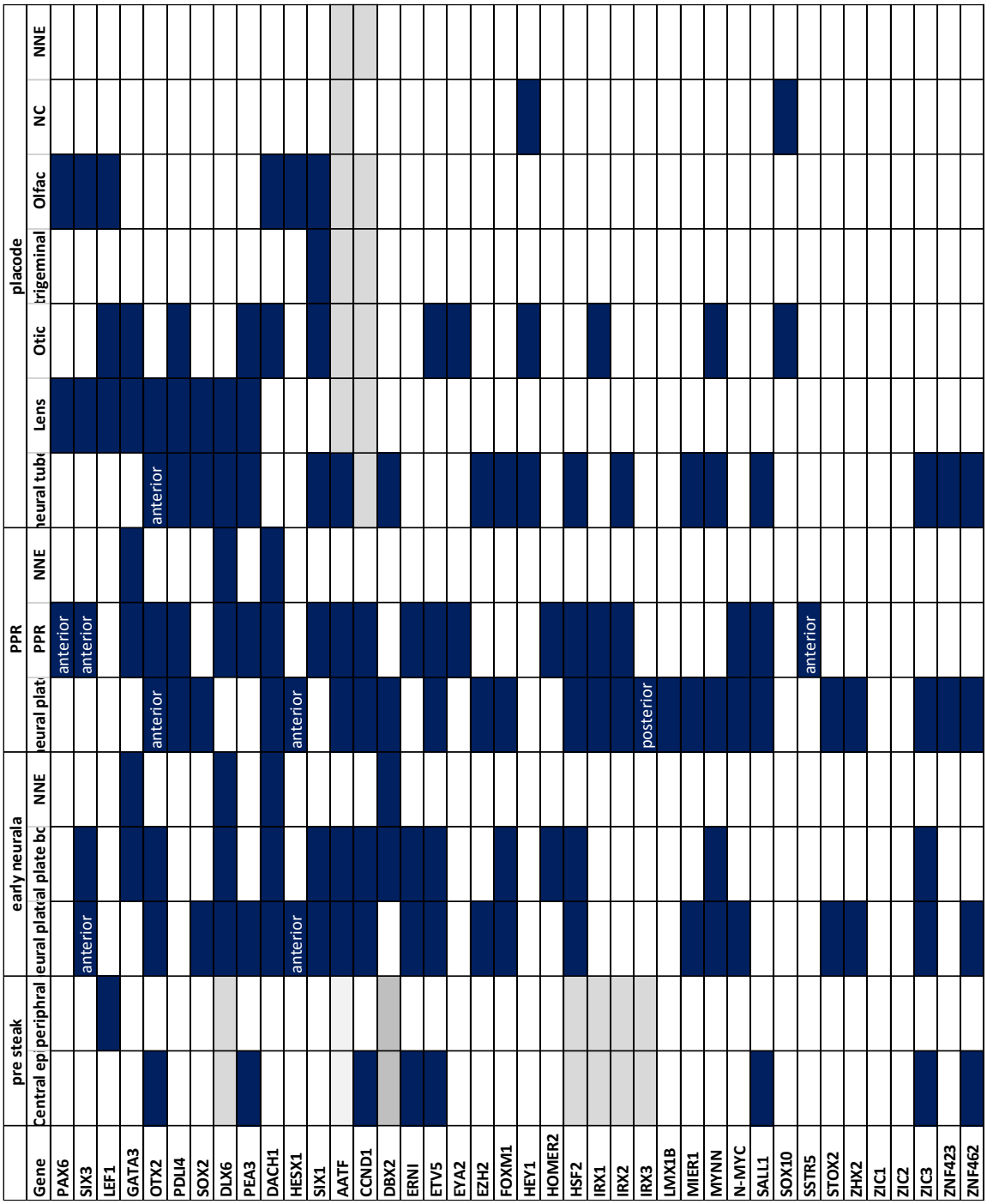


**Appendix 9.1: Map of known expression patterns for statistically significant gene at; pre-streak, early neurula (HH6); placode stage (HH10); blue = expressed, white = not expressed, grey = unknown**

```
#Specify row name.
row.names(data2)<-Data$Gene
#Convert to a data matrix
A<-data.matrix(data2)
hr <- hclust(as.dist(1-cor(t(A), method="spearman")), method="complete"); hc <- hclust(as.dist(1-cor(A, method="spearman")), method="complete")
# Generates row and column dendrograms.
mycl <- cutree(hr, h=max(hr$height)/3); mycolhc <- rainbow(length(unique(mycl)), start=0.1, end=0.9); mycolhc <- mycolhc[as.vector(mycl)]
# Cuts the tree and creates color vector for clusters.
library(gplots); myheatcol <- colorpanel(100, "purple", "gray", "yellow")
# Assign your favorite heatmap color scheme. Some useful examples: colorpanel(40,"black" "darkblue","gray", "yellow");
# heat.colors(75); cm.colors(75); rainbow(75); redgreen(75); library(RColorBrewer); rev(brewer.pal(9,"Blues")[-1]).
# Type demo.col(20) to see more color schemes.
heatmap.2(A, Rowv=as.dendrogram(hr), Colv=as.dendrogram(hc), col=myheatcol, scale="row", density.info="none", trace="none", RowSideColors=mycolhc)
# Creates heatmap for entire data set where the obtained clusters are indicated in the color bar.
x11(height=6, width=2); names(mycolhc) <- names(mycl); barplot(rep(10, max(mycl)), col=unique(mycolhc[hr$labels[hr$order]]), horiz=T, names=unique(mycl[hr$order]))
# Prints color key for cluster assignments. The numbers next to the color boxes correspond to the cluster numbers in 'mycl'.
clid <- c(7); Asub <- A[names(mycl[mycl%in%clid]),]; hrsub <- hclust(as.dist(1-cor(t(Asub), method="spearman")), method="complete")
# Select sub-cluster number (here: clid=c(1,2)) and generate corresponding dendrogram.
x11(); heatmap.2(Asub, Rowv=as.dendrogram(hrsub), Colv=as.dendrogram(hc), col=myheatcol, scale="row", density.info="none", trace="none", RowSideColors=mycolhc[mycl%in%clid])
# Create heatmap for chosen sub-cluster.
B<-data.frame(GeneID=rev(hrsub$labels[hrsub$order]))
# Print out row labels in same order as shown in the heatmap.
write.table(B, "Cluster7.csv", sep=",", row.names=FALSE,col.names=TRUE , append=TRUE)
#Below is a script fpr matching and extracting genes....to pair them with values from the input file
L1<-read.csv("neural plate.csv", sep=",", header=T)
L2<-read.csv("Probes.csv", sep=",",header=T)
input<-(L1)
lib<-(L2)
input_df = as.data.frame(input)
lib_df = as.data.frame(lib)
input_in_lib = input_df$Gene%in% lib_df[,1]
input_in_lib_df = input_df[input_in_lib,]
head(input_in_lib_df)
write.table(input_in_lib_df, "np_extracted.csv", sep=",", row.names=FALSE, col.names=T, append=TRUE)
```

**Appendix 9.2 Clustering and heatmap code: used to generate heatmaps in R-studio**

| | | | | |
|---|---|---|---|---|
| AATF | ETV5 | IRX1 | PCNA | TBL1XR1 |
| ADNP2 | EYA1 | IRX2 | PDLIM4 | TBX1 |
| AP-2 | EYA2 | IRX3 | PEA3 | TBX2 |
| AXIN2 | EZH2 | KERATIN 1 | PHF10 | TBX3 |
| BCL11A | FGF3 | klf4 | PHF20 | TGIF2 |
| BCL2 | FOLLISTA | KREMEN | PNOC | TOX3 |
| BCL7A | FOXG1 | LEF1 | POGZ | TP53 |
| Blimp1 | FOXI1 | LMX1A | PSIP1 | TRIM24 |
| BMP4 | FOXI3 | LMX1B | ripplya3 | WHSC1 |
| CCND1 | FOXM1 | LRP11 | RRN3 | YEATS4 |
| CDKN1B | FOXN2 | LZTR1 | RX1 | ZFHX1B |
| CHD7 | fzd7 | MEF2D | RYBP | ZHX2 |
| CITED2 | GAPDH | meis 1 | SALL1 | ZIC1 |
| CNTNAP5 | GATA2 | MIER1 | SALL4 | ZIC2 |
| CXCl14 | GATA3 | MLLT10 | SDHA | ZIC3 |
| CXXC6 like | GBX2 | MORC2 | SETD2 | ZNF217 |
| Cyp26A | GEMININ | MSX1 | SIX1 | ZNF423 |
| Cyp26C1 | Hand1 | MTA3 | Six2 | ZNF462 |
| DACH1 | HDAC1 | Myb | SIX3 | |
| DBX2 | HESX1 | MYNN | SIX4 | |
| DLX3 | HEY1 | NFKB1 | SMAD6 | |
| DLX5 | HEY2 | Nkx6.2 | Snail 2 | |
| DLX6 | HIF1A | N-MYC | SOX10 | |
| DNAJC1 | HMGXB4 | NPAS3 | SOX2 | |
| DNMT3A | HMX3 | NSD1 | SOX3 | |
| DNMT3B | HOMER2 | OTX2 | SOX9 | |
| E2F8 | HPRT1 | patched 1 | SP4 | |
| ECE1 | HSF2 | PAX2 | SPRY1 | |
| EEF1A1 | Id1 | PAX3 | SPRY2 | |
| en2 | Id2 | PAX6 | SSTR5 | |
| ERNI | ING5 | PAX7 | STOX2 | |

**Appendix 9.3 List of genes used in NanoString probeset**

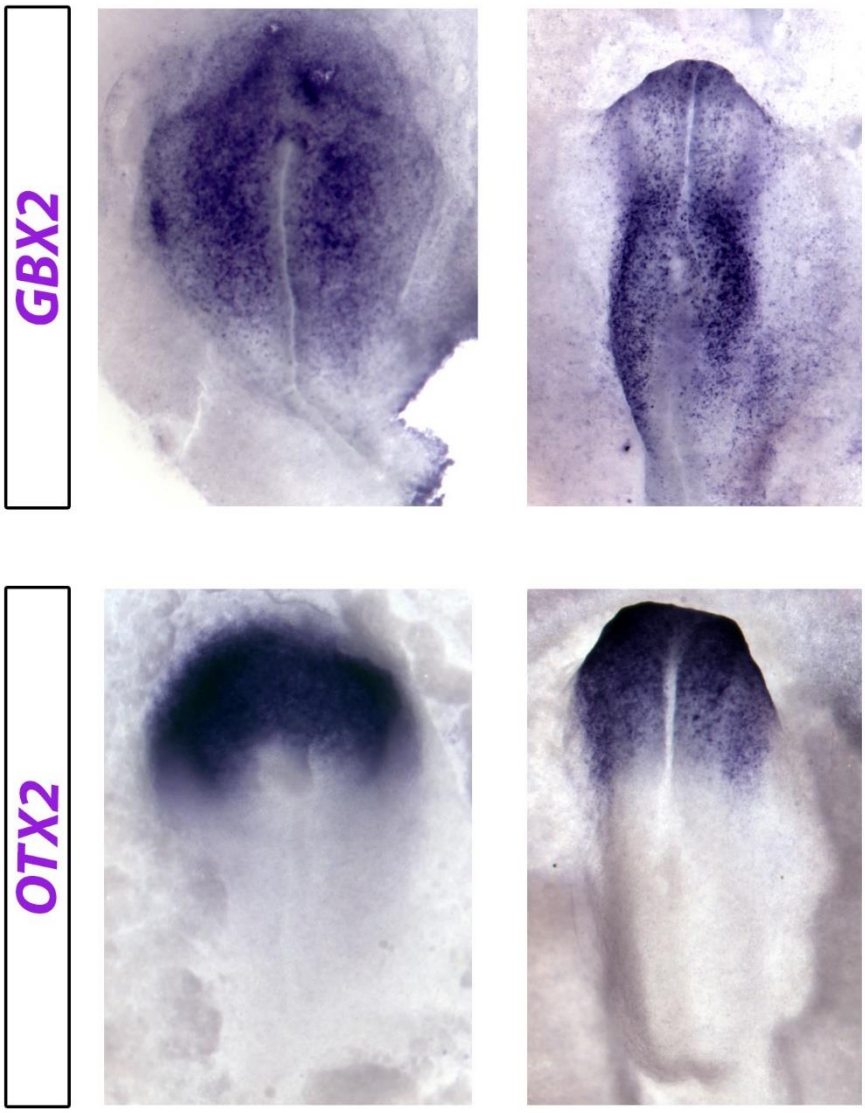


**Appendix 9.4**

**Insitu hybridisation of *Otx2* and *Gbx2* (Blue), displaying early overlapping domains at HH4, before becoming refined into anterior and posterior expression domains respectively.**

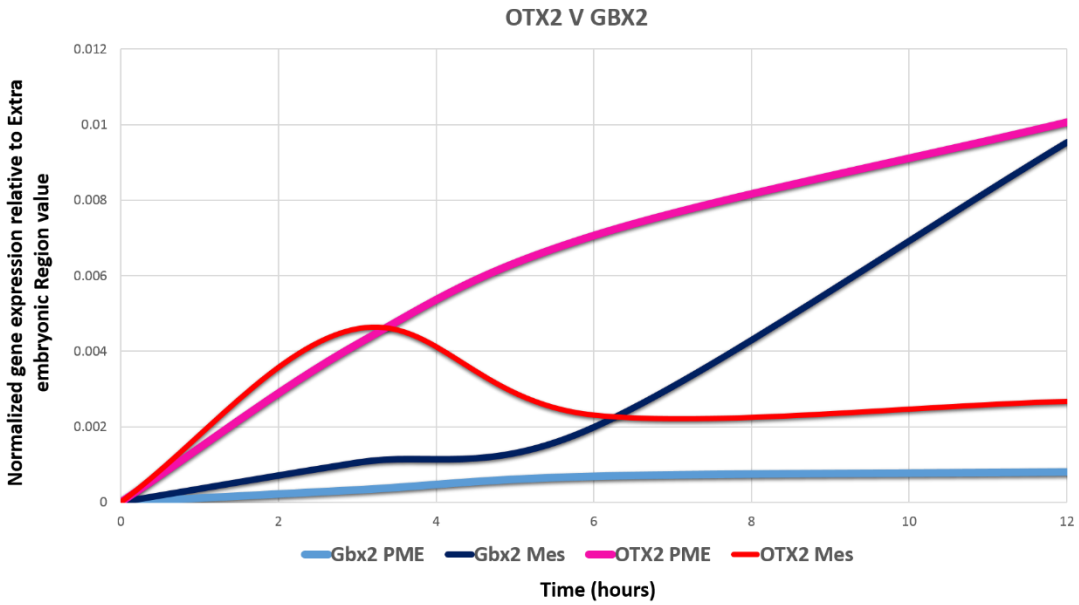


**Appendix 9.5**

**Normalised mean expression of Otx2 and Gbx2 plotted as a curve against time for the lHM (Otx2, Red; Gbx2, Dark blue) and pME (Otx2, Pink; Gbx2 Light blue). The expression of OTx2 and Gbx2 mirror the embryonic overlap at early stages before becoming refined to the anterior (Otx2, pME) or posterior (Gbx2, lHM) conditions.**

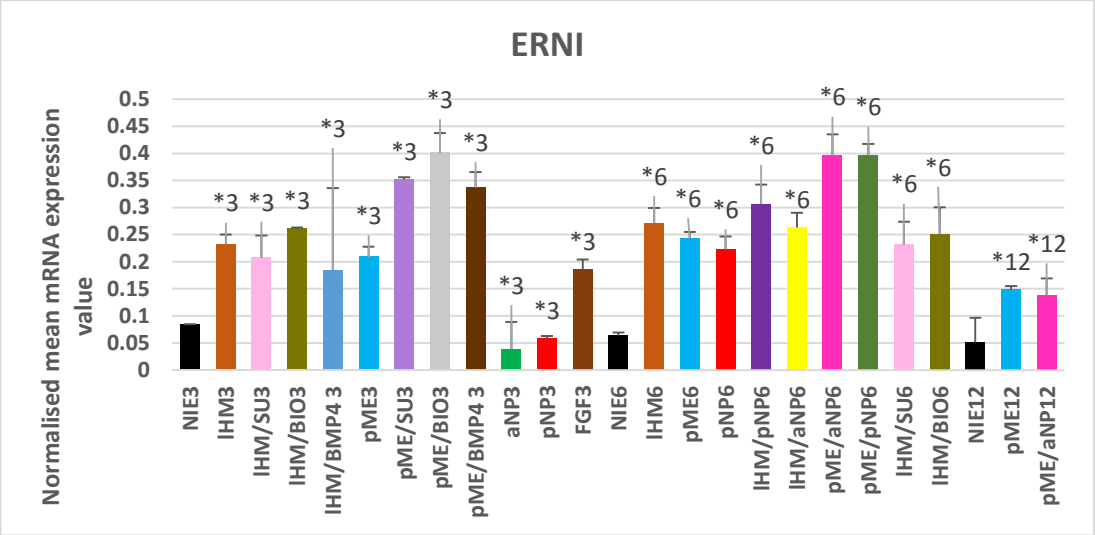


**Appendix 9.6**

**Bar chart showing experiments at which time points *ERNI* is significant when compared to time matched NIE (P-value<0.05, *n – indicates which NIE experiment was significantly different from when compared; Students t-test 2 tailed). X-axis represents normalised mean mRNA expression value. Y-axis displays experimental condition. ERNI was removed from all bar charts due to high expression values which skewed graphs and made visualisation difficult.**

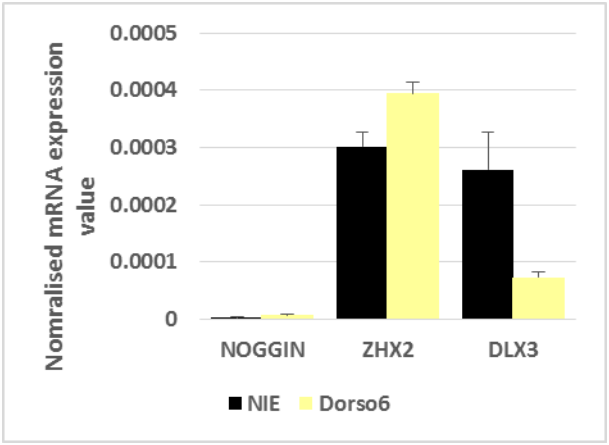


**Appendix 9.7 Genes regulated at 6 hours by Dorsomorphin.**

**Appendix 9.8 Electronic appendix: File containing all NanoString data,**

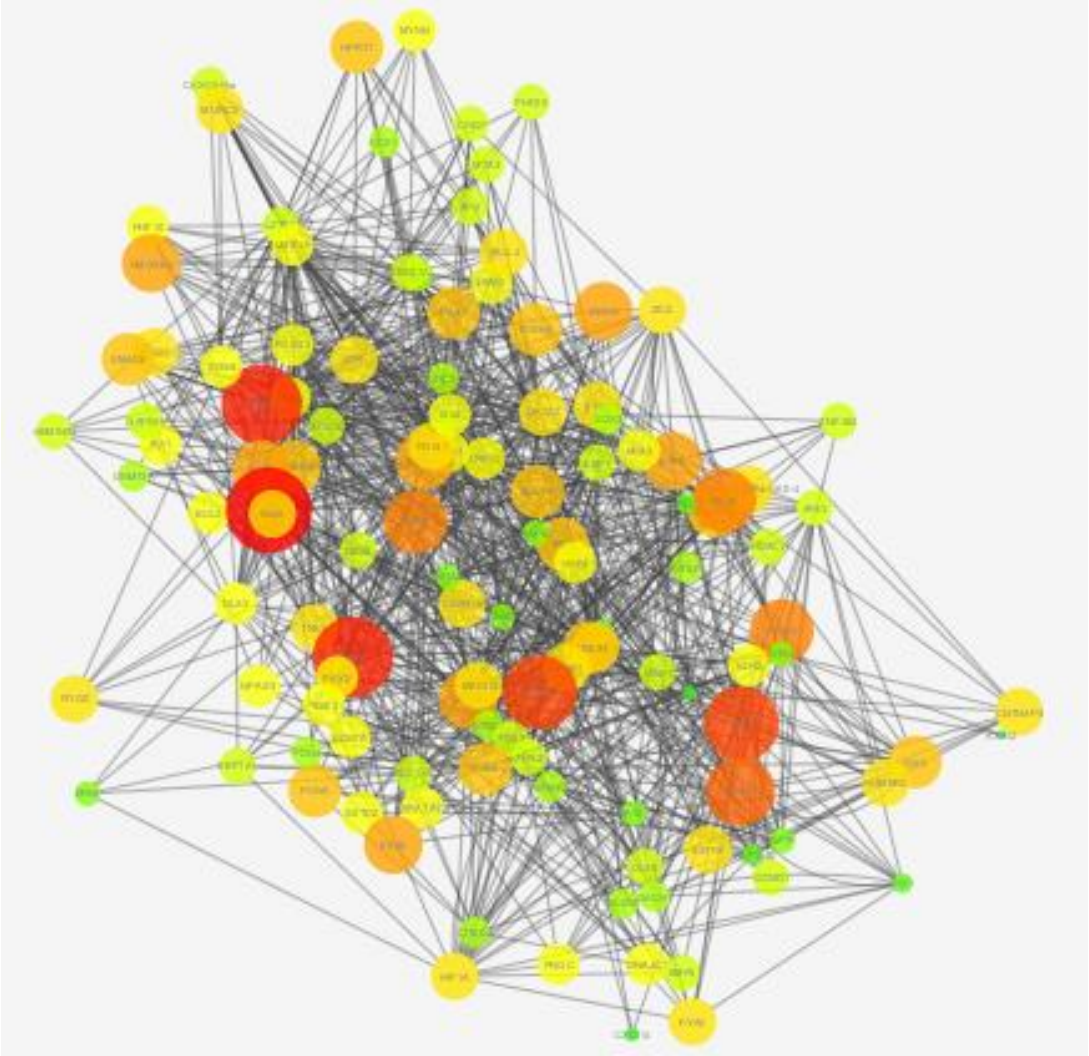

**Appendix 9.10 Predicted network of interactions for Chapter 4**